Viktoria H. Gessner   *Editor*

Modern Ylide Chemistry

Applications in Ligand Design, Organic
and Catalytic Transformations

Springer

177
Structure and Bonding

Series Editor:

D.M.P. Mingos, Oxford, United Kingdom

Aims and Scope

Structure and Bonding is a publication which uniquely bridges the journal and book format. Organized into topical volumes, the series publishes in depth and critical reviews on all topics concerning structure and bonding. With over 50 years of history, the series has developed from covering theoretical methods for simple molecules to more complex systems.

Topics addressed in the series now include the design and engineering of molecular solids such as molecular machines, surfaces, two dimensional materials, metal clusters and supramolecular species based either on complementary hydrogen bonding networks or metal coordination centers in metal-organic framework materials (MOFs). Also of interest is the study of reaction coordinates of organometallic transformations and catalytic processes, and the electronic properties of metal ions involved in important biochemical enzymatic reactions.

Volumes on physical and spectroscopic techniques used to provide insights into structural and bonding problems, as well as experimental studies associated with the development of bonding models, reactivity pathways and rates of chemical processes are also relevant for the series.

Structure and Bonding is able to contribute to the challenges of communicating the enormous amount of data now produced in contemporary research by producing volumes which summarize important developments in selected areas of current interest and provide the conceptual framework necessary to use and interpret mega-databases.

We welcome proposals for volumes in the series within the scope mentioned above. Structure and Bonding offers our authors and readers:

- OnlineFirst publication. Each chapter is published online as it is finished, ahead of the print volume
- Wide dissemination. The chapters and the volume will be available on our platform SpringerLink, one of the largest collections of scholarly content in the world. SpringerLink attracts more than 50 million users at 15.000 institutions worldwide.
- Easy manuscript preparation. Authors do not have to spend their valuable time on the layout of their contribution. Springer will take care of all the layout related issues and will provide support throughout the complete process.

More information about this series at http://www.springer.com/series/430

Viktoria H. Gessner
Editor

Modern Ylide Chemistry

Applications in Ligand Design, Organic
and Catalytic Transformations

With contributions by

M. Alcarazo · B. Borthakur · W.-C. Chen · V. H. Gessner ·
S. Liu · N. Maulide · J. Merad · J. D. Neuhaus · T.-G. Ong ·
R. Oost · A. K. Phukan

Springer

Editor
Viktoria H. Gessner
Chair of Inorganic Chemistry II
Ruhr-Universität Bochum
Bochum, Germany

Preface

Ylide chemistry has quite a long history. However, despite their age, ylides have never gone out of fashion. Historically, first studies on ylidic compounds were already reported at the end of the nineteenth century by Michaelis [1] as well as Staudinger, who reported the first isolation and reactions toward C=X bonds [2]. The full potential of this reaction, however, was only recognized years later by Wittig in the 1950s [3]. His well-known olefination reaction coined "ylide chemistry" for many years and – without doubt – ranks among the most outstanding achievements in synthetic chemistry of the twentieth century, rightly recognized by the Nobel Prize in 1979 [4]. Many variations of the original Wittig reaction were reported since then, thus uncovering the utility of ylidic compounds in organic synthesis. The impact of the Wittig and related reactions is impressively demonstrated by many protocols for the synthesis of pharmaceutically or biologically active substances, natural products, or flavors, which rely on ylide-based olefination reactions.

But where does ylide chemistry stand today? Despite this intimate relationship between ylides and Wittig-type reactions, ylide chemistry is by far not restricted to olefin formation reactions. In contrast, ylidic compounds are the subject of vivid research activities in most diverse fields of chemistry and have been part of countless fascinating experimental as well as theoretical studies. Particularly recent years have uncovered new applications of ylidic compounds such as in coordination chemistry and homogeneous catalysis by also focusing on ylide systems that have long been neglected particularly compared with classical phosphorus ylides. The numerous examples reported over the years demonstrate the exciting properties of ylidic compounds as well as their versatility as important reagents in organic synthesis and as highly potent donor ligands.

The continuous developments in ylide chemistry and the special properties of this class of compounds are clearly reflected by their unique electronic structure. The question about the "best" description of the bonding situation has been the subject of perseverative controversial discussions that are ongoing even today. Initial debates argued on the competing contributions of the double bonded ylene

structure **A′** and the ylidic ionic structure **A** but have ended in favor of the ylide description due to the unfavorable energy of the *d*-orbitals of the main group elements. However, recent debates incited by publications based on detailed computational studies centered around a predominant contribution of a dative bonding situation to the electronic structure of ylidic compounds as depicted by structure **A″**. While phosphorus ylides can thus be viewed as phosphine coordinated carbenes, bisylidic compounds such as carbodiphosphoranes **B** can be regarded as coordination compounds of carbon with carbon being in the oxidation state of zero. This picture has led to their denotation as carbones **B″** [5]. The captodative bonding mode in carbones (indicated by an arrow between the two atoms bound to each other) is comparable to the well-known Dewar–Chatt–Duncanson model which is routinely used to describe ligand metal interactions in transition metal chemistry. Consequently, this has led to the conclusion that the carbon atom in ylidic compounds can also serve as the "central atom" comparable to a metal center in a complex [6].
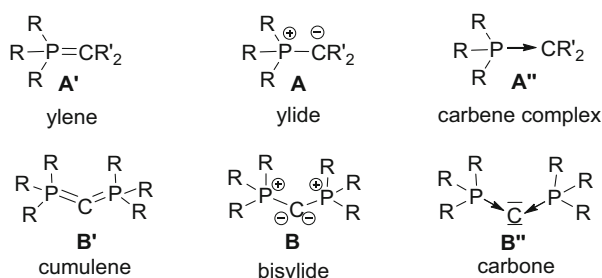
The dative description of ylidic compounds has resulted in most controversial discussions within the chemistry community and revived fundamental debates about differences between dative and polar covalent bonding situations [7–9]. Furthermore – and probably most importantly – it has also led to a "rethinking" of the nature of ylidic compounds and thus stimulated increased research activities particularly with focus on the coordination chemistry of ylides [10]. Regardless of the question of the correct description of the electronic structure, the discussion impressively reflects the unique properties and reactivities of ylidic compounds and demonstrates the vivid and exciting nature of this research.

This volume focuses on recent trends in ylide chemistry. Thus, it brings together ylidic compounds with unique electronic properties and reactivities that have received particular interest in the past decade. While simple phosphorus ylides without doubt still belong to the most important and frequently used reagents in organic synthesis, this volume deliberately neglects the chemistry of simple phosphorus ylides which have been the subject of many other review articles and book chapters. In contrast, this book concentrates on ylidic compounds, which are less elaborated but have attracted increased research interest in recent years, thus already revealing their huge synthetic potential. Hence, the chemistry of bisylides,

carbodicarbenes, yldiides, and sulfur ylides is summarized in this book with special focus on unusual structures and bonding situations as well as advanced synthetic applications such as the development of new versatile reagents for organic synthesis and catalytic transformations with ylide compounds acting as reagents as well as supporting ligands for metal catalysts.

The first chapter provided by A. K. Phukan picks up recent computational studies on ylide chemistry particularly focusing on two different areas: As such, the first part deals with carbon(0) compounds, i.e., the bonding situation, electronic structure, and properties of bisylidic compounds, especially summarizing those studies which gave way to the disputed description of these compounds as carbones. The second part discusses the impact of ylide functionalization of carbenes, thus demonstrating the utility of ylide moieties in electronic manipulation of molecules. This chapter is followed by a summary of the experimental work on carbodiphosphoranes and related compounds by M. Alcarazo. The compound class of carbodiphosphoranes is a prime example for compounds which have been synthesized early and known for several years, but whose exciting and unique chemistry – above all their excellent ligand properties for the coordination of unusual main group element species – has only been appreciated in recent times. Here, the synthesis and properties as well as the coordination chemistry toward main group elements and transition metals are highlighted. The third and fourth chapters are then concerned with catalytic applications of ylidic compounds. At first T.-G. Ong and W.-C. Chen provide an overview on the use of carbodicarbenes – a particularly interesting subclass of bisylidic compounds – as ligands to support catalytically active transition metal catalysts, while N. Maulide highlights the synthetic value of sulfur-based ylides as powerful reagents in transition metal-catalyzed reactions. The last chapter finally picks up the chemistry of α-metallated ylides, which can be regarded as the anionic congeners of bisylides. Their structure, unique reactivity, and applications in organic synthesis as well as main group element and transition metal chemistry are summarized together with the use of ylide functionalization to manipulate the electronic properties of reactive species.

The diversity of the compounds discussed in this volume demonstrates the multifariousness of ylide chemistry and its breadth of applications. Continuously, novel types of compounds have been discovered or rediscovered and their utility broadened in most different fields of chemistry. The examples selected in this volume prove the dynamic nature of ylide chemistry that will ensure the discovery of many more fascinating properties and reactivities in the future.

Bochum, Germany   Viktoria H. Gessner
December, 2017

References

1. Michaelis A, Gimborn Hv (1894) Über das Betain und Cholin des Triphenylphosphins. Ber 27:272
2. Staudinger H, Meyer J (1919) Über neue organische Phosphorverbindungen III. Phosphinmethylenderivate und Phosphinimine. Helv Chim Acta 2:635
3. Wittig G, Geissler C (1953) Zur Reaktionsweise des Pentaphenyl-phosphors und einiger Derivate. Liebig Ann Chem 580:44
4. Wittig G (1980) From diyls to ylides to my idyll. Science 210:600
5. Tonner R, Öxler F, Neumüller B, Petz W, Frenking G (2006) Carbodiphosphoranes: the chemistry of divalent carbon(0). Angew Chem Int Ed 45:8038
6. Alcarazo M, Lehmann CW, Anoop A, Thiel W, Fürstner A (2009) Coordination chemistry at carbon. Nat Chem 1:295
7. Himmel D, Krossing I, Schnepf A (2014) Dative bonds in main-group compounds: a case for fewer arrows! Angew Chem Int Ed 53:370
8. Frenking G (2014) Dative bonds in main-group compounds: a case for more arrows! Angew Chem Int Ed 53:6040
9. Himmel D, Krossing I, Schnepf A (2014) Dative or not dative? Angew Chem Int Ed 53:6047
10. Dyker A, Bertrand G (2009) Rethinking carbon. Nat Chem 1:265

Contents

Structure and Reactivity of Carbones and Ylide Stabilized Carbenes: Contributions from Theory

Bitupon Borthakur and Ashwini K. Phukan

Abstract This chapter presents the results of theoretical studies on divalent C(0) bases as well as on ylide stabilized carbenes. The primary difference between C(0) and C(II) compounds is the presence of two lone pairs at the central carbon atom of the former, unlike one in the latter. Theoretical studies reveal that the first and especially second proton affinity values can be used to distinguish carbenes from carbones. Further, the difference in reactivity of C(0) and C(II) compounds towards electrophiles such as H^+, BH_3 and AuCl is also found to be effective in distinguishing these two classes of compounds. Moreover, the ^{13}C NMR chemical shifts of the central carbon atom as well as reactivity towards nucleophiles such as CNMe provide another criteria for distinguishing not only C(0) and C(II) compounds but also those having hidden C(0) characters. In addition, this chapter also deals with the recent studies carried out on ylide stabilized carbenes which possess excellent electron donation abilities. However, the ylide substituted carbenes are found to be ineffective towards activation of small molecules like H_2 and NH_3 due to the absence of a suitable low-lying π-acceptor orbital at the carbene centre.

Contents

B. Borthakur and A. K. Phukan (✉)
Department of Chemical Sciences, Tezpur University, Napaam, Assam, India
e-mail: ashwini@tezu.ernet.in

1 Introduction

The tetravalent nature of carbon in most of the organic compounds where it uses all the four valence electrons in bonding is a common knowledge. However, there exists an unusual situation where the central divalent carbon atom possesses a pair of non-bonding electrons (**A**, Scheme 1) which may reside either in a single orbital with anti-parallel spin (singlet carbenes) or in two mutually perpendicular orbitals with parallel spins (triplet carbenes). Even though the first stable singlet carbene was synthesized by Bertrand et al. in 1988 [1], the chemistry of divalent carbon compounds came to the fore when Arduengo et al. isolated the first bottleable cyclic carbene known as NHC (*N*-heterocyclic carbene) in 1991 [2]. Before that, carbenes were considered as reactive reaction intermediates [3–6]. Following the discovery of NHC, a number of their skeletally substituted derivatives were also isolated which possess varying degree of electronic properties [7–14]. NHCs are popular as very good electron donors even better than the classical σ-donors like phosphines and amines and later, both experimental and theoretical studies reported their non-negligible π-accepting abilities as well ([15–24], and references therein). In 2005, Bertrand and co-workers isolated a saturated version of NHC where one of the α-nitrogen atoms was replaced by a quaternary carbon atom known as cyclic (alkyl) (amino)carbene (CAAC) [9]. CAAC possesses significantly enhanced electron donation and acceptance ability compared to typical NHCs [11]. Owing to such enhanced electronic properties, CAAC was found to be advantageous for many catalytic processes [25, 26] and can be compared to a transition metal complex because of its ability to activate small molecules like H_2, NH_3 and P_4, etc. [27–30]. On the other hand, both theoretical [31, 32] and experimental [33–36] studies confirm the strong electron donation abilities of ylide substituted NHCs. It is believed that by virtue of the significant π-stabilization ability, installation of ylide moieties may even help in the isolation of hitherto unknown free remote NHCs [32].

    There is another class of divalent carbon compounds but unlike carbenes, they possess two non-bonding electron pairs at the central carbon atom (**B**, Scheme 1)
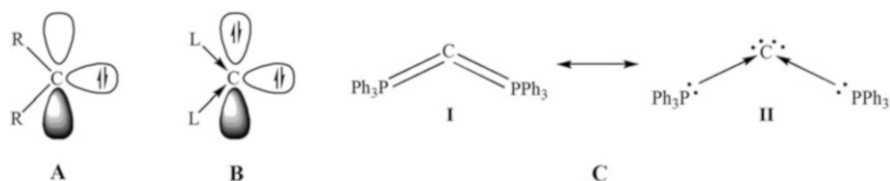
Scheme 1 Schematic representations of carbene (**A**), carbone (**B**) and bonding situation in carbodiphosphorane (CDP) (**C**)
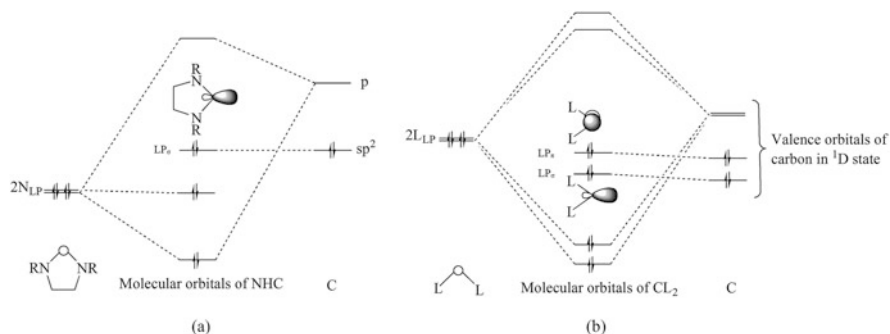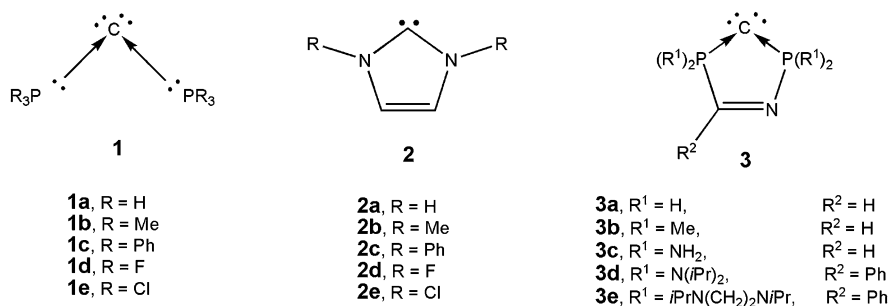
Scheme 2 Qualitative molecular orbital diagrams of (**a**) *N*-heterocyclic carbene (NHC) and (**b**) carbone

[37, 38] popularly known as carbones [39]. The first molecule of this kind, carbodiphosphorane (CDP) was isolated as early as in 1961 [40] but it came to prominence only after the description of its bonding situation by Frenking et al. in terms of donor–acceptor bonds between the phosphine ligands and the central carbon atom (structure **C II**, Scheme 1) [41]. It should be noted that in this case none of the valence electrons of the central carbon atom is involved in bonding and hence it is thought to possess a formal oxidation state of zero, i.e. C(0) unlike C(II) in carbenes. Further, the central carbon atom in carbones possesses an electron octet with one σ- and one π-symmetric lone pairs while it is a sextet for carbenes with only one lone pair of electrons residing in an in-plane σ-symmetric orbital. An inspection of the qualitative molecular orbital diagrams for NHC and carbone (Scheme 2) shows that in case of NHC, the interactions between the nitrogen lone pairs with the carbon out-of-plane vacant p-orbital result in the formation of a singlet carbene with a lone pair of electron concentrated at the carbon atom. In contrast, the formation of carbones results from interaction of the lone pairs of Lewis donor groups with the formally vacant p orbitals of an excited singlet carbon atom thereby stabilizing two carbon-based lone pair orbitals. In the next sections, we will discuss different types of carbones as well as ylide substituted carbenes with special emphasis on the respective theoretical studies carried out till date.

2 Carbodiphosphoranes

In 1961, Ramirez et al. synthesized the first CDP (**1c**, Scheme 3) [40]. Later in 2006, theoretical studies by Frenking et al. showed that the bonding interaction in CDP is mainly dative in nature where the phosphorus lone pairs are being donated to the empty valence orbitals on carbon thereby generating two lone pairs at the central carbon atom (C_0) having π- and σ-symmetry, respectively (Fig. 1) [41]. The calculated NBO (Natural Bond Orbital) atomic partial charge at the C_0 atom was found to be significantly negative ($-1.43e$) which is in accordance with the presence of two

1

1a, R = H
1b, R = Me
1c, R = Ph
1d, R = F
1e, R = Cl

2

2a, R = H
2b, R = Me
2c, R = Ph
2d, R = F
2e, R = Cl

3

3a, R^1 = H, R^2 = H
3b, R^1 = Me, R^2 = H
3c, R^1 = NH_2, R^2 = H
3d, R^1 = N(iPr)$_2$, R^2 = Ph
3e, R^1 = iPrN(CH$_2$)$_2$NiPr, R^2 = Ph

Scheme 3 Schematic representation of all the CDPs (**1** and **3**) and NHCs (**2**) discussed in this section
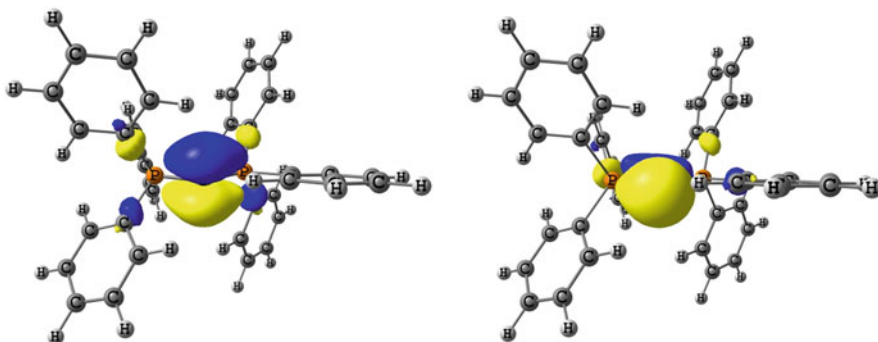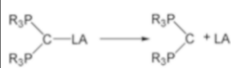

Fig. 1 HOMO (left) and HOMO-1 (right) of C(PPh$_3$)$_2$ (**1c**) [41]

non-bonding pairs of electrons at C_0. DFT calculations were also carried out on the smaller congeners of CDPs with L = PH$_3$ (**1a**) and PMe$_3$ (**1b**) [41, 42]. All these three CDPs (**1a–c**) were found to be significantly bent with P-C-P bond angles in the range 125°–137°. However, the energy difference between the equilibrium and linear geometry (i.e. with ∠P-C-P = 180°) is very small (2.0, 0.9 and 3.1 kcal mol^{-1} for **1a**, **1b** and **1c**, respectively) and interestingly, very recently Parkin et al. were able to synthesize and isolate the linear isomer of C(PPh$_3$)$_2$ [43]. The four electron donor ability (i.e. the presence of two lone pairs at the central carbon atom) in CDPs was supported by the calculated first and second proton affinity (PA) values [44]. Frenking and co-workers reported that CDPs not only have very high first PA values but also large second PA values (Table 1). However, carbenes (**2a–e**) possess much smaller second PA values compared to the CDPs. Thus, it was proposed that PA values can be used to distinguish carbones from carbenes. However, the PA values for the halophosphine compounds **1d** and **1e** were reported to be comparatively lower than the PAs for **1a–c**. The difference between the C(0) and C(II) compounds also comes from the calculated atomic partial charges at the central carbon atom of the parent molecule as well as of the corresponding singly and

Table 1 Calculated (MP2/TZVPP//BP86/SVP) first and second proton affinities (PA-1 and PA-2 in kcal mol^{-1}) and NBO partial charges (BP86/TZVPP//BP86/SVP) at the central carbon atom [q(C)] for **1–3** as well as in their protonated derivatives [41, 44]

Molecule	PA-1	PA-2	q(C)	q(C)$_{H+}$	q(C)$_{2H+}$
1a	255.7	114.4	−1.32	−1.26	−1.01
1b	278.4	156.2	−1.47	−1.36	−1.07
1c	280.0	185.6	−1.43	−1.33	−1.07
1d	209.3	70.6	−1.69	−1.53	−1.30
1e	227.9	116.4	−1.35	−1.36	−1.13
2a	254.2	47.7	0.04	0.20	−0.14
2b	262.3	71.8	0.04	0.21	−0.12
2c	264.7	100.1	0.08	0.21	−0.10
2d	228.9	38.9	0.04	0.12	−0.17
2e	244.3	57.6	0.07	0.18	−0.13
3a	251.5	110.5	−1.26	−1.26	−1.04
3b	270.8	143.3	−1.34	−1.32	−1.08
3c	271.4	138.1	−1.38	−1.36	−1.15
3d	284.2	188.3	−1.49	−1.40	−1.18
3e	284.5	179.0	−1.44	−1.39	−1.19

Table 2 Calculated (RI-MP2/TZVPP//RI-BP86/SVP) bond dissociation energies (BDEs, kcal mol^{-1}) of CDP complexes with various Lewis acids (LA) [41]

Molecule	R	BH$_3$	BCl$_3$	AlCl$_3$	BH$_3$	BCl$_3$	AlCl$_3$
1a	H	29.3	33.9	44.0	25.5	14.8	23.1
1b	Me	34.0	36.4	51.0	28.4	9.6	27.0
1c	Ph	27.5	35.9	50.9	15.8	−32.7	−3.9

doubly protonated species. Table 1 clearly shows that for the CDPs, the central carbon centre carries a negative charge not only in the neutral molecule but also in the respective singly and doubly protonated species while this is not the case with carbenes. For carbenes **2a–e**, the atomic partial charge on C(II) is almost close to zero which becomes slightly positive in the singly protonated species. But the doubly protonated carbenes have a central carbon atom with slightly negative atomic partial charge which is due to the change in bonding situation in the doubly protonated species. The C(0) character of CDPs were also revealed by the presence of two (3,+3) critical points (CP) in **1a** as evident from the molecular electrostatic potential (MESP) analysis [45]. In contrast, **2a** exhibits only one (3,+3) CP thereby indicating the presence of only one lone pair at the central carbon atom.

The calculated values of bond dissociation energies (BDEs, Table 2) indicate that CDPs with smaller PR$_3$ groups (**1a–b**) can easily bind two Lewis acids other than H$^+$ [41]. The BDE values for the donor–acceptor complexes of **1a** and **1b** with one/two molecules of BH$_3$, BCl$_3$ and AlCl$_3$ are significantly positive. Later, this theoretical prediction was confirmed by the successful isolation of a dicoordinated adduct of **1c** where it binds two BH$_3$ molecules [46]. However, CDP with bulky phenyl

groups (**1c**) can bind with only one molecule of BCl_3 and $AlCl_3$ as the calculated BDE values for the respective adducts of **1c** with two molecules of BCl_3 and $AlCl_3$ are found to be negative.

In 2006, the group of Baceiredo reported the isolation of cyclic five-membered CDPs (**3d–e**, Scheme 3) which were found to exhibit unusual stability [47]. Calculations were also carried out on cyclic CDPs having different substituents on the ring framework [41, 44] and the results are summarized in Table 1. The calculated first and second PA values for the cyclic CDPs are akin to the acyclic CDPs (**1**). Further, the atomic partial charges on the central carbon atom of **3a–e** are also significantly negative in the neutral molecule as well as in the singly and doubly protonated species which indicates the presence of divalent C(0) character in these cyclic CDPs as well.

3 Carbodicarbenes

Following the bonding description of CDP [41], it was envisaged that NHC could be a suitable replacement for phosphine towards stabilization of the C(0) species (**4a**, Scheme 4) [48]. Similar to the CDPs, the central C_{NHC}-C_0-C_{NHC} angle was found to be acute (125.8°) in the equilibrium geometry **4a** with a torsion angle of 81.6° between the NHC planes. An analysis of the frontier molecular orbitals of **4a** shows the resemblance of the two highest occupied molecular orbitals HOMO and HOMO-1 with those of CDPs. The shapes of HOMO and HOMO-1 indicate that both are lone pair orbitals and thus the bonding situation in carbodicarbenes (CDCs) can be described in terms of L → C donor–acceptor interactions. The experimental verification of CDC came soon after when Bertrand et al. synthesized and structurally characterized a benzannulated derivative of **4a** in a two-step process [49] which was followed by the synthesis of another CDC by Fürstner and co-workers [50].

As explained in the case of CDPs, the first and especially second proton affinity values can be used as a decisive indicator for the presence of C(0) character in a particular ligand. The theoretically predicted values of both first and second PAs for **4a** (292.3 and 155.3 kcal mol^{-1}, respectively) and **4b** (294.3 and 168.4 kcal mol^{-1}, respectively) were found to be significantly higher and comparable to those of CDPs (Table 1) thereby supporting the C(0) character of CDCs. However, unlike in CDPs, MESP analysis of **4a** indicated the presence of only one (3,+3) CP which is ascribed

Scheme 4 Schematic representation of carbodicarbenes (CDCs) with different substituents at the heteroatoms of NHCs

4a, R = H
4b, R = Me
4c, R = NH$_2$
4d, R = OH
4e, R = Cl
4f, R = F
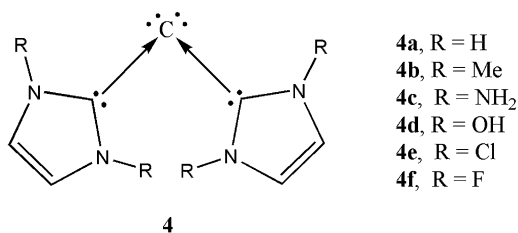
to the greater extent of delocalization of the π-type lone pair in **4a** compared to that in **1a** [45]. The strong donation ability of CDCs was further tested by their complexation with Lewis acids other than proton (H$^+$) [51]. The dissociation energies of the donor–acceptor complexes of both **4a** and **4b** with one and two BH$_3$ molecules are significantly higher. In addition, the changes in Gibb's free energies indicate that both **4a** and **4b** can easily bind two molecules of BH$_3$ thereby further confirming the double donor ability of CDCs. Interestingly, in 2008, Frenking et al. predicted that the use of carbones as ligands in Grubbs' catalysts will show better activity [52] which has recently been confirmed in experimental studies by Grubbs and co-workers [53]. In addition, recent studies have also shown that not only the transition metal complexes of CDCs [54–57] but also metal free CDCs [58, 59] exhibit high efficiency in catalytic transformations including small molecule activations.

In 2012, we predicted the stabilization of cyclic and acyclic carbon(0) compounds by differential coordination of heterocyclic carbenes (Scheme 5) [60]. Except **6**, all other CDCs possess a bent central C$_c$-C$_0$-C$_c$ angle (C$_c$ = carbenic carbon atom). The stronger interaction between the central C$_0$ atom and the C$_c$ of remote NHCs in **6** resulted in a linear geometry. Even though NBO analysis did not show any L $\rightarrow$ C $\leftarrow$ L type donor–acceptor interactions in the equilibrium geometries, the calculated natural charges at the central carbon atom were found to be negative which indicate the presence of C(0) character in these compounds. However, the slight positive charge at the central carbon atom of **6** arises from a high degree of electron delocalization from the central carbon atom to the vacant p$_\pi$ orbital of the adjacent C$_c$ atoms. Further, the frontier occupied orbitals (HOMO and HOMO-1) of all these CDCs were found to be largely localized at the central C$_0$ atom implying that these molecules possess double donor character. The calculated first and second PAs were also very high (Table 3) and comparable to that of CDPs and interestingly, the C$_0$ atom of **5–10** has significant negative charge even after first protonation thus supporting the description of donor–acceptor interaction L $\rightarrow$ C $\leftarrow$ L. Further, we obtained a nice correlation between the orbital energies and the computed PA
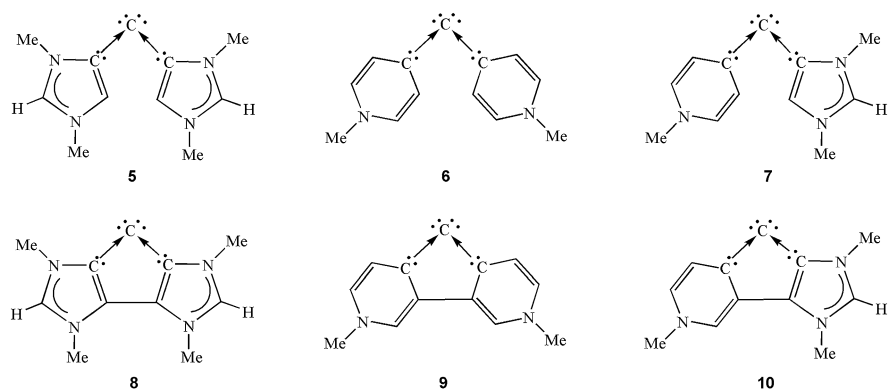
Scheme 5 Schematic representations of acyclic (**5–7**) and cyclic (**8–10**) CDCs [60]

Table 3 Calculated (BP86/TZVP) first and second proton affinities (in kcal mol^{-1}), BDEs (in kcal mol^{-1}) and energies including thermal and vibrational corrections (BDE_0^{298} in kcal mol^{-1}) calculated using reaction (1) [60]

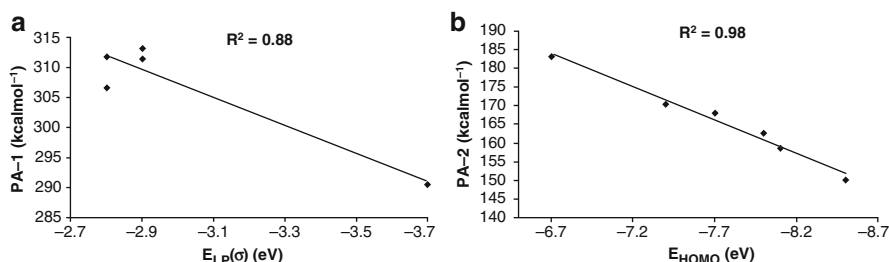| Molecule	PA-1	PA-2	BDE	BDE_0^{298}
5	311.9	183.6	221.2	220.6
6	290.6	162.9	285.9	284.2
7	306.7	170.6	250.9	248.7
8	313.4	168.3	193.6	186.4
9	312.0	150.3	255.4	246.5
10	311.5	158.7	228.7	220.2

Fig. 2 Correlation plot between (**a**) first proton affinity and energy of the σ-symmetric lone pair orbital, and (**b**) second proton affinities and energies of the π-symmetric HOMO of the first protonated derivatives of **5–10** [60]

values (Fig. 2). The second PAs for the acyclic CDCs (**5–7**) are slightly larger than those computed for their cyclic derivatives (**8–10**) which was reasoned to the lower energies of the π-symmetric lone pair orbital (HOMO) of the first protonated derivatives of **8–10**. Further, the calculated BDEs (Table 3) of the carbon-ligand donor–acceptor bonds using Eq. (1) indicated that the acyclic CDCs follow the trend **5** < **7** < **6**. The BDE trend was found to be similar for the cyclic counterparts as well (i.e. **8** < **10** < **9**). Further, the calculated ΔG values for the formation of all these CDCs (**5–10**) are found to be significantly negative implying their high thermodynamic stability.

$$CL^1L^2 \rightarrow C(^3P) + L^1 + L^2 \tag{1}$$
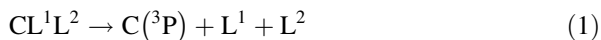
In another study, we found that the substituents present at the nitrogen atoms of the NHCs in CDCs govern not only the structures but also the electron donation ability of CDCs [61]. Calculations showed that NHCs having substituents like F (**4e**) and Cl (**4f**) at the heteroatoms (Scheme 4) give rise to CDCs with a quasi-linear geometry which "mask" their C(0) character. Further, the QTAIM (quantum theory of atoms in molecules) [62, 63] analysis of **4a** indicates that the bond between carbenic carbon and the central carbon has significant covalent character as evident from large negative value of both the Laplacian and local electronic energy density $H(r)$ (Fig. 3) [64].
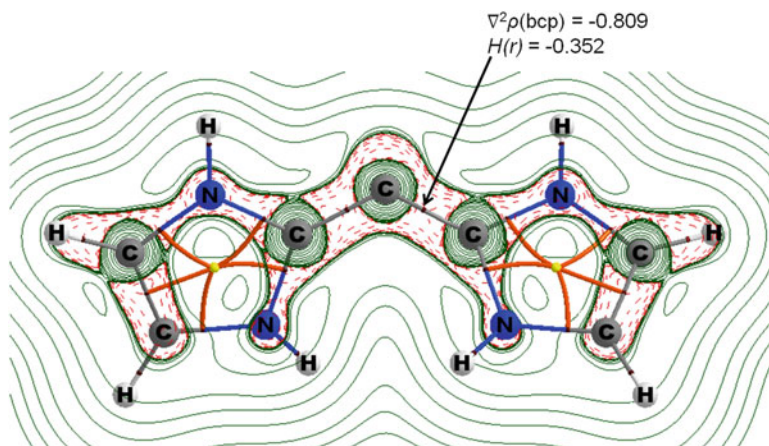
Fig. 3 Laplacian of electron density $[\nabla^2\rho(\text{bcp})]$ in the C_c–C_0–C_c plane for **4a**. Solid green lines represent charge depletion $[\nabla^2\rho(\text{bcp}) > 0]$, while dashed red lines represent charge concentration $[\nabla^2\rho(\text{bcp}) < 0]$. Reddish brown dots represent bond critical points. The values of Laplacian $[\nabla^2\rho(\text{bcp})]$ and local energy density $H(r)$ are in atomic units [61]

4 Compounds with Hidden C(0) Character

Theoretical studies were also available for CDCs with acyclic carbenes (**11**, Scheme 6) [42, 48, 65] and these compounds were previously known as tetraaminoallenes (TAAs). The fact that TAAs can exhibit the property of typical carbones such as CDP or CDC is supported by the experimental observation of donor–acceptor complexes between CO_2 and TAA as well as isolation of a diprotonated species.

There is another intriguing class of compound known as "bent allenes" which were first synthesized by Bertrand and co-workers [66]. As clear from its name, unlike TAAs, in bent allenes, the central C=C=C moiety is not linear (Scheme 6). Here, the divalent central carbon atom is stabilized by a "push–push" substitution pattern of a bidentate diaminocarbene (**12a**) or oxoaminocarbene (**12b**) ligand. Further, in 2009 Bertrand et al. reported the synthesis of an extremely bent allene ($\angle$C-C-C = 85°) which possesses all carbon four-membered ring [67]. The bonding analysis of **12b** had shown that both σ- and π-symmetric lone pair orbitals are strongly localized on the central carbon atom thereby indicating the presence of C(0) character in these bent allenes.

The calculated first PA values for these allenes (Table 4) suggest that all of them can be considered as super bases (PA > 239 kcal mol^{-1}). More importantly, the second PA values were also found to be significantly high and comparable to those reported for CDPs/CDCs thereby providing unequivocal confirmation of the presence of C(0) character in these compounds. Similar to the case with CDPs, all these TAAs and bent allenes carry partial negative charge at the central carbon atom which remains even after second protonation. In addition, the calculated dissociation energies (Table 5) for the mono BH$_3$ adducts with all these allenes are significantly

11a, R = CH$_3$
11b, R = C$_2$H$_5$

12a, R =   **12b**, R =
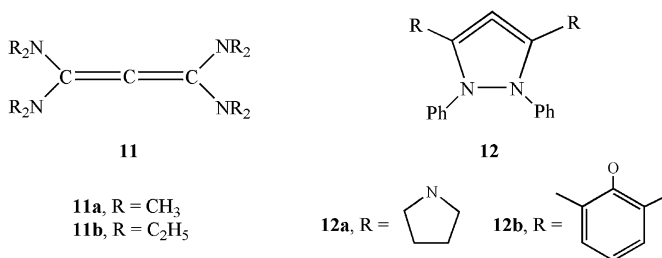
Scheme 6 Schematic representation of linear and bent allenes

Table 4 Calculated (MP2/TZVPP//BP86/SVP) first and second proton affinities (in kcal mol^{-1}) and NBO partial charges at the central carbon atom (qC) of **11–12** as well as in their protonated derivatives [39, 51]

Molecule	PA-1	PA-2	q(C)	q(C)$_{H+}$	q(C)$_{2H+}$
11a	282.5	151.6	−0.21	−0.47	−0.51
11b	268.2	175.8	−0.22	−0.47	−0.57
12a	296.5	158.7	−0.48	−0.42	−0.52
12b	284.3	133.3	−0.48	−0.44	−0.61

Table 5 Calculated (MP2/TZVPP//BP86/SVP) dissociation energies (D_e, in kcal mol^{-1}) and changes in Gibb's free energies ($-\Delta G$, in kcal mol^{-1}) of one and two BH$_3$ molecules for some selected allenes [**A**] [51]

[**A**]	[**A**] − BH$_3$ → [**A**] + BH$_3$		H$_3$B − [**A**] − BH$_3$ → [**A**] − BH$_3$ + BH$_3$	
	D_e	$-\Delta G$	D_e	$-\Delta G$
11a	39.8	23.4	17.4	0.2
12a	58.4	42.7	20.0	5.8
12b	53.0	38.2	9.5	−4.5

higher and the changes in Gibb's free energies indicate that they can easily bind two molecules of BH$_3$. However, the coordination of the second equivalent of BH$_3$ was found to be thermodynamically unfavourable for **12b**. Therefore, all the calculated parameters, viz., geometric parameters, shapes of frontier occupied molecular orbitals, reactivity towards different electrophiles and the calculated atomic partial charges confirmed the presence of hidden C(0) character in these allenes.

Another interesting candidate of this category is 2,2′-bipyridyl carbene (**13**, Scheme 7) which was synthesized by Weiss et al. [68] in 1998. Earlier, based on ab initio calculations, this compound was assigned as a carbene. However, due to the availability of a geminal diprotonated derivative of **13**, our group reinvestigated its electronic nature as well as reactivity towards electrophiles [69]. Interestingly, NBO analysis showed that the HOMO and HOMO-1 of **13** are akin to those observed for **4b**. Further, the calculated values of both first and second PAs (261.0 and 133.8 kcal mol^{-1}, respectively) are significantly higher than those reported for other carbenes and almost comparable to those of C(0) compounds indicating the
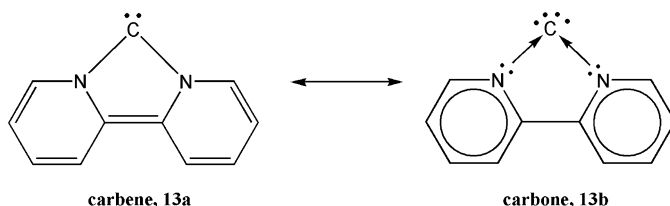
Scheme 7 Possible resonance forms of 2,2′-bipyridyl carbene (**13**) [69]

presence of hidden C(0) character in **13** thereby highlighting the importance of the resonance form **13b** (Scheme 7). Further support for the presence of C(0) character in **13** came from the significant values of BDEs calculated for gem-dimetallation (37.1 and 33.1 kcal mol^{-1} for complexation with AuCl and Ni(CO)$_2$, respectively). It should be noted that the computed BDEs for gem-dimetallation of normal NHC (**2b**) was also found to be significant (35.0 and 31.3 kcal mol^{-1} for complexation with AuCl and Ni(CO)$_2$, respectively) and comparable to that of **13** thereby indicating the possibility of hidden C(0) character even in Arduengo type NHCs [68].

5 Carbodiylides

Frenking et al. carried out the theoretical investigations on a series of compounds (CL$_2$ = **14**–**18**, Scheme 8) where they have used diyl ligands (L = ECp*, E = B − Tl) as substituents on a divalent carbon atom [70]. The choice of diyl ligands to stabilize the central carbon atom was based on the strong σ-donation and weaker π-acceptance ability of these ligands than CO. It was found that except for the boron compound **14**, all others possess significantly bent structures and the bending angles (∠E-C-E) were found to be smaller than those reported for CDPs and CDCs. The two Cp* groups in **14** are coordinated to the boron atom in η^1 fashion and rotated with respect to each other by almost 90° about the C-B-C axis. However, in case of the higher analogue **15**, all the Al-C bonds to the carbon atoms of Cp* were calculated to be almost identical (2.259–2.272 Å) implying η^5 mode of coordination between Al and the two Cp* rings. For the remaining homologues (i.e. **16**–**18**), the bonding between the group 13 element (E) and the Cp* groups was characterized as intermediate between η^3 and η^1 as suggested by the calculated E-C$_{Cp*}$ bond lengths. For example, the calculated Ga-C$_{Cp*}$ bonds were found to be in three different ranges with one having short (2.063 Å), two moderately long (2.479 and 2.558 Å) and the remaining two with very long (3.003 and 3.047 Å) Ga-C bonds and this situation holds true for **17** and **18** as well. Analysis of the frontier molecular orbitals indicates the presence of two lone pairs (except in **14**), one having π-symmetry (HOMO) and the other one with σ-symmetry (HOMO-1) in these carbodiylides thereby demonstrating their double donor character. However, for **14**, both HOMO and HOMO-1 were found to be delocalized over the entire molecule which is in accordance with its

E = B(**14**), Al(**15**), Ga(**16**), In(**17**), Tl(**18**)
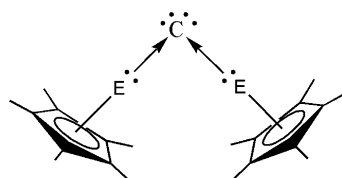
Scheme 8 Schematic representation of the carbodiylides **14–18**

Table 6 Calculated (MP2/TZVPP//BP86/SVP) values of first and second proton affinities (in kcal mol^{-1}), BDEs (in kcal mol^{-1}) and natural charges (BP86/TZVPP//BP86/SVP) at the central carbon atom for **14–18** [70]

Molecule	PA-1	PA-2	BDE	L → C(^{1}D)	q(C)
14	288.1	197.0	216.2	122.7	−1.29
15	287.8	191.6	125.2	77.2	−1.81
16	292.8	195.2	83.4	56.3	−1.57
17	279.0	190.0	53.7	41.4	−1.47
18	270.7	184.9	26.1	27.6	−1.35

almost linear geometry ($\angle$B-C-B = 178.9°). Further, the calculated first and second PAs for all the carbodiylides are very high (Table 6). It should be noted that for most of the C(ECp*)$_2$ compounds, the second PAs are even higher than those reported for CDPs and CDCs. Therefore, the highly bent geometries as well as the very high second PA values clearly confirm the C(0) character of the heavier carbodiylides (**15–18**). However, even though **14** possesses an almost linear geometry, based on the high second PA value it can be thought to possess hidden C(0) character like TAAs. The C$_0$-E bond strength becomes weaker with the increase in size of the group 13 element in the order B < Al < Ga < In < Tl as evident from the calculated BDEs for the reaction C(ECp*)$_2$ → C(^{3}P) + 2ECp*. In addition, the calculated donor–acceptor bond strength (L → C(^{1}D)) suggests that the thallium compound possesses much stronger donor–acceptor interaction between C$_0$ and TlCp* compared to those in majority of the typical Lewis donor–acceptor complexes of main group elements. Further support for the donor–acceptor interaction present in C(ECp*)$_2$ compounds came from the fact that in all the molecules, the central carbon atom carries significantly negative partial charge which is comparable to CDPs.

6 Distinction of Different Carbon Bases

As discussed earlier, the very high value of first and especially second PA values of C(0) compounds can be used as a measure to distinguish them from C(II) compounds. In addition, complexation with Lewis acidic groups other than protons

(such as BH_3) also suggests their double donor character. In this context, Frenking et al. proposed that different divalent carbon bases can be further distinguished by their complexation to one or two molecules of AuCl [71]. Recently, we have also proposed two new approaches to distinguish different carbon bases which are discussed in the next subsections.

6.1 Complexation to AuCl

Theoretical calculations carried out on a number of mono- and diaurated complexes of different divalent carbon bases revealed that there is a difference in the coordination mode for all the ligands [72]. While carbones were found to bind to AuCl groups in η^1 mode, allenes bind them in η^2 form. It should be noted that the diaurated complex of the CDP $C(PPh_3)_2$ is also experimentally known [73]. Complexation of carbon suboxide (C_3O_2) to one molecule of AuCl prefers the η^1 coordination mode while the optimized equilibrium structures for the diaurated complexes possess comparable energies for both η^1 and η^2 coordination modes. Divalent carbon bases with hidden carbon(0) character can coordinate in more than one way where the dominant coordination mode indicates the extent of C(0) or allene character. Calculations were also carried out for complexation of AuCl with NHC and the computed BDE for dissociation of one AuCl molecule is very high. Interestingly, NHC was also found to coordinate with two molecules of AuCl exhibiting the presence of an aurophilic interaction between the two η^1 bonded AuCl groups. However, the BDE for dissociation of the second AuCl from [NHC(AuCl)$_2$] is smaller than those obtained for similar reactions in case of typical carbones. Therefore, this difference in BDEs for the dissociation of the second AuCl moiety can be used to distinguish C(II) ligands from C(0) ones.

6.2 Reactivity Towards Nucleophiles

Theoretical calculations indicate that the ylide substituted carbenes (**19** and **20**, Scheme 9a) possess a high energy lone pair orbital at the carbenic centre as well
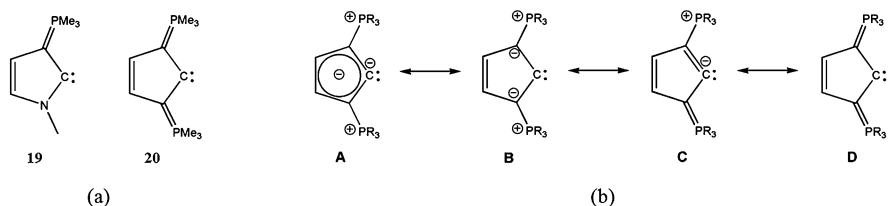
Scheme 9 Schematic representation of (**a**) ylide substituted carbenes, (**b**) different resonance forms of bis-ylide carbene [74]

Table 7 Computed (BP86/TZVP, SDD (Au)) natural charge at the central carbon atom (q_C), occupancies of the lone pair orbitals, first and second PAs (in kcal mol^{-1}) and BDEs (in kcal mol^{-1}) for the dissociation of one molecule of AuCl from L-AuCl and L-(AuCl)$_2$ [74]

Molecule	q_C	Occ(σ)	Occ(π)	PA-1	PA-2	BDE-1	BDE-2
19	−0.160	1.377	0.735	290.2	124.9	89.5	41.8
20	−0.368	1.436	0.799	310.5	161.8	98.5	48.4
1b	−1.419	1.442	1.163	279.5	160.4	72.0	62.3
4b	−0.499	1.347	1.146	287.4	169.8	72.2	50.8

as a 3c-2e π-donor orbital [31, 74]. The bis-ylide substituted carbene exhibit different resonance forms (Scheme 9b) out of which **A** and **C** better describe the π-donating ability of the central carbon atom. Further, the calculated natural charges at the carbenic carbon indicate an increase in electron density at C_c as a result of ylide substitution and these values are found to be comparable to CDCs (Table 7). While the occupancies of the σ-symmetric lone pair orbital of both C(II) and C(0) compounds are comparable, those for the π-symmetric molecular orbital (MO) are found to be lower in carbenes than in carbones. This can be explained by the fact that the occupied π-symmetric MO of carbones represents a lone pair while it represents the 3c-2e delocalized MO for carbenes. Interestingly, the calculated first and second PAs as well as BDEs for gem-dimetallation of these ylide substituted carbenes are very high and comparable to those for typical carbones like **1b** and **4b**, etc. Therefore, both carbones and carbenes with strong π-donating substituents may show similar reactivity towards electrophiles such as H$^+$ and AuCl. However, unlike carbones, carbenes were found to be more prone to nucleophilic attack due to the presence of a suitable low-lying π^* orbital. Interestingly, reactions of **19** and **20** with a nucleophile (CNMe) were found to be exergonic while the same turned out to be significantly endergonic for C(NHC)$_2$. Indeed, addition of the nucleophile CNMe to C(PMe$_3$)$_2$ leads to a broken geometry undergoing P-C bond cleavage giving rise to a phosphinocarbene adduct and a free PMe$_3$ molecule. Further, in order to determine the difference in energy barrier for the formation of nucleophilic adduct of C(0) and C(II) compounds, we located the transition states for some typical carbenes like normal NHC (TS1, Fig. 4) and abnormal NHC (TS2) as well as for CDCs (TS3 and TS4). Interestingly, the energy barriers are found to be smaller for carbenes compared to those for carbones (Fig. 4). Thus, the presence or absence of a low-lying π-acceptor orbital is a key electronic feature which may distinguish a carbene from carbone. The presence or absence of π accepting ability has an implication on their reactivity towards nucleophiles. Although both carbenes and carbones may show similar reactivity towards electrophiles, they behave differently when subjected to nucleophilic attack.

6.3 ^{13}C NMR Spectroscopy

In addition to the above mentioned reactivity parameter, we have recently proposed the use of ^{13}C NMR spectroscopy as a tool to distinguish different divalent carbon
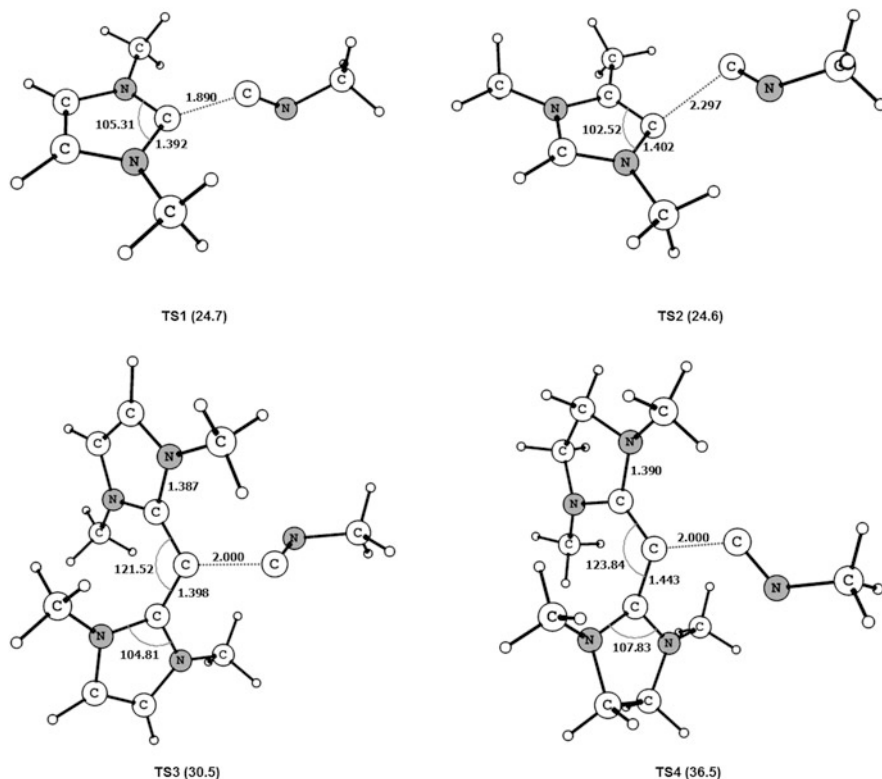
Fig. 4 Optimized (BP86/TZVP) geometries of the transition states for the addition of CH$_3$CN to NHC (TS1), abnormal NHC (TS2) and CDCs (TS3 and TS4). Bond lengths and angles are in Å and degrees, respectively. The respective activation energies (E$_A$ in kcal mol^{-1}) are given within parenthesis [74]

bases (Scheme 10) [75]. As we know, carbones possess an extra lone pair of electron than carbenes and accordingly, there is a larger concentration of electron density at the central carbon atom of carbone than at carbenes. As a result, the ^{13}C NMR chemical shifts (δ^{13}C) of carbenes are expected to be more downfield compared to those of carbones. The calculated values of δ^{13}C are in reasonable agreement with the available experimental data (Table 8). As expected, the δ^{13}C values for the C(II) compounds are computed to be larger than those for C(0) ones (Table 8). However, the δ^{13}C values for the carbon bases with hidden carbon(0) character (e.g. ylide substituted carbenes) fall between those of typical carbenes and carbones. Interestingly, the calculated δ^{13}C value for **30** which may be thought to show the properties of C(0) compounds is found to be significantly larger compared to other C(0) compounds. This discrepancy can be explained by the dominant contribution of the resonance form **30A** (Scheme 11) in describing its reactivity thereby clearly establishing its carbene characteristics. Thus, the calculated ^{13}C NMR shift values of these divalent carbon bases can be used to distinguish these two classes of
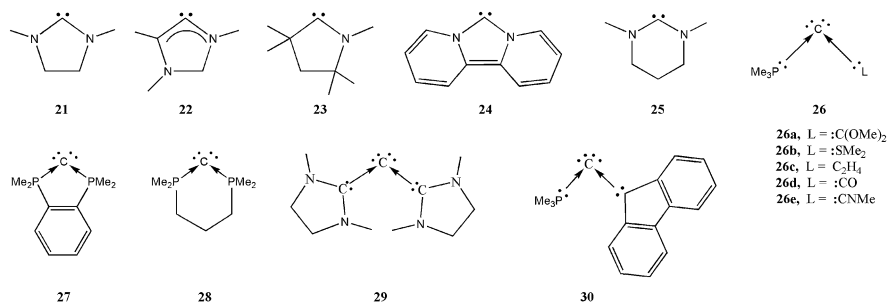
Scheme 10 Schematic representation of different C(II) and C(0) bases [75]

Table 8 Calculated (PBE0/6-311++G*//PBE0/6-31+G*) values of ^{13}C chemical shifts ($\delta^{13}C$) of different carbenes and carbones

Molecule	$\delta^{13}C$	Molecule	$\delta^{13}C$
1b	18.1	**25**	231.9 (242.7)
2b	214.9 (215.2)	**26a**	72.7
3b	20.5	**26b**	40.1
4b	107.3 (110.2)	**26c**	13.3
11a	163.0 (136.0)	**26d**	−3.4
19	218.4	**26e**	29.8
20	208.9	**27**	21.9
21	236.1 (239.8)	**28**	14.5
22	196.4	**29**	124.4
23	314.5 (304.2)	**30**	197.4 (198.8)
24	200.3 (196.4)		

Experimental values are given within parenthesis [75]
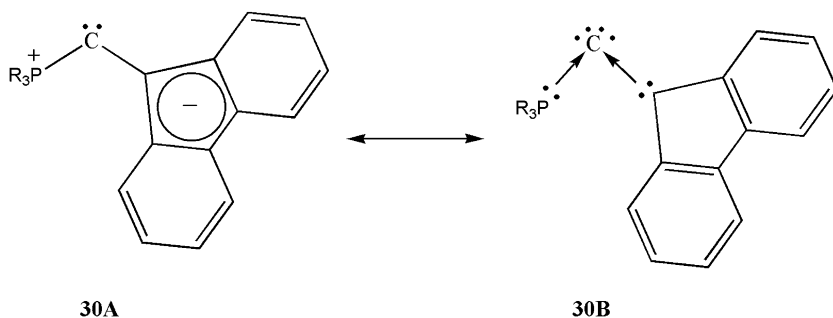
Scheme 11 Resonance forms of **30** showing the carbene (**30A**) and carbone (**30B**) characteristics [75]

compounds. Further, the $\delta^{13}C$ values follow a similar trend for the protonated derivatives as well. As shown in Scheme 12, carbene has a single lone pair of electrons at C_c which after donation to a proton becomes electron deficient. However, the central carbon atom of carbone still has a non-bonding pair of electrons
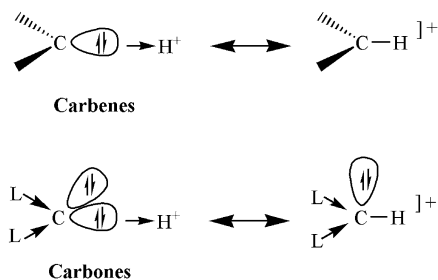
Scheme 12 Bonding situation in the protonated derivatives of carbenes and carbones [75]
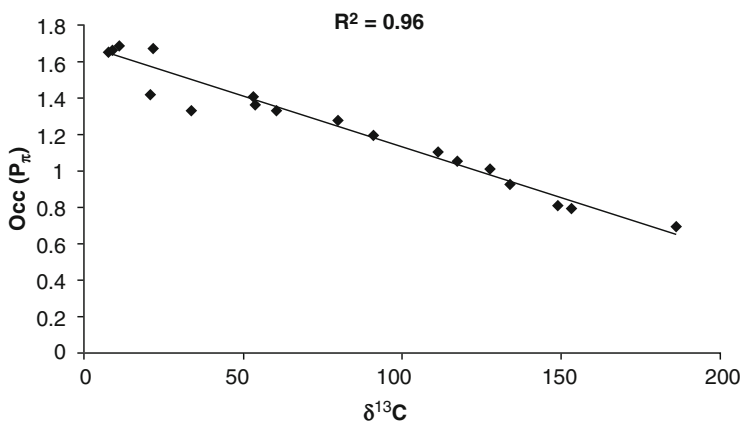
Fig. 5 Correlation plot between $\delta^{13}C$ and out-of-plane p_π occupancy at the central carbon atom of the protonated derivatives [75]

even after single protonation and accordingly, the ^{13}C shifts are significantly upfield for carbones than carbenes. Similar to the case with parent molecules, the C_c of the protonated forms of the hidden C(0) compounds also experiences a lesser downfield shift than the C(II) ones. Indeed, we obtained an excellent correlation between the out-of-plane p_π occupancy at the central carbon atom and $\delta^{13}C$ values (Fig. 5). Thus, this spectroscopic approach can be considered as an effective tool to distinguish different carbon bases.

7 Ylide Stabilized Carbenes

In addition to the above discussed divalent C(0) compounds, ylide moieties were found to stabilize divalent C(II) compounds too [33–36]. Inspired by the seminal works of Kawashima [33] and Fürstner [35], in 2015, we carried out a systematic theoretical study towards designing a number of mono- and bis-ylide substituted

carbenes (**31–46**, Scheme 13) [31]. Interestingly, majority of the ylide substituted cyclic carbenes possess comparable thermodynamic stabilities with those of the experimentally known ones as evident from the calculated singlet–triplet separation and stabilization energy values. Further, evaluation of the energies of the σ-symmetric donor orbitals suggested that ylide substitution significantly enhances the electron donation ability and this effect is found to be additive in nature (i.e. the bis-ylide substituted carbenes are better donors than the mono-ylidic ones; Table 9). The stability of the ylide substituted carbenes can be attributed to effective π-donation from the ylide carbanion to the adjacent carbene centre while the enhanced σ-donation ability results from a smaller inductive effect of the ylide groups relative to the amino group present in normal NHCs. The better electron donation ability of the ylide substituted carbenes was further corroborated by the calculated proton affinities (PAs) as well as the average carbonyl stretching frequencies (ν_{CO}) in the respective metal complexes. Interestingly, the calculated PAs for the bis-ylide substituted carbenes were found to be significantly high (>300 kcal mol^{-1}) which is in agreement with their excellent electron donation abilities. In fact, we obtained good correlation between the energies of the σ-donor orbitals (E_σ) and PAs as well as E_σ vs. ν_{CO} values (Fig. 6). Recently, it was proposed that the basicity of a carbene ligand may be correlated with the degree of gallium pyramidalization (θ_{Ga}; $\theta_{Ga} = 360° - \Sigma(\text{Cl-Ga-Cl})$) in the corresponding GaCl$_3$ adducts [76]. Gratifyingly, the extent of gallium pyramidalization (θ_{Ga}) for all these ylide stabilized carbenes (**31–46**) was found to correlate well with the respective nucleophilicity index (N) values. Furthermore, we obtained a nice correlation between the Ga-C$_c$ BDEs and bond lengths (Fig. 7). With an intent to understand the ability of ylide stabilized carbenes towards small molecule activation, very recently we designed a variety of

31; X = CH$_2$, Y = C(CH$_3$)$_2$
32; X = Y = CH
33; X = N, Y = CH
34; X = CH, Y = N

35; X = CH$_2$, Y = C(CH$_3$)$_2$
36; X = Y = CH
37; X = N, Y = CH

38; X = CH$_2$, Y = C(CH$_3$)$_2$
39; X = Y = CH
40; X = N, Y = CH

41; X = NMe
42; X = C(PMe$_3$)

43; X = NMe
44; X = C(PMe$_3$)

45; X = NMe
46; X = C(PMe$_3$)
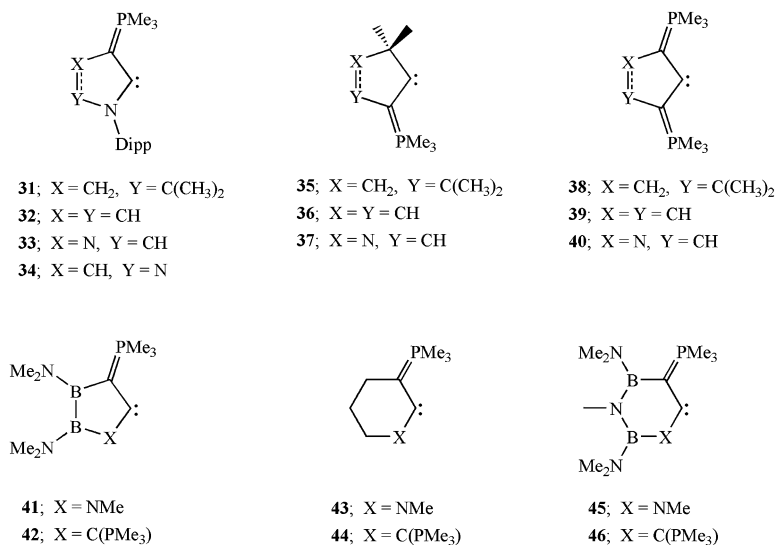
Scheme 13 Schematic representation of ylide substituted carbenes **31–46**

Table 9 Calculated (PBE0/6-31+G*, SDD (Rh)) values of energies of the σ-donor orbitals (E_σ, in eV), proton affinities (PA, in kcal mol^{-1}) and average carbonyl stretching frequencies (ν_{CO}, in cm^{-1}) in L-Rh(CO)$_2$Cl (L: **31–46**) complexes [31]

Molecule	E_σ	PA	ν_{CO}
31	−4.8	291.8	2,120
32	−5.0	292.9	2,125
33	−5.2	287.4	2,129
34	−5.3	284	2,131
35	−4.5	295	2,122
36	−4.6	294.5	2,123
37	−4.9	285.9	2,129
38	−4.1	308.3	2,112
39	−4.0	313.1	2,112
40	−4.2	308.4	2,112
41	−4.4	297.9	2,122
42	−3.5	311.2	2,110
43	−4.3	293.2	2,122
44	−3.9	309.4	2,110
45	−4.3	294.7	2,120
46	−3.8	307.8	2,101
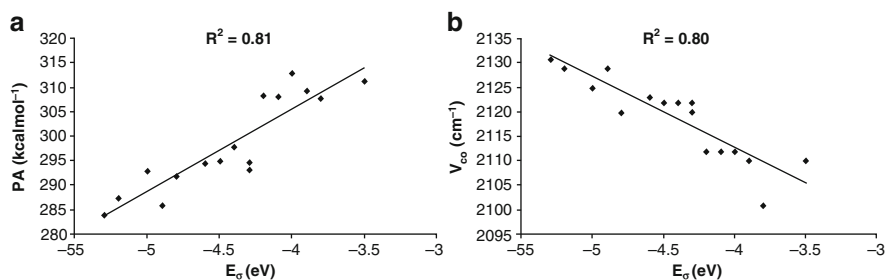
Fig. 6 Correlation plots between the energies of the σ-donor orbitals (E_σ) and (**a**) proton affinities and (**b**) carbonyl stretching frequencies (ν_{CO}) for **31–46** [31]

cyclic carbenes where ylide substitution was combined with boron or silicon centres (**47–55**, Scheme 14) [77]. As expected, here also, ylide substitution leads to increase in stability as well as substantial enhancement of σ-donation abilities which may be attributed to the reasons explained earlier. The calculated PA and the nucleophilicity index values (Table 10) were found to be in excellent agreement with the respective electron donation ability of the carbenes. Further support for the increased σ-donation ability of the ylide substituted carbenes came from the degree of gallium pyramidalization (θ_{Ga}) as well as the BDEs of the Ga-C$_c$ bonds in the corresponding GaCl$_3$ adducts which were found to correlate well with the energies of the σ-donor orbitals. It may be noted that while ylide substitution significantly enhances the σ-donation ability of a particular carbene, at the same time it decreases the
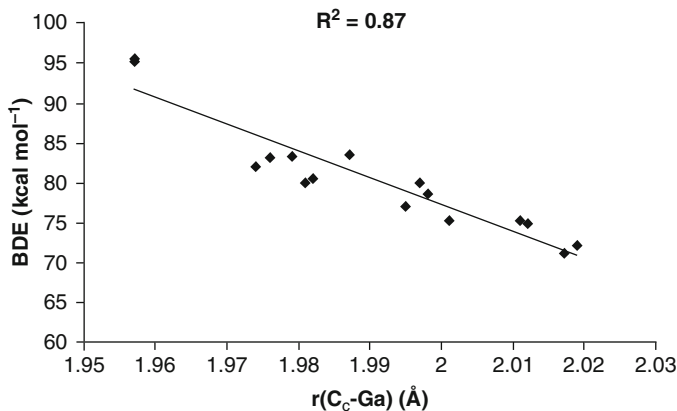
Fig. 7 Correlation plot between the Ga-C_c bond dissociation energies (BDEs, in kcal mol^{-1}) and the Ga-C_c bond lengths (in Å) of the GaCl$_3$ adducts of **31–46** [31]
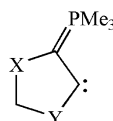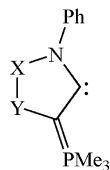
47; X = C(CH$_3$)$_2$, Y = CH$_2$	**52**; X = Y = C(CH$_3$)$_2$
48; X = C(CH$_3$)$_2$, Y = B(NMe$_2$)	**53**; X = C(CH$_3$)$_2$, Y = Si(CH$_3$)$_2$
49; X = B(NMe$_2$), Y = CH$_2$	**54**; X = B(NMe$_2$), Y = C(CH$_3$)$_2$
50; X = C(CH$_3$)$_2$, Y = Si(CH$_3$)$_2$	**55**; X = Si(CH$_3$)$_2$, Y = C(CH$_3$)$_2$
51: X = Si(CH$_3$)$_2$, Y = CH$_2$	

Scheme 14 Schematic representation of ylide substituted carbenes **47–55**

π-acceptance ability of the same as evident from the calculated higher energies of the π-accepting orbitals of **47–55** (Table 10). However, in order to activate enthalpically strong bonds such as H–H, C–H, N–H, etc., a given carbene should not only possess strong electron donation ability but it should also have substantial π-accepting ability [27]. Accordingly, **47–55** were found to be ineffective towards activation of small molecules like H$_2$ and NH$_3$. Interestingly, it was found that the transition states characterized for the activation of H$_2$ by considering **47**, **52** and **53** as representative molecules were quite different from those using ambiphilic carbenes such as CAAC (Fig. 8a). It is clear from Fig. 8a that while the positively polarized hydrogen atom (H$^{\delta+}$) of dihydrogen interacts effectively with the lone pair orbital of C_c, the hydridic one (H$^{\delta-}$) was found to be far away from the formally vacant p$_\pi$ orbital of C_c in case of **47**, **52** and **53**. The inability of H$^{\delta-}$ to interact efficiently with C_c is attributed to the absence of a suitable low-lying p$_\pi$-acceptor orbital at C_c. In addition, the reaction free energies for splitting of H$_2$ by **47**, **52** and **53** (−20.45, −34.52 and

Table 10 Calculated (M06/Def2-TZVP) energies of σ-symmetric lone pair orbital (E_σ in eV) and π-symmetric unoccupied orbital ($E_{\pi*}$ in eV), proton affinities (PA in kcal mol^{-1}), nucleophilicity indices (N in eV), degree of pyramidalization at the gallium atom (θ_{Ga} in degree) and BDEs of the Ga-C$_c$ Bond (kcal mol^{-1}) of **47–55** [77]

Molecule	E_σ	$E_{\pi*}$	PA	N	θ_{Ga}	BDE
47	−4.91	0.26	289.1	4.79	32.53	65.00
48	−4.66	0.20	291.6	5.04	33.76	62.63
49	−4.78	0.41	292.9	4.92	34.54	64.44
50	−4.68	0.21	288.8	5.02	35.72	60.25
51	−4.90	0.22	289.0	4.80	34.75	60.15
52	−4.69	0.42	290.9	5.01	36.40	67.03
53	−4.70	0.02	287.5	5.00	33.76	64.90
54	−4.43	0.21	294.6	5.27	35.06	67.54
55	−4.44	0.21	292.7	5.26	35.86	65.85
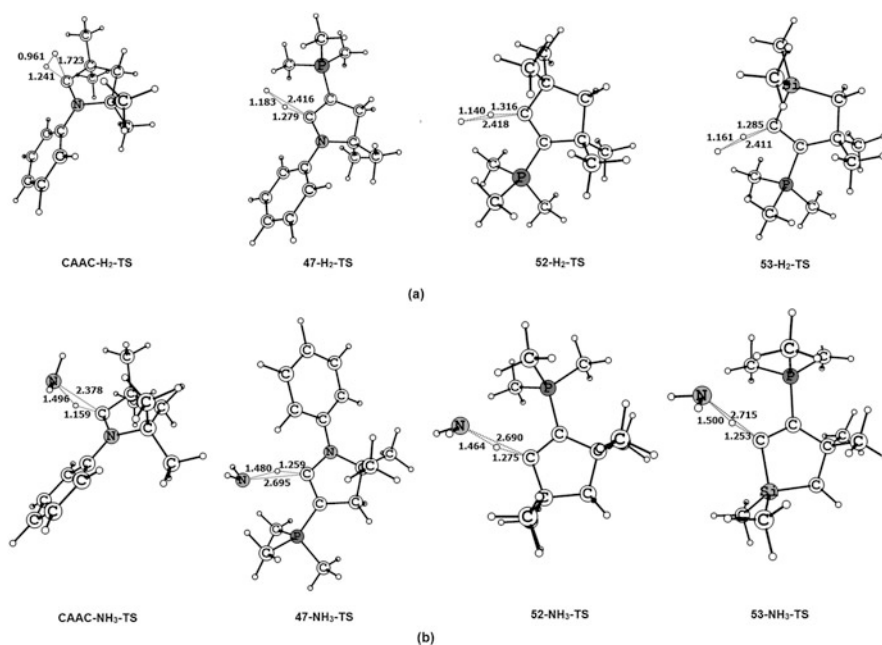
Fig. 8 Optimized (M06/Def2-TZVP) geometries of the transition states for activation of dihydrogen and ammonia by **CAAC** and **47**, **52** and **53** [77]

−32.22 kcal mol^{-1}, respectively) were also found to be significantly less exergonic compared to those using the ambiphilic ones (e.g. −44.2 kcal mol^{-1} for **CAAC**). Similar results were obtained for the activation of NH$_3$ using **47**, **52** and **53** where the interaction between the NH$_2{}^{\delta-}$ fragment and C$_c$ (Fig. 8b) is not strong enough to cleave the N-H bond due to the absence of a low-lying π-acceptor orbital at C$_c$.

8 Summary

This chapter provides a comprehensive overview of the theoretical works on carbones as well as on ylide stabilized carbenes. The primary difference between C(II) and C(0) comes from the difference in bonding between the central carbon atom and the α-substituents, as a result of which carbones possess an extra lone pair of electrons than carbenes. Theoretical studies reveal that the calculated first and second proton affinity values as well as complexation with AuCl may be used to distinguish carbenes from carbones. In addition, carbene and carbones can also be distinguished by considering their reactivity towards nucleophiles as well as their ^{13}C NMR chemical shifts. This chapter also deals with the recent studies carried out on ylide stabilized carbenes which possess excellent electron donation abilities. However, the ylide substituted carbenes are found to be ineffective towards activation of small molecules like H_2 and NH_3 due to the absence of a suitable low-lying π-acceptor orbital at the carbene centre.

References

1. Igau A, Grutzmacher H, Baceiredo A, Bertrand G (1988) J Am Chem Soc 110:6463
2. Arduengo III AJ, Harlow RL, Kline M (1991) J Am Chem Soc 113:361
3. Moss RA, Jones Jr M (1978) Reactive intermediates, vol 1. Wiley, New York, p 69
4. Jones Jr M, Moss RA (eds) (1973) Carbenes, vol 1. Wiley, New York, p 153
5. Jones Jr M, Moss RA (eds) (1975) Carbenes, vol 2. Wiley, New York, p 101
6. Jones Jr M, Moss RA (eds) (2004) Reactive intermediate chemistry. Wiley-Interscience, Hoboken
7. Arduengo III AJ, Goerlich JR, Marshall WJ (1997) Liebigs Ann 2:365
8. Martin D, Baceiredo A, Gornitzka H, Schoeller WW, Bertrand G (2005) Angew Chem Int Ed 44:1700
9. Lavallo V, Canac Y, Präsang C, Donnadieu B, Bertrand G (2005) Angew Chem Int Ed 44:5705
10. Lavallo V, Canac Y, DeHope A, Donnadieu B, Bertrand G (2005) Angew Chem Int Ed 44:7236
11. Soleilhavoup M, Bertrand G (2015) Acc Chem Res 48:256
12. Präsang C, Donnadieu B, Bertrand G (2005) J Am Chem Soc 127:10182
13. Krahulic KE, Enright GD, Parvez M, Roesler R (2005) J Am Chem Soc 127:4142
14. Iglesias M, Beetstra DJ, Knight JC, Ooi L, Stasch A, Coles S, Male L, Hursthouse MB, Cavel KJ, Dervisi A, Fallis IA (2008) Organometallics 27:3279
15. Boehme C, Frenking G (1996) J Am Chem Soc 118:2039
16. Tukov AA, Normand AT, Nechaev MS (2009) Dalton Trans:7015
17. Bazinet P, Yap GAP, Richeson DS (2003) J Am Chem Soc 125:13314
18. Kuhn N, Al-Sheikh A (2005) Coord Chem Rev 249:829
19. Nair V, Bindu S, Sreekumar V (2004) Angew Chem Int Ed 43:5130
20. Alcarazo M, Stork T, Anoop A, Thiel W, Fürstner A (2010) Angew Chem Int Ed 49:2542
21. Seo H, Roberts BP, Abboud KA, Merz KM, Hong S (2010) Org Lett 12:4860
22. Hudnall TW, Bielawski CW (2009) J Am Chem Soc 131:16039
23. Tonner R, Heydenrych G, Frenking G (2007) Chem Asian J 2:1555
24. Jacobsen H, Correa A, Poater A, Costabile C, Cavallo L (2009) Coord Chem Rev 253:687
25. Lavallo V, Frey GD, Kousar S, Donnadieu B, Bertrand G (2007) Proc Natl Acad Sci U S A 104:13569

26. Chu J, Munz D, Jazzar R, Melaimi M, Bertrand G (2016) J Am Chem Soc 138:7884
27. Frey G, Lavallo V, Donnadieu B, Schoeller WW, Bertrand G (2007) Science 316:439
28. Masuda JD, Schoeller WW, Donnadieu B, Bertrand G (2007) Angew Chem Int Ed 46:7052
29. Back O, Kuchenbeiser G, Donnadieu B, Bertrand G (2009) Angew Chem Int Ed 48:5530
30. Lavallo V, Canac Y, Donnadieu B, Schoeller WW, Bertrand G (2006) Angew Chem Int Ed 45:3488
31. Borthakur B, Phukan AK (2015) Chem Eur J 21:11603
32. Borthakur B, Silvi B, Dewhurst RD, Phukan AK (2016) J Comput Chem 37:1484
33. Nakafuji S, Kobayashi J, Kawashima T (2008) Angew Chem Int Ed 47:1141
34. Asay M, Donnadieu B, Baceiredo A, Soleilhavoup M, Bertrand G (2008) Inorg Chem 47:3949
35. Fürstner A, Alcarazo M, Radkowski K, Lehmann CW (2008) Angew Chem Int Ed 47:8302
36. Kobayashi J, Nakafuji S, Yatabe A, Kawashima T (2008) Chem Commun:6233
37. Frenking G, Hermann M, Andrada DM, Holzmann N (2016) Chem Soc Rev 45:1129
38. Zhao L, Hermann M, Holzmann N, Frenking G (2017) Coord Chem Rev 344:163
39. Frenking G, Tonner R (2009) Pure Appl Chem 81:597
40. Ramirez F, Desai NB, Hansen B, McKelvie N (1961) J Am Chem Soc 83:3539
41. Tonner R, Öxler F, Neumüller B, Petz W, Frenking G (2006) Angew Chem Int Ed 45:8038
42. Tonner R, Frenking G (2008) Chem Eur J 14:3260
43. Quinlivan PJ, Parkin G (2017) Inorg Chem 56:5493
44. Tonner R, Heydenrych G, Frenking G (2008) ChemPhysChem 9:1474
45. Deshmukh MM, Gadre SR, Tonner R, Frenking G (2008) Phys Chem Chem Phys 10:2298
46. Petz W, Öxler F, Neumüller B, Tonner R, Frenking G (2009) Eur J Inorg Chem:4507
47. Marrot S, Kato T, Gornitzka H, Baceiredo A (2006) Angew Chem Int Ed 45:2598
48. Tonner R, Frenking G (2007) Angew Chem Int Ed 46:8695
49. Dyker CA, Lavallo V, Donnadieu B, Bertrand G (2008) Angew Chem Int Ed 47:3206
50. Fürstner A, Alcarazo M, Goddard R, Lehmann CW (2008) Angew Chem Int Ed 47:3210
51. Frenking G, Tonner R (2011) WIREs Comput Mol Sci 1:869
52. Tonner R, Frenking G (2008) Chem Commun 13:1584
53. Liberman-Martin AL, Grubbs RH (2017) Organometallics 36:4091
54. Pranckevicius C, Fan L, Stephan DW (2015) J Am Chem Soc 137:5582
55. Hsu YC, Shen JS, Lin BC, Chen WC, Chan YT, Ching WM, Yap GPA, Hsu CP, Ong TG (2015) Angew Chem Int Ed 54:2420
56. Goldfogel MJ, Roberts CC, Meek SJ (2014) J Am Chem Soc 136:6227
57. Roberts CC, Matías DM, Goldfogel MJ, Meek SJ (2015) J Am Chem Soc 137:6488
58. Chen WC, Shen JS, Jurca T, Peng CJ, Lin YH, Wang YP, Shih WC, Yap GPA, Ong TG (2015) Angew Chem Int Ed 54:15207
59. Chen WC, Shih WC, Jurca T, Zhao L, Andrada DM, Peng CJ, Chang CC, Liu SK, Wang YP, Wen YS, Yap GPA, Hsu CP, Frenking G, Ong TG (2017) J Am Chem Soc 139:12830
60. Phukan AK, Guha AK (2012) Dalton Trans 41:8973
61. Guha AK, Konwar B, Sarmah S, Phukan AK (2012) Theor Chem Accounts 131:1134
62. Bader RWF (1990) Atoms in molecules: a quantum theory. Oxford University Press, Oxford
63. Bader RFW (1991) Chem Rev 91:893
64. Cremer D, Kraka E (1984) Angew Chem Int Ed 23:627
65. Patel DS, Bharatam PV (2011) J Org Chem 76:2558
66. Lavallo V, Dyker CA, Donnadieu B, Bertrand G (2008) Angew Chem Int Ed 47:5411
67. Melaimi M, Parameswaran P, Donnadieu B, Frenking G, Bertrand G (2009) Angew Chem Int Ed 48:4792
68. Weiss R, Reichel S, Handke M, Hampel F (1998) Angew Chem Int Ed 37:344
69. Guha AK, Phukan AK (2012) Chem Eur J 18:4419
70. Klein S, Frenking G (2010) Angew Chem Int Ed 49:7106
71. Tonner R, Frenking G (2008) Chem Eur J 14:3273
72. Esterhuysen C, Frenking G (2011) Chem Eur J 17:9944
73. Vicente J, Singhal AR, Jones PG (2002) Organometallics 21:5887

74. Guha AK, Gogoi U, Phukan AK (2013) Int J Quantum Chem 113:2471
75. Guha AK, Borthakur B, Phukan AK (2015) J Org Chem 80:7301
76. El-Hellani A, Monot J, Tang S, Guillot R, Bour C, Gandon V (2013) Inorg Chem 52:11493
77. Bharadwaz P, Chetia P, Phukan AK (2017) Chem Eur J 23:9926

Synthesis, Structure, and Reactivity of Carbodiphosphoranes, Carbodicarbenes, and Related Species

Manuel Alcarazo

Abstract The unique electronic distribution in carbodiphosphoranes has attracted the attention of chemists early since their first isolation. These molecules can be seen as two simultaneous ylide functionalities localized at the same carbon atom; thus, their central carbon possesses two perpendicular electron pairs available for coordination. Recent theoretical studies point that the bonding situation in these compounds is best described using a captodative model; that means, in terms of donor acceptor interactions $L \rightarrow \overline{\underline{C}} \leftarrow L$. Hence, carbodiphosphoranes can be seen as C(0) atoms stabilized by two flanking phosphines. Although not always free of controversy, the fact is that this analysis is extremely useful to predict and understand the reactivity of carbodiphosphoranes of different structure as well as that of analogous molecules such as carbodicarbenes, carbon suboxide, and mixed systems. This chapter reviews theoretical and experimental research on carbodiphosphoranes $C(PR_3)_2$ and related compounds of formula $C(L)_2$ as both, free molecules and ligands in transition metal or main group coordination complexes. Special emphasis will be given to highlight the unique reactivity derived from localizing two electron pairs at the same carbon atom.

Contents

M. Alcarazo (✉)
Institut für Organische und Biomolekulare Chemie, Georg-August-Universität Göttingen, Göttingen, Germany
e-mail: manuel.alcarazo@chemie.uni-goettingen.de

1   Introduction: The Electronic Structure of Carbodiphosphoranes and Related Species

In 1961, Ramírez succeeded in synthesizing the first ever isolated carbodiphosphorane $(Ph_3P)_2C$ (**1**) as a yellow crystalline solid, which is indefinitely stable when kept under Ar atmosphere [1]. In this seminal paper Ramírez and coworkers described the bonding situation in this compound as a resonance hybrid between structures **1A** (cumulene) and **1B** (bisylide) (Scheme 1). The detailed analysis of resonance structure **1B** is especially instructive; two electron pairs are localized at the central carbon atom. As first recognized by Kaska, this leads to an alternative and very unique description of **1** as a coordinatively unsaturated carbon-based complex **1B′**, in which the carbon atom is in the formal oxidation state of zero and the two flanking phosphine ligands donate electron density to this atom as they would do it to metal centers [2].

This analysis, in conjunction with other unexpected observations such as the strongly bent P–C–P bond angle determined by X-ray (140°) [3], or the observed triboluminescence of **1** [4], immediately attracted the attention of many research groups, who studied their reactivity towards organic reagents and metallic fragments, as well as the influence of structural changes on their electronic properties and reactivity [5–12]. Probably, the most crucial report published in these early times of carbodiphosphorane chemistry was the one of Schmidbaur, in which the first *gem*-dimetallated derivative of a carbodiphosphorane was characterized [7]. The synthesis of **2** was only possible by the intelligent selection of AuCl as a linear, sterically non-demanding metal fragment. Importantly, the isolation of that compound
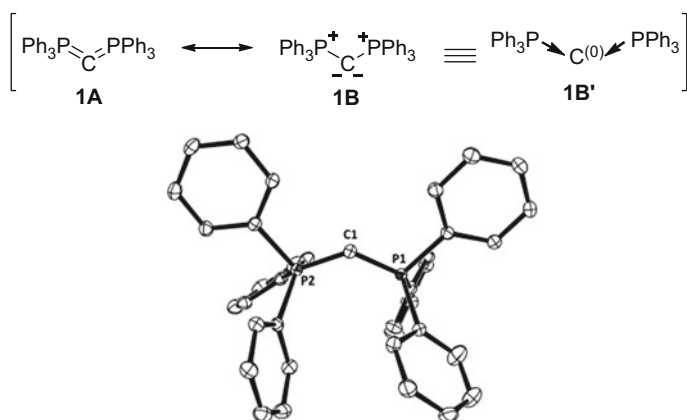
Scheme 1 (*Top*) Conceivable resonance structures of **1**. Compound **1** can also be described using a captodative model. Thus, **1** is also a biphosphine carbon(0) complex. (*Bottom*) Molecular structure of **1**

highlighted for the first time the weight of resonance form **1B** on the electronic structure of carbodiphosphoranes, since it is the only resonance structure able to adequately explain this reactivity. In 2002, Vicente and coworkers were able to obtain the first X-ray structure of a *gem*-diaurated derivative of **1**, compound **3** (Fig. 1) [13].

The next breakthrough in carbodiphosphorane chemistry came from the Frenking group shortly after Vicente's publication. In a series of papers orientated to unveil the true electronic distribution in **1**, they carried out in-depth computational analyses, in which Kaska's original hypothesis was validated [14–16]. Frenking and coworkers concluded from these studies that carbodiphosphoranes should be better described as consisting of two phosphine ancillary ligands coordinated to a central zero-valent carbon atom. Two orthogonal lone pairs available for coordination, one of σ-symmetry and the other depicting a strong π-character correspond to the HOMO-1 and HOMO orbitals, being both mainly localized at the zero-valent carbon atom (Fig. 2). This analysis explains the cumulus of experimental evidences collected to date; namely, the already mentioned highly bent structure of carbodiphosphoranes, their excellent donor properties and their ability to bind up to two transition metals at the central carbon. Moreover, through the calculation of the first and second proton affinity, these authors offered for the first time a tool to quantify the C(0) character of different species, which is fundamental to compare and predict their reactivities.

Soon after these theoretical studies were published, carbodiphosphorane chemistry underwent a renaissance. Keeping in mind the captodative formalism already described, it was only a small step to recognize that the substitution of the flanking phosphines by other commonly used ligands such as carbon monoxide, isonitriles, or *N*-heterocyclic carbenes should lead to new types of "carbon complexes" (carbones following the nomenclature proposed by Frenking). The answer to this query incited the reinvestigation of several already known compounds and the synthesis of new ones. For example, Fürstner revisited cumulenes **4–6** and demonstrated that **6** could be diaurated and therefore it has C(0) character; however in **4** and **5**, the π-acceptor character of the flanking CO or isonitrile ligands favors the delocalization of the original π-electron pair at carbon onto these groups and hampers the coordination of a second metal center. Remarkably, the divergent reactivity of the cumulenes studied, which puts clear borders to what can be considered a C(0) compound, could still be interpreted using a captodative bonding model (Scheme 2) [17].

Fig. 1 (*Left*) Diaurated complexes **2** and **3** and (*right*) X-ray structure of **3**
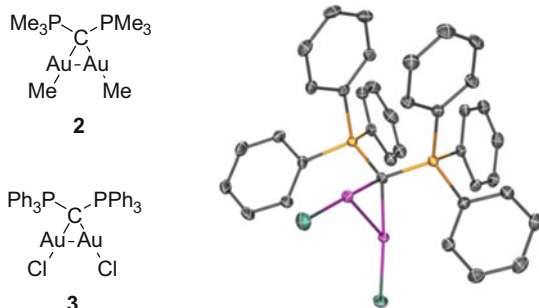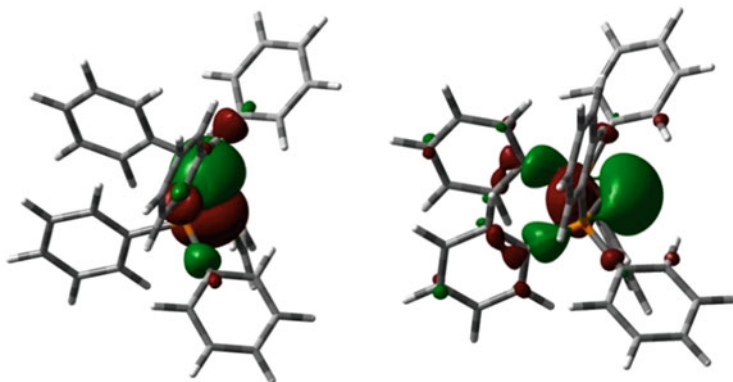
Fig. 2 Frontier molecular orbitals in hexaphenylcarbodiphosphorane **1** (HOMO, *left*; HOMO-1, *right*)

Simultaneously to this study one or even both flanking phosphines were formally exchanged by prototypical poor π-acceptor ligands that were not available at the time the first carbodiphosphorane was prepared: *N*-heterocyclic carbenes (NHC). Thus, the concept was extended to "carbophosphinocarbenes" **10** and "carbodicarbenes" **11–12**, demonstrating the scope of the bonding model developed (Scheme 3) [18–23]. It is worth mentioning that dimetallation of carbodicarbenes has proved to be a difficult task, probably due to the steric requirements imposed by the short C(0)-C (NHC) bond (double protonation of these species is much easier); however, the differences between carbodicarbenes and typical allenes are obvious already after monometallation: carbodicarbenes bind the metal in η^1 fashion, whereas allenes prefer to coordinate metals along the π-system in a η^2 mode [24, 25].

Taken together all experimental evidence accumulated during the past years, the defining characteristics of carbon(0) species can be resumed as follows:

– All these compounds show strongly bent L–C–L angle which deviates substantially from $180°$, the one expected for typical allenes.
– Moreover, their valence electrons are teamed up in the form of two electron pairs mainly localized at the carbon(0) atom, which depict strong Lewis base character. Both pairs should be available for coordination or at least for protonation. This can be verified theoretically by high first and second proton affinities (PAs).

Along this chapter a general perspective of the research done in the area will be presented, making a special emphasis on the description of situations in which the particular electronic distribution of the C(0)-center is essential to either isolate elusive species or to explain the reactivity (and catalytic activity) of the resulting system. The detailed theoretical study of the electronic distribution in these compounds and their heavier analogues is not within the scope of this chapter; it has been already discussed along a previous chapter in this same volume ([26–30], in addition, see [13]).
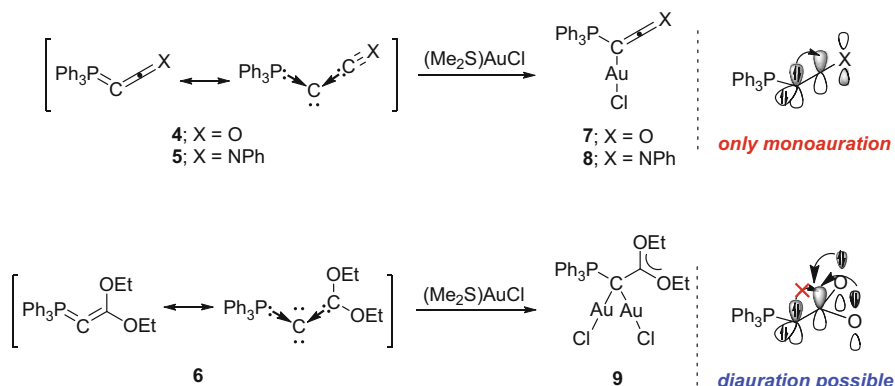
Scheme 2 Influence of the "internal ligand" nature on the coordination properties of cumulenes
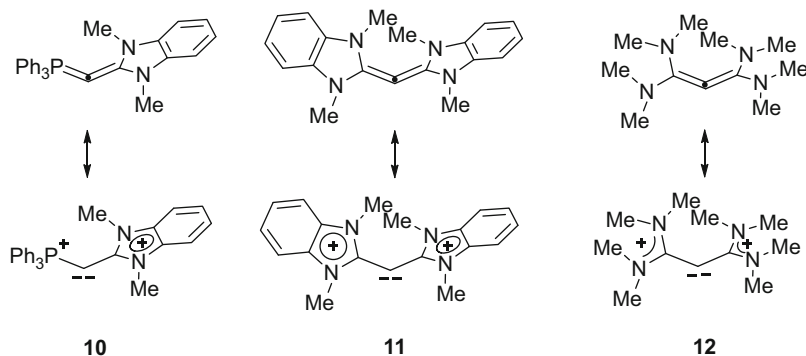
Scheme 3 Selected examples of "carbophosphinocarbenes" and "carbodicarbenes"

2 Synthesis of Carbodiphosphoranes and Carbodicarbenes

Since the publication of the synthesis of **1** a relatively high number of carbodiphosphoranes depicting different substitution patterns have been prepared and some of them even structurally characterized by X-ray diffraction. These compounds can be classified into acyclic and cyclic ones. Acyclic carbodiphosphoranes **13–19**, **21–22** and carbodiarsenane **20** have been mainly prepared following three general methods. In the case of symmetric per-aromatic substituted compounds, Ramírez' synthesis is the most adequate: reaction of dibromo−/diiodomethane with two equivalents of the desired phosphine followed by double deprotonation of the intermediate diphosphonium salt. If the desired carbodiphosphorane is asymmetric such as **14–17** or **22**, the first phosphine can be made to react with excess of CH_2Br_2 to obtain an intermediate bromomethyl-phosphonium salt that later can be condensed with a second phosphine. Finally, alkyl substituted carbodiphosphoranes are more adequately obtained by double alkylation of

methylene-bridged diphosphines and subsequent deprotonation with appropriate bases such as NaNH$_2$ (Fig. 3) [31–37].

Several cyclic carbodiphosphoranes have also been synthesized by Schmidbaur and coworkers **23–25**. Compound **23** was prepared following Ramirez methodology by reaction of 1,2-bis(diphenylphosphanyl)benzene with CH$_2$Br$_2$ followed by deprotonation. Aliphatic derivatives **24** and **25** were prepared by reaction of methylenebis(diphenyl)phosphine with the corresponding 1,*n*-dibromoalkanes (*n* = 2–4) affording the corresponding cyclic diphosphonium salts, which were deprotonated with strong bases (normally (CH$_3$)$_3$P=CH$_2$) to produce the desired carbodiphosphoranes [38–41]. Embedding the carbodiphosphorane moiety into a six- or seven-membered cyclic scaffold does not disturb the natural P–C–P bond angle, making the isolation of these species uncomplicated. However, in five-membered rings the strain introduced in the P–C–P angle is much higher. This is probably the reason why **23** shows considerable thermal lability towards isomerization already at room temperature.

It was not until Baceiredo formally substituted all alkyl/aryl substituents by dialkylamino groups that thermally robust cyclic carbodiphosphorane **29** was isolated and its coordination chemistry studied [42]. The same group has recently extended the concept from P- to S-ylides, being able to isolate and structurally characterize the first C(0) moiety supported by a P,S-bisylide scaffold **32** [43, 44]. Carbon(0) species stabilized by S(II), Se(II), and S(IV) such as **36** have also been recently isolated by Fujii and coworkers (Scheme 4) [45].

As already mentioned in the introduction, an obvious extension to this chemistry consists of the substitution of one or both phosphine termini by NHCs. However, the synthetic routes leading to the preparation of carbodicarbenes and carbophosphinocarbenes differ substantially from those used for carbodiphosphoranes. For example, to avoid side reactions derived
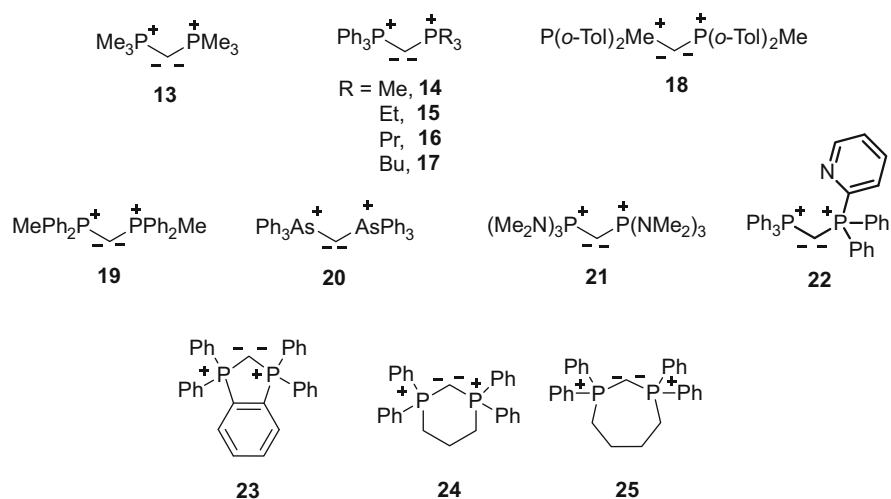
Fig. 3 Prototypical acyclic **13–22** and cyclic **22–26** carbodiphosphoranes and mixed P,S- and S,S-bisylides **27** and **28**

from the higher basicity of *N*-heterocyclic carbenes when compared with phosphines, Bertrand found it more convenient to first prepare the parent methylene-bridged bisimidazole skeleton **37**, which after *N*-alkylation followed by deprotonation afforded the desired carbodicarbene **11** (Scheme 5a) [19]. An alternative and more general route to carbodicarbenes, which also avoids the use of free carbenes, has been subsequently reported by Ong and coworkers. The key step of this synthesis consists of the reaction of a methylthio (imidazolium) salt **39** with either a Wittig ylide or an *N*-heterocyclic olefin to afford the protonated carbone precursor. Simple deprotonation with excess of KN(SiMe$_3$)$_2$ produces the desired carbophosphinocarbene **40** or carbodicarbene **41** species (Scheme 5b) [21, 22].

Bearing in mind the precedents regarding cyclic carbodiphosphoranes and the experimental C=C=C angle in **11** (134.8°), Bertrand and coworkers also attempted with success the synthesis of cyclic carbodicarbenes, which they named bent allenes **44** and **47**. The route used to prepare the first member of this family of compounds is shown in Scheme 6a [46]. Of special interest when analyzing the bonding situation in these compounds are resonance structures **44B** and **47B**, which suggest that bent allenes are potentially four-electron donors. In fact, double protonation of these species at the central carbon is possible [47]. It must be mentioned however that the description of compounds **44**, **47** and analogue as bent allenes has generated controversy; some authors have pointed that the ground state of **44** and related molecules is better described by zwitterionic structure **44C** where the allenic character is residual if any [48, 49].

A similar synthetic route to the one used for the preparation of **44** has been applied with success to obtain the corresponding four-membered analogue structure
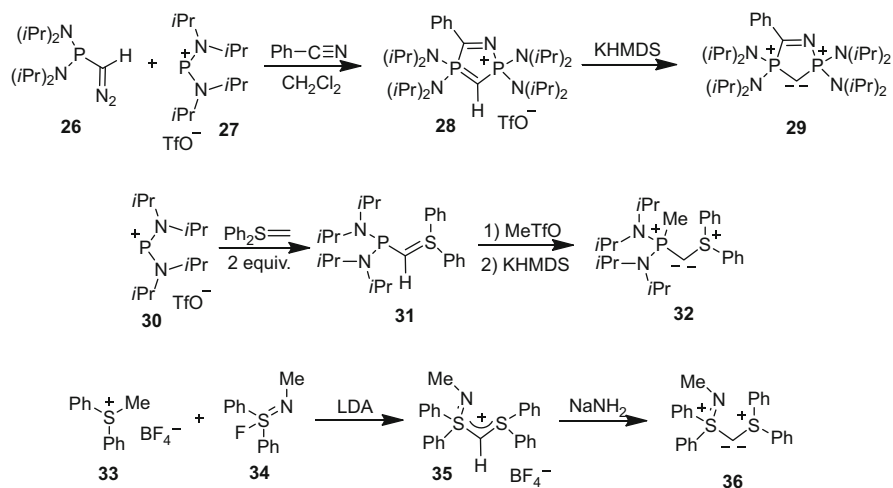
Scheme 4 Prototypical acyclic carbon(0)-containing molecules stabilized by mixed P,P-, P,S-, and S,S-bisylides **29**, **32** and **36**

route a)

route b)

Dipp = 2,6-diisopropylphenyl
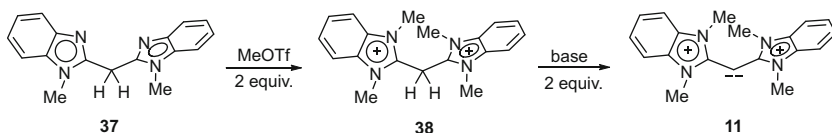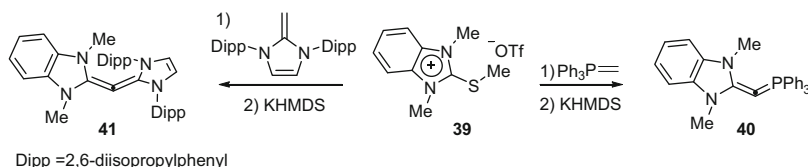
Scheme 5 Prototypical acyclic carbodicarbenes **11**, **41** and carbophosphinocarbenes **40**

a)

b)
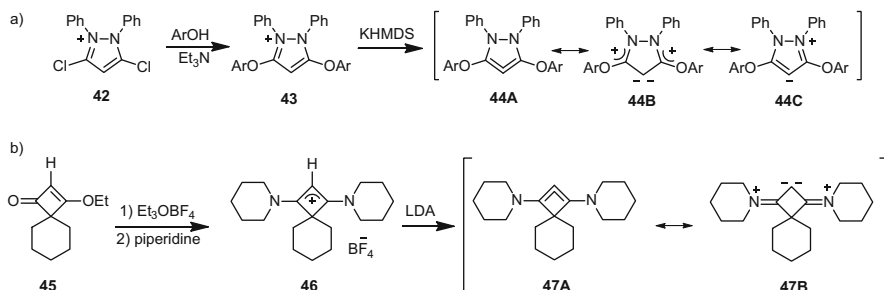
Scheme 6 Synthesis of bent allenes **44** and **47**

47, which could be isolated as a surprisingly thermally stable crystalline material (Scheme 6b) [50].

Very recently, a new breakthrough in carbodicarbene chemistry has been reported through a joint effort of the Bertrand and Stephan groups. These authors designed a carbodicyclopropenylidene system, **49**, which is just a hydrocarbon; yet, its central carbon atom can be protonated twice and forms η^1-complexes with Lewis acids, both typical characteristics of a carbon(0) center [51]. An X-ray structure of **49** is still not available; its geometry, however, has been calculated to be almost linear (Scheme 7).

3 Donor Properties of Carbodiphosphoranes

Although the comparison of the electronic properties among ligands of very different structure and bonding properties using only a single parameter is not always adequate [52], the Tolman electronic parameter (TEP) still remains as the most common method used to compare donor/acceptor abilities [53]. Note,

Scheme 7 Synthesis of carbodicyclopropenylidene **49**
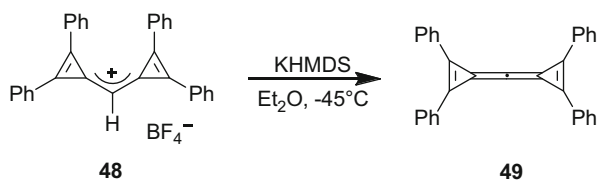
however, that in the case of C(0)-based ligands the situation is even more complex since there are, a priori, two electron pairs that could be used for donation to the metal center. Thus, the TEPs measured will reflect the result of the complete bonding interaction but the discrimination between the relative contributions of the σ- and π- components to the net donation will not be possible. In addition, the available data have been collected using Ni, Mo, and Rh scales, and the IR spectra were not always recorded under identical conditions, making the direct comparison of the data available not always straightforward.

Figure 4 compiles the values for selected [RhCl(CO)$_2$**L**] complexes, by far the largest experimentally available data set. It also includes a series of selected amino (ylide)carbenes **50** and NHCs **51–55** for comparison purposes [54–57]. The obvious conclusion from this figure is that carbodiphosphoranes and carbodicarbenes share the area of the Tolman stereoelectronic map reserved for the strongest donors. They clearly surpass all other known neutral ligands in this regard. Bent allenes are only slightly weaker donor ligands and occupy the second position in the rank followed by NHCs and phosphines (not shown). It is worth also mentioning that the TEP values for carbodiphosphoranes, carbodicarbenes, and many other typical ligands have been theoretically calculated. The values obtained, although different in absolute magnitude to the experimental ones, lead to identical rankings [52, 58].

An alternative methodology to determine the global electron density donated by the ligand has been proposed by Gandon and coworkers employing X-ray diffraction data of **L**GaCl$_3$ complexes instead of spectroscopic ones. They argue that according to Bent's rule, the atomic *s* character in main group elements tends to concentrate in orbitals directed towards electropositive groups, while the *p* character concentrates in orbitals directed towards electronegative atoms [60–62]. Hence, in the model Ga complexes the stronger the donor ligand is, the higher *p* character of the Ga orbitals pointing to the chlorides will be. As a result, for strong donor ligands the pyramidalization of the Ga atom should increase, or what is the same, the sum of the Cl-Ga-Cl angles ($\Sigma_{Cl\text{-}Ga\text{-}Cl}$) should decrease [63]. As can be seen by comparison of Figs. 4 and 5, the data obtained by Gandon's method and those based on IR spectroscopy afford very similar rankings of ligands. The small discrepancies observed are probably due to the influence of crystal packing forces on the conformation of these relatively flexible molecules.
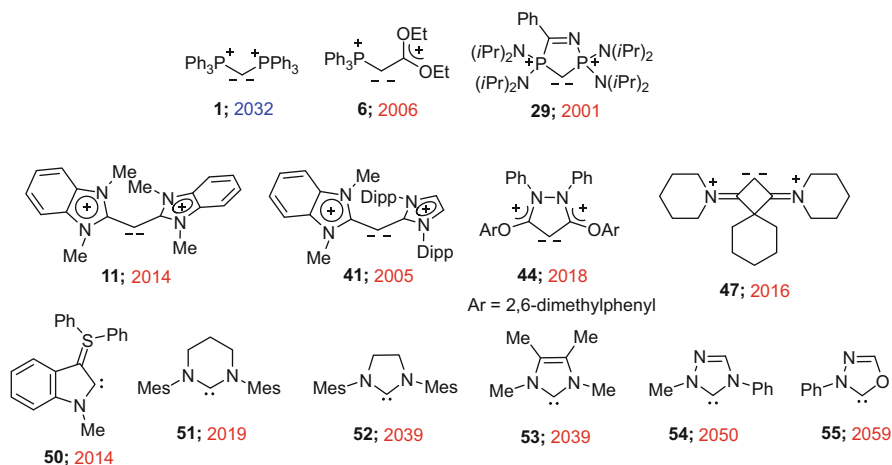
Fig. 4 Average IR frequencies [cm^{-1}] for *cis*-[RhCl(CO)$_2$**L**] complexes. The value depicted for the carbodiphosphorane **1** (blue) is the one of the [Ni(CO)$_3$**L**] complex [59]
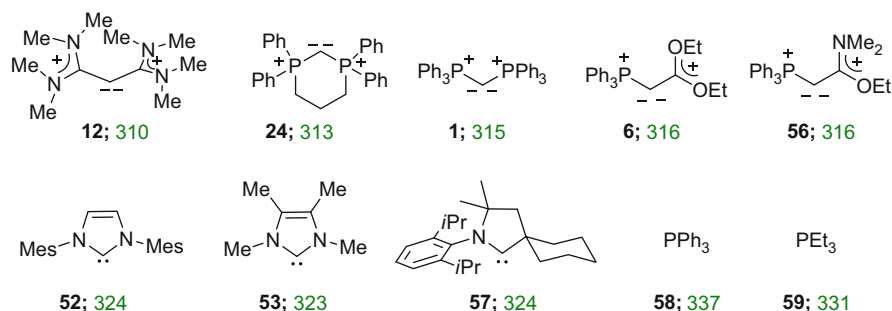
Fig. 5 Ranking of ligands according to the $\Sigma_{Cl\text{-}Ga\text{-}Cl}$ of their **L**GaCl$_3$ complexes (shown in *green*)

4 Applications of Carbodiphosphoranes and Carbodicarbenes in Main-Group-Element Chemistry

The use of C(0) species in the area of main group chemistry is not new; however, it was only recently recognized that the double donation (σ- and π-) of these ancillary ligands could be used to stabilize otherwise elusive, low coordinated main-group-based compounds. In this regard the isolation of the first dihydrido borenium cation **61** by hydride abstraction form adduct **60** was essential, as it probed the validity of this strategy for the preparation of unconventional electrophilic species (Scheme 8) [64].

That seminal work was continued by Petz and coworkers, who were able to isolate the dicationic olefin **63** by alkoxide abstraction from **62** [65], and also by

Ong and coworkers, who prepared the first ever characterized dicationic borohydride **65** employing the less sterically demanding carbodicarbene **64**, as ancillary ligand (Scheme 9) [66].

The possibility of simultaneous σ- and π-donation from carbodiphosphoranes to the same Lewis acidic center is not limited to second row elements. Vidović and coworkers have demonstrated that carbodiphosphoranes are also useful ancillary ligands for the stabilization of two-coordinated P(III) di- and trications. For example, in compound **67**, which was prepared by chloride abstraction from cationic **66**, the central phosphorus atom accepts π-electron density from the carbodiphosphorane as manifested by the P–C–P–N torsion angle of only 9° and the shortening of the C–P bond distance if compared with **66** (Scheme 10). Interestingly, when the less sterically demanding carbodicarbene **11** is used as ancillary ligand, even the tricationic dicoordinated P species **69** could be isolated and structurally characterized [67–69].

Independently, Alcarazo extended the range of application of this double interaction to elements of the fourth row such as Ge(II) centers, being able to isolate the dicoordinated cation **71** by chloride abstraction from adduct **70** [70]. Here again, the P–C–Ge–Cl torsion angle of 8° suggests efficient overlap between the C and Ge π-orbitals, as was later confirmed by DFT calculations (Scheme 11, right side). Because the efficiency of the orbital overlap between the π-systems of the carbon
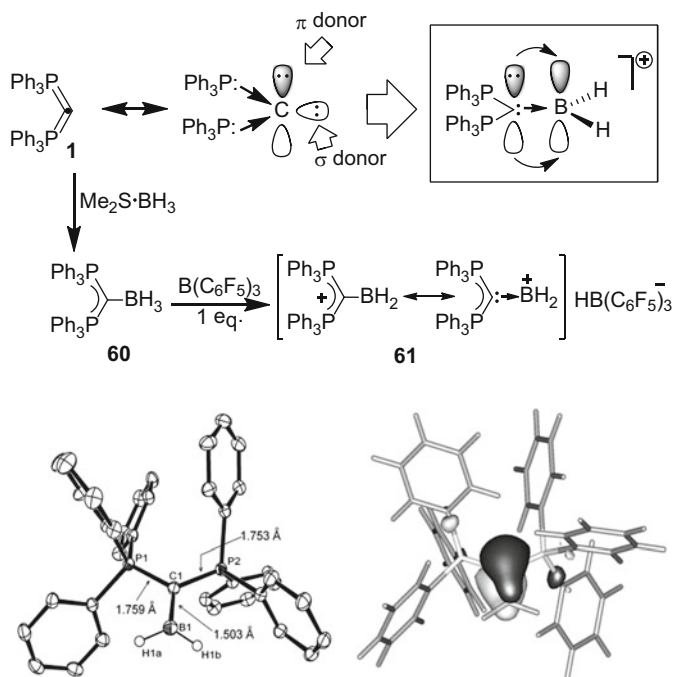
Scheme 8 (*Top*) Synthesis of the dihydroborenio cation **61**; (*Bottom*) X-ray structure of its cationic part, and HOMO of the molecule showing the stabilizing interaction between the π-systems of the C and B atoms
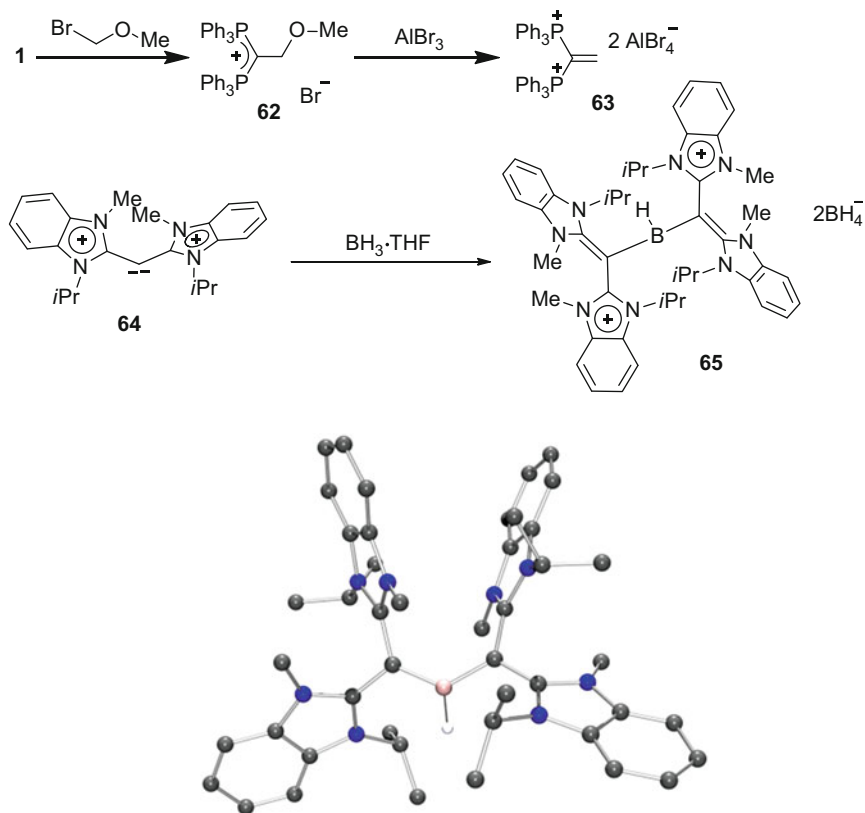
Scheme 9 (*Top*) Synthesis of the dicationic borohydride **65** and (*bottom*) ORTEP representation of its cationic part

(0) atom and that of the element directly attached diminishes for heavier atoms, the stabilization provided by the π dative C → E bond gets also reduced in these cases. This seems to be the reason why during the attempts to synthesize the Sn (II) analogue of **71**, dimeric species **73** is isolated instead. In this case the stabilization energy provided by a plausible π(C–Sn) bond is relatively weak and for this reason it is overridden by dimerization of the transient Sn-cations with concomitant formation of two chloride bridges between the Sn atoms.

In this regard it is worth to mention the very unique situation of beryllium dichloride complex **74**. A priori, it would be expected from $BeCl_2$, a second row-based fragment having two vacant valence orbitals, to participate in πC → Be-donation. However, the P2–C1–Be1–Cl2 torsion of 41.4°, which is probably caused by the steric interaction between the chlorides and the phenyl substituents, makes the p-orbital overlap quite unfavorable. On the other hand, the short C1–Be1 bond distance (1.742(9) Å) combined with the size of the carbodiphosphorane moiety prevents the formation of putative
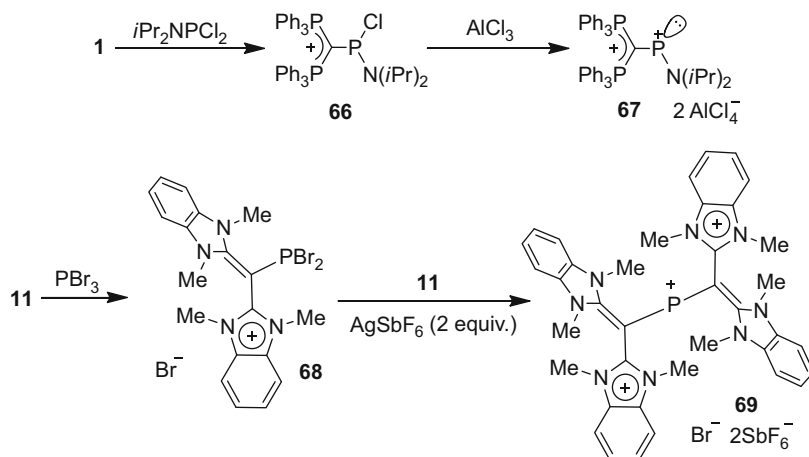
Scheme 10 Synthesis of dicoordinated P^{+2} and P^{+3} species stabilized by carbodiphosphorane and carbodicarbene moieties, respectively
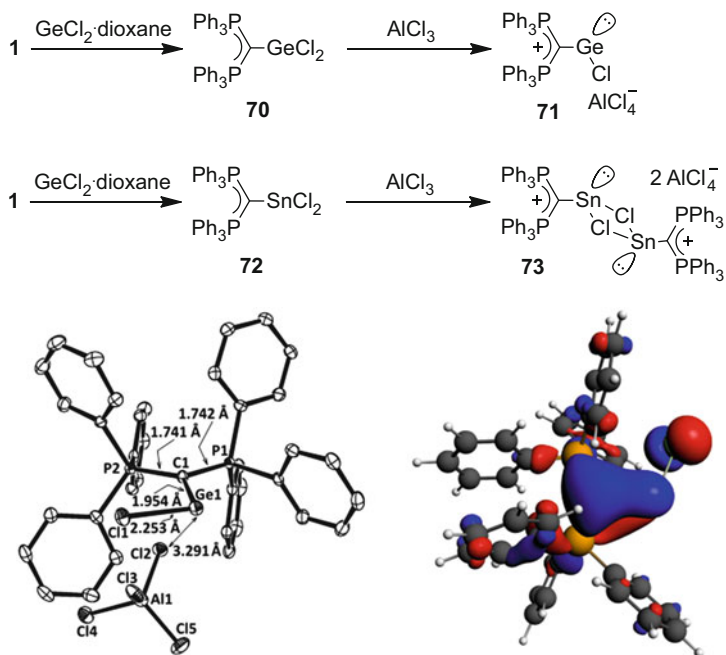
Scheme 11 Synthesis of dicoordinated P(III) and Ge(II) species (*top*); ORTEP representation and HOMO (BP86/def2-TZVP level) of **71** (*bottom*)

Cl-bridged dimeric structures (Scheme 12) [71]. Hence, **74** remains as a monomer although it cannot substantially benefit from simultaneous σ- and π-donation.

Also very informative is the analysis of the structure of carbodiphosphorane-halonium complexes **75–78**, which is included in Fig. 6 [72]. Comparison of the C1-halogen bond length with those of NHC derivatives **79–82** reveals a significant elongation of this bond in carbodiphosphorane derivatives, probably as a consequence of the repulsion between the filled p-orbitals of the halogen and the carbon atom. In NHC derivatives this destabilizing interaction is not present making the bond length shorter [73–78]. The same effect, although less pronounced in magnitude, can be observed when comparing $[\mathbf{1}\cdot\mathrm{SAr}]^+$ and $[\mathrm{NHC}\cdot\mathrm{SAr}]^+$ cations (Ar=p-tol) [79, 80].

Along the preceding pages, only examples in which the C(0) ligand donates two electron pairs to the same main-group Lewis acid have been reviewed. Given the electronic structure of carbones, the coordination of these ligands to up to two main group-based Lewis acids should be expected as well, in the same way that it happens with some transition metals. However, to date only one complex depicting this coordination mode has been reported **83** [81]. Probably, the steric demand of tridimensional ER_n groups is determinant to hinder the attachment of two of these fragments at the same carbon atom. In **83** this problem is solved by the formation of a hydride bridge, which ties together the two boron atoms, thus reducing their steric demand (Scheme 13).

This section about the coordination of carbones to main group elements will not be complete without an analysis of the structure of compound **84** [82, 83]. This Fe-complex was prepared by reaction of carbon disulfide with Fe(II) tetrafluoroborate in the presence of etriphos **85**. As can be seen in Scheme 14, a carbodiphosphorane moiety bonded to two sulfur atoms can be identified as a fragment in the coordination sphere from iron (shown in red). No mechanism for the formation of this compound is proposed by the authors; however, consecutive attack of two phosphines to the central carbon atom of a Fe-activated carbon sulfide seems to be a plausible pathway. Free ligand **86** or any other
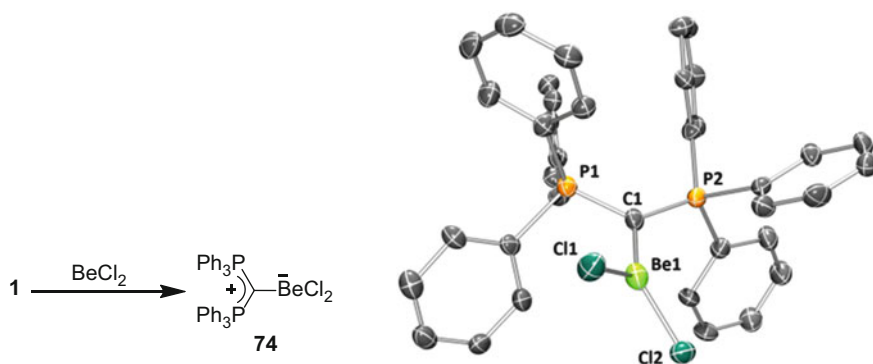
Scheme 12 Synthesis and X-ray structure of **74**
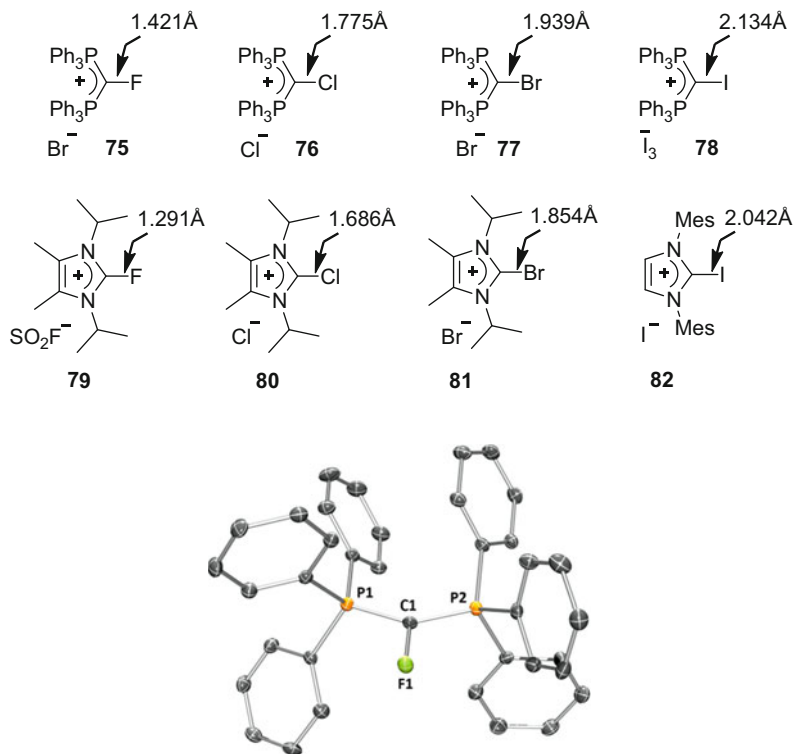
Fig. 6 Comparison of the C-Halogen distances in carbodiphosphorane and NHC-stabilized halonium cations
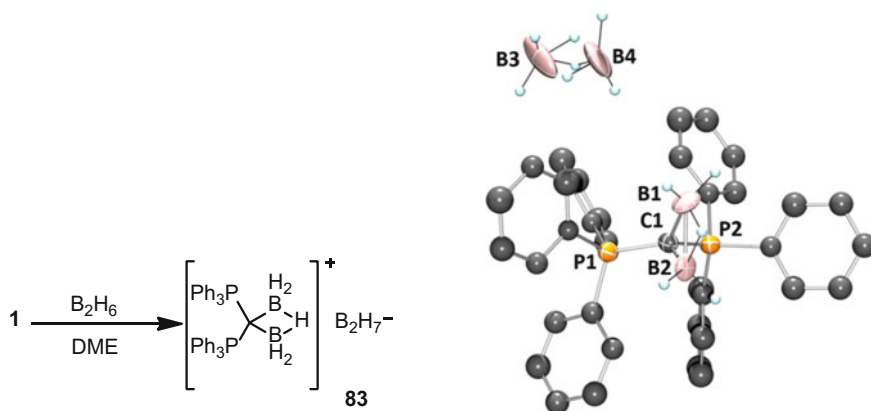
Scheme 13 Synthesis and X-ray structure of **83**

chalcogen analogue has never been isolated; the typical products obtained by reaction of carbones with elemental sulfur being thioketones such as **87** [84].

5 Carbodiphosphorane- and Carbodicarbene-Transition Metal Complexes

As in the case of coordination to main group elements, three possible coordination modes can be envisaged for carbone-transition metal complexes; all them having been experimentally confirmed: (1) the central carbon atom donates only two electrons and therefore it behaves as a strong σ-donor ligand; (2) both electron pairs serve to bind the same metal center through simultaneous σ- and π-donation, or (3) the electron pairs localized at the C(0) center are used to coordinate an electrophile each, affording geminally dimetallated complexes. Most of the known complexes of carbodiphosphoranes and carbodicarbenes belong to the first group described; relevant examples **88–99** are shown in Fig. 7. It is not within the scope of
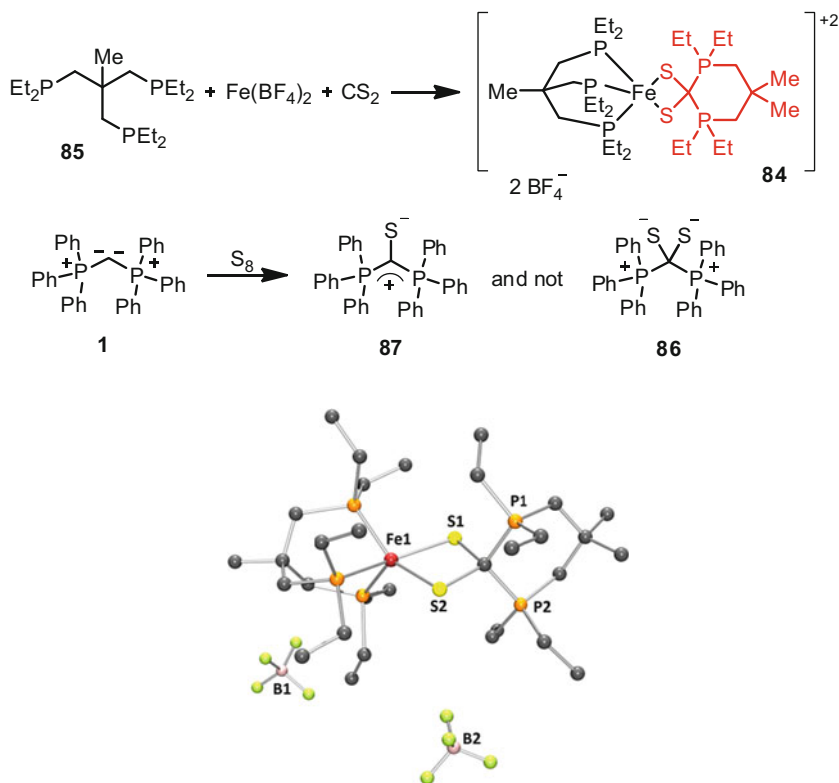
Scheme 14 Synthesis and X-ray structure of **84** and synthesis of **87**

this chapter to discuss in detail all these complexes because the mode of coordination that they exhibit is not specific of C(0) species [85–90]. An exception will be made however, if the extraordinary σ-donation from the ligand influences the catalytic activity of the resulting complex. These cases will be discussed along the next section of this chapter.

Regarding the second mode of coordination, it could be argued that some π-interaction should be present in any carbodiphosphorane/carbodicarbene metal complex. However, this C → M π-donation is usually marginal. Even in the coordinatively unsaturated Ni complex **100**, the carbodiphosphorane ligand has been calculated to act as a nearly exclusive σ-donor [59]. Rhenium compound **101** is one of the few exceptions in which double σ- and π-donation from the carbodiphosphorane unit to the metal is documented [91]. No calculations are available to support the π-interaction; however, a comparative analysis of the X-ray structures of **101** and the isolobal rhenium carbene **102** clearly suggests its presence. In **102** the Re1–C1 and Re1–C2 bond distances are 1.869(9) Å and 2.114(9) Å, respectively, while in **101** the Re1–C1 bond length was determined to be 1.991(7) Å [92]. Taking together, this value, which is intermediate between a single and double C–Re bond, and the highly oxidized nature of the Re(VII) center, the authors concluded that a significant Re=C double bond character should be present in **101** (Fig. 8).

Arguably, the most unique coordination mode of carbones is that in which each from both electron pairs at the formal C(0) atom coordinate a metal center. Several structures of this type are known employing mainly low sterically demanding linear AuCl fragments and were commented earlier along this chapter [7, 13, 17, 93]. In fact, it was the possibility to isolate these gem-dimetallated complexes that first
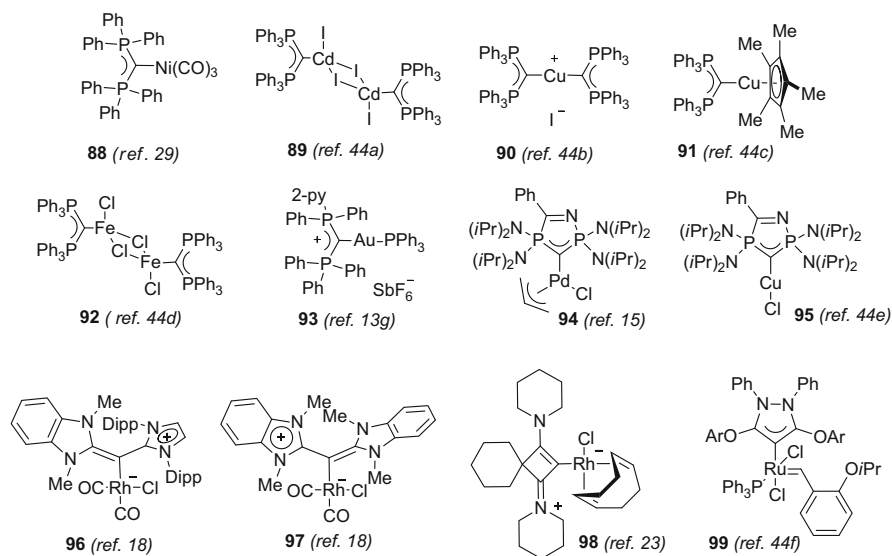
Fig. 7 Representative examples of carbodiphosphorane- and carbodicarbene-transition metal complexes in which the C(0) atom mainly acts as σ-donor ligand

attracted the attention of many researchers on this field. On the other hand, the use of carbones as platforms for the synthesis of heterobimetallic species is even more provocative. These complexes might be interesting from a structural point of view since they possess a new architecture to study metal–metal interactions; moreover, their applications in the area of cooperative bimetallic catalysis can be envisaged.

The first heterobimetallic complex derived from a carbodiphosphorane, complex **103**, was not reported until 2009. To achieve such an architecture, the authors designed a carbodiphosphorane ligand containing two pendant phosphines, which were first used to trap a Pd(II) center affording chelate **104**. In the second step **104** was made to react with one equivalent of AuCl obtaining the desired bimetallic complex **103** [94]. The X-ray structure of this compound confirms the coordination of the central carbon atom to both metal centers, being the Au atom nearly perpendicular to the Pd coordination plane (Au1–C1–Pd1 angle of 86.80(11)°). Additionally, the Pd-Au separation of only 2.8900(3) Å, shorter than the sum of both van der Waals radii (3.29 Å), indicates a d^8–d^{10} interaction between the two metals (Scheme 15).

A similar strategy was followed by Fürstner and coworkers to prepare dimetallated carbodiphosphoranes containing Au and Cu centers [37]. Firstly these authors synthesized ligand **22** containing a pendant pyridine moiety and subsequently, they made it react with Ph_3PAuCl in the presence of $NaSbF_6$ to give complex **105** in which the Au atom coordinates the C(0) center. This complex was able to intercept CuCl affording **106** (Scheme 14). In **106** the Cu atom is tightly bound to the central carbon of the ligand, the Cu(1)–C(1) bond length of 1.981(5) Å being only slightly longer than the one found in closely related complexes **90** and **91**. In addition, the Cu atom also coordinates the nitrogen of the pyridyl rest, and there is a weak metallophilic interaction between Cu and Au, with a Cu1–Au1 bond distance of 2.8483(10) Å (Scheme 16).

Kubo and Mizuta have also exploited a similar strategy to the one already described to obtain carbon(0)-bridged Pt_2Ag_2 clusters. In this case a pincer carbodiphosphorane framework was constructed by successive cyclometalation reaction of **1** with a half equivalent of $[Me_2Pt[\mu\text{-}SMe_2]]_2$ in the presence of PEt_3 to produce complex **107**, with subsequent release of methane (Scheme 15). Reaction of **107** with an equimolar amount of AgOTf afforded **108** in which, apart from the expected Pt ← C(0) → Ag dative bonds, Pt(II)–Ag(I) and Ag(I)–Ag(I) interactions are observed [95]. Cluster **108** is quite labile and rapidly reacts with phosphines causing the cleavage of the tetranuclear core and formation of dinuclear species such as **109,** in which the phosphane coordinates the vacancy available at silver (Scheme 17).
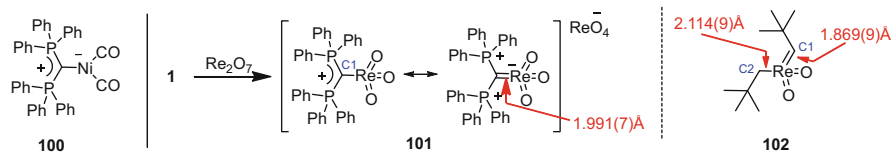
Fig. 8 Simultaneous σ- and π-interaction in carbodiphosphorane-transition metal complexes
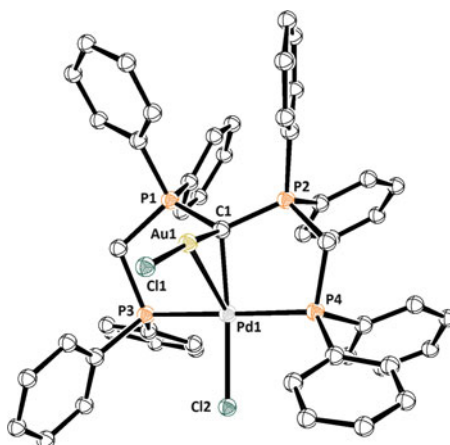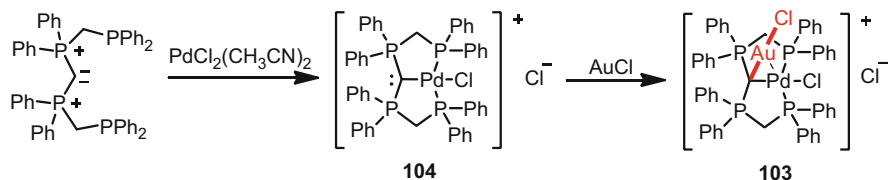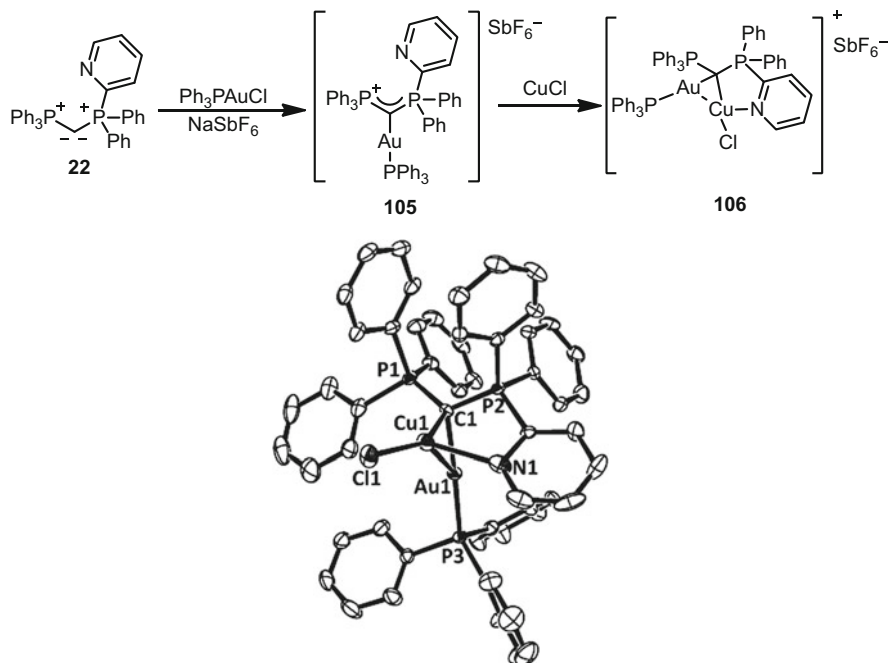
Scheme 15 Synthesis and X-ray structure of the cationic part of **103**

6 Application of Carbon(0) Compounds on the Activation of Small Molecules

Given the exceptional nucleophilicity of carbon(0) species, which surpasses the values reported for amines, phosphines or even *N*-heterocyclic carbenes, and the possibility to modulate their steric demand, these compounds are well qualified to act as based in the framework of frustrated Lewis pairs chemistry. In fact, the combination of **1** and $B(C_6F_5)_3$ at low temperature generates a quite reactive frustrated Lewis pair able to activate H–H, Si–H, C–O, and even C–F bonds (Scheme 18) [96]. It worth to mention that the first cleavage of C–F bonds employing the concept of frustrated Lewis pair chemistry was achieved using carbodiphosphorane 1 as base.

Quite interesting is also the report of Stephan about the reduction of CO_2 to CO employing Et_3P as stoichiometric reductant [97]. As can be observed in the proposed catalytic cycle reproduced in Scheme 19, an in situ generated carbodiphosphorane species acts as catalysts. After optimization a TON of 24.8 could be achieved.

Scheme 16 Synthesis and X-ray structure of the cationic part of **106**

Scheme 17 Synthesis of bimetallic complexes **107–109** and X-ray structures of the cationic parts of **108** and **109**
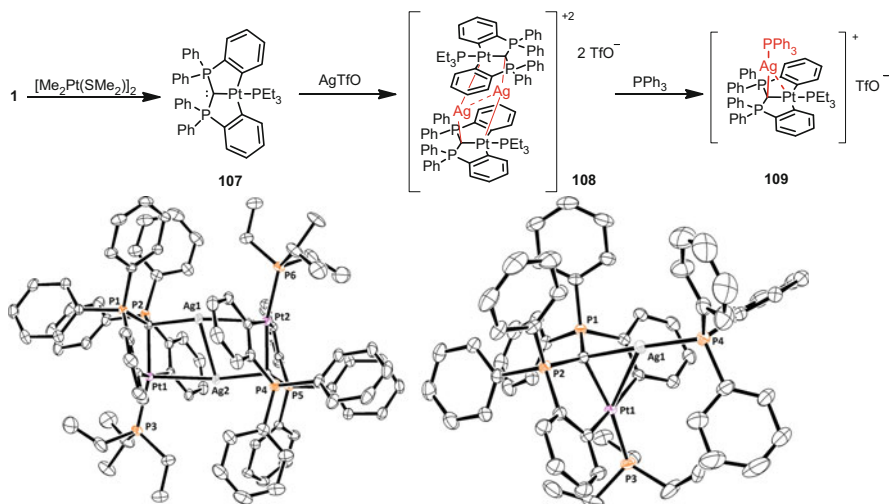
7 Application of Carbone Ligands in Transition Metal Catalysis

The opportunities offered by carbones in catalysis arise from their ability to increase the electron richness of the metal they coordinate. Thus, if in a hypothetical catalytic cycle the step that determines the rate is facilitated by an increase of the electron density at the metal, then an acceleration of the whole process is expected by their use as ancillary ligand. Interestingly, this situation is relatively often found; common elementary steps such as oxidative addition belong to this category and are thus fostered by electron rich metal centers. Apart from this, the use of strongly donating ligands can also be determinant for the stabilization of the catalytic active species along the whole cycle. This increase of catalyst robustness should not be underestimated; in fact, it might be decisive for the design of a catalyst with practical utility.

A case where this last influence is determinant is the Cu-catalyzed Michael addition of anilines to acrylonitrile, which is one of the seminal catalytic applications of a carbodiphosphorane-containing metal complexes (Scheme 20). Most probably compound **116** improves the catalytic performance over NHC–Cu(I) analogues by providing a more efficiently stabilization of the catalytically relevant species **117** [84].

The electron richness of carbodiphosphoranes can also be employed to influence the product outcome of a catalytic cycle. Scheme 21 shows how the cycloisomerization of eneallene **118** can provide different ratios of mixtures containing the [2 + 2] and the [3 + 2] cycloadducts **119** and **120a/b**, respectively. Interestingly, an increase in the ratio of **119** was observed as the metal becomes more electron rich [98]. This can be explained as follows. An electron rich gold template, such as the one provided by precatalyst **121**, could make the carbon adjacent to Au from the vinyl rest more electron rich and therefore, it favors the direct vinylation/demetallation via pathway **I**. In contrast, the catalyst derived from Ph_3PAuCl is more electron deficient; thus, it preferentially induces the attack of the carbon atom bearing the two methyl group substituents
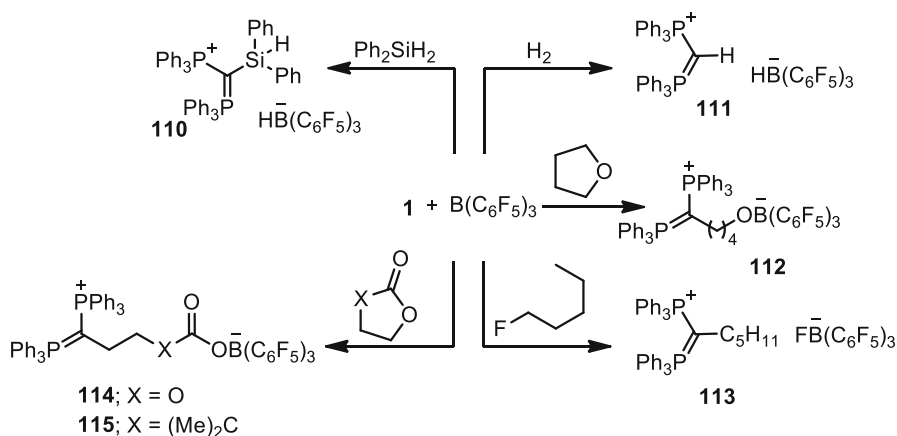
Scheme 18 Reactivity of the frustrated Lewis pair form by mixtures of **1** and $B(C_6F_5)_3$
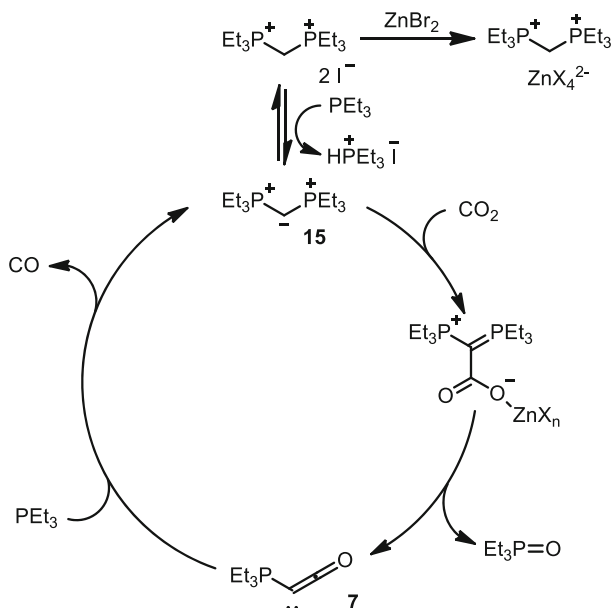
Scheme 19 Reduction of CO_2 to CO promoted by carbodiphosphoranes
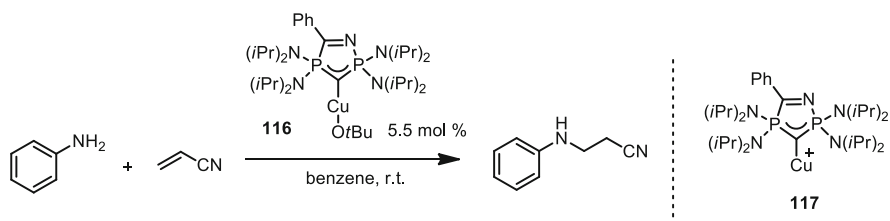
Scheme 20 Seminal application of carbodiphosphorane ligands in catalysis

via **II**. In this case cyclopentenes **120a/b** are delivered by a formal [3 + 2] cycloaddition followed by migration of a methyl group [99]. The picture is certainly more complex when diaurated carbodiphosphoranes are used as catalysts since dual activation mechanism could be also operative [98].

Finally, the strong σ-donation of carbodicarbenes has been employed even more efficiently to prepare interesting catalysts. In this regard it needs to be mentioned the work of Stephan in hydrogenation [100], the one of Ong in cross-coupling chemistry [21], and the one of Meek in hydroarylation reactions [101–103]. This research is compiled in another chapter of this book and therefore will not be discussed here.
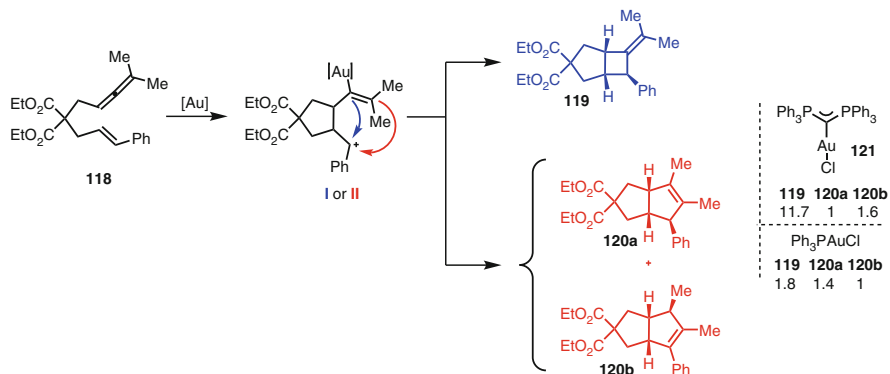
Scheme 21 Ligand influence over the cycloisomerization of enallene **118**

8 Conclusions and Outlook

The presence of two electron pairs around the central carbon atom in carbodicarbenes and carbodiphosphoranes makes them unique ligands in coordination chemistry. Due to this characteristic, these species can formally display three coordination modes, namely σ-donation (using only one electron pair), σ- and π-donation (to the same metal/Lewis acid) and double σ-donation to two different acceptors, which can be identical or not. This versatility multiplies the range of possible applications of these compounds.

However, up to now carbodicarbenes and carbodiphosphoranes have been mainly employed for the stabilization of coordinately unsaturated species, and to some extension for the synthesis of a series of metal complexes, whose catalytic activities may overcome those of NHC-analogues. Hence, most of the potential of C(0)-based ligands remains unexploited. The synthetic applications of dimetallated carbodiphosphoranes are completely underdeveloped, and the cooperative effect invoked by the presence of two (different) metal centers in close proximity has never been exploited in catalysis. In addition, the synthesis of enantiomerically pure carbodicarbenes/carbodiphosphoranes and their subsequent use in asymmetric catalysis would be desirable. It is therefore not adventurous to say that the most interesting applications of carbone chemistry are still to come.

References

1. Ramírez F, Desai NB, Hansen B, McKelvie N (1961) J Am Chem Soc 83:3539
2. Kaska WC, Mitchell DK, Reichelderfer RF (1971) J Organomet Chem 47:391
3. Vincent AT, Wheatley PJ (1972) J Chem Soc Dalton Trans 617
4. Hardy GE, Zink JI, Kaska WC, Baldwin JC (1978) J Am Chem Soc 100:8001
5. Daly JJ, Wheatley PJ (1966) J Chem Soc A 1703
6. Birum GH, Matthews CN (1969) Acc Chem Res 2:373

7. Schmidbaur H, Gasser O (1976) Angew Chem Int Ed Eng 15:502
8. Bestmann HJ (1977) Angew Chem Int Ed Eng 16:349
9. Schmidbaur H, Schier A (2013) Angew Chem Int Ed 52:176
10. Petz W, Frenking G (2010) Top Organomet Chem 30:49
11. Alcarazo M (2011, 1839) Dalton Trans 40
12. Frenking G, Hermann M, Andrada DM, Holzmann N (2016) Chem Soc Rev 45:1129
13. Vicente J, Singhal AR, Jones PG (2002) Organometallics 21:5887
14. Tonner R, Öxler F, Neumüller B, Petz W, Frenking G (2006) Angew Chem Int Ed 45:8038
15. Tonner R, Frenking G (2008) Chem Eur J 14:3260
16. Tonner R, Frenking G (2008) Chem Eur J 14:3273
17. Alcarazo M, Lehmann CW, Anoop A, Thiel W, Fürstner A (2009) Nat Chem 1:295
18. Viehe HC, Janousek Z, Gompper R, Lach D (1973) Angew Chem 85:581
19. Dyker CA, Lavallo V, Donnadieu B, Bertrand G (2008) Angew Chem Int Ed 47:3206
20. Fürstner A, Alcarazo M, Goddard R, Lehmann CW (2008) Angew Chem Int Ed 47:3210
21. Kaufhold O, Hahn FE (2008) Angew Chem Int Ed 47:4507
22. Hsu YC, Shen JS, Lin BC, Chen WC, Chan YT, Ching WM, Yap GPA, Hsu CP, Ong TG (2015) Angew Chem Int Ed 54:2420
23. Chen WC, Shen JS, Jurca T, Peng CJ, Lin YH, Wang YP, Shih WC, Yap GPA, Ong TG (2015) Angew Chem Int Ed 54:15207
24. Esterhuysen C, Frenking G (2011) Chem Eur J 17:9944
25. Brown TJ, Sugie A, Leed MGD, Widenhoefer RA (2012) Chem Eur J 18:6959
26. Tonner R, Frenking G (2007) Angew Chem Int Ed 46:8695
27. Takagi N, Shimizu T, Frenking G (2009) Chem Eur J 15:3448
28. Klein S, Tonner R, Frenking G (2010) Chem Eur J 16:10160
29. Frenking G, Tonner R, Klein S, Takagi N, Shimizu T, Krapp A, Pandey KK, Parameswaran P (2014) Chem Soc Rev 43:5106
30. Zhao L, Hermann M, Holzmann N, Frenking G (2017) Coord Chem Rev 344:163
31. Gasser O, Schmidbaur H (1975) J Am Chem Soc 97:6281
32. Hussain MS, Schmidbaur H (1976) Z Naturforsch 31b:721
33. Schmidbaur H, Hasslberger G, Deschler U, Schubert U, Kappenstein C, Frank A (1979) Angew Chem Int Ed Eng 18:408
34. Appel R, Baumeister U, Knoch F (1983) Chem Ber 116:2275
35. Schmidbaur H, Herr R, Zybill CE (1984) Chem Ber 117:3374
36. Schmidbaur H, Nusstein P (1985) Organometallics 4:344
37. Alcarazo M, Radkowski K, Mehler G, Goddard R, Fürstner A (2013) Chem Commun 49:3140
38. Schmidbaur H, Costa T, Milewski-Mahrla B, Schubert U (1980) Angew Chem Int Ed Eng 19:555
39. Schmidbaur H, Costa T (1981) Chem Ber 114:3063
40. Bowmaker GA, Herr R, Schmidbaur H (1983) Chem Ber 116:3567
41. Schmidbaur H, Herr R, Zybill CE (1984) Chem Ber 117:3380
42. Marrot S, Kato T, Gornitzka H, Baceiredo A (2006) Angew Chem 118:2660
43. Pascual S, Asay M, Illa O, Kato T, Bertrand G, Saffon-Merceron N, Branchadell V, Baceiredo A (2007) Angew Chem Int Ed 46:9078
44. Dellus N, Kato T, Bagán X, Saffon-Merceron N, Branchadell V, Baceiredo A (2010) Angew Chem Int Ed 49:6798
45. Morosaki T, Suzuki T, Wang WW, Negase S, Fujii T (2014) Angew Chem Int Ed 53:9569
46. Lavallo V, Dyker CA, Donnadieu B, Bertrand G (2008) Angew Chem Int Ed 47:5411
47. Fernández I, Dyker CA, DeHope A, Donnadieu B, Frenking G, Bertrand G (2009) J Am Chem Soc 131:11875
48. Christl M, Engels B (2009) Angew Chem Int Ed 48:1538
49. Lavallo V, Dyker CA, Donnadieu B, Bertrand G (2009) Angew Chem Int Ed 48:1540

50. Melaimi M, Parameswaran P, Donnadieu B, Frenking G, Bertrand G (2009) Angew Chem Int Ed 48:4792
51. Panckevicious C, Liu L, Bertrand G, Stephan DW (2016) Angew Chem Int Ed 55:5536
52. Gusev DG (2009) Organometallics 28:763
53. Tolmann CA (1977) Chem Rev 77:313
54. Denk K, Sirsch P, Herrmann WA (2002) J Organomet Chem 649:219
55. Mayr M, Wurst K, Ongania KH, Buchmeiser MR (2004) Chem Eur J 10:1256
56. Alcarazo M, Fernández R, Álvarez E, Lassaletta JM (2005) J Organomet Chem 690:5979
57. Fürstner A, Alcarazo M, Radkowski K, Lehmann CW (2008) Angew Chem Int Ed 47:8302
58. Tonner R, Frenking G (2009) Organometallics 28:3901
59. Petz W, Weller F, Uddin J, Frenking G (1999) Organometallics 18:619
60. Bent HA (1960) J Chem Educ 37:616
61. Huheey JE (1981) Inorg Chem 20:4033
62. Jonas V, Boehme C, Frenking G (1996) Inorg Chem 35:2097
63. El-Hellani A, Monot J, Tang S, Guillot R, Bour C, Gandon V (2013) Inorg Chem 52:11493
64. Inés B, Patil M, Carreras J, Goddard R, Thiel W, Alcarazo M (2011) Angew Chem Int Ed 50:8400
65. Celik MA, Frenking G, Neumüller B, Petz W (2013) ChemPlusChem 78:1024
66. Chen WC, Lee CY, Lin BC, Hsu YC, Shen JS, Hsu CP, Yap GPA, Ong TG (2014) J Am Chem Soc 136:914
67. Tay MQY, Lu Y, Ganguly R, Vidović D (2013) Angew Chem Int Ed 52:3132
68. Tay MQY, Ilić G, Werner-Zwanziger U, Lu Y, Ganguly R, Ricard L, Frison G, Carmichael D, Vidović D (2016) Organometallics 35:439
69. Dordević N, Ganguly R, Petković M, Vidović D (2016) Chem Commun 52:9789
70. Khan S, Gopakumar G, Thiel W, Alcarazo M (2013) Angew Chem Int Ed 52:5644
71. Petz W, Dehnicke K, Holtzmann N, Frenking G, Neumüller B (2011) Z Anorg Allg Chem 637:1702
72. Petz W, Kuzu I, Frenking G, Andrada DM, Neumüller B, Fritz M, Münzer JE (2016) Chem Eur J 22:8536
73. Kuhn N, Bohnen H, Fahl J, Blaeser D, Boese R (1996) Chem Ber 129:1579
74. Kuhn N, Abu-Rayyan A, Eichele K, Piludu C, Steimann M (2004) Z Anorg Allg Chem 630:495
75. Kuhn N, Abu-Rayyan A, Ströbele M (2002) Z Anorg Allg Chem 628:2251
76. Arduengo AJ, Tamm M, Calabrese JC (1994) J Am Chem Soc 116:3625
77. Schmidbaur H, Zybill C, Neugebauer D, Müller G (1985) Z Naturforsch 40:1293
78. Petz W, Heimann S, Öxler F, Neumüller B (2007) Z Anorg Allg Chem 633:365
79. Inés B, Holle S, Goddard R, Alcarazo M (2010) Angew Chem Int Ed 49:8389
80. Palomas D, Holle S, Inés B, Bruns H, Goddard R, Alcarazo M (2012) Dalton Trans 41:9073
81. Petz W, Öxler F, Neumüller B, Tonner R, Frenking G (2009) Eur J Inorg Chem 4507
82. Bianchini C, Meli A, Orlandini A, Sacconi L (1980) Angew Chem 92:1055
83. Bianchini C, Meli A, Orlandini A, Sacconi L (1981) J Organomet Chem 218:81
84. Schmidbaur H, Zybill CE, Neugebauer D (1982) Angew Chem 94:321
85. Petz W, Neumüller B (2011) Eur J Inorg Chem 4889
86. Petz W, Neumüller B, Klein S, Frenking G (2011) Organometallics 30:3330
87. Zybill C, Müller G (1987) Organometallics 6:2489
88. Pranckevicius C, Iovan DA, Stephan DW (2016) Dalton Trans 45:16820
89. Corberán R, Marrot S, Dellus N, Merceron-Saffon N, Kato T, Peris E, Baceiredo A (2009) Organometallics 28:326
90. DeHope A, Donnadieu B, Bertrand G (2011) J Organomet Chem 696:2899
91. Sundermeyer J, Weber K, Peters K, von Schnering HG (1994) Organometallics 13:2560
92. Toreki R, Schrock RR, Davis WM (1992) J Am Chem Soc 114:3367
93. Reitsamer C, Shuh W, Kopacka H, Wurst K, Ellmerer EP, Peringer P (2011) Organometallics 30:4220

 94. Reitsamer C, Schuh W, Kopacka H, Wurst K, Peringer P (2009) Organometallics 28:6617
 95. Kubo K, Okitsu H, Miwa H, Kume S, Cavell RG, Mizuta T (2017) Organometallics 36:266
 96. Alcarazo M, Gomez C, Holle S, Goddard R (2010) Angew Chem Int Ed 49:5788
 97. Dobrovetsky R, Stephan DW (2013) Angew Chem Int Ed 52:2516
 98. El-Hellani A, Bour C, Gandon V (2011) Adv Synth Catal 353:1865
 99. Alcarazo M, Stork T, Anoop A, Thiel W, Fürstner A (2010) Angew Chem Int Ed 49:2542
100. Pranckevicious C, Fan L, Stephan DW (2015) J Am Chem Soc 137:5582
101. Goldfogel MJ, Roberts CC, Meek SJ (2014) J Am Chem Soc 136:6227
102. Roberts CC, Matías DM, Goldfogel MJ, Meek SJ (2015) J Am Chem Soc 137:6488
103. Goldfogel MJ, Roberts CC, Manan RS, Meek SJ (2017) Org Lett 19:90

Synthesis and Structure of Carbodicarbenes and Their Application in Catalysis

Shukai Liu, Wen-Ching Chen, and Tiow-Gan Ong

Abstract Carbodicarbenes are a special class of bisylidic CL_2 compounds, the so-called carbones. Carbones are divalent carbon compounds, in which a four-electron carbon atom in the oxidation state of zero is bound by two σ-donor ligands L via donor-acceptor interactions, resulting in the formulation L→C(0)←L. In carbodicarbenes (CDCs), the L ligand is a *N*-heterocyclic carbene (NHC) or any other singlet carbene species. Comparable to "classical" bisylides, CDCs possess two lone pairs of electrons at the central carbon atom, thus making them stronger σ-donors than conventional carbenes like NHCs. These unusual donor properties make CDCs unique and highly potent ligands for transition metals and catalysis. This chapter summarizes the exciting developments of the last 10 years in CDC chemistry. A concise overview of this new class of carbone compounds is given by summarizing the synthesis of different CDC frameworks as well as their application in transition metal chemistry and homogenous catalysis.

Keywords Carbene · Carbodicarbene · Carbone · Homogeneous catalysis · Ligand design

S. Liu
Institute of Chemistry, Academia Sinica, Taipei, Taiwan, Republic of China

Department of Applied Chemistry, National Chiao Tung University, Hsinchu, Taiwan, Republic of China

Sustainable Chemical Science and Technology, Taiwan International Graduate Program, Academia Sinica and National Chiao Tung University, Hsinchu, Taiwan, Republic of China

W.-C. Chen (✉)
Institute of Chemistry, Academia Sinica, Taipei, Taiwan, Republic of China

T.-G. Ong (✉)
Institute of Chemistry, Academia Sinica, Taipei, Taiwan, Republic of China

Department of Applied Chemistry, National Chiao Tung University, Hsinchu, Taiwan, Republic of China
e-mail: tgong@gate.sinica.edu.tw

Contents

1   Introduction

The search for interesting electronic and bonding configurations in carbonic species has always been an important theme in organic chemistry. The best-known examples of carbonic species are carbenes, where the carbon atom contains a free electron pair. The most Common members of this class of divalent carbon compounds are cyclic (alkyl)(amino)carbenes (CAACs) and *N*-heterocyclic carbenes (NHCs) (Scheme 1a). The distinct electronic structure of singlet carbenes engenders them with a strong σ-donating ability, which has allowed them to play a key role in the field of coordination
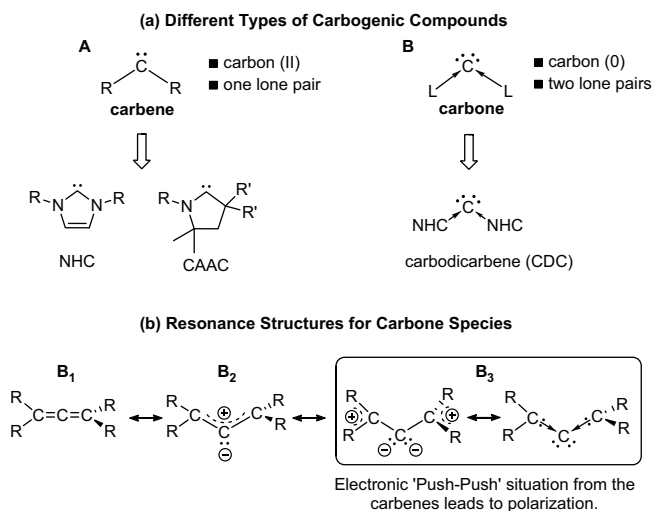
Scheme 1 (**a**) Carbene **A** versus carbone **B**. (**b**) Resonance Lewis structures of carbone

chemistry and catalysis [1–3]. Seminal efforts in developing NHCs and other strong carbon ligands have led to the generation of another remarkable class of nonconventional carbon bases, the *carbones* CL_2 consisting of a bent dicoordinated carbon atom [4–8]. In general, carbones can be viewed as compounds with a divalent carbon atom in an oxidation state of zero. Here, the central carbon atom possesses four electrons and is flanked by two neutral donor ligands L that supply the remaining electrons to fulfill the octet rule.

Carbodicarbenes (CDCs) are one of the main carbone subgroups. Therein, the coordinated ligand units (L) in their respective scaffolds are NHCs or other common carbene ligands. Scheme 1a illustrates the atom connectivity in CDCs in comparison to carbenes. The Lewis resonance description of carbodicarbene can be written in several forms ($\mathbf{B_1}$, $\mathbf{B_2}$, and $\mathbf{B_3}$ formalism). In $\mathbf{B_1}$ formalism, the CDC could be strictly regarded as a traditional allene with an sp. hybridized central carbon containing two orthogonal π-bonds. However, in reality, CDCs have a nonlinear C–C–C skeleton with electron configuration more closely resembling $\mathbf{B_2}$ and $\mathbf{B_3}$ formalisms. This is due to an electronic polarization resulting from the push-push substitution from both flanked units. In an extreme form of $\mathbf{B_3}$, the CDC behaves like a dicarbanionic resonance form and manifests a feature more like a captodative bonding model of transition metals, a departure from the classical Lewis electron sharing description. In this case, the central carbon accepts a dative σ-donation from its flanking carbon units rather than covalently sharing electrons in the bonding. Thus, the flanking carbon units can be formally treated as a singlet carbene subunit, datively donating its lone pair to the central carbon atom. It should be noted that this dative model description of carbodicarbenes has its share of controversy and criticism, which was brought up by Himmel, Krossing, and Schnepf [9–11]. Also the "classical" covalent ylidic bonding situation of $\mathbf{B_3}$ is valid to describe the chemical character of CDCs particularly their bent structure and the presence of two lone pairs of electrons at the central carbon atom. The latter is probably the most striking feature of CDCs, which promises a new coordination behavior and complementary reactivity with respect to ubiquitous NHCs. The aim of this "chapter" is to highlight several recent advances in the development of CDCs and similar species. In addition, this article also describes several attempts to make known CDCs and their implication in both main-group chemistry and catalysis.

2   Preparation and Properties of Carbodicarbenes

The term "carbodicarbene" was firstly proposed by Frenking and Tonner in 2007 in their theoretical studies, predicting that these divalent carbon(0) compounds flanked by two NHC fragments should be stable enough for being synthesized and isolated [5]. These calculations indicated that free stable carbodicarbene (CDC) could be isolated based on the two simple computational model systems, **1-H$_4$** and **1-Me$_4$** (Scheme 2). Interestingly, the energetically most stable geometry of **1-H$_4$** was proposed to exhibit – in contrast to parent allene $H_2C=C=CH_2$ – a nonlinear C–C–C angle of 125.8° with bond lengths of 1.359 Å and two NHC planes with a torsion angle of 81.6°.

Scheme 2 (Left) Predicted C(NHC)$_2$ structures of **1-H$_4$** and **1-Me$_4$** at the BP86/TZ2P level of theory. (Right) HOMO and HOMO-1 of **1-H$_4$**, lone pair orbitals (some pictures adapted from [5])

HOMO (π type)

HOMO-1 (σ type)

Orbitals representing the two lone pairs at the central carbon atom of **1-H$_4$**
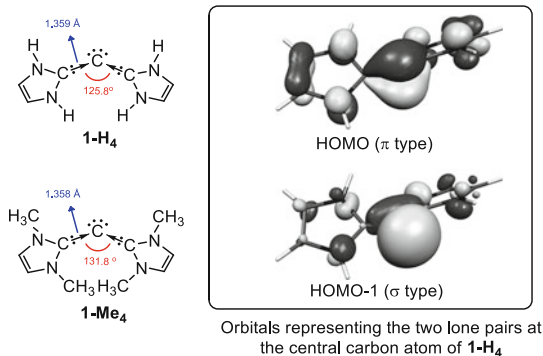
Analogously, the **1-Me$_4$** form with methyl substituents should feature a C–C–C angle of 131.8° with bond distances of 1.358 Å. The loss of classical sp. hybridization in **1-H$_4$** and **1-Me$_4$** resulted in molecular orbitals of σ- (HOMO-1) and π-symmetry (HOMO) localized at the central carbon, which indicates the presence of two electron lone pairs. The existence of two lone pairs at the carbon atom in carbodicarbenes was evidenced by high first (292.3 kcal/mol) and second proton affinities (168.4 kcal/mol). This theoretical prediction by Frenking and Tonner has inspired many research groups and served as foundation for the developments in the preparation of CDCs in the following years. Apart from the synthetic challenge, CDCs also promised a high potential as auxiliary ligands for metal complexes, potentially rivaling their NHC counterparts for distinct reactivities where the strong σ-donating feature of CDCs could prove advantageous. Additionally, the prospect of geminally coordinating two metal centers has broad implication to many fields of organometallic chemistry and catalysis and thus led to special research interest.

2.1 The First Free Carbodicarbenes

The groups of Bertrand and Fürstner first undertook the synthetic challenge to replicate the theoretical prediction of Frenking and Tonner and prepare a stable free carbodicarbene (Scheme 3) [12, 13]. Bertrand prepared the corresponding CDC **4** containing benzimidazoline-2-ylidene as the donating ligands. The synthetic route for CDC **4** started from methylene-bridged benzimidazole **2**. N-alkylated reaction of **2** could be performed with 2 equivalents of MeOTf to afford conjugate acid **3**. Twofold deprotonation of conjugate acid **3** by strong potassium base afforded free CDC **4** (32% yield) (Scheme 3) [12]. The structure of **4** was confirmed by single crystal X-ray diffraction analysis and showed a highly nonlinear C–C–C moiety, which clearly confirmed to the electronic structure of **B$_3$** (see Scheme 1). The bond distance of 1.343(2) Å with an angle of 134.8(2)° along the C–C–C moiety was in agreement with the computational values by Frenking and Tonner. The structural parameters clearly showed that carbodicarbene are uniquely different from normal
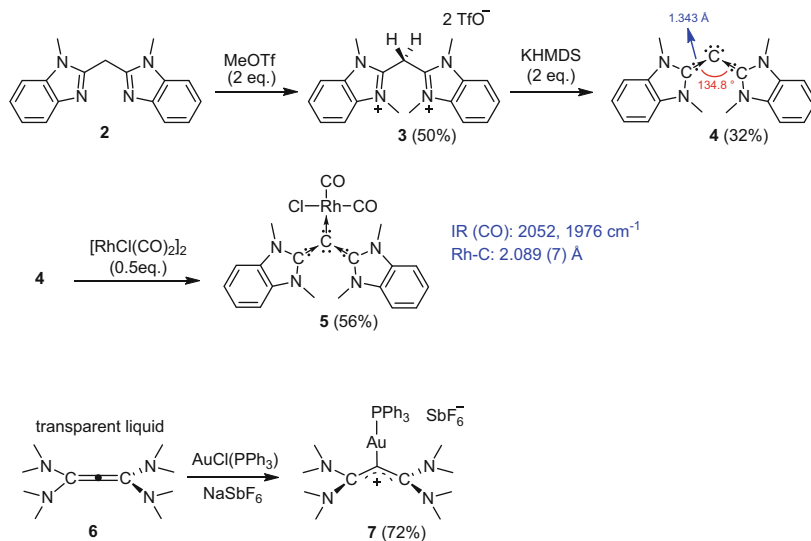
Scheme 3 First known stable carbodicarbenes and complexes thereof

allenes. In this work, Bertrand also defined compound **4** as a "bent allene" although its reactivity was found to be significantly different from the reactivity behavior of normal organic allenes. For example, in the Rh complex **5**, the metal binds to CDC **4** in an η^1-mode, while a conventional allene would coordinate to the metal in η^2 manner via the C=C π-bond. The low IR carbonyl stretching frequency of **5** (2,052 and 1,976 cm^{-1}) indicated a stronger donor ability of **4** compared to most known NHCs. In the same year, Fürstner and coworkers also studied the long-known tetradimethylaminoallene **6**. Compound **6** is a moisture-sensitive compound and readily reacted with Ph$_3$PAuCl/NaSbF$_6$ to furnish gold complex **7**. Again, complex **6** displays an η^1-binding mode of the ligand to the metal, indicating its unique nature compared to traditional allenes [13]. It should be noted that allenes typically coordinate to a metal via a η^2 coordination mode which thus distinguishes them from CDC ligands.

2.2 CDC with Symmetrical Supporting L Units: Scaffold's Variety

Despite of the potential of CDCs as effective σ-donating auxiliary ligands for metal complexes, the use of CDC for such purposes was not seen for many years after the first isolation in 2008 (CDC **4**). This was also due to the fact that compound **4** and its metal complexes have very poor solubility in organic solvents, which frustrated subsequent experimental efforts. More importantly, there was a notable

lack of variability to the framework of CDCs that is essential for modulating the catalytic activity and selectivity of the catalyst.

Ong and coworkers' work represents the first attempt to expand the collection of acyclic CDC's beyond methyl pendant arms since the isolation of the first CDC. The Ong group devised a synthetic strategy based on modification of the pendant group at nitrogen to both increase solubility and broaden the scaffold diversity of CDCs [14, 15] (Scheme 4). The work has focused on the development of CDC scaffolds derived from a bis(benzimidazole-2-yl)methane bearing isopropyl (**12a**) and cyclohexyl (**12b**) pendant arms [14]. The synthesis begins with nitroaniline precursors **8a** and **8b** to make diamine **9a** (isopropyl) and **9b** (cyclohexyl), respectively. Subsequently, reaction of the diamino substrates with diethyl malonate afford *bis* (benzimidazole-2-yl)methanes **10a** and **10b** which are then transformed to the CDC precursor salts **11a,b** via a reaction with either CH$_3$I or MeOTf. The deprotonation of **11** afforded the moisture-sensitive CDCs **12a** and **12b** in good yields. Fortunately, the solubility of CDCs **12** was greatly improved in organic solvents.

The molecular structure of **12a** was elucidated by single crystal X-ray diffraction analysis studies. It also displayed a bent C–C–C moiety with a bond angle of 136.6 (5)° and short bond lengths of 1.335(5) Å. The structural parameters of **12a** are comparable to the first CDC isolated by Bertrand, illustrating that sterically demanding isopropyl pendant arms on the framework did not make any significant change to the CDC structure. The two benzimidazoyl planes in **12a** are twisted by 71° from the typical perpendicular arrangement found for normal allenes. The coordination ability of carbodicarbene **12** toward metal complexes was also examined by means of rhodium carbonyl palladium allyl complexes **13** and **14a** (Scheme 5) [14]. The molecular structures of the metal complexes have been determined: the metal-carbone bond distances were 2.109(2) and 2.123(2) Å in Rh complexes **13a** and
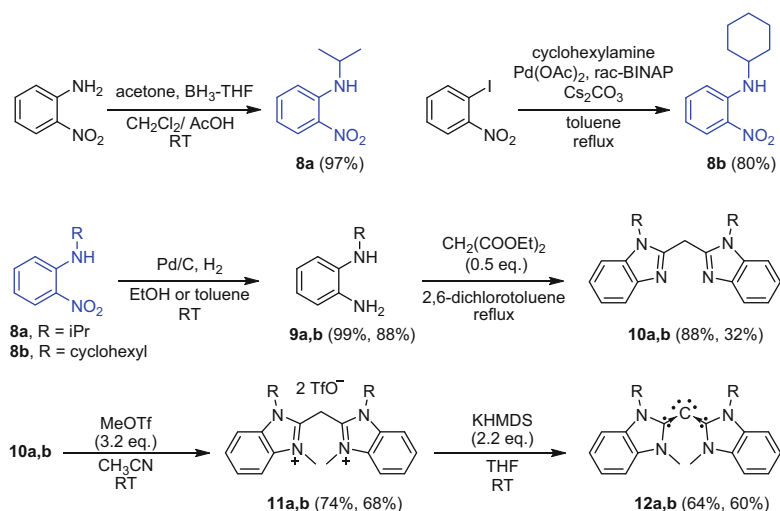
Scheme 4 Synthetic routes for CDC **12**
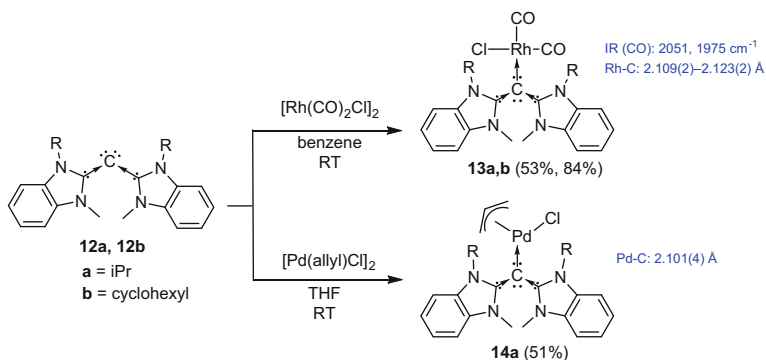
Scheme 5 Coordinated CDC Pd and Rh complexes

13b, respectively, and 2.101(4) Å in the Pd complex **14a**. These metal-carbon bond distances are slightly longer, which could be attributed to steric hindrance invoked by CDC.

2.3 Preparation of Unsymmetrical CDCs

Ong and Chen continued to construct carbodicarbene scaffolds with the goal of generating a carbone center bearing two unsymmetrical ligand units. The introduction of modular scaffolds to the CDC framework would greatly advance the tunability and, as a result, the potential use of these ligands in catalysis. The synthetic strategy outlined in Scheme 6 utilized an S_N2 route to construct unsymmetrical CDCs [15]. To this end, the *N*-heterocyclic olefin (NHO) **17** was selected as a nucleophile, together with the thioether containing **19** as the electrophile (the thioether is considered a good leaving group). Compound **17** and **19** reacted very smoothly to afford the unsymmetrical CDC precursor **20** in good yield (56%). The free CDC **21** was eventually obtained in satisfactory yield (73%). A series of CDC frameworks (**22–25**) could thus be prepared modularly and with ease via this S_N2 route.

In this work, the diversity of CDC structures expanded beyond benzimidazole-related NHC to comprise an Arduengo NHC (**24**) and PPh$_3$ (**25**) in the framework. Structure analysis of CDC **24** bearing the IPr carbene unit revealed unequal C–C bond distances of 1.318(3) and 1.344(3) Å. The shorter bond is located to the benzimidazole fragment, thus indicating a more effective π-interaction. The C–C–C bond angle (146.11(19)°) is less bent than that found in other CDCs because of less electronic repulsion from the two electron lone pairs. The molecular structure of **25** with an PPh$_3$ ligand showed a P–C bond length of 1.6435(12) Å, which is shorter than normal P–C single bonds (1.8 Å). This is in agreement with the carbodiphosphorane structure reported by the groups of Alcarazo and Fürstner (P–C bond length = 1.6398–1.6416 Å) [16].
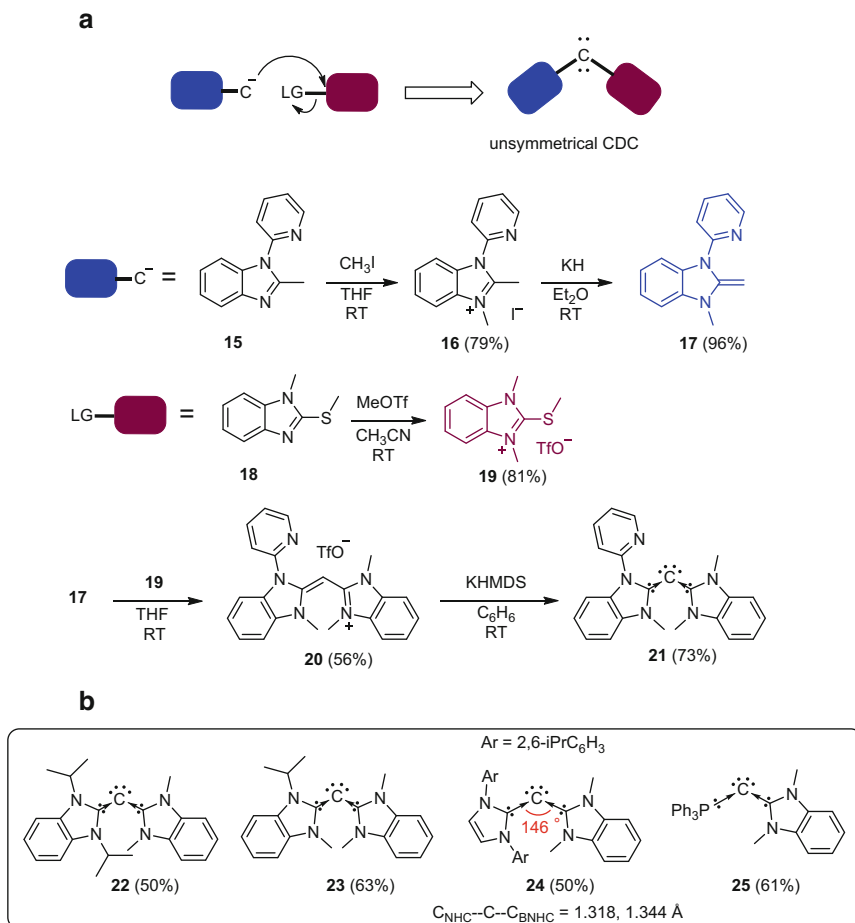
Scheme 6 Synthetic strategy based on S_N2 route for preparing the unsymmetrical CDCs **21–25**. (**a**) S_N2 strategy, (**b**) Library of CDCs

2.4 Cyclic Carbodicarbenes

Incorporating a C=C=C moiety into a five-membered cycloalkane ring presents a synthetic challenge due to unfavorably high-energy ring strain resulting from the large C–C–C angle. Bertrand postulated that electronic push-push substitution to favor the CDC structure over the allene structure within the system could reduce the ring strain by inducing deviations from the classical allene geometry [17]. To test this hypothesis, the synthetically easily available 3,5-diaminopyrazolium salt **27** was examined as a possible precursor to generate a five-membered cyclic CDC or bent allene **28** (Scheme 7). The four amino groups within cyclic CDC **28** could
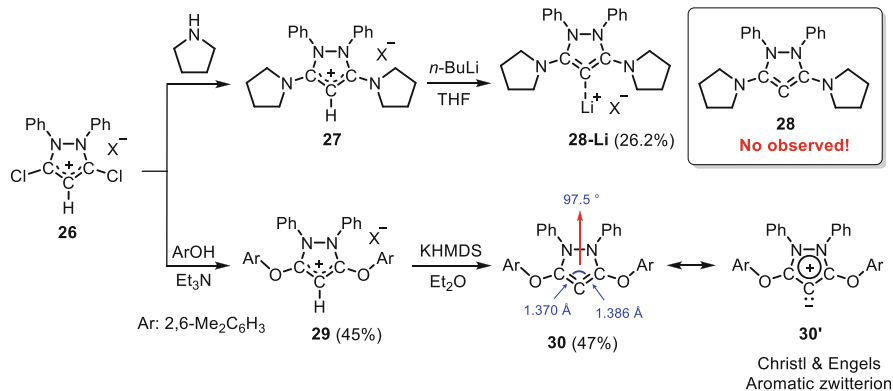
Scheme 7 Cyclic carbodicarbenes based on five-membered ring

potentially provide effective π-donor conjugation to offset the ring strain. Indeed, deprotonation of the precursor **27** using *n*-butyl lithium base yielded **28-Li** adduct, but free cyclic CDC **28** could not be obtained without the use of Li. In contrast, cyclic CDC **30** was successfully isolated by exchanging the exocyclic pendant groups to aryloxy moieties, i.e., to weaker π-donors than the amino analogues. CDC **30** contained an extremely acute C–C–C angle of 97.5° with longer C–C bond distances of 1.370 and 1.386 Å (Scheme 7) [17]. Interestingly, the two nitrogen and two oxygen centers in **30** were found to be coplanar with the C–C–C allenic fragment. The π-donation from lone pairs at oxygen of compound **30** played a key role, as evidenced by the very short O–C bond distances (1.358 and 1.347 Å). Computational analysis rationalized that exocyclic delocalization by the 3,5-substituted donor enhanced the stability of cyclic CDCs. The aromaticity stabilization of endo-nitrogen atoms within pyrazolium played a lesser role [18]. Nonetheless, Christl and Engels have argued against the bent allene formalism in **30** as the most stable ground state but stated that the ground-state structure should contain aromatic conjugation stabilization [19]. The group proposed that the cyclic CDC should be described as a "zwitterion derived from pyrazole" as depicted by Lewis structure **30′**. However, Bertrand and coworkers defended their formalism as an intuitive nomenclature classification of the compound to avoid any further confusion in the chemical community [20].

Subsequently, Bertrand, Melaimi, and Frenking continued to prepare a more strained four-membered cyclic CDC **32** in the absence of aromatic stabilization within the ring (Scheme 8) [21]. The ^{13}C NMR signals for the central and terminal carbon atoms in allene moiety appeared at δ = 151 and 185 ppm, respectively. The unstable nature of CDC **32** prevented any further structural analysis. Computational studies on the BP86/def-SVP level of theory found that the energy-optimized geometry of **32** features a very acute C–C–C bond angle of 85.0° and co-planarity of the ring carbon atoms and two nitrogen centers. The reaction of [Rh(cod)Cl]$_2$ or [Ir(cod)Cl]$_2$ with **32** afforded the corresponding solid η^1-complexes **33** and **34**, respectively, thus providing evidence of a less allenic nature of **32** but its CDC character. The average IR stretching frequency of iridium carbonyl complex **36** was found to be about 2,002 cm^{-1}, which

Structure based
computational prediction
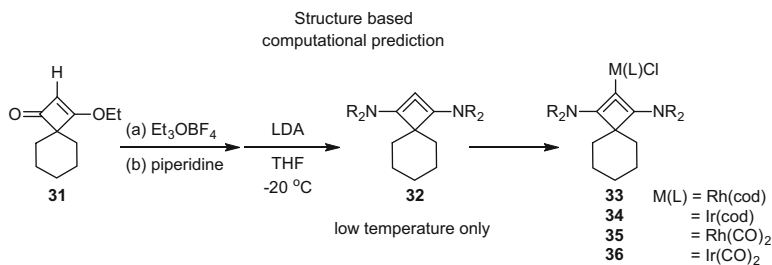
Scheme 8 Cyclic carbodicarbene based on a four-membered ring

was at the lower end of the range of strong donors such as abnormal carbenes ($1{,}999–2{,}020$ cm^{-1}). The molecular orbital analysis also disclosed that the central carbon atom exhibited the largest coefficients of HOMO and HOMO-1 at the central carbon atom, literally implicating the existence of two lone pairs of electrons at the central carbon atom which were σ- and π-symmetric, respectively. The theoretical analysis and the CDC character were further supported by a successful double protonation of cyclic **32** via addition of tetrafluoroboric acid.

2.5 Pincer-Type Carbodicarbenes

To extend CDCs to multidentate systems, Meek and coworkers developed the tridentate P–C–P carbodicarbene ligands **39**, which unfortunately could not be isolated in free form. The corresponding CDC precursors **38**, 1,4-diazepenium salts, were obtained in good yields via phosphination of substrate **37** with PR$_2$Cl in the presence of Et$_3$N. The salts **38** could directly be converted to the square-planar Rh complexes **40** using [Rh(cod)Cl]$_2$ and NaOMe as base (Scheme 9) [22]. Addition of AgBF$_4$ to complex **40** afforded cationic compounds **41**, which were used for crystal structure analysis. The Rh-CDC bond distance is around 2.043 Å, but the Rh-NCMe bond length of 2.029 Å is slightly longer than literature-reported values, showing a strong trans influence induced by the CDC.

Ong and coworkers also reported pincer CDC ligands with *bis*(pyridine) units covalently linked to the pendant arms of the CDC. The synthetic work derived from their previous work [14, 15] on CDC was employed to prepare the N–C–N scaffold. The synthesis of the dicationic salt **46** (pincer-type carbodicarbene precursor) started with a commercially available 1-iodo-2-nitrobenzene (**42**) (Scheme 10) [23], which was aminated with 2-aminopyridine in the presence of a palladium catalyst followed by a hydrogenation step to furnish diamine **44** in good yields (92%). The diamine **44** could subsequently be easily converted to the dicationic salt **46** in two steps, which eventually afforded the stable free pincer CDC **47** after deprotonation. The allenic moiety in **47** featured bond lengths of 1.333(2) and 1.324(2) Å, which were similar to those of monodentate CDC (see above). In contrast, the C–C–C bond angle was
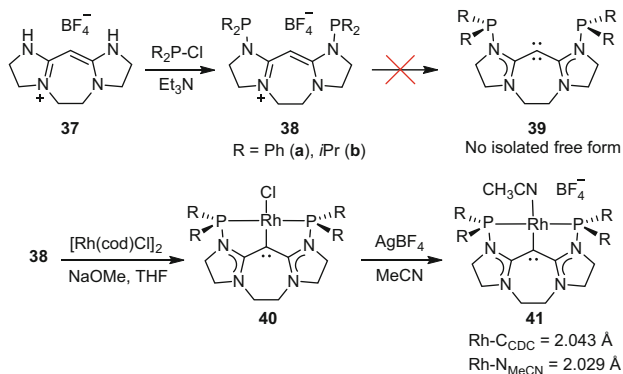
Scheme 9 Pincer carbodicarbene with P–C–P coordination sites
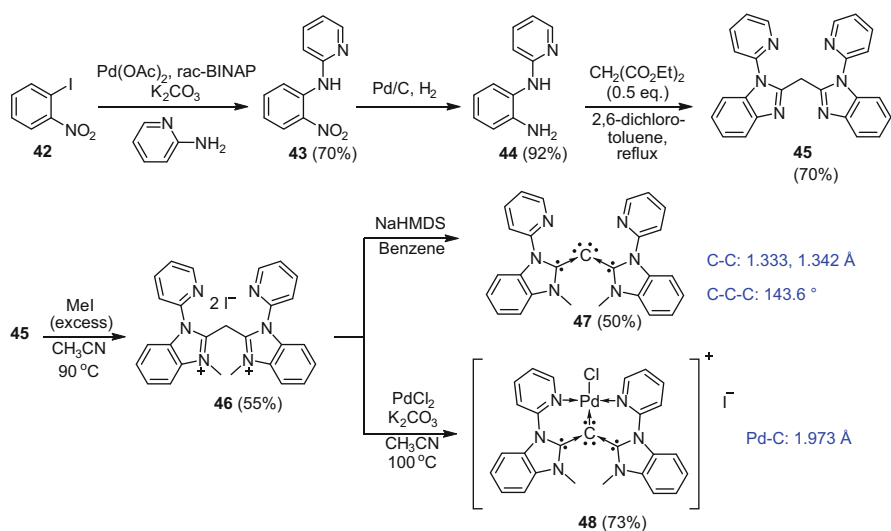
Scheme 10 Synthesis of pincer carbodicarbene **47** with N–C–N coordination sites

found to be rather large (143.6°) with an almost orthogonal torsion angle between the NHC planes (84°), which suggested some allenic character in **47**. Computational studies using the TopMod program were performed to understand this phenomenon. "TopMod" is a computational program used to study the electron density of bonding and lone pairs by performing the electron localization function (ELF) analysis of a molecular structure. The valence basin near this central atom of **47** was found to contain an electronic population with a value of 1.54 e⁻, displaying a pronounced CDC character at the central C atom of the pincer CDC. However, it also behaved more like an allene with less significant electronic population. This is likely due to the electron-withdrawing pyridine potentially diminishing the carbone character in

the CDC framework. Pd complex **48** supported by the pincer CDC ligand could be obtained by the reaction of PdCl$_2$ with the dicationic salt **46** in the presence of K$_2$CO$_3$ with heating. The structure of **48** consisted of a cationic palladium center with a square-planar environment of tridentate NCN and chloride coordination. The Pd-CDC bond distance of 1.973(3) Å is shorter than in the non-pincer CDC-Pd complex **14a** (2.101(4) Å).

2.6 Acyclic Carbodicarbenes Supported by Benzoxazol-2-Ylidene

In addition to the NHC-based CDCs, Bertrand and Ruiz examined the more π-accepting benzoxazol-2-ylidene moieties as supporting ligand units for possible CDC preparation. The synthetic route of CDC precursor **50** is depicted in Scheme 11 [24], which has similarities to the acyclic CDC **4** (see above). The strong metal base potassium bis(trimethylsilyl)amide (KHMDS) was used to deprotonate compound **50** to afford dimer **52** at room temperature, but no product related to expected free CDC **51** was observed. Free CDC **51** was only seen at −40°C by ^{1}H NMR spectroscopy, which then quickly dimerized to compound **52** at temperatures above −20°C. The dimerization is exothermically favorable with −99.0 kJ/mol based on theoretical analysis. The electronegativity of the oxygen atom in the benzoxazol-2-ylidene fragment unit has actually made the carbone center more electrophilic for the dimerization process. As a consequence, this allowed the intermolecular attack by another CDC molecule. The proposed hypothesis is consistent with the
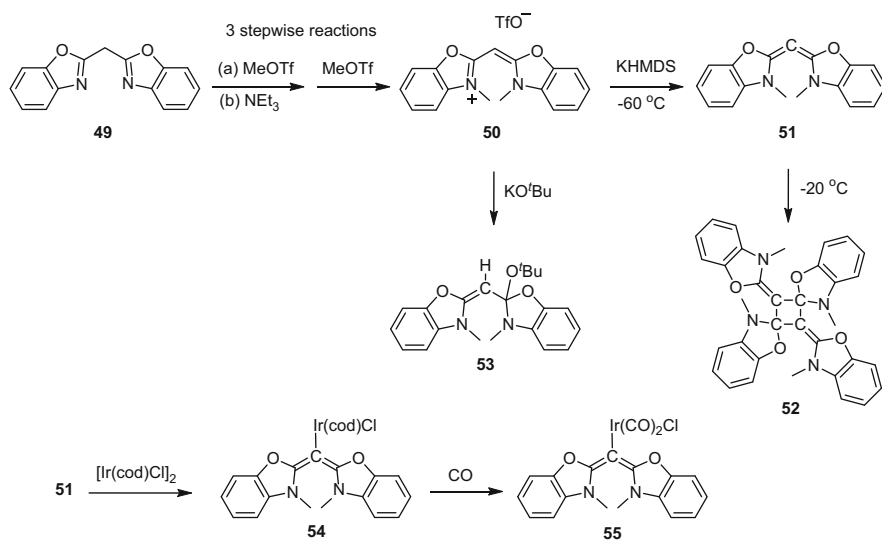
Scheme 11 Synthesis and reactivity of carbodicarbene **51** based on benzoxazol-2-ylidene subunit

experimental evidence that potassium *tert*-butoxide reacted with the cationic precursor **50** to give **53**. Nonetheless, the highly reactive **51** could be trapped by complexation of [Ir(cod)Cl]$_2$ to afford complex **54**, which was further transformed into **55** by treatment with carbon monoxide. The average carbonyl stretching frequency was about 2,009 cm^{-1} and corresponded to a Tolman electronic parameter (TEP) of 2,037 cm^{-1}, which is a weaker donor than normal CDC but is still stronger than typical NHCs (2,040–2,055 cm^{-1}).

2.7 Nontraditional Carbodicarbenes

Stephan and coworkers have prepared a nontraditional CDC supported by flanking cyclopropenylidene units. Starting from compound *bis*(1,2-diphenylcyclopropen-3-yl)methane **56**, they could effectively produce a conjugate acid of CDC precursor **57** in 76% yield by using two equivalents of trityl tetrafluoroborate (Scheme 12) [25]. The molecular structure of **57** indicated that both three membered rings are canted with each other by an angle of 16.5° arising from steric restrictions imposed by axial phenyl groups. The distances of the central carbon atom to the adjacent rings are 1.378(3) Å and 1.381(3) Å, respectively, supporting the presence of a 3-center 2-electron (3c-2e) π-bond. The free CDC **59** can be obtained by deprotonation of **57** using a strong metal base. Unfortunately, CDC **59** was only stable at low temperature thus only allowing NMR characterization. Stephan and Frenking calculated the structure of **59** based on DFT at the M06-2X/Def2-SVP level and found that the central carbon is in an almost linear environment (179.98°) with short C–C distances of 1.308 Å. The natural bond analysis pointed out that the HOMO and HOMO-1 orbitals are delocalized on the central carbon with double bond character along C–C–C moiety, thus suggesting an allenic character. Experimentally however, the conjugate acid **57** can be further protonated at the central carbon using an excess HOTf to form the methylene bridged dicyclopropenium salt **58**, confirming the CDC character of **59**. The synthesis of η^1-Lewis acid-base adducts of B(C$_6$F$_5$)$_3$ **60** and GaCl$_3$ **61** confirmed its strong binding
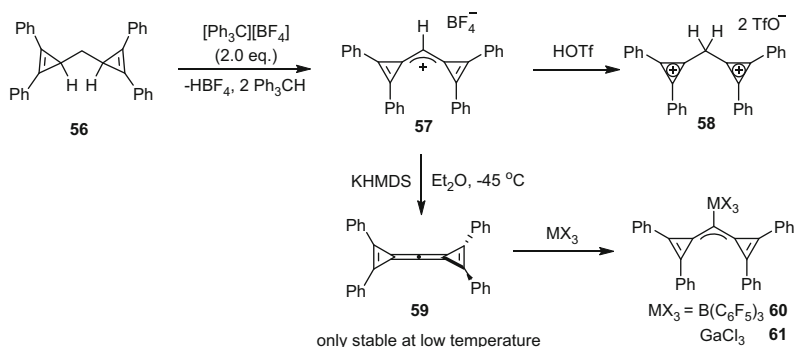
Scheme 12 Carbodicarbene **59** flanked with cyclopropenylidene subunits

ability for Lewis acid components. Both complexes have C–C bond distances of ~1.39 Å observed between the flanking carbon and the central carbon, signifying a more CDC type than allenic character. The molecular structure of the $GaCl_3$ adduct **61** featured a pyramidalization of the gallium center (Σ ClGaCl) of ~320.7°, which correlated with a Tolman electronic parameter (TEP) of 2,044.5 cm^{-1}. This indicated that CDC **59** is a stronger donor than both NHCs and CAACs but weaker than other CDCs (see above).

As outlined by the different CDCs described in this section variation of their structures allows for the controlled manipulation of their electronic structure and donor properties. Overall, CDCs are extremely strong donor ligands which surpass even NHCs and other singlet carbenes. For comparison, some of these features and parameters of various carbodicarbenes and selected carbenes are again highlighted in Table 1, thus underlining the unique properties of CDCs.

Table 1 Comparison of spectroscopic properties of CDCs and NHCs
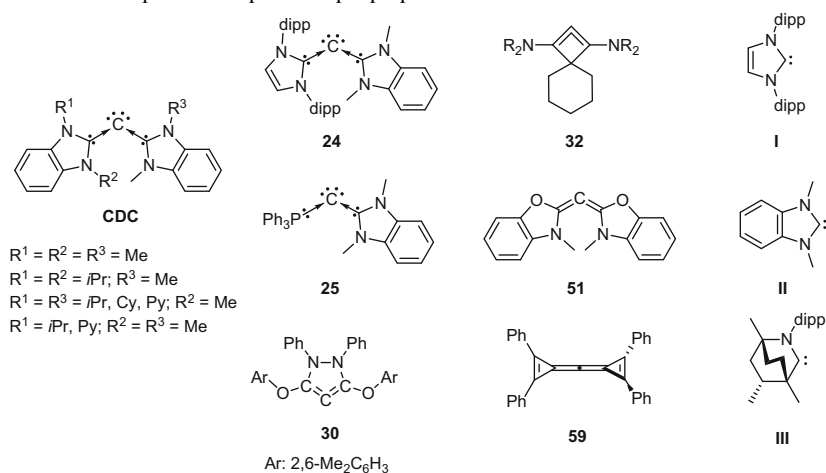
Compounds	^{13}C NMR	TEP	C–C (Å)	C(P)–C–C (°)
CDC	109.8–119.1	2,009–2,024	1.318–1.346	134.8–146.1
24	109.9	2,009	1.344, 1.318	146.1
25	64.4	–	1.338	143.0
30	115.5	2,027	1.370, 1.386	97.5
32	151.6	2,025	–	–
51	105.5	2,037	–	–
59	133.4	2,045	–	–
I	220.6	2,045	–	–
II	224.9	2,045	–	–
III	334.4	2,045	–	–

3 Carbodicarbenes in Catalysis

Homogeneous catalysis using transition metal complexes supported by *N*-heterocyclic carbenes is a common and mature field. Interestingly, endeavors involving CDC-based catalysts have long been neglected since the first isolation of CDC in 2008. The groups of Meek and Ong have been the first who employed CDCs as supporting ligands in catalysis and thus applied the particularly strong σ-donor properties of CDCs in this direction. This section highlights the success in this chemistry thus demonstrating the huge potential of this class of ligands.

3.1 Alkene Hydroamination and Hydroheteroarylation

The Meek group has demonstrated that pincer CDC Rh(I) complex **40** effectively promotes intermolecular hydroamination of 1,3-diene substrates with various aryl and alkyl amines with good regioselectivity (Scheme 13) [22]. As such, complex **40** (1–5 mol% loading) in the presence of AgBF$_4$ for halide abstraction was found to catalyzed the hydroamination of phenyl 1,3-butadiene (**S1-a**) with *p*-CF$_3$ or *p*-methoxy-substituted anilines (**S2**) to afford allylic amines (**S4**) with >98% γ-selectivity in high yield. Alkyl amines (**S3**) were also successfully applied in the hydroamination process; however, higher temperatures (80°C) than for aryl amines (50–60°C) were required to obtain good yields. Complex **40** also catalyzed the hydroamination of alkyl diene substrates to deliver allylic amine products bearing di- or tri-substituted olefins (up to >98% γ-selectivity, **S1-b**, **S1-c**, **S1-e**). In addition, numerous functional groups
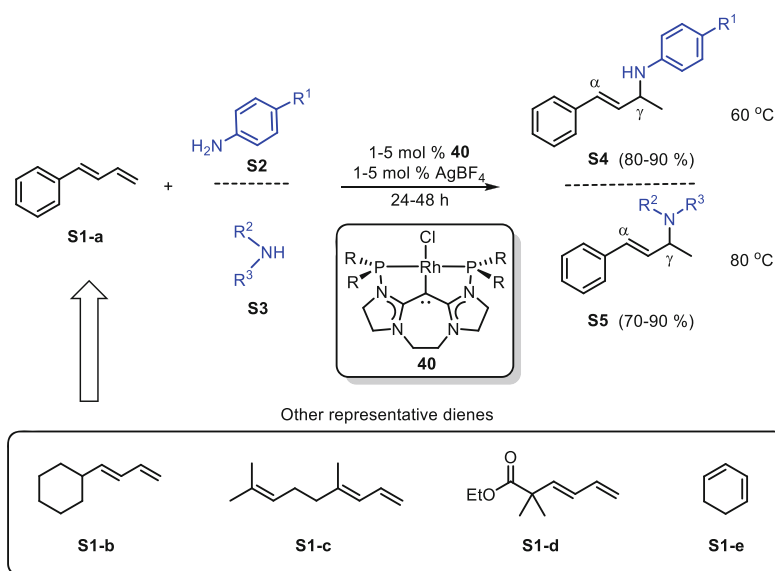
Scheme 13 Hydroamination of diene with amines using CDC-Rh complex **40**

are also tolerated with this protocol, as demonstrated by representative substrate containing ester (**S1-d**).

In a remarkable study, Meek and coworkers utilized Lewis acids to improve the catalyst reactivity by secondary binding to the carbon(0) ligand in a transition metal complex thus making use of both lone pairs of electrons at the central carbon atom. Rhodium complex **62** and its activated congener **63** were used to provide proof to this concept (Scheme 14) [26]. Interestingly, the activity of the CDC-Rh pincer complex **62** in the hydroheteroarylation reaction of dienes with indole and heteroarenes could be considerably accelerated by adding LiBF$_4$ or other Lewis acid salts. The reaction is highly selective with excellent yields (up to 98% yield and >98:2 γ:α) for hydroheteroarylation of indoles and pyrroles (**S6–S7**). Mechanistic investigation revealed that the Lewis acid reversibly binds in secondary fashion to the central carbon atom of the coordinated CDC in the metal complex. This phenomenon of secondary binding effect could be evidenced by reaction of complex **64** with HBF$_4$. The resulting protonation at C(0) center in complex **65** increased the IR stretching frequency of the carbonyl ligand (2,016 cm^{-1}), indicating a significant decrease in π-back-donation and decrease in electron density at Rh. Such a secondary binding feature has not been reported for other traditional ligands so far. The binding of the Lewis acid creates a more electron-deficient Rh center in **63** and subsequently invokes a more positive charge at the bound alkene thus resulting in a further activation. This methodology was compatible with a variety of terminal and internal dienes containing ester, alkyl halide, as well as boronate ester functional groups.
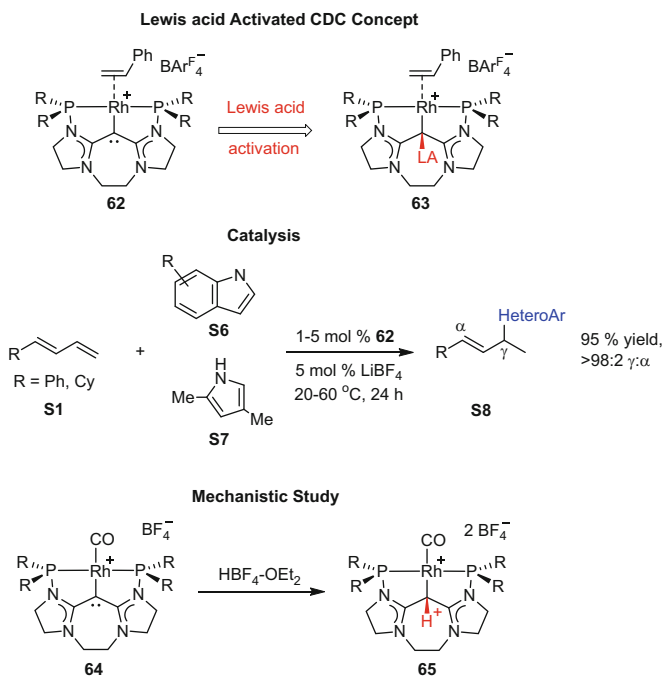
Scheme 14 Hydroheteroarylation of diene with amines

3.2 Carbon-Carbon Cross-Coupling Reaction

Ong and Hsu have examined carbodicarbene to explore the catalytic activity of the pincer palladium complex **48** for the Mizoroki-Heck cross-coupling reaction (Scheme 15) [23]. The coupling stilbene product **S11** with different functional groups could be obtained with aryl bromides or chlorides (**S9**) and styrene (**S10**) in high yields. The loading of palladium catalyst was very low (0.5 mol%), and catalysis could be performed under organic solvent-free conditions using aqueous media with ammonium salts. The flexibility of catalyst **48** was also demonstrated in the Suzuki-Miyaura cross-coupling reaction between boronic acids (**S12**) and aryl bromides (**S13**). In general, the yields for various scopes of aryl bromide and phenyl boronic acid with electron withdrawing and donating functionalities were excellent. In addition, the relatively hindered 2-bromo-1,3,5-trimethyl benzene was also found to be a capable coupling partner with different boronic reagents.

3.3 Olefin Hydrogenation

Stephan's group has probed cyclic CDC **30**'s role in catalytic hydrogenation processes. They postulated that strongly σ- and π-basic ligands would make the ruthenium complex a highly active catalyst. Equimolar combinations of complex RuHCl(CO)
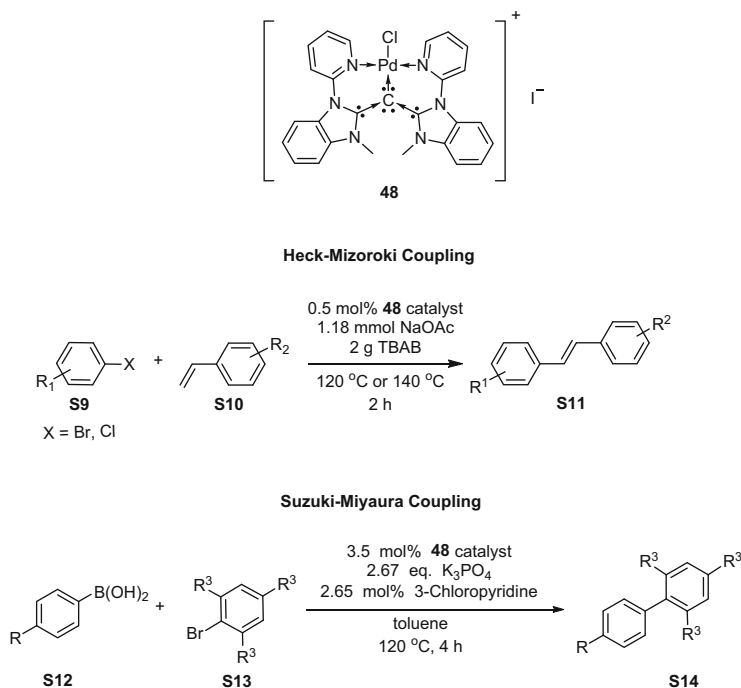
Scheme 15 Carbon-carbon cross-coupling reactions based on Pd complex **48**

(CDC)(SIMes) (**67**) and Me$_3$SiOSO$_2$CF$_3$ gave Ru complex **68**, which acts as a catalyst for olefin hydrogenation (Scheme 16) [27]. It was further postulated that hydrogenation activity could be increased if the halide ligand of the complex could be substituted with a weakly coordinating anion, which could more easily generate an empty site for effective binding. By doing so, quantitative hydrogenation of 1-hexene could be achieved in 15 min with 0.01 mol% catalyst loading of **68** under 20 bar of H$_2$ pressure at 25°C. Even unreactive alkenes like cyclohexene or the tertiary olefin 2-methyl-2-butene were also completely hydrogenated within an hour. However, the methodology employing **68** is not suitable for those tetra-substituted olefinic 2,3-dimethyl-2-
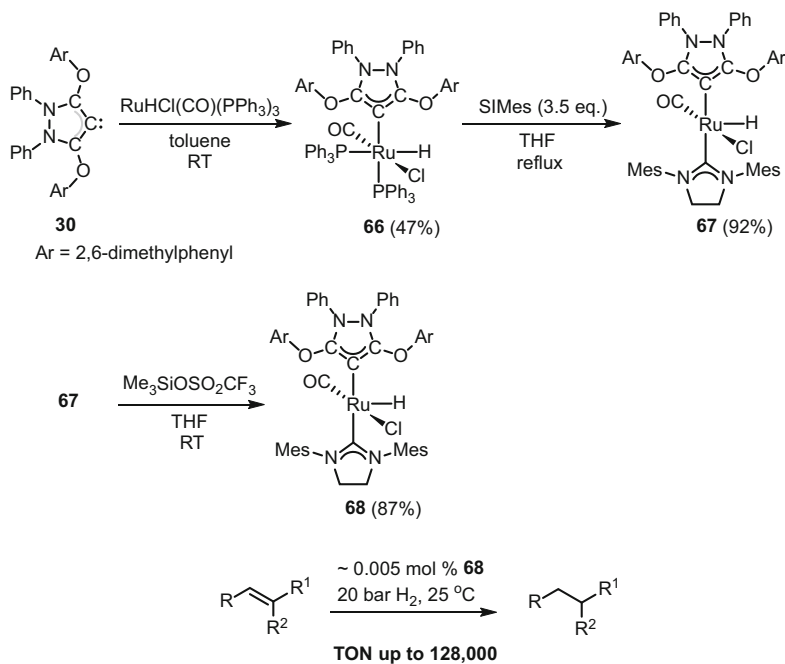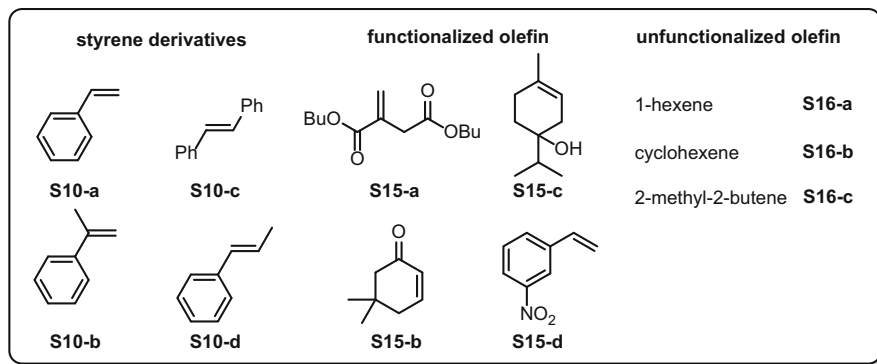
Scheme 16 Olefin hydrogenation using carbodicarbene Ru complex **68**

butenes. To date, the hydrogenation reactivity of **68** is superior to that of other known [NHC]-Ru and phosphine complexes like Ru(PCy$_3$)$_2$(CO)HCl, Ru(SIMes)(PPh$_3$) (CO)HCl, and Wilkinson's catalyst, RhCl(PPh$_3$)$_3$. Several functional olefins (**S15**) and styrene derivatives (**S10**) are also suitable for this reaction.

3.4 CO$_2$ Activation via Metal-Free Carbodicarbene Catalysis

The first application of CDCs in organocatalysis was reported by Ong and Chen by means of the methylation of amines with CO$_2$ as C1 source [15]. The reaction was performed in THF solution with diphenylamine (**S17**) and 9-borabicyclo[3.3.1] nonane (9-BBN) under 1 atmosphere of CO$_2$ using 10 mol% CDC **24** catalyst to afford *N*-methyldiphenylamine **S19** in excellent yields of 90%. The substrate library was extended to many secondary and primary aryl amines, all affording the products in good yields. In addition, cyclic alkylamine such as piperidine (**S17b**), morpholine (**S17c**), and sterically hindered primary anilines (**S18a**) were also readily methylated using metal-free CDC catalyst **24**. The proposed mechanism is illustrated in Scheme 17. Adduct **69** was found to be the crucial intermediate
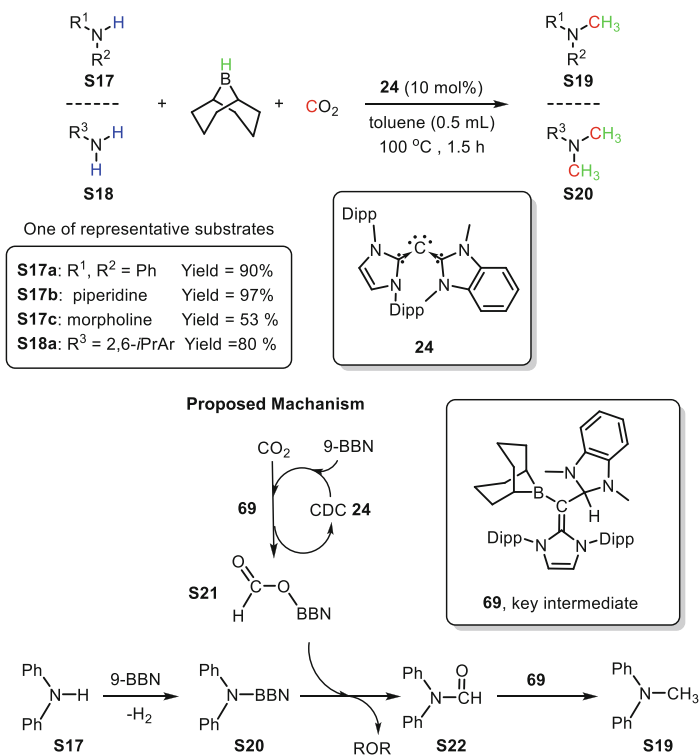
Scheme 17 Methylation of amine via CO$_2$ fixation process catalyzed by carbodicarbene **24**

along the reaction pathway. Its formation could be evidenced by the stoichiometric reaction of **24** with 9-BBN giving way to the 1,2 addition of the B–H bond across one of the C–C bonds in the allenic moiety. **69** was thought to be a hydride transporter in this process to reduce CO_2 to methyl. In short, this work impressively showed for the first time the potential utility of CDCs also as organic catalysts for the synthesis of valuable platform chemicals from renewable carbon feedstocks.

4 Conclusions and Outlook

Carbodicarbenes are a unique subclass of carbone ligands consisting of a divalent carbon(0) center with two lone pairs of electrons coordinated by two σ-donor NHC/carbene ligands, which stabilize the otherwise electronic deficient carbon center. The captodative bonding situation between the central carbon atom and the flanking carbene ligands results in a unique chemical character of CDCs that distinguishes them from classical allenes. Instead CDCs possess unusual electronic properties, which lead to new reactivity patterns and a special coordination behavior which also substantially differs from conventional NHCs. Thereby, the most prominent feature of carbodicarbenes concerns their strong σ-donor capacity. This makes them even more electron-rich and thus stronger donors than NHCs and other carbenes in general, which has impressively been demonstrated by the application of CDCs in homogenous catalysis. Several key developments in carbodicarbene chemistry have been made in the last 10 years, which provide foundation for more interesting chemistry to come. This includes innovations in synthetic routes to allow for a greater diversity in the framework of carbodicarbenes as well as the development of applications in organocatalysis and as supporting ligands for transition metal complexes and catalysts.

Despite these advancements in CDC chemistry, there is still room for improvement in many directions, above all in the development of further (also stereoselective) catalytic applications. Also, the electronic structure remains subject of controversial discussions. While the electronic structure of carbodicarbenes described by a dative model has proven useful to rationalize many chemical phenomena in carbodicarbene chemistry, the covalent ylidic Lewis structure brought up by Himmel, Krossing, and Schnepf [9, 11] also explains the special reactivity of CDCs. Thus, it remains a critical task for many theoreticians and experimentalists to put more efforts in providing more insights into the bonding of carbodicarbenes. Another challenge that remains for both, the experimental and synthetic community, is the use of the second latent lone pair at the central carbon in carbodicarbenes for synthetic applications. So far, most applications only rely on the strong σ-donation of CDCs, while the π-basicity remains unused. The realization of processes employing the σ- as well as π-basicity of carbones would broaden their application in coordination with chemistry such as by introducing cooperative effects invoked by bimetallic interactions.

References

1. Enders D, Niemeier O, Henseler A (2007) Chem Rev 107:5606–5655
2. Díez-González S, Marion N, Nolan SP (2009) Chem Rev 109:3612–3676
3. Hopkinson MN, Richter C, Schedler M, Glorius F (2015) Nature 510:485–496
4. Tonner R, Öxler F, Neumüller B, Petz W, Frenking G (2006) Angew Chem Int Ed 45:8038–8042
5. Tonner R, Frenking G (2007) Angew Chem Int Ed 46:8695–8698
6. Inés B, Patil M, Carreras J, Goddard R, Thiel W, Alcarazo M (2011) Angew Chem Int Ed 50: 8400–8403
7. Alcarazo M (2011) Dalton Trans 40:1839–1845
8. Zhao L, Hermann M, Holzmann N, Frenking G (2017) Coord Chem Rev 344:163–204
9. Himmel D, Krossing I, Schnepf A (2014) Angew Chem Int Ed 53:370–374
10. Frenking G (2014) Angew Chem Int Ed 53:6040–6046
11. Himmel D, Krossing I, Schnepf A (2014) Angew Chem Int Ed 53:6047–6048
12. Dyker CA, Lavallo V, Donnadieu B, Bertrand G (2008) Angew Chem Int Ed 47:3206–3209
13. Fürstner A, Alcarazo M, Goddard R, Lehmann CW (2008) Angew Chem Int Ed 47:3210–3214
14. Chen W-C, Hsu Y-C, Lee C-Y, Yap GPA, Ong T-G (2013) Organometallics 32:2435–2442
15. Chen W-C, Shen J-S, Jurca T, Peng C-J, Lin Y-H, Wang Y-P, Shih W-C, Yap GPA, Ong T-G (2015) Angew Chem Int Ed 54:15207–15212
16. Alcarazo M, Radkowski K, Mehler G, Goddard R, Fürstner A (2013) Chem Commun 49: 3140–3142
17. Lavallo V, Dyker CA, Donnadieu B, Bertrand G (2008) Angew Chem Int Ed 47:5411–5414
18. Fernández I, Dyker CA, DeHope A, Donnadieu B, Frenking G, Bertrand G (2009) J Am Chem Soc 131:11875–11881
19. Christl M, Engels B (2009) Angew Chem Int Ed 48:1538–1539
20. Lavallo V, Dyker CA, Donnadieu B, Bertrand G (2009) Angew Chem Int Ed 48:1540–1542
21. Melaimi M, Parameswaran P, Donnadieu B, Frenking G, Bertrand G (2009) Angew Chem Int Ed 48:4792–4795
22. Goldfogel MJ, Roberts CC, Meek SJ (2014) J Am Chem Soc 136:6227–6230
23. Hsu Y-C, Shen J-S, Lin B-C, Chen W-C, Chan Y-T, Ching W-M, Yap GPA, Hsu C-P, Ong T-G (2015) Angew Chem Int Ed 54:2420–2424
24. Ruiz DA, Melaimi M, Bertrand G (2013) Chem Asian J 8:2940–2942
25. Pranckevicius C, Liu L, Bertrand G, Stephan DW (2016) Angew Chem Int Ed 55:5536–5540
26. Roberts CC, Matías DM, Goldfogel MJ, Meek SJ (2015) J Am Chem Soc 137:6488–6491
27. Pranckevicius C, Fan L, Stephan DW (2015) J Am Chem Soc 137:5582–5589

Sulfur Ylides in Organic Synthesis and Transition Metal Catalysis

Rik Oost, James D. Neuhaus, Jérémy Merad, and Nuno Maulide

Abstract Sulfur-based ylides have long been used for a number of classical transformations, in particular for the synthesis of small ring systems and various rearrangement reactions. By combining the unorthodox reactivity of such ylides with the strength and flexibility of transition-metal catalysis, a growing number of groups have in recent years looked to expand their application in organic synthesis. This chapter aims to summarise recent developments in transition-metal-catalysed sulfonium/sulfoxonium ylide reactions as well as to offer historical perspective. In overviewing the successes in this area, the authors hope to encourage others into this growing field.

Contents

R. Oost, J.D. Neuhaus, J. Merad, and N. Maulide (✉)
Institute of Organic Chemistry of the University of Vienna, Vienna, Austria
e-mail: nuno.maulide@univie.ac.at

1   Introduction

Sulfonium and sulfoxonium ylides are versatile precursors for a diverse range of chemical transformations. They are, for example, widely used as methylene synthons in the formation of small rings such as cyclopropanes, epoxides and aziridines. Sulfonium/sulfoxonium ylides can be visualised as carbanions, stabilised by an adjacent positively charged sulfur atom. Their stability and reactivity are largely governed by the nature of substituents adjacent to the carbanion; thus, electron-withdrawing groups (such as ester, keto or amide groups) stabilise sulfonium/ sulfoxonium ylides and lead to more practical, bench-stable reagents. This additional stabilisation is, however, accompanied by a marked reduction of reactivity. Recently, sulfur ylides have been reported as versatile substrates in transition-metal catalysis, a combination that vastly expands the potential of such ylides in organic synthesis. In this chapter, recent advances in the field of transition-metal-catalysed reactions of sulfonium and sulfoxonium ylides are highlighted, grouped into three broad sections: carbene-free processes, reactions that employ sulfonium ylides as carbene precursors, or reactions that form sulfonium ylides in situ from metal carbenoids for cascade reactions.

2   Metal-Ylide Complexes

Sulfonium ylides are known to react with a variety of electrophilic substrates, in particular electron-poor olefins. Simple olefins, however, are not attacked by even the most nucleophilic ylides. Activation of these olefins by complexation with a transition metal is a good strategy to increase their electrophilicity. However, stoichiometric studies on such activation employing Pd(II) salts only afforded metal-ylide complexes [1].

Sulfonium ylides can behave as ligands, due to the ability of the carbanion to donate electron density to a transition metal. In the case of α-keto-stabilised ylides, various binding modes have been reported, due to their ambidentate character [2]. The coordination chemistry of these compounds has been intensively studied. The more frequently observed carbanion coordination mode can be found in complexes with Pd(II) [1], Pt(II) [1, 3], Hg(II) [4], Cd(II) [5] and Ag(I) [6], whilst enolate oxygen coordination is limited to a small number of complexes with hard oxophilic metals such as W(0) [7].

Although the coordination chemistry of sulfonium ylides to transition metals has been extensively studied, to date, very few applications of these complexes to synthesis have been reported. Pd(II) complexes with sulfonium ylide ligands can serve as catalysts in Suzuki-Miyaura coupling of aryl bromides or chlorides with aryl boronic acids [8–10] (Scheme 1). The same catalyst was also employed in the Mizoroki-Heck coupling of aryl halides [11]. These complexes are efficient catalysts and can be used in catalyst loadings as low as 0.05 mol%. Moreover, their stability under aerobic conditions and ease of preparation makes them interesting replacements for phosphine ligands. However significant development is necessary before these ligands can be routinely employed.

3 Non-carbene-Based Transition-Metal-Mediated Reactions of Sulfur Ylides

3.1 Sulfur Ylides as Single-Carbon Synthons in Formal (n + 1) Cycloadditions

The first publication detailing the combination of sulfur ylides and transition metals for the purpose of synthesis came in 1976 from the group of Norman Holy [12]. The preparation of the cyclopropane derived from β-nitrostyrene **1** was unsuccessful using palladium and diazomethane, and so investigations moved on to look at achieving a Corey-Chaykovsky style cyclopropanation. When exposed to sulfoxonium ylide **2**, the β-nitrostyrene (**1**) was fully consumed, and only an amorphous solid was obtained. Although this solid could not be characterised, Holy et al. decided to temper the reactivity of the sulfoxonium ylide through treatment with stoichiometric copper iodide. This time when the β-nitrostyrene was introduced to a solution containing the preformed Cu-sulfoxonium species, a smooth reaction proceeded, without affording any of the amorphous precipitate. What was observed following workup and purification, however, was not the expected (2 + 1)-Corey-Chaykovsky cyclopropanation, but a five-membered 2-isoxazoline N-oxide **3**, resulting from a formal (4 + 1) process (Scheme 2). Following the Michael addition
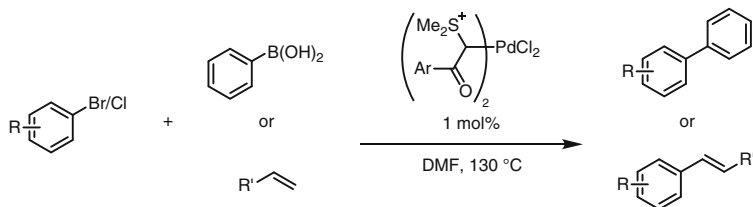
Scheme 1 Sulfonium ylides as ligands in cross-coupling chemistry
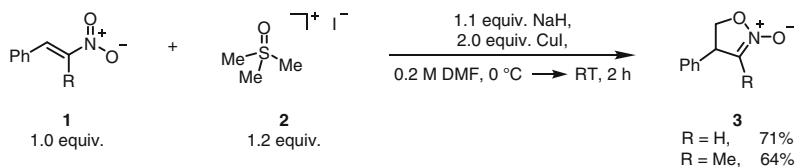
Scheme 2 The first Cu-promoted formal (4 + 1) cycloaddition

of the sulfoxonium ylide, 3-exo-tet, C-based ring closure to the cyclopropane was less favourable than a 5-exo-tet, O-based ring closure.

Exploration of this process found that similar Michael acceptors did not behave analogously, either resulting in polymerisation (cinnamonitrile and diethyl benzylidenemalonate), cyclopropanation (chalcone), or the recovery of the majority of the starting material (ethyl cinnamate and cyclohexenone).

A number of similar formal (4 + 1)-cycloadditions involving sulfoxonium and sulfonium ylides have been reported over the following decades. They generally involved the use of simple Lewis acidic or hydrogen-bonding catalysts to activate systems for the initial conjugate addition event, often in an enantioselective manner [13].

In 2012, the group of Bolm published a report involving a formal (4 + 1) cycloaddition of a sulfonium ylide, catalysed by a chiral copper complex (Fig. 1) [14]. By treating α-halo hydrazones (4) with a weak base, a simple elimination reaction afforded highly reactive azoalkenes, which had been previously shown to undergo conjugate addition reactions [15]. Bidentate coordination with a chiral Cu-BINAP complex facilitated a controlled (4 + 1)-type process, which resulted in the formation of enantioenriched dihydropyrazoles (5). The enantioselectivity of the process ranged from good to excellent, over a wide range of substrates (Scheme 3). Furthermore the reaction was successful on a gram scale, reflecting the robust nature of this chemistry.

In 2014, a conceptually distinct process emerged from the group of Xiao [16]. In this report, the generation of a suitable coupling partner for the sulfonium ylide was achieved through an asymmetric, decarboxylative Tsuji-Trost-like allylic functionalisation. A range of enantioenriched 2-acyl, 3-vinyl indoles was synthesised in this manner, tolerating electron-withdrawing, electron-donating and halide functionality on the aromatic backbone and a broad scope of mono-stabilised sulfonium ylides (Scheme 4).

The postulated mechanism for this transformation is relatively straightforward (Fig. 2). Following oxidative addition of the Pd(0) species into the allylic C–O bond, decarboxylation affords zwitterionic intermediate 6. Electrostatic interactions then control the addition of the stabilised sulfonium ylide, affording the AAA (asymmetric allylic alkylation) product chelated to the metal complex. Decomplexation must occur to allow for bond rotations required to achieve the stereoelectronic requirements for the ring-closing S_N2 attack.

2014 saw the application of nucleophilic iron complexes to the decarboxylative (4 + 1)-cycloaddition reaction by the same group (Scheme 5) [17]. Although the
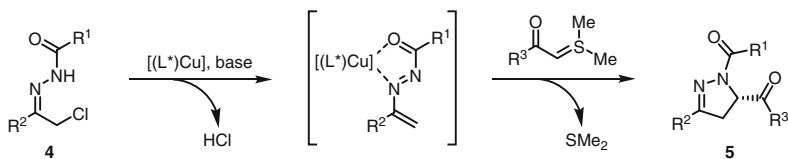
Fig. 1 Chiral Lewis acid-promoted, formal (4 + 1) cycloaddition

(84%, 87:13 er)   (91%, 97:3 er)   (88%, 94:6 er)   (93%, 93:7 er)
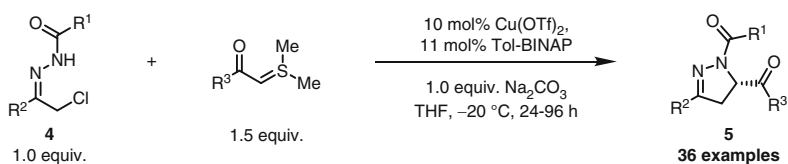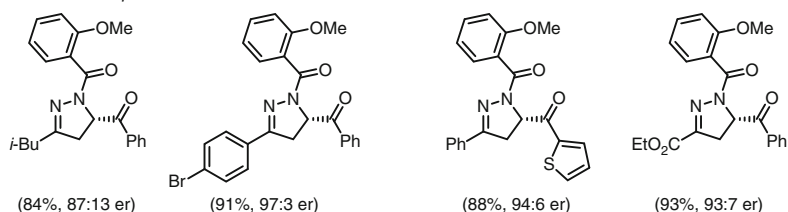
Scheme 3 Scope of dihydropyrazole formation

(86%, 99% *ee*)   (81%, 92% *ee*)   (86%, 93% *ee*)   (86%, 95% *ee*)
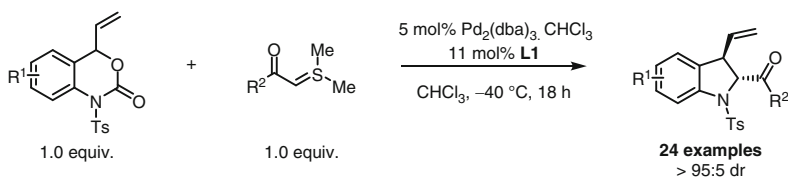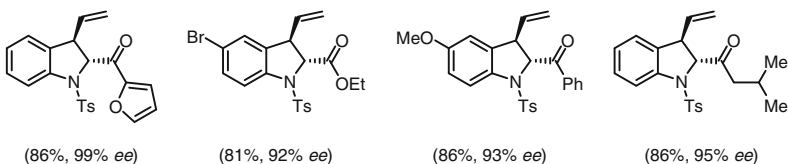
Scheme 4 Palladium-catalysed decarboxylative (4 + 1) cycloaddition for the asymmetric synthesis of indoles

reaction was no longer asymmetric, high yields were achieved for a wide range of substrates, and the excellent diastereoselectivity was maintained. The high abundance and low price of iron catalysts, coupled with their low biological and environmental impact, make them highly applicable for practical systems, which have been reflected in a recent renaissance in Fe-catalysis [18].
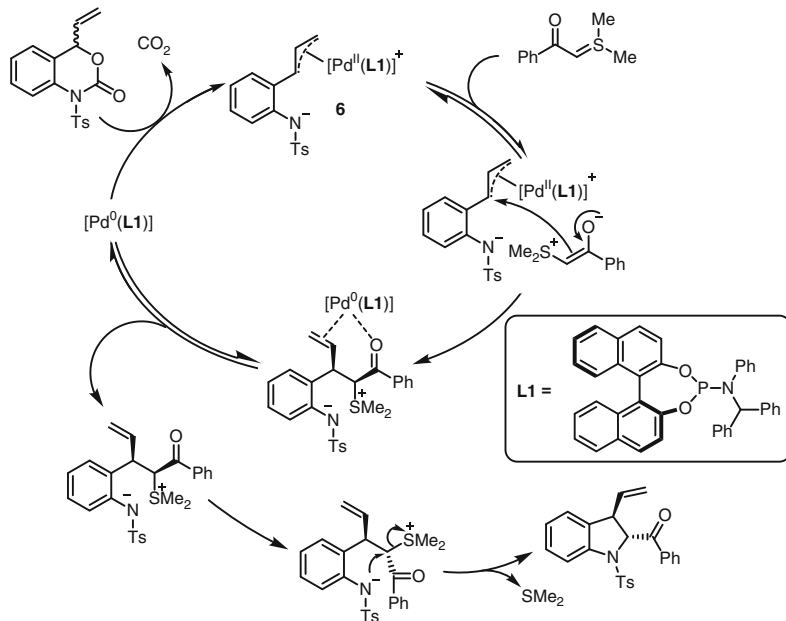
Fig. 2 The mechanism of Pd-catalysed decarboxylative formal (4 + 1) cycloaddition
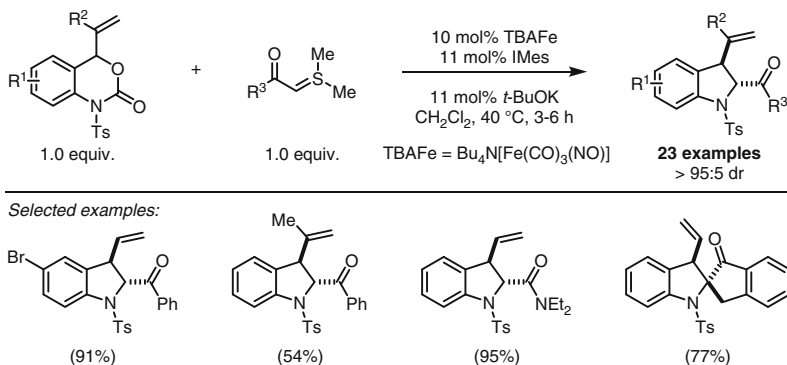
Scheme 5 Iron-catalysed decarboxylative formal (4 + 1) cycloadditions

Swiftly following the aforementioned publication was a Cu-based report, in which instead of an asymmetric *allylic* alkylation, the *propargylic* variant was accomplished (Scheme 6). The combination of copper triflate and a PyBOX ligand achieved excellent yields and good to excellent enantioselectivity over a wide range of substrates. Unlike the previous reports, it was found that generation of the sulfonium ylide in situ from the readily available and bench-stable sulfonium salt with Hünig's base afforded higher enantioselectivity [19]. Although the authors do
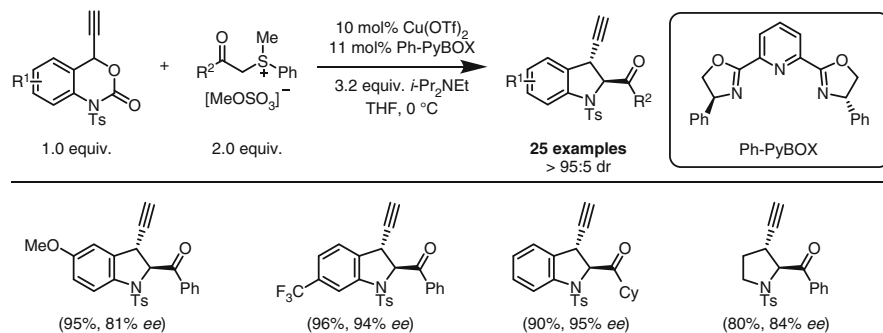
Scheme 6 Cu-catalysed decarboxylative formal (4 + 1) cycloadditions

not propose a rationale for this observation, mechanistic work by van Maarseveen has suggested that Hünig's base can play a key role in promoting the formation of the active enantioselective multinuclear complex [20].

The mechanism (see Fig. 3) of this process is similar to the previously discussed reports. However, the mode of activation by the transition-metal catalyst is subtly different. Deprotonation of the Cu-complexed terminal alkyne affords copper acetylide **7**. Decarboxylation of this intermediate generates a copper-allenylidene species, an intermediate exploited in a number of catalytic processes involving Ru and Cu over the past decade [21].

In 2017 Doyle and co-workers demonstrated that sulfonium ylide cycloaddition chemistry was not limited to just the examples described so far in this section. By utilising enoldiazo compounds as three carbon synthons [22], they successfully demonstrated the first transition-metal-mediated formal (3 + 1)-cycloaddition of stabilised sulfonium ylides (Scheme 7) [23]. By employing a bulky BOX-ligand, excellent enantio- and diastereoselectivities were observed.

Based on previous observations on the reactivity of enoldiazo compounds, the authors proposed the mechanism outlined in Fig. 4. An active metal-carbenoid species, generated from the enoldiazo precursor, is attacked at the vinylogous carbon by the sulfonium ylide, followed by an intramolecular S_N2 to generate a Cu-cyclobutyl complex. The key copper-carbenoid **8** can also be generated from the donor-acceptor cyclopropene **9**, in identical enantioselectivity and yield as with the enoldiazo precursor.

3.2 Transition Metals as π-Acid Catalysts

Both the Holy [12] and Bolm [14] methods detailed previously involve the addition of nucleophilic sulfur-based ylides to electron-poor π-bonds in Michael-type reactivity. Based on this encouraging precedent, a number of groups have investigated the potential of using an external π-acid to activate otherwise unreactive π-systems to nucleophilic attack.
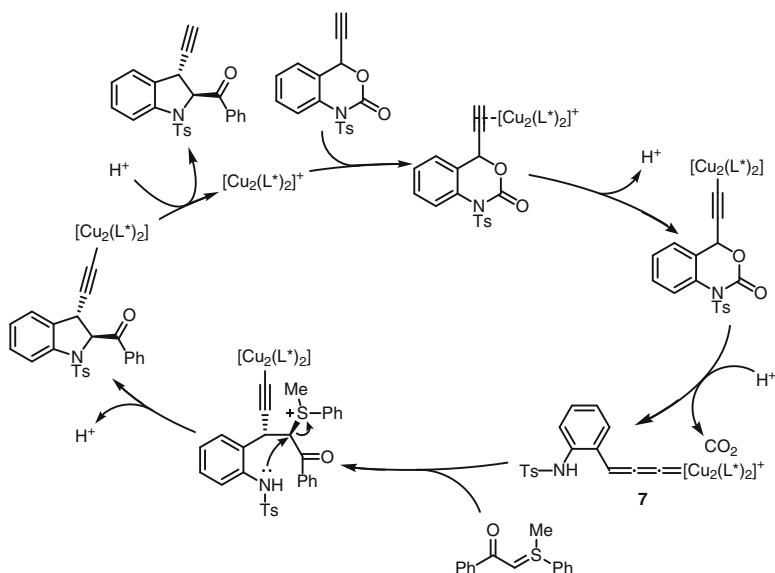
Fig. 3 Cu-allenylidene intermediates in decarboxylative formal (4 + 1) cycloadditions
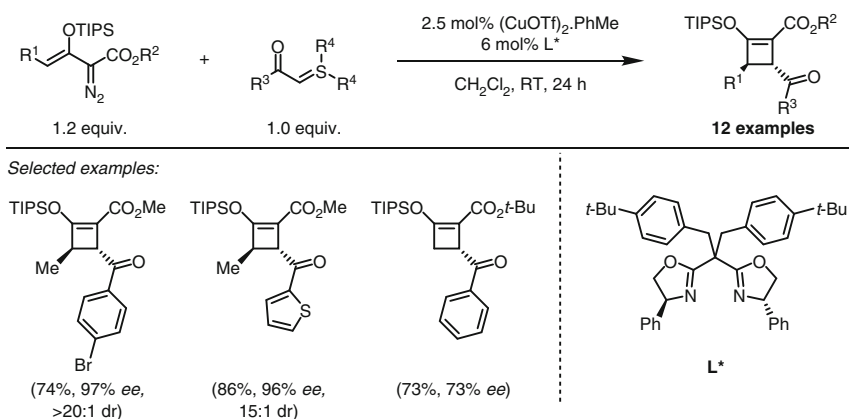
Scheme 7 Doyle's Cu-catalysed asymmetric formal (3 + 1) cycloaddition

In 2012 two publications were released within months of each other from the groups of Skrydstrup and Maulide, each detailing the synthesis of furans through the combination of stabilised sulfonium ylides and unactivated alkynes. The first of these, from the Skrydstrup group, used a cationic Au^I complex to couple simple terminal alkynes with mono-stabilised sulfonium ylides in an intermolecular process, yielding 2,4-disubstituted furans (Scheme 8) [24].

The second involved the intramolecular cyclisation of doubly stabilised sulfonium ylides, synthesised through an ylide transfer reaction [25], to generate a
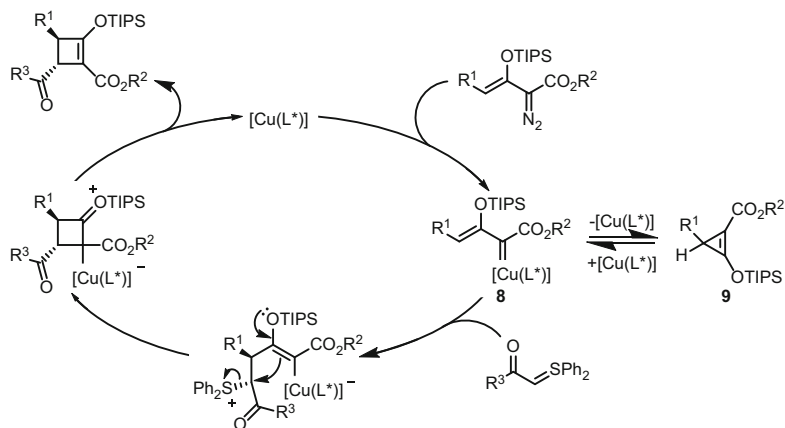
Fig. 4 Mechanism of the formal (3 + 1) cycloaddition involving sulfonium ylides
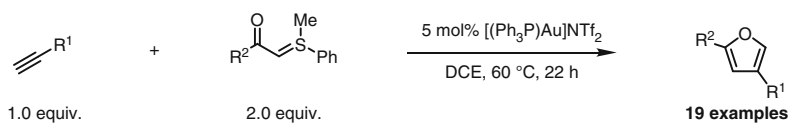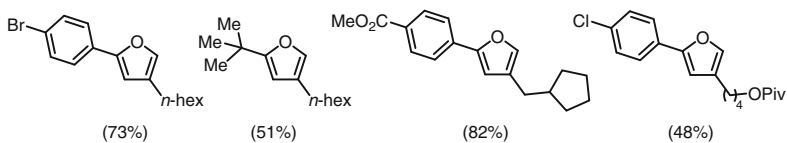
Scheme 8 Skrydstrup's intermolecular furan synthesis
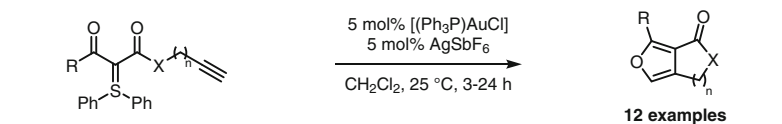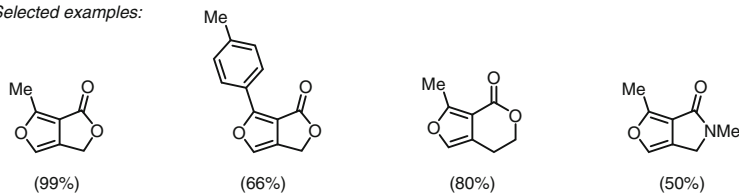
Scheme 9 Maulide's intramolecular furan synthesis

lactone-fused furan ring [26]. A similar catalyst was used to effect the transformation, and a number of different tethers were evaluated (Scheme 9).

The mechanisms proposed in these papers differ in the key cyclisation step (Fig. 5). Following the activation of the alkynes to nucleophilic attack by the π-acidic gold catalyst, and subsequent reaction with the nucleophilic sulfonium ylide, a vinyl-gold species is generated (10 and 13, respectively). The Skrydstrup group then proposed an initial expulsion of phenylmethylsulfide to generate gold-carbenoid species 11, which can then be trapped in an intramolecular fashion to form the five-membered ring (12), which then can easily undergo deauration to afford the furan product. In contrast the mechanism favoured by the Maulide group involves a rearrangement of the vinyl-gold species via a [3,3]-sigmatropic shift to form intermediate 14, which can then undergo a 5-exo-trig cyclisation, expelling the diphenylsulfide as part of the ring-forming step (affording 15), as opposed to a preceding step, as proposed by Skrydstrup et al. Computational modelling carried out by the Maulide group could not identify an energy minimum corresponding to the free carbene, analogous to intermediate 11.

In the same publication, Maulide et al. showed that doubly stabilised ylides were suitable starting materials for the synthesis of 2,3,4-trisubstituted furans via the intermolecular Skrydstrup-based procedure (Scheme 10). However, higher temperatures were now required due to the reduced nucleophilicity of the ylide. Additionally it was found that when the electron-withdrawing stabilisation was provided by an allyl ester, the final products were able to rearrange via a [3,3] shift to furanone derivatives (Scheme 11). The strength of the C=O bond is seemingly sufficient to counter the loss of pseudo-aromaticity in the process.

Whilst investigating these allyl-ester-based substrates, it was found that a competing process involving activation of the olefin moiety was also operative. When the external alkyne was removed from the reaction, the π-acidic Au-catalyst was found to promote an intramolecular cyclopropanation reaction. In addition to achieving good to excellent yields over a wide range of substrates, excellent diastereoselectivities were observed when more highly substituted allyl-groups
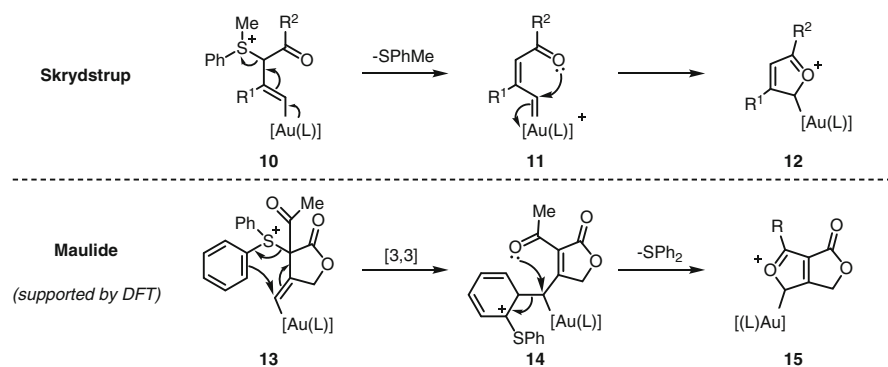
Fig. 5 Proposed mechanisms for furan formation
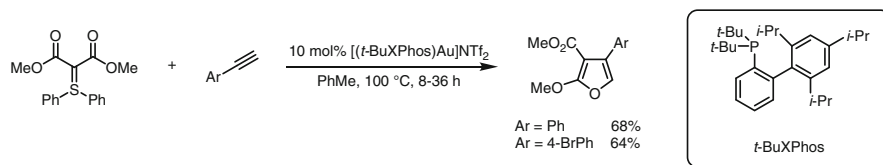
Scheme 10 Intermolecular synthesis of trisubstituted furans
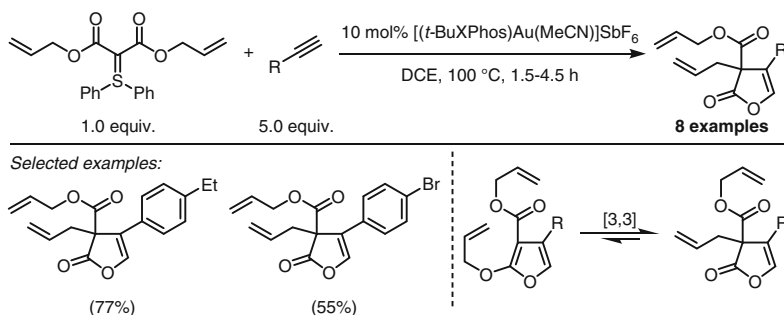
Scheme 11 Maulide's intermolecular furanone formation
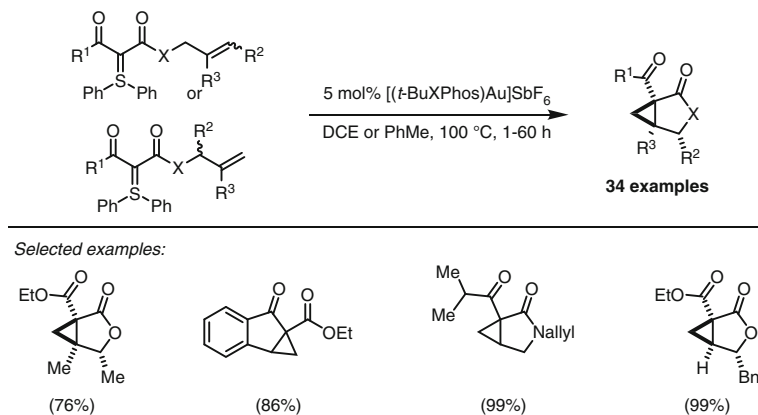
Scheme 12 Maulide's Au-promoted intramolecular cyclopropanation

were employed. With these substrates it also appeared that when X = O, both of the starting materials represented in Scheme 12 afforded the same product, in similar yields and near-identical diastereoselectivities. This observation was to have significant mechanistic implications (vide infra).

Whilst diastereoselectivities were extremely high for these substrates, the products were necessarily produced as racemates. Following extensive mechanistic studies [27], it was found that the use of cationic gold, complexed by a dimeric chiral TADDOL-based phosphoramidite, could achieve the cyclopropanation in an

enantioselective manner [28]. Starting from both the 'linear' and 'branched' isomers, it was possible to synthesise the lactone-fused cyclopropanes in good to excellent yields, near-perfect diastereoselectivities, and good to excellent enantioselectivities (Scheme 13).

The proposed mechanism for this remarkable process (Fig. 6) relies heavily on the aforementioned mechanistic paper [27] and consists of a domino deracemisation-cyclopropanation sequence. As previously observed, the cyclopropanation of the branched substrates (i.e. the mono-substituted alkenes) occurs more favourably than that of the disubstituted 'linear' substrates. By exposing allylic β-keto esters to Au-based π-acidic catalysts, equilibration of the 'linear' and 'branched' isomers was observed by ^{1}H-NMR. The mechanism for this interconversion involves the formation of a six-membered intermediate (**16**), via attack of the ester carbonyl on the Au-activated olefin. The consequent elimination (i.e. the reverse process) can afford either the 'linear' or 'branched' isomer, the latter of which can be formed as either enantiomer. The reversible attack of the carbonyl onto the olefin appears to be the faster process. When the carbon-based attack occurs, the generated alkyl-gold intermediate **17** can undergo a nucleophilic substitution to generate the cyclopropane with simultaneous expulsion of the diphenylsulfide leaving group. The gold catalyst selectively activates one enantiomer of the branched isomer, on just one face of the olefin, and it is in this key step that the stereochemistry of each centre is set, in an elegant dynamic kinetic resolution (DKR). As a result, the single chiral gold catalyst is responsible for the formation of each of the stereocentres, through catalyst-controlled deracemisation, enantioselective recognition and diastereoselective cyclopropane formation.

Whilst, in these highly selective examples, the process is only applicable to intramolecular cyclopropanation, the Maulide group has shown that certain highly activated unsaturated partners can undergo intermolecular cyclopropanation [29]. The coordinating effect of the enamide moiety in terminal allenamides allows for successful cyclopropanation of the terminal double bond (Scheme 14). Evidence
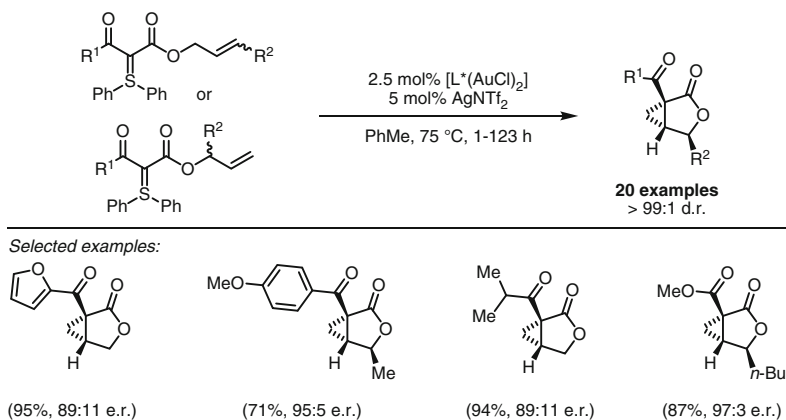
Scheme 13 Domino deracemisation-cyclopropanation of sulfonium ylides
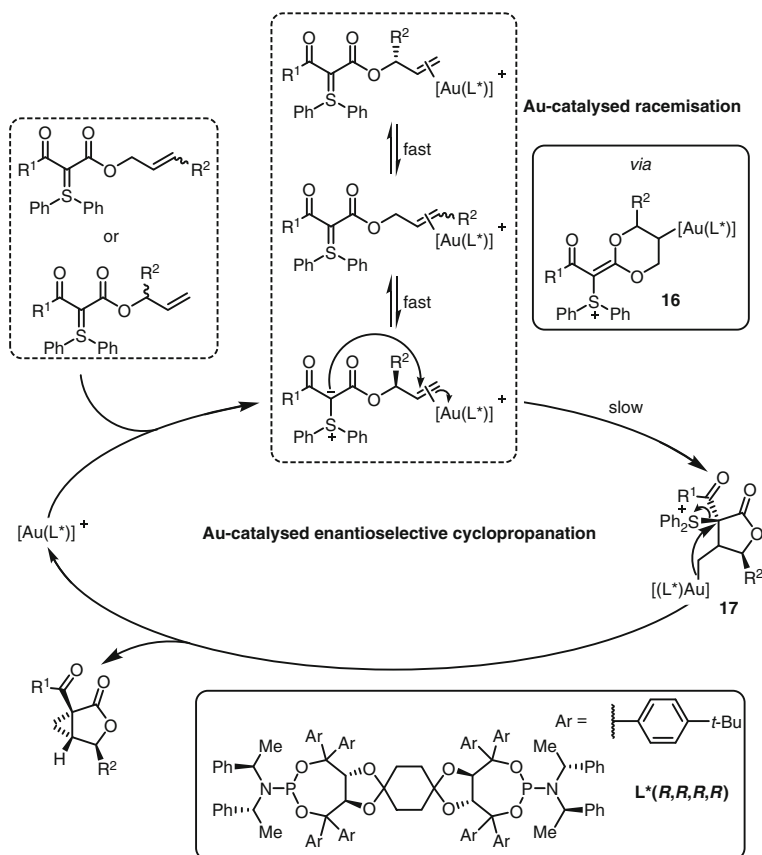
Fig. 6 Mechanistic rationale behind the deracemisation-cyclopropanation cascade

in support of this extra interaction was again provided in the form of computational studies. Such a process provides an alternative to the use of diazo compounds for the generation of similar structures.

In each of the previous examples, the sulfide acts as a leaving group, and therefore the identity of the groups on the departing sulfide was of little consequence (with the exception of the involvement of the phenyl group in the key [3,3] sigmatropic rearrangement en route to furans [26]). The addition of suitable nucleophiles to vinylic sulfonium salts has been used by the Aggarwal group as a method of generating sulfonium ylides in situ for various onward reactions [30–33]. In contrast, stabilised vinylic sulfonium ylides can be induced to transfer the vinyl substituent from *S* to *O*, in a Smiles-type rearrangement (Scheme 15). Reported by Maulide et al. [34], this process can occur either thermally or through the use of a gold catalyst, although the *E/Z* selectivity is much lower in the thermal variant. The mechanism proposed for this process involves nucleophilic attack through the carbonyl substituent in a 5-exo-trig manner, followed by intramolecular
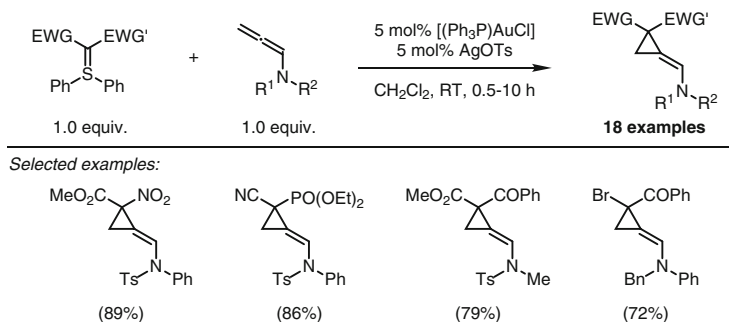
Scheme 14 Intermolecular cyclopropanation of allenamides
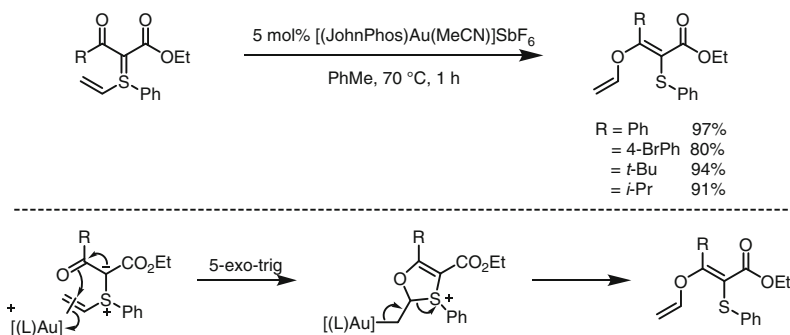
Scheme 15 Au-catalysed [1, 4] vinyl migration

elimination of the sulfide. Deuterium labelling experiments were used to disprove a 6-endo-trig alternative. The enol ether products were subsequently subjected to photocatalytic conditions and a number of onward reactions reported.

3.3 Sulfonium Ylides as C–S Activation Precursors

As mentioned in Sect. 2, the coordination chemistry of sulfonium ylides with transition-metal centres has been extensively investigated. In the overwhelming majority of cases, however, this analysis was restricted to structural elucidation with no onward reactions investigated. In 2013, Maulide et al. demonstrated that the coordination of stabilised ylides (generated through ylide transfer) to a number of Pd(II) salts could promote the reductive cleavage of the S-Ph non-ylidic bond to generate simple sulfide products [35]. Whilst the activation of the ylidic C–S bond through carbene transfer to metals such as copper, rhodium and iridium (to be discussed in Sect. 4) is well documented, this report represented the first selective cleavage of a non-ylidic S–C bond. A number of ylides were cleanly converted into

3-sulfenyl-indoles, 2-sulfenyl-pyrroles or α-sulfenyl-β-diketones, as depicted in Scheme 16. Whilst the exact mechanism for this process remains unclear, mechanistic experiments showed that the H-atom introduced into the indole ring does not originate from the silane but more likely the acetic acid additive. X-ray crystallographic analysis revealed that coordination to Pd(II) significantly affected the nature of both the ylidic and neighbouring bonds.

This concept of non-ylidic C–S bond activation has been further developed by the group of Li [36]. By utilising simple mono-stabilised dimethylsulfide-derived sulfonium ylides, an alkyne methylation reaction could be promoted by a Pd (II) catalyst. A wide range of terminal alkynes were methylated (Scheme 17), and the authors also showed that a number of sulfonium ylides were suitable as coupling partners, although only a methyl group could be transferred. In this paper a possible mechanism involving oxidative addition into the S-Me bond was postulated. Nevertheless beyond proving that a trideuteromethyl group was transferred without loss of deuteration in a crossover experiment – discounting a Pd-carbene intermediate – there is no concrete evidence in support of the proposed mechanism.

Despite the uncertainty as to the pathway by which the reaction proceeds, it remains a highly interesting transformation as a simple S-alkyl bond has been activated by Pd. Even simple S-Ar bonds are notoriously difficult to activate via transition-metal catalysis without resorting to oxidation to sulfonyl chlorides [37], transformation into a sulfonium salt [38] or use of directing group strategies [39]. Sulfonium salts are increasingly being used as stable alkyl halide equivalents, and this report suggests that a similar strategy is feasible with sulfonium ylides, which, depending on the substitution pattern, can be simpler to prepare.

3.4 Photocatalysis Involving Sulfonium Ylides

In recent years there has been an explosion in the number of reports of reactions promoted by photoactive catalysts, either by simple energy transfer to the reactants or through photoredox catalysis [40, 41]. The nature of these photoredox catalytic
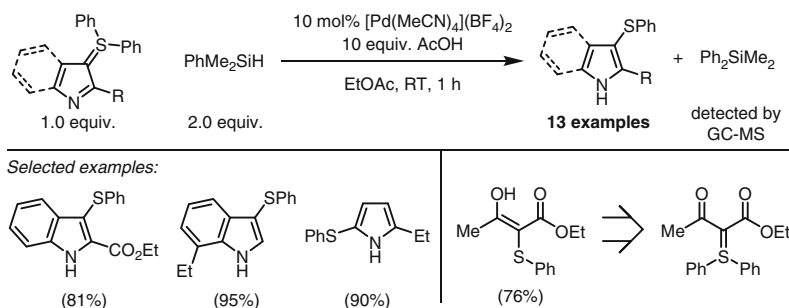
Scheme 16 Pd-catalysed sulfur-to-silicon group transfer
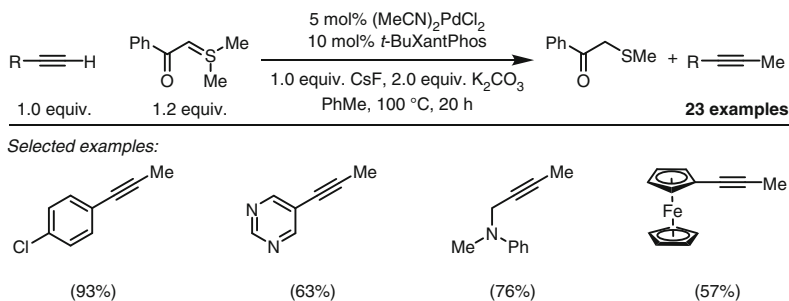
Scheme 17   C–S activation for the methylation of terminal alkynes

cycles enables transformations that are completely unknown using classical chemistry or even conventional transition-metal catalysis. The range of these transformations, the relatively mild reaction conditions often employed and the high functional group tolerance of such reactions are amongst the reasons behind this surge.

To date, there has only been one report looking to combine the use of photocatalysts and stabilised sulfonium ylides, which takes advantage of the high stability of the ylides in their ground state due to delocalisation of the formal anion. In 2016, Xiao et al. reported that, in the presence of a photoactive iridium complex, sulfonium ylides of the general structure shown in Scheme 18 could be cyclised to oxindoles through a formal C–H insertion reaction [42].

In contrast to previous studies involving the direct photochemical activation of sulfonium ylides with UV light to generate free carbenes [43], the excitation of the photocatalyst by blue LEDs generates an excited iridium species (termed [Ir]* in Fig. 7, however in reality a cationic complex). This excited complex is thought to then oxidise the sulfonium ylide to a highly reactive radical cation **18**, which rapidly reacts with the aryl ring to form five-membered-ring-containing intermediate **19**. The following steps, involving elimination of dimethyl sulfide and reduction to close the photoredox cycle, could feasibly follow either path a or path b.

4   Sulfonium and Sulfoxonium Ylides as Metal-Carbene Precursors

Sulfonium and sulfoxonium ylides have been further used as carbene precursors in transition-metal-catalysed reactions [44]. They are promising alternatives to diazo compounds and may offer a more stable and safer alternative. The chemistry of metal carbenoids, generated from diazo compounds, has found numerous applications in the field of organic synthesis. In particular, cyclopropanation and insertion into C–H and X–H (X = N, O, S, P, Se) bonds have been extensively studied [45–49]. The same chemistry can conceivably be accessed with metal carbenoids
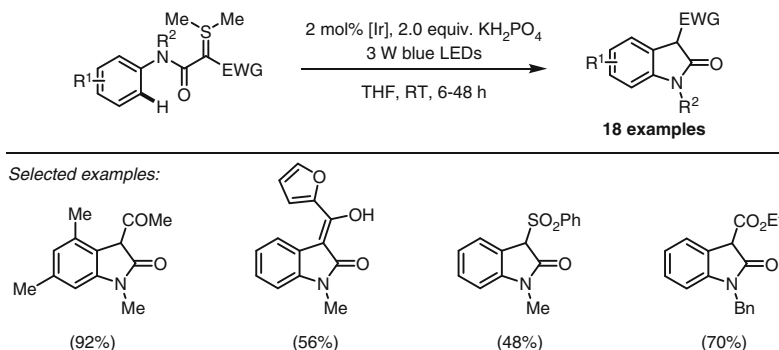
Scheme 18 Xiao's photocatalytic insertion of sulfonium ylides into C–H bonds for oxindole synthesis

Fig. 7 Mechanism of the photocatalysed C–H insertion
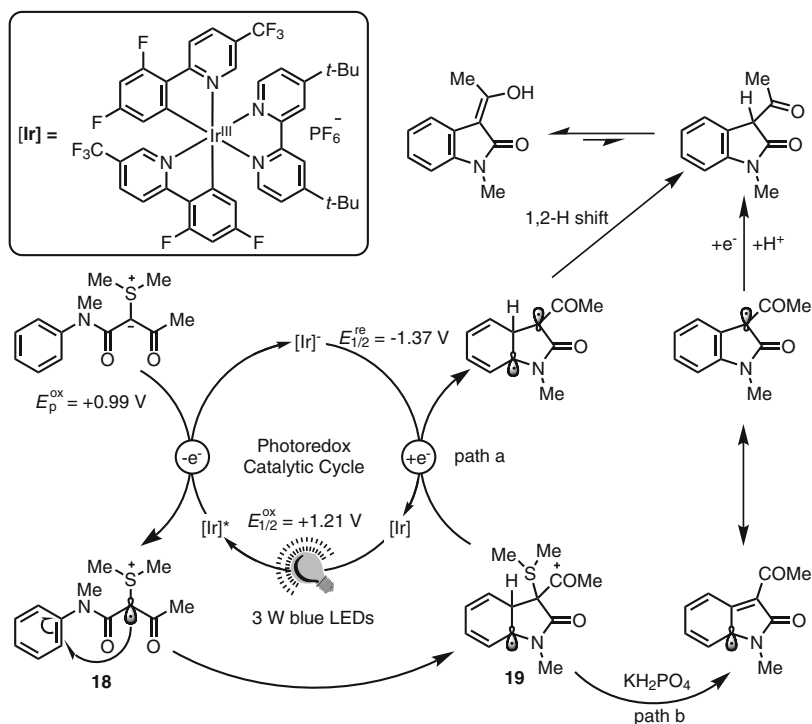
derived from sulfonium and sulfoxonium ylides. However, the generation of metal carbenoids from these compounds is much more challenging, especially because the reverse reaction, i.e. the formation of sulfonium ylides from the combination of metal-carbenoid species with sulfides, is both well studied and facile.

4.1 Cyclopropanation Reactions

The first example of a metal-catalysed cyclopropanation using sulfonium ylides was described by Trost in 1966 (Scheme 19a) [43]. The cyclopropane **21** derived from cyclohexene and ylide **20** was obtained in only 5% yield. The major product isolated was in fact **22**, formed by cyclopropanation of a dimerised intermediate. Following this report, Cohen et al. also demonstrated Cu(II)-catalysed cyclopropanation of olefins with diphenylsulfonium methylide [50]. The yields are only moderate at 31–48%, although a significant improvement compared to the work of Trost. No cyclopropanation of a dimerised intermediate was reported. Later, in 1991, Julia reported improved yields of this reaction as a result of changing the ligand on the copper from acac to pentacac (Scheme 19b) [51]. This allowed the catalyst loading to be lowered from 44 to 15 mol%. The improved yield was most significant when cyclohexene was employed as the olefin substrate, whilst for other olefins only a slight yield enhancement was observed.

In 1999, Müller reported the first example of an asymmetric metal-catalysed cyclopropanation using sulfonium ylides (Scheme 20) [52]. Both Cu(I) and Rh(II)-catalysts could be employed in the generation of the metal carbenoid from sulfonium ylide **23**. Only moderate yields were obtained when using the diphenylsulfonium ylides however. When the dimethyl counterpart was used instead, generation of the expected cyclopropanes was not observed. This pioneering report also provides a direct comparison between diazo compounds and sulfonium ylides as metal carbene precursors. In all cases, the reactivity of the diazo compounds is much higher, leading to higher yields, but the same diastereo- and enantioselectivity is obtained for each olefin, suggesting that a similar mechanism takes place.

Recently, the group of Gu reported a Fe-catalysed cyclopropanation of olefins with trifluoroethylidenesulfonium ylide **24** (Scheme 21) [53]. Previously reported catalysts such as $Cu(acac)_2$ achieved only a 16% yield, whilst others like $CuSO_4$ and
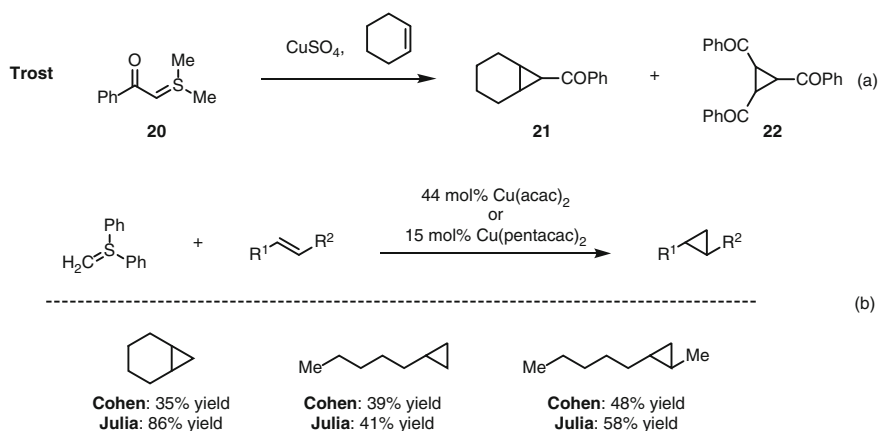
Scheme 19 Initial investigations towards the use of sulfonium ylides as diazo surrogates
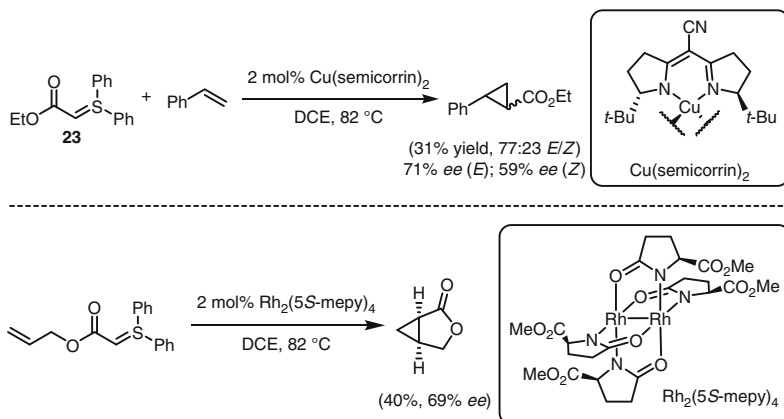
Scheme 20 Asymmetric metal-catalysed cyclopropanations
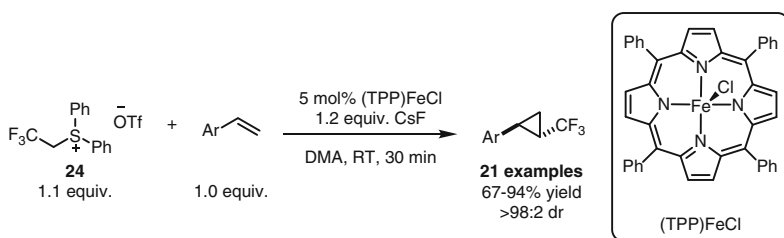
Scheme 21 Iron-catalysed carbenoid transfer to generate CF$_3$-substituted cyclopropanes

Rh$_2$(OAc)$_4$ were not able to promote the reaction at all. A porphyrin-based (TPP) FeCl catalyst was found to give the best results, and a wide range of styrenes could be transformed into the CF$_3$-cyclopropanes in good *trans*-diastereoselectivity. Unfortunately, no alkyl substituted alkenes or 1,2-disubstituted alkenes could undergo this cyclopropanation reaction.

The same group has recently extended the scope to the synthesis of difluoromethyl cyclopropanes [54]. The same catalyst was used, but the reaction conditions were slightly modified. In particular 20 mol% of Zn dust was introduced. This additive is believed to reduce the Fe(III) to Fe(II), which is the active cyclopropanation catalyst.

4.2 Insertion Reactions into X–H Bonds

Insertion into polar X–H bonds represents another common transformation of metal carbenoids. A number of sulfoxoniums have been used as precursors for this process, although to date no sulfonium ylide has been successfully employed. The first

example of such a reaction was described in 1993 by Baldwin and co-workers [55]. They demonstrated that ring opening of lactams with dimethylsulfoxonium methylide led to β-keto sulfoxonium ylides of type **25**. Treatment of this ylide with 5 mol% Rh$_2$(TFA)$_4$ led to the desired 4-oxopyrrolidinone in 77% yield (Scheme 22a). However, the use of the same copper catalysts described previously by Trost, Cohen and Julia did not furnish the N–H insertion product. The extension of this method to γ-lactams was also evaluated, and 5-oxopipecolic acid was produced in a 51% yield.

In 2009, Mangion and co-workers at Merck investigated a more general methodology for the intermolecular N–H insertion of α-keto sulfoxonium ylides (Scheme 22b) [56]. Treatment of a sulfoxonium ylide of type **26** in the presence of aniline and 5 mol% Rh$_2$(TFA)$_4$ only gave 22% yield of the desired product. The authors stated that the catalyst was deactivated by DMSO, which is released after decomposition of the sulfoxonium ylide, a conclusion supported by a control reaction involving the addition of DMSO prior to the reaction, in which the previous reactivity was supressed. Much better results were obtained with ruthenium- and iridium-based catalysts, especially [Ir(COD)Cl]$_2$. Under the optimised reaction conditions, a range of primary and secondary amines, alcohols and thiols could be applied to afford the insertion product in good yields (63–93%). In addition, a range of intramolecular N–H insertion reactions related to the prior Baldwin report could also be achieved with this catalyst in good yields (Scheme 22a).

In 2010, Mangion et al. extended this study to other catalytic systems, including gold and platinum salts [57]. The reaction was even more efficient with AuCl (SMe$_2$) as catalyst, providing the X–H insertion products in a 94% yield. Alternative catalysts such as Pt(COD)Cl$_2$ and AuCl$_3$ afforded yields of around 80%. Whilst, in reactions that employed [Ir(COD)Cl]$_2$ as catalyst, the metal-carbenoid intermediate could be observed by NMR spectroscopy, no direct evidence was provided for a gold carbene intermediate. The authors proposed that the gold-
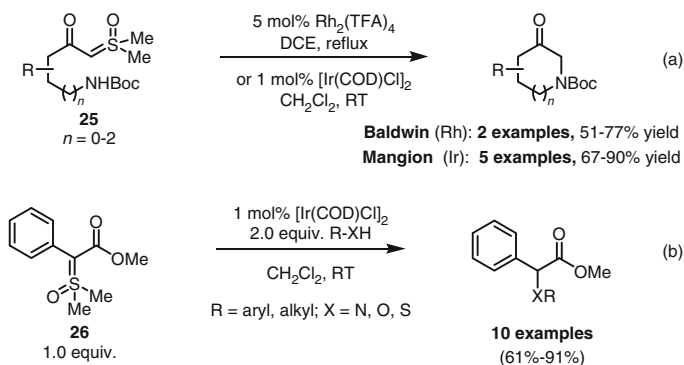
Scheme 22 Rh- and Ir-catalysed X–H bond insertion reactions

catalysed reaction follows the same pathway as the iridium-catalysed, rather than via a simple Lewis acid activation.

An interesting application of the N–H insertion of sulfoxonium ylides was disclosed by Merck in 2012 (Scheme 23a). The synthesis of MK-7246, a selective CRTH2 antagonist with potential in the treatment of respiratory disease could be achieved in eight steps [58]. The key step of the synthesis is the Ir-catalysed intramolecular N–H insertion reaction of **27**, which could be achieved in 83% isolated yield to afford six-membered ring **28**. The synthesis requires no chromatographic purification and was scaled up to more than a ton scale in a pilot plant.

Also developed by Merck was the synthesis of MK-7655, a β-lactamase inhibitor, again through N–H insertion of a sulfoxonium ylide (Scheme 23b) [59]. The authors found once more that iridium catalysts are the most suitable for this transformation and the N–H insertion product **29** was obtained in 87% yield.

Recently, the group of Shekhar reported the Ir-catalysed insertion of sulfoxonium ylides into the N–H bond of 2-aminopyridine derivatives (Scheme 24) [60]. When $[Ir(COD)Cl]_2$ was employed as the catalytic species, N–H insertion to yield the β-keto amine **30** was the favoured reaction pathway. When 1,10-phenantroline was employed as ligand in the presence of NaOTf to generate a cationic active catalyst, the major reaction product was now azole **31** which the authors propose is formed through preferential reaction of the metal carbenoid at the pyridine nitrogen, rather than with the free NH_2.
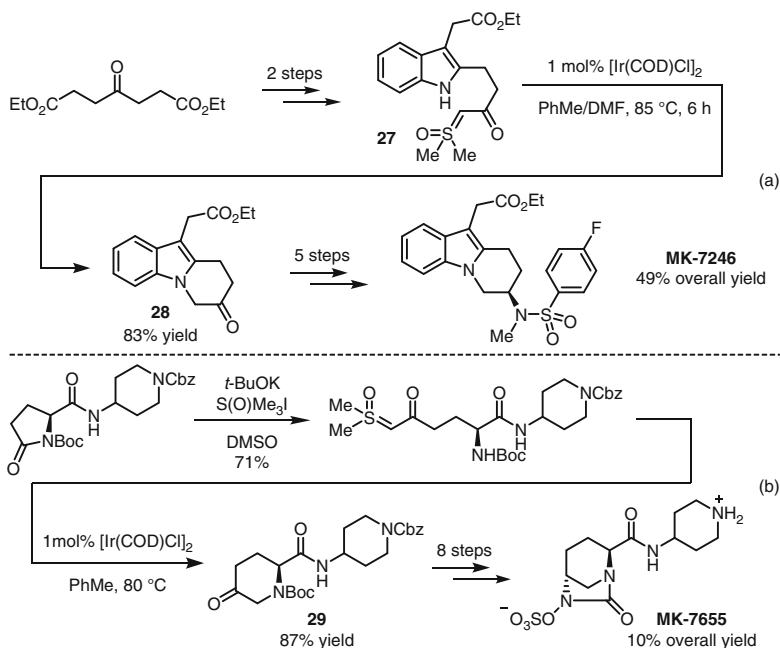
Scheme 23 Ir-catalysed N–H insertion in the synthesis of biologically relevant targets
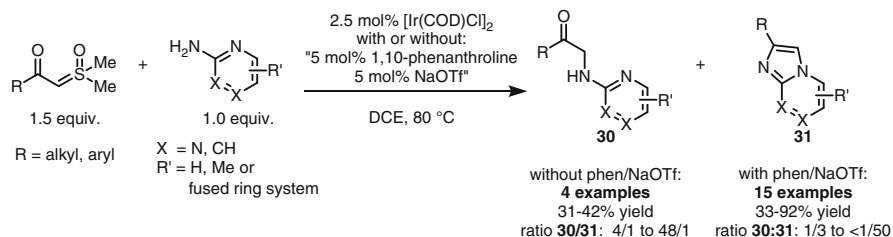
Scheme 24 Ligand effects in X–H insertion reactions

Similarly, the group of Hopmann reported the N–H insertion of sulfoxonium ylides into anilines, followed by one-pot acid-catalysed cyclisation to afford indoles [61]. Reactions with aniline derivatives proceed through a cascade of carbenoid formation, N–H insertion, imine formation, substitution and aromatisation to generate a range of indoles (Scheme 25).

4.3 Insertion Reactions into C–H Bonds

Whilst the insertion of metal carbenes generated from diazo compounds into C–H bonds has been extensively described, only a limited number of examples of C–H insertion employing sulfonium/sulfoxonium ylides have been published. To date, the only report describing the successful use of sulfonium ylides for such a process details the reaction of ylide **32** under rhodium catalysis (Scheme 26a) [52]. Only 9% of lactone **33** was isolated whilst the majority of the starting material dimerised. The same problem was observed by Mangion et al., when they subjected **34** to iridium catalysis [56]. Cycloheptanone **35**, which is the major product isolated from when the diazo-analogue of **34** is used as the starting material was not found; instead only dimerisation product **36** was isolated in 94% yield (Scheme 26b).

The group of Hopmann notably showed that enamines are suitable substrates for C–H insertion with iridium carbenoids, derived from sulfoxonium ylides (Scheme 27) [61]. Combined with concomitant acid-catalysed cyclisation, the reaction afforded a range of substituted pyrroles. The applicability of this method was also demonstrated by the synthesis of the pyrrole subunit (**37**) of atorvastatin (Lipitor), a cholesterol-lowering drug.

From this short section, it becomes apparent that C–H insertion is the poor relation of N–H insertion and cyclopropanation when sulfur-based ylides are employed. The key challenge here lies in the fact that sulfur ylides are more nucleophilic than diazo compounds and will attack the metal-carbenoid complex. This side reaction is much faster than a C–H insertion reaction and needs to be overcome in order to develop a more general C–H insertion reaction employing sulfur ylides.
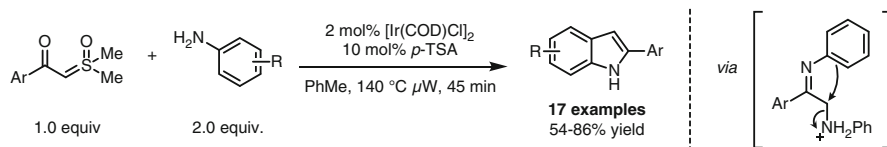
Scheme 25 Hopmann's N–H insertion for indole synthesis
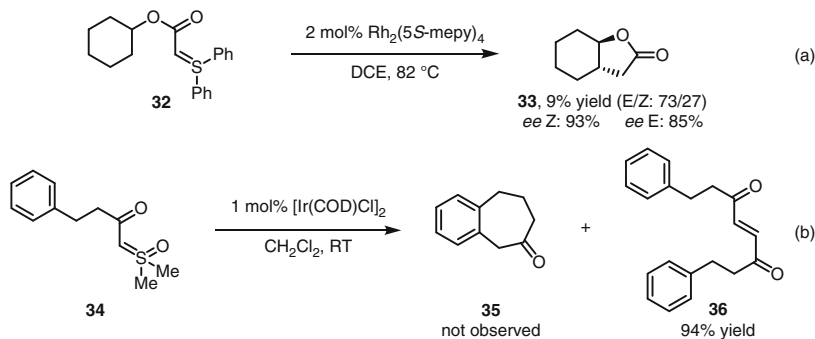
Scheme 26 Limitations in C–H insertion reactions
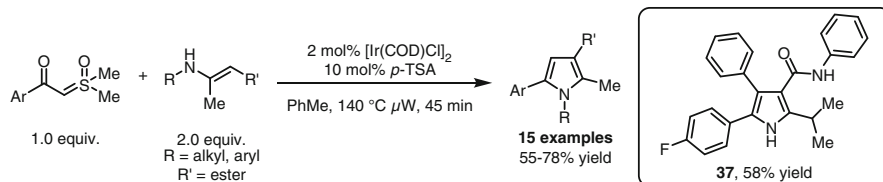
Scheme 27 Ir-catalysed C–H insertion for pyrrole synthesis

4.4 Miscellaneous Sulfonium-Derived Metal-Carbenoid Reactions

Milstein and co-workers described the synthesis of metal-carbenoid complexes employing sulfonium ylides as carbenoid donors [62, 63]. The method was applied to various metals, such as rhodium, iridium, ruthenium and osmium as well as a number of alkylidene units. These reactions were initially carried out using sulfonium ylides in solution, but later polymer-supported sulfonium ylides were developed, allowing for the recycling of the sulfide. In both cases, diaryl sulfides were used as leaving groups and gave good yields. Using this method, the first generation Grubbs' catalyst and Werner's carbene could be prepared.

The use of sulfonium ylides in polymerisation reactions, via metal-carbenoid intermediates, was demonstrated by de Bruin and co-workers [64]. When exposed

to rhodium catalysis, dimethylsulfoxonium methylide was found to polymerise to produce polymethylene in yields of 15–80%. The co-polymerisation of sulfonium ylides with diazo compounds was also reported using the same catalyst.

5 Cascade Reactions Involving Transition-Metal-Catalysed Ylide Formation

For a long time, the deprotonation of sulfonium/sulfoxonium salts was the only method to efficiently access sulfonium/sulfoxonium ylides. This approach, although convenient on some levels, suffers serious limitations resulting from the use of a base to generate the carbanionic species. Indeed, such conditions appear incompatible with a broad range of base-sensitive functional groups, and the selected bases have to be poor nucleophiles to avoid the dealkylation of the electrophilic sulfonium. Additionally, serious chemoselectivity issues are observed if the substrate contains several acidic positions. As a result of these considerations, the range of sulfonium ylides routinely studied tends to consist of ylides stabilised by either one or two electron-withdrawing groups. However, considerable steps to address these limitations have been made with the development of alternative strategies consisting of the formation of the desired ylide by reaction between a sulfide and an electron-poor carbene intermediate [44, 65]. This reactivity was reported for the first time by Diekmann, in 1965, with the formation of sulfonium/sulfoxonium ylides by photochemical decomposition of bis(phenylsulfonyl) diazomethane in sulfur-containing solvents like dimethylsulfide, dibutylsulfide and dimethylsulfoxide [66]. Thereafter, Ando demonstrated that the presence of copper sulfate allowed the reaction to occur without requiring UV irradiation [67, 68]. This major contribution significantly improved the synthetic value of this transformation, which tolerates a broad range of substrates including cyclic sulfides or diaryl sulfides. Through a systematic comparison with the photochemical activation, they highlighted the higher efficiency of this copper-triggered ylide formation (Scheme 28). In 1978, Porter achieved a breakthrough by using rhodium acetate in the synthesis of sulfonium ylides [69]. Due to the high efficiency of rhodium salts in the promotion of these reactions, only 0.12 mol% of catalyst was necessary to deliver the desired thiophenium ylide in 95% yield.

From a mechanistic point of view, this ylide synthesis can be described as a double umpolung of the carbenic carbon atom (Fig. 8). Indeed, the nucleophilic diazo compound **38** is decomposed in the presence of a metal salt to form a metal carbene complex **39**. In this intermediate, the carbon atom becomes electrophilic by electron donation to the metal and can undergo nucleophilic attacks from sulfides to form the desired ylide **40**. In practice, this transformation is highly attractive as it proceeds under mild reaction conditions and displays good chemoselectivity. During recent decades, this approach has been extensively used for the in situ generation of sulfonium ylides in cascade reactions. Depending on their structure, these
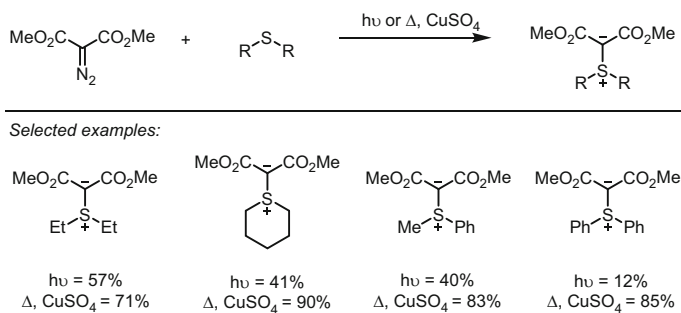
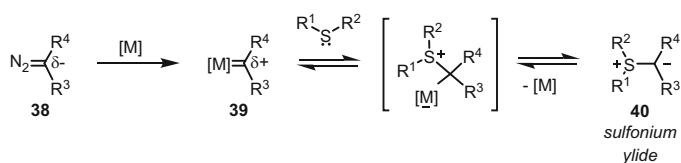Scheme 28 Thermal versus photochemical formation of sulfonium ylides by Ando et al.

Fig. 8 General mechanism for the metal-catalysed synthesis of sulfonium ylides from diazo compounds

ylides can undergo a number of transformations, which are the topic of several reviews [70–72]: [2,3]-sigmatropic rearrangements, 1,2-migrations and Corey-Chaykovsky-type reactions represent the major families of onward reactions. Hence, the purpose of this section is to offer an overview of metal-catalysed sequences involving sulfonium ylides as reaction intermediates through significant and recent examples.

5.1 [2,3]-Rearrangement of Sulfonium Ylides

[2,3]-sigmatropic rearrangements constitute powerful tools for the formation of C–C bonds. Classically, the migrations of σ-bonds are significantly accelerated if one or several bonds of the system are polarised, the fastest reactions occurring when an atom bears a formal charge. Therefore, sulfonium ylides constitute valuable substrates in such transformations. Given the classical requirement for preparation and deprotonation of complex sulfonium salts, the in situ formation of sulfonium ylides from simple starting materials followed by their subsequent rearrangement rapidly emerged as a synthetically appealing approach. The combined sequence of diazo decomposition in the presence of an appropriate catalyst and an allylic or propargylic sulfide, followed by spontaneous [2,3]-rearrangement of the zwitter-ionic intermediate, is known as the Doyle-Kirmse reaction (Fig. 9) [73, 74]. This

Fig. 9 General proposed
mechanism for the Doyle-
Kirmse reaction
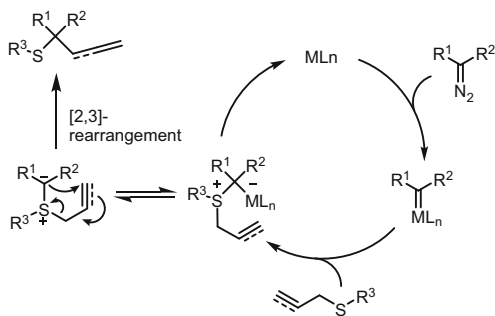
transformation is the most studied domino reaction based on sulfonium ylide
intermediates and offers a unique access to *S*-substituted quaternary centres.

Due to their high efficiency in the decomposition of diazo derivatives, copper
and rhodium complexes constitute the most extensively used catalysts in Doyle-
Kirmse reactions. However, a broad range of metals can promote the same type of
transformation including Co [75], Ag [76], Pd [77], Ru [78–80] and Fe [81–
84]. This multiplicity of reaction conditions results in a plethora of applications
and a broad diversity of substrates. This transformation allows the one-step forma-
tion of sophisticated sulfur-containing molecules. Typically, allyl sulfides and
propargylsulfides are converted to homoallyl and homoallenyl sulfides, respec-
tively, as demonstrated by the iron porphyrin-catalysed process in Scheme 29
[85]. Because of the lower costs associated with iron catalysts, their application
has attracted considerable interest in recent years. When employed for the decom-
position of ethyl diazoacetate in the presence of sulfides **41** and **42,** only 0.2 mol%
of catalyst **45** was required to afford rearranged compounds **43** and **44** in excellent
yields at room temperature in very short reaction times. Another interesting aspect
of the Doyle-Kirmse reaction is its noteworthy chemoselectivity. The functional
group tolerance is particularly high using TBAFe as a catalyst and includes
boronates, allyl ethers, secondary anilines, disulfides and free alcohols (Scheme
30) [86]. Interestingly, the metal complex used in this reaction is electron-rich and
decomposes the diazo compound via a nucleophilic attack.

When the π-system involved in a [2,3]-sigmatropic rearrangement is embedded
in an aromatic ring, the reaction is known as the Sommelet-Hauser rearrangement.
Wang reported the first rhodium-catalysed thia-Sommelet-Hauser reaction between
diazo(aryl)acetates and aryl sulfides (Scheme 31) [87]. The mechanism involves an
unusual ylide transposition. The intermediate arising from the initial reaction
between the sulfide and the metal carbene complex underwent reversible proton
transfer to form a second sulfonium ylide, itself stabilised by an additional electron-
withdrawing group. It is this second species that participates in the [2,3]
sigmatropic rearrangement. That the reaction proceeds smoothly at room temper-
ature despite requiring a dearomatisation step is particularly noteworthy. The
reaction represents a selective *ortho*-substitution and delivers di- and trisubstituted
arenes that are otherwise difficult to prepare. Electron-rich and electron-poor
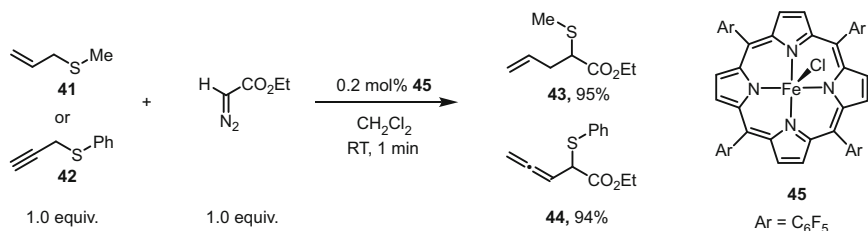
Scheme 29 Iron-catalysed Doyle-Kirmse reaction of allyl and propargylsulfides
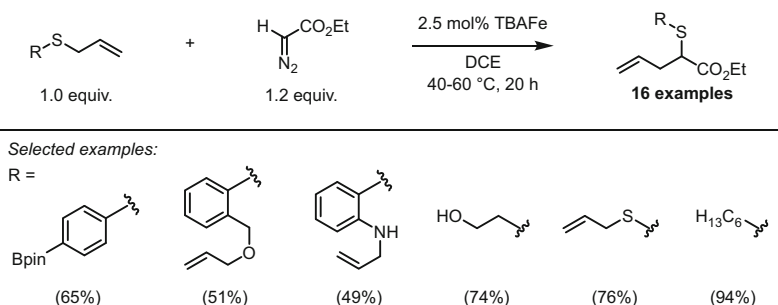
Scheme 30 Highly chemoselective TBAFe-catalysed Doyle-Kirmse reaction
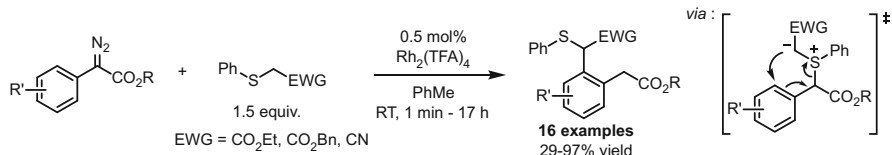
Scheme 31 Rhodium-catalysed thia Sommelet-Hauser rearrangement of benzylsulfides

aromatic substituents were well tolerated, affording the rearranged products in moderate to excellent yields.

In 2011, Wang extended this approach to report a modification of Gassman's oxindole synthesis triggered by Rh-catalysed decomposition of diazo compounds in the presence of sulfonamides [88]. In this way, oxindoles with a quaternary centre in position 3 are obtained in one step in moderate to good yields (Scheme 32).

[2,3]-Sigmatropic rearrangements of ylides generally result in the formation of chiral molecules. The development of an enantioselective variant of this transformation is highly appealing, as it would allow the stereocontrolled formation of a C–S and a C–C bond on the same carbon atom. Over the last two decades, many efforts were made to achieve this goal based on the use of chiral metal complexes. However, until recently, only moderate enantioselectivities have been achieved in pure catalyst-controlled transformations. The main challenge is the requirement to

Scheme 32 Wang's modified Gassman oxindole synthesis

control the stereoselectivity over the entire sequential process. Additionally, the reaction mechanism remains unclear concerning the role of the metal catalyst at the different steps of the reaction, and contradictory observations have been reported.

In 1995, Uemura demonstrated the concept by reporting the first enantioselective Doyle-Kirmse reaction between ethyl diazoacetate and (E)-cinnamyl phenyl sulfide in the presence of Cu(I)/bisoxazoline and $Rh_2(5S$-MEPY)$_4$ [89]. Regardless of the nature of the chiral complex, homoallyl sulfides were obtained with poor enantio- and diastereoselectivities (Scheme 33). Due to the complexity of the reaction mechanism, the low degrees of enantiocontrol could have several explanations (Fig. 10). Indeed, the global enantioselectivity of the reaction could be traced to the discrimination between the two enantiotopic lone pairs of the sulfur atom during the initial attack of the chiral metal carbene. However, good stereocontrol at this step could be partially or totally negated by a fast racemisation process. The configurational stability of sulfonium ylides proved to be high in the absence of transition-metal complexes but remains unclear for metal-catalysed Doyle-Kirmse reactions. Additionally, [2,3]-sigmatropic rearrangements of enantiopure sulfonium ylides have shown perfect chirality transfer under metal-free conditions, but possible coordination by the metal complex in this case could result in important matched/mismatched effects.

This last question was investigated by Katsuki and co-workers who compared, in a similar reaction, the diastereoselectivities obtained using various Co-salen catalysts (Scheme 34) [75]. In each case, unchanged levels of diastereocontrol were observed, whilst the enantiomeric ratios appeared catalyst-dependent. This result suggests that the configuration of the sulfonium ylide intermediate is under catalyst control but that the ylide is not coordinated to the catalyst in the course of the rearrangement step. Thus, the final diastereomeric ratio is a result of the difference in the potential energy in the two envelope transition states **A** and **B**.

Thereafter, Hashimoto [90] reached the same conclusions, whilst Aggarwal observed a strong correlation between the ligand and the diastereoselectivity in Doyle-Kirmse reactions involving allyl sulfides and trimethylsilyl diazomethane [91]. Additional mechanistic studies undertaken by Wang support a metal-free rearrangement step. Although the combination of Cu(MeCN)$_4$PF$_6$ and ligand **46** delivered rearranged sulfides with moderate enantioselectivities, no stereocontrol was observed starting from the symmetric substrate **47** (Scheme 35) [92].

This observation is inconsistent with a rearrangement under catalyst control, the intermediate ylide being achiral. On the other hand, the same author demonstrated,
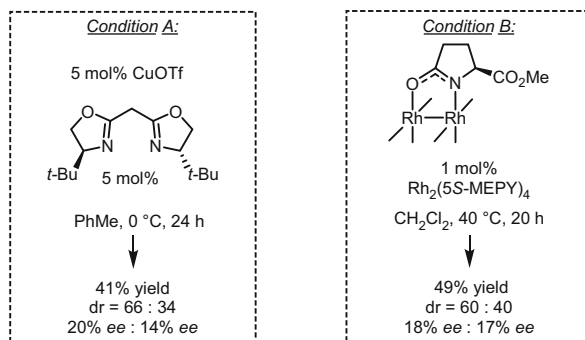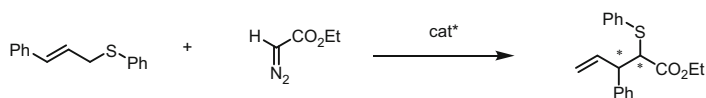
Scheme 33 Enantioselective Doyle-Kirmse reaction by Uemura and co-workers
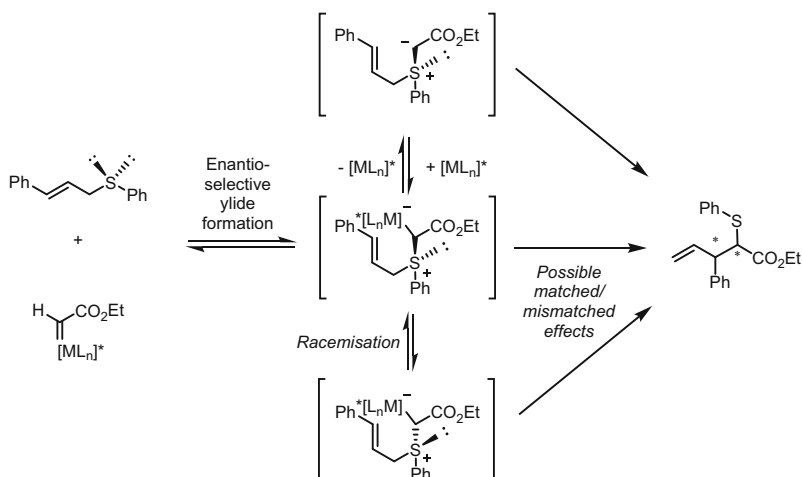

Fig. 10 Plausible reaction pathways in enantioselective metal-catalysed Doyle-Kirmse reactions

predominantly by IR spectroscopy, a strong affinity between the copper catalyst and the sulfonium ylide (Fig. 11) [93]. Such results suggest that the installed equilibrium is displaced towards the formation of the metal-ylide complex but that only the free ylide undergoes the sigmatropic rearrangement. Other experiments undertaken by Trost proved that this final rearrangement step is much faster than the racemisation of free sulfonium ylides in the reaction conditions [94]. Taking all these observations into account, the enantioselectivity of the whole sequence
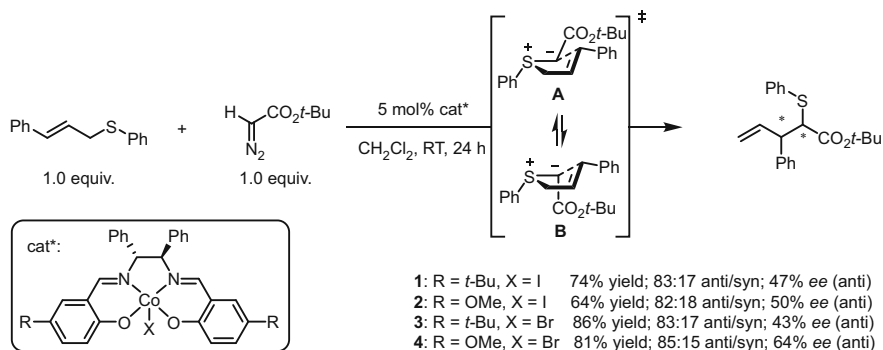
Scheme 34 Cobalt salen-catalysed Doyle-Kirmse reaction
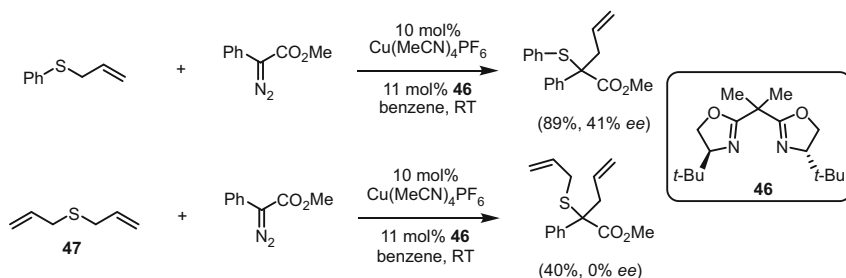
Scheme 35 Difference of enantioinduction starting from nonsymmetric and symmetric allyl sulfides
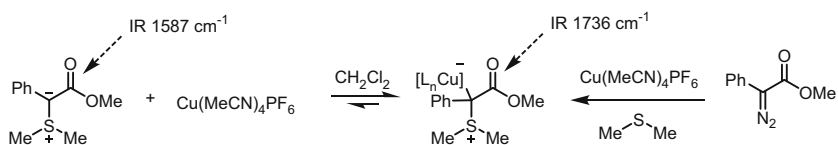
Fig. 11 Evidence of the strong affinity of sulfonium ylides for electrophilic copper complexes

appears to only reflect the degree of enantiodiscrimination obtained during the formation of the chiral ylide intermediate.

For many years, the best yields and enantioselectivity were to be found in the use of double asymmetric induction, developed by Wang, and involving the combined actions of an enantiopure copper catalyst and Oppolzer's chiral auxiliary (Scheme 36) [93]. Because the reaction is primarily under substrate control, uniformly good to excellent enantiomeric excesses were observed. The reaction is highly versatile and allyl- and propargylsulfides as well as aryl-, methyl-, cinnamoyl- and propenyldiazoacetamides are well tolerated. Following the reaction, the auxiliary

Selected examples:

(70%, 90% *ee*) (81%, 90% *ee*) (82%, 95% *ee*) (74%, 82% *ee*) (97%, 94% *ee*) (95%, 93% *ee*)
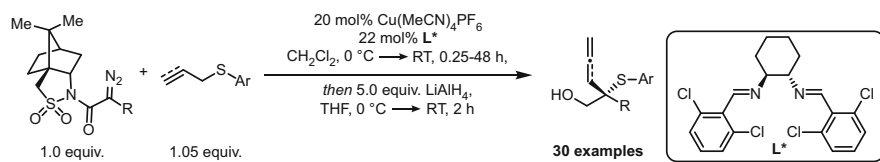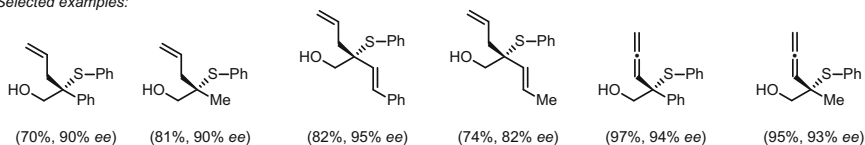
Scheme 36 Double asymmetric induction in copper-catalysed Doyle-Kirmse reaction

is easily removed by reduction of the amide bond in the presence of LiAlH$_4$. Whilst representing the most practical procedure to carry out this transformation, the need for both a chiral catalyst and a chiral auxiliary does detract from the process.

Shortly before the publication of this chapter, the Wang group achieved similar levels of enantioinduction without the use of a chiral auxiliary in a publication dedicated to the formation of enantioenriched trifluoromethylthio-substituted compounds (Scheme 37) [95]. The combined effect of new ligand sets and the highly electron-poor trifluoromethyl sulfides afforded extremely high enantiocontrol over an unprecedented range of diazonium salts, including aryl-, alkenyl- and hetero-aryl- substituted diazoacetate derivatives. When internal olefins were employed, low diastereoselectivities were observed, and similar to the previous reports discussed, these new catalysts imparted negligible enantiocontrol when diallyl sulfide was employed (as in Scheme 35). These observations are in accordance with the active species prior to [2,3]-rearrangement being decomplexed from the chiral TM-catalyst.

Diazo compounds constitute the prototypical metal carbene precursors, and their decomposition in the presence of transition-metal salts offers good chemoselectivity and requires soft conditions. However, diazo derivatives suffer major drawbacks including toxicity and explosive properties. Moreover, their preparation is limited to stabilised compounds bearing one or two electron-withdrawing groups. During recent decades, many efforts have been made to develop new alternatives to the direct use of diazo compounds as carbenoids precursors to extend the scope and the efficiency of the Doyle-Kirmse reaction. These improvements included the in situ generation of diazo intermediates or the direct formation of metal carbenes from unsaturated C–C bonds in the presence of π-acid complexes.

In this framework, tosylhydrazones represent valuable precursors of unstabilised diazo compounds through the so-called Bamford-Stevens reaction. Under basic conditions, in the presence of Rh$_2$(OAc)$_4$ and suitable sulfides, tosylhydrazones are converted to sulfonium ylides able to undergo [2,3]-rearrangement [96]. In comparison with previously reported methodologies, this approach allows the formation of rearranged products without the electron-withdrawing groups usually necessary for the stability of the diazo starting materials. More recently, the ability of 1-sulfonyl-
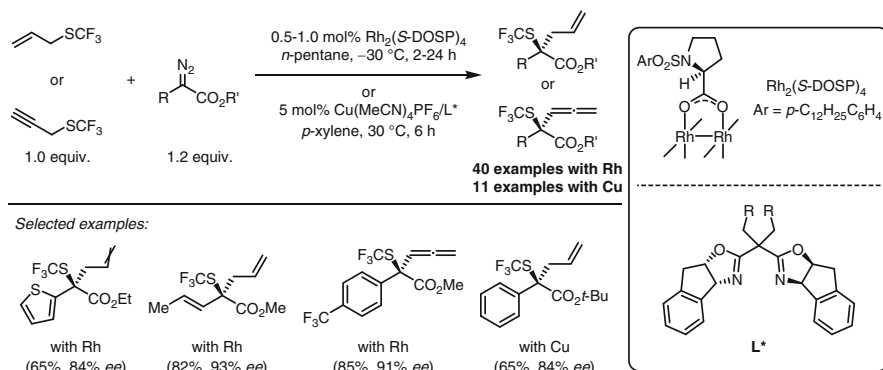
Scheme 37 Enantioselective Doyle-Kirmse reaction under full catalyst control

1,2,3-triazoles to tautomerise to diazoimines was also interestingly exploited. Murakami and co-workers were the first to exploit the reactivity of triazoles in the [2,3]-rearrangement of allylsulfonium ylides [97]. The authors proposed a cascade reaction involving a copper-catalysed (3 + 2)-cycloaddition from easily available alkynes and tosylazides (Scheme 38). Diazoimine tautomers are then converted to rhodium carbene complexes by decomposition in the presence of $Rh_2(O_2Ct\text{-}Bu)_4$ as a second catalyst. The attack by an allyl sulfide moiety followed by a [2,3]-sigmatropic rearrangement delivered the desired sulfenylated imines that can be hydrolysed under acidic conditions or reduced to the corresponding tosylamines through the final addition of $LiAlH_4$. In view of the sequence complexity, the yields are surprisingly high and demonstrated a remarkable chemoselectivity in this dual-catalysed process. Shortly after, a similar strategy was used by Anbarasan in the rhodium-catalysed denitrogenative synthesis of α-sulfenylated imines [98].

In tandem with strategies relying on the in situ generation of diazo compounds, alternative approaches to forming metal carbenoids, not requiring the intermediacy of diazo compounds, have been established. In 2002, Ohe and Uemura developed a method to synthesise (2-furyl)carbenoids in situ via cyclisation of ene-yne-carbonyl compounds **48** in the presence of rhodium acetate [99]. By combining this approach with the Rh-catalysed Doyle-Kirmse reaction, they subsequently developed a high-yielding procedure (Scheme 39) [100]. When diallyl sulfide **47** was employed, the product was able to undergo a further thermal [4 + 2] Diels-Alder process in the same pot to form polycyclic heterocycles of type **49**.

Alternative rearrangement strategies have been successful, including a number employing simple alkynes as masked carbenoids. In a pioneering work, Davies described the gold-catalysed formation of sulfonium ylides from propargylic carboxylates and allyl sulfides (Scheme 40) [101]. The products of this reaction were not the products of the expected [2,3]-shift, but rearranged products **50**, probably the result of a Cope-rearrangement of the expected Doyle-Kirmse products.

In 2009, the same author investigated a similar strategy in the synthesis of cyclic sulfides [102]. Based on the works of Toste [103] and Zhang [104], alkyne
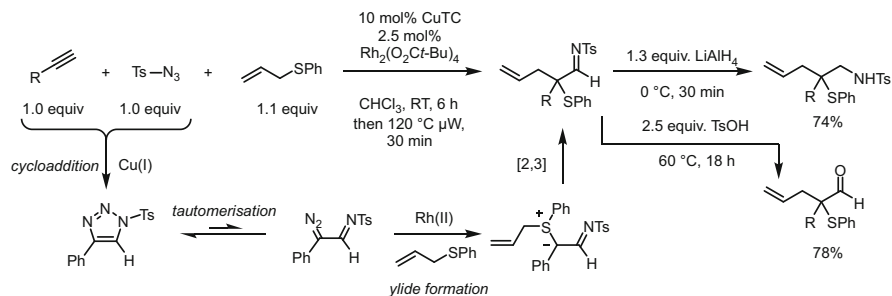
**Scheme 38** In situ generation of diazo intermediate the Doyle-Kirmse synthesis of thioamines
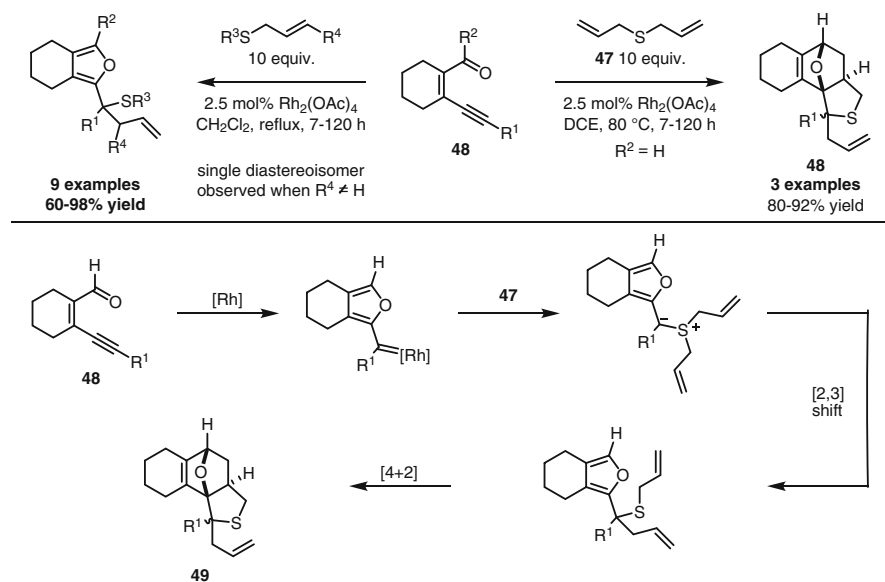
Scheme 39 Doyle-Kirmse reactions from in situ generated (2-furyl)carbenoids

oxidation was triggered by the intramolecular addition of a sulfoxide moiety (Scheme 41). The subsequent cleavage of the S–O bond released both a metal carbene and a sulfide that, in turn, react chemoselectively to form ylide **52**. A final [2,3]-rearrangement provided the heterocyclic products. Optimisation of the reaction conditions revealed PtCl$_2$ to be the best catalyst to promote the reaction with terminal alkynes. Internal alkynes, on the other hand, required the action of dichloro (pyridine-2-carboxylato)gold(III) **51** to be transformed efficiently into the cyclic sulfide bearing a quaternary centre. Propargyl and aryl esters were well tolerated, whilst the presence of 1,2-disubstituted olefins resulted in poor diastereoselectivity.

More recently, methodologies involving the intermolecular oxidation of C–C triple bonds in the presence of stoichiometric amounts of amine N-oxides were
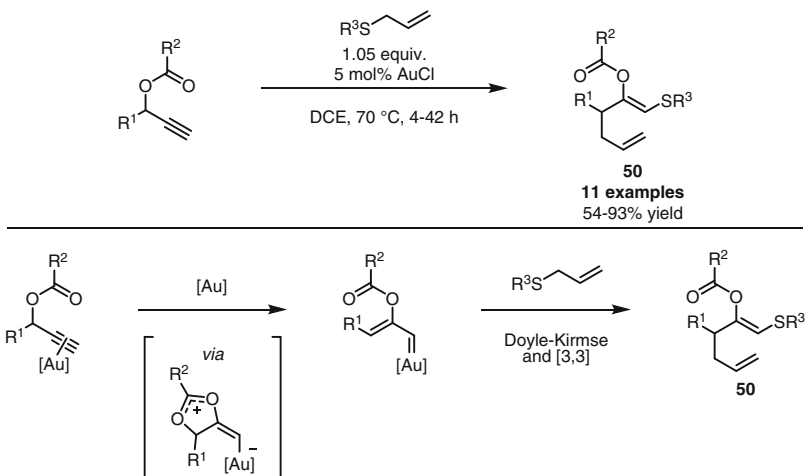
Scheme 40 Alkynes as masked ylides in Doyle-Kirmse chemistry
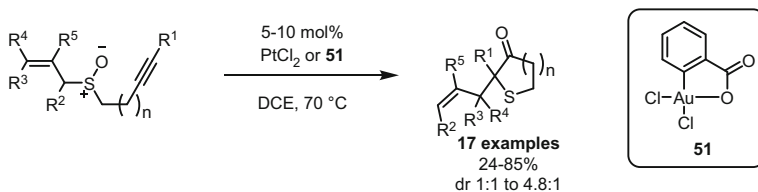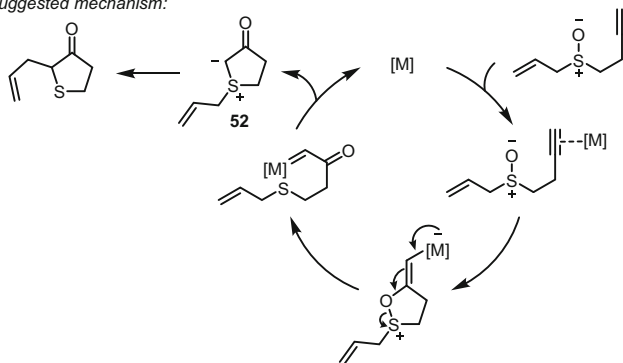
Scheme 41 Synthesis of sulfur heterocycles from alkynyl sulfoxides

reported. Such transformations have the advantage that they rely on simple substrates but could theoretically suffer regioselectivity issues. Therefore, polarised alkynes like ynamides were used as substrates in the oxidative synthesis of 2-(thio) amides bearing a α-quaternary centre [105]. However, the narrow scope of

ynamides belied the difficult control of the chemoselectivity due to the presence of alternative external nucleophiles that would be able to react with the gold carbene intermediate. In an independent publication, Zhang addressed this competition issue in the three-component synthesis of α-aryl(alkyl)thio-γ,δ-unsaturated ketones directly starting from terminal alkynes [106]. To achieve this reaction efficiently, the oxidising agent was added with a syringe pump, and, most importantly, *P*,*S*-bidentate ligands were used to decrease the electrophilicity of the α-oxo gold carbene complex.

The most recent developments for the diazo-free Doyle-Kirmse sequence relied on the cyclic strain displayed by cyclopropenes [107]. In the presence of Rh₂(OAc)₄ catalyst, cycloprop-2-ene-1,1-diyldibenzene **53** spontaneously ring opened to form the corresponding rhodium carbene **54** (Scheme 42). This intermediate can be trapped by allyl(phenyl)sulfide leading to the formation of a sulfonium ylide, with this approach, reported by Wang, revealed to be quite general allowing the synthesis of sulfur-containing alkenes and allenes in good yields. However, attempts to deliver an enantioselective version resulted in low enantiomeric excesses.

5.2 1,2-Migration of Sulfonium Ylides

In certain cases the presence of allyl, propargyl or benzyl substituents is not necessary to trigger rearrangements of ylides. The direct 1,2-migration of an alkyl substituent from the heteroatom to the carbanionic centre of an ylide is known as the Stevens rearrangement. Although well described with oxonium and ammonium ylides, the Stevens rearrangement of sulfonium ylides remains relatively underutilised. However, combined with the ability of sulfides to convert diazo compounds to ylides in the presence of appropriate metal complexes, this reaction has proved to be a powerful tool in C–C (and C–N bond [108]) formation and the synthesis of quaternary centres. Specifically, it has mainly been used for the preparation of sulfur-containing heterocycles by ring expansion. A significant example was reported by Diver with the formation of macrocycles via a rhodium-catalysed double-Stevens rearrangement [109]. The decomposition of diethyl diazomalonate in the presence of Rh₂(OAc)₄ (2 mol%) and disulfide **55** results in the formation the bisylide **56** that spontaneously rearranges when the reaction is performed in refluxing xylenes (Scheme 43). This intermediate can, however, be isolated when generated at low temperature. The regioselectivity of the reaction
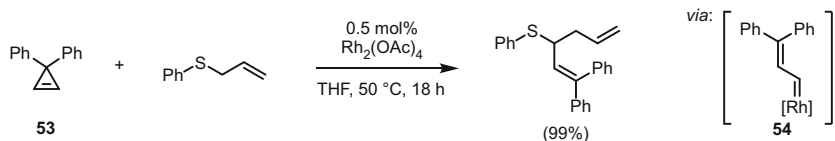
**Scheme 42** Doyle-Kirmse reaction from cyclopropenes

suggested a radical pathway for the 1,2-migration. Interestingly, sulfur extrusion and a new C–C bond formation can be triggered by UV irradiation in the presence of $P(OEt)_3$ to give the corresponding [3]-heterophanes.

Rhodium-catalysed expansions of four-membered thietanes into tetra-hydrothiophenes were also explored [110] and were used by Zakarian to propose a synthesis of the *Nuphar* thioalkaloids thiolane core (Scheme 44) [111].

More recently, West achieved the formal synthesis of (+)-Laurencin, the key step of which involves the 1,2-migration of a monothioacetal-derived ylide [112]. The Cu(hfacac)$_2$-catalysed formation of a cyclic ylide and the subsequent Stevens rearrangement delivered a medium-sized thioether **57** in a 60% yield under optimised conditions (Scheme 45). Interestingly, the 1,2-shift occurred with perfect retention of configuration of the α-stereogenic centre rendering this strategy synthetically useful. If the Stevens rearrangement indeed proceeds with high levels of fidelity, the potential for developing an enantioselective version of this reaction is highly attractive.

In 2009, Tang described the copper-catalysed sequence of sulfonium ylide formation/asymmetric Stevens rearrangement starting from diazomalonates and racemic 1,3-oxathiolanes (Scheme 46) [113]. The optimisation of the reaction conditions revealed the mixture of Cu(OTf)$_2$ and chiral bisoxazoline **58** as the best combination to furnish rearranged products in good yields and promising enantiopurities. However, more electron-rich substrates require the use of ligand **59,** and the enantioselectivity was decreased. It is interesting to note that in cases in which the Doyle-Kirmse reaction could occur, only the Stevens rearrangement product was observed. In subsequent studies, the discrimination between these two competing transformations has been shown to be strongly dependent on the reaction conditions and the electronic properties of the substrates.

Indeed, whilst studying the hemin-catalysed formation and rearrangement of benzyl sulfonium ylides (Scheme 47) [114], Pan and co-workers determined that the outcome of the reaction was modulated by the nature of the solvent and moreover by the presence of electron-withdrawing substituents of the benzylic aromatic ring. They established that the [2,3]-Sommelet-Hauser rearrangement
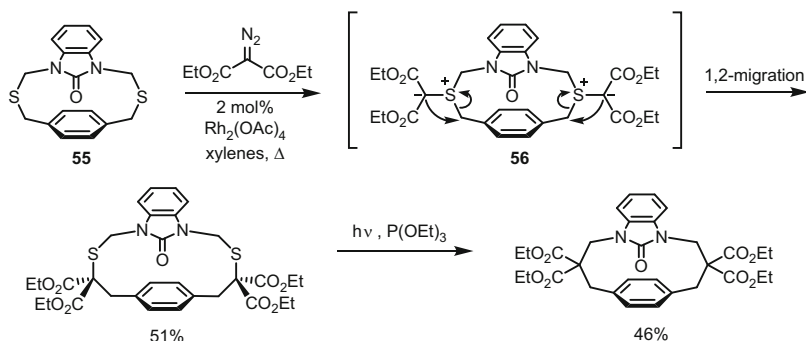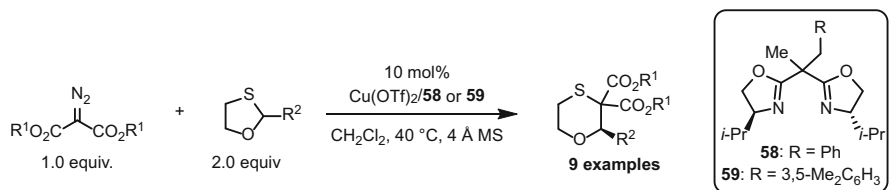

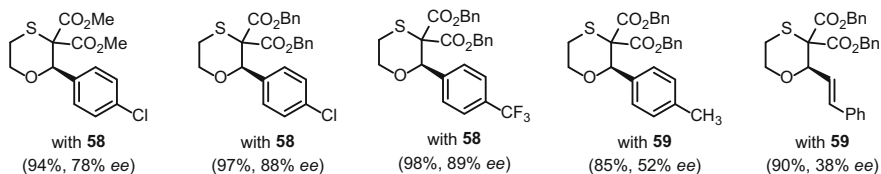Scheme 43 Macrocycle ring expansion by double-Stevens rearrangement
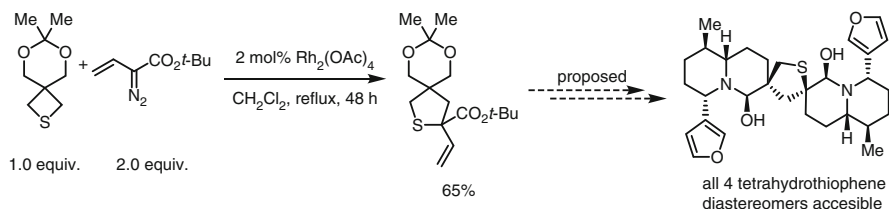
Scheme 44 Proposed synthesis of *Nuphar* thioalkaloids through ring expansion of thietanes
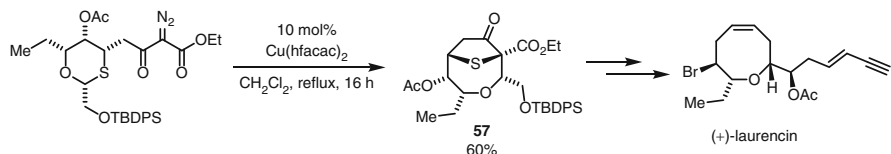
Scheme 45 Stevens rearrangement as a key step in the formal synthesis of (+)-laurencin


Scheme 46 Copper-catalysed enantioselective 1,2-migration of dithioacetals

(leading to **60**) was favoured by performing the reaction in protic solvents and with electron-poor benzylic substituents. On the other hand, electron-rich substrates formed an ylide that underwent a Stevens rearrangement (leading to **61**).

5.3 Epoxidation, Aziridination and Cyclopropanation

In addition to simple rearrangement reactions, the concept of in situ generated sulfonium ylides is theoretically applicable to any classical reaction in which one would usually preform the ylide. This concept has been employed in the synthesis

THF, 80 °C, 8 h, R = Me: **60a** = 71%, **61a**= 0%
H_2O, 40 °C, 4 h, R = NO_2: **60b** = 0%, **61b**= 94%
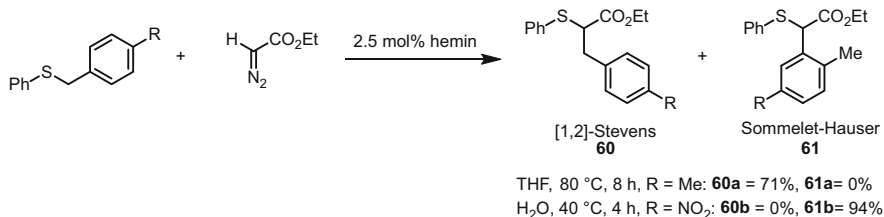
Scheme 47 Chemoselectivity between 1,2-migration and Sommelet-Hauser rearrangement

of small rings via the Corey-Chaykovsky reaction, itself a topic rich with precedent for highly diastereo- and enantioselective reaction pathways. The reader is referred to several in-depth reviews and book chapters on this topic for further information [115, 116].

5.3.1 Epoxidation

Epoxides are important functional groups due to their biological properties, although more often they serve as reactive intermediates in organic synthesis. More interesting are enantiomerically pure epoxides, as they can be used for the preparation of chiral bifunctional compounds after stereoselective ring opening by a nucleophile. Although many catalytic enantioselective methods for the synthesis of epoxides have been developed, most of these methods concern the oxidation of an alkene. Direct epoxidations from carbonyl compounds can also be achieved in an enantioselective manner by using a chiral sulfonium ylide. First stoichiometric, but later also catalytic, amounts of chiral sulfide have been reported by alkylation, deprotonation and epoxidation steps. The main disadvantages of this reaction are the basic conditions and the low reactivity of sulfides and alkyl halides that limit the substrate scope.

In 1994, Aggarwal exploited the previously discussed transition-metal-catalysed sulfonium ylide synthesis to generate transient chiral ylides capable of achieving epoxidation chemistry [117]. Such a procedure was catalytic in both transition metal and chiral sulfide **62**. Slow-addition of the diazo compound as well as dilution of the reaction mixture was crucial for obtaining good yields. Both Cu(acac)$_2$ and Rh$_2$(OAc)$_4$ were effective in the formation and transfer of the carbene to the sulfide. A number of follow-up studies were undertaken, including the use of chiral sulfides (Scheme 48a) [118–120]. A major drawback to this method, however, is the requirement to handle stoichiometric quantities of diazo compounds, which are hazardous and potentially explosive.

Therefore, a modified procedure was introduced, where tosylhydrazones were used as source of diazo compounds (Scheme 48b) [121, 122]. Sodium tosylhydrazone salts decomposed to give diazo compounds in acetonitrile at 30–40°C in the presence of phase-transfer catalysts (5–20 mol%). Sulfide loadings
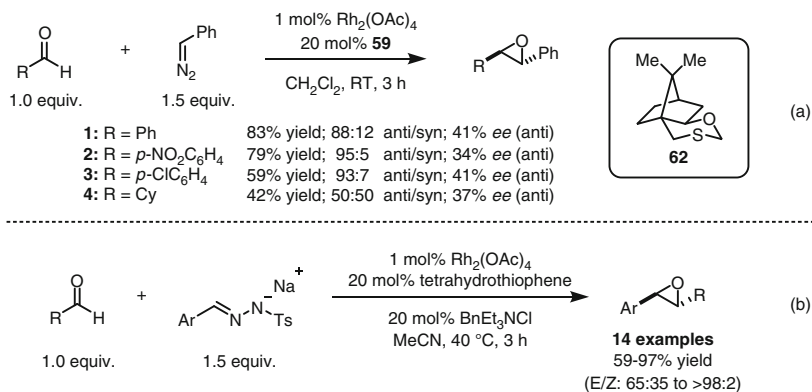
Scheme 48 Diazo-based and diazo-free sulfide-mediated epoxidation of aldehydes

as low as 5 mol% could be employed, albeit with an accompanying extension of the reaction time (up to 48 h). A wide range of aromatic, aliphatic and α,β-unsaturated aldehydes could be epoxidised in moderate to good yields and high diastereo- and enantioselectivities using camphor-derived sulfide **63** (Fig. 12). The scope of tosylhydrazone salts showed that electron-rich aryl-substituted examples gave the best yields and enantioselectivities. Electron-poor, heteroaromatic and α,-β-unsaturated tosylhydrazone salts gave more varied results.

5.3.2 Aziridination

Analogously to epoxides, aziridines are useful synthetic building blocks, and many methods have been developed for their asymmetric synthesis. In 1996, Aggarwal showed that his previously reported epoxidation procedure could also be applied for the synthesis of aziridines, by replacing the aldehyde with an imine [123]. A complication in this process is that metal carbenoids can react directly with imines to give the aziridine. This was overcome by placing electron-withdrawing groups on the imine nitrogen, thus making the π-system less reactive towards the metal carbenoid and more reactive towards sulfonium ylides. As in the epoxidation reactions, the diazo compound could be generated in situ from the corresponding tosylhydrazone salt [124, 125]. This in situ process gave in many cases better yields and enantioselectivities than when diazo compounds were used directly. However, the diastereoselectivities were only moderate (2:1 to 8:1). The scope of imines could be expanded to ketimines and alkyl aldimines, without reduction in yield.

5.3.3 Cyclopropanation

Cyclopropanation reactions can be carried out using the same strategy [126]. Similarly to the epoxidations and aziridinations, a sulfonium ylide was generated

Fig. 12 Camphor-derived
chiral sulfides for
epoxidation, aziridination
and cyclopropanation
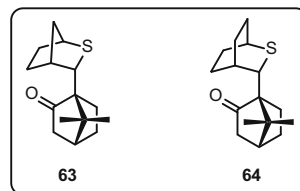
in situ from the sulfide and diazo compound, in the presence of a transition-metal catalyst. This sulfonium ylide could then react with Michael acceptors to afford the cyclopropane in moderate yield but with excellent enantioselectivities. The reaction could also be carried out with tosylhydrazones salts as diazo precursors [124]. However, sulfide **63**, which was effective for the epoxidations and aziridination, gave only low yields for the cyclopropanation. It was later shown that sulfide **64** (Fig. 12) is a more effective catalyst, leading to higher yields of the cyclopropane product [30].

6 Outlook

We have seen in each of the previous sections how the unconventional reactivity of sulfonium and sulfoxonium ylides can be paired with the strength and flexibility of transition-metal catalysis to achieve interesting new transformations. Sulfonium ylides, predominantly representing carbene synthons, traditionally react as nucleophiles, restricting their application to a handful of key reactions. However, when paired with transition-metal catalysts, a considerable breadth of reactivity can be accessed. Many of the aforementioned studies utilise chiral transition-metal catalysis to achieve enantioselective transformations, often through the asymmetric synthesis of sulfonium ylides for further transformations. Be it through carbene transfer, oxidative addition pathways or Lewis acid activation, the use of transition-metal catalysts in combination with sulfur ylides represents an underexplored and underutilised area of synthetic organic chemistry, where further exciting developments can be anticipated in coming years.

References

1. Bravo P, Fronza G, Ticozzi C, Gaudiano G (1974) J Organomet Chem 74:143–154
2. Weber L (1983) Angew Chem Int Ed 22:516–528
3. Koezuka H, Matsubayashi G, Tanaka T (1974) Inorg Chem 13:443–446
4. Sabounchei SJ, Akhlaghi Bagherjeri F, Hosseinzadeh M, Boskovic C, Gable RW (2014) C R Chim 17:1257–1263
5. Sabounchei SJ, Akhlaghi Bagherjeri F, Boskovic C, Gable RW (2013) J Mol Struct 1046:39–43

6. Sabounchei SJ, Akhlaghi Bagherjeri F, Mozafari Z, Boskovic C, Gable RW, Karamian R, Asadbegy M (2013) Dalton Trans 42:2520–2529
7. Kawafune I, Matsubayashi G-E (1983) Inorg Chim Acta 70:1–5
8. Sabounchei SJ, Hashemi A (2014) Inorg Chem Commun 47:123–127
9. Sabounchei SJ, Yousefi A, Ahmadianpoor M, Hashemi A, Bayat M, Sedghi A, Akhlaghi Bagherjeri F, Gable RW (2016) Polyhedron 117:273–282
10. Sabounchei SJ, Hashemi A, Sedghi A, Bayat M, Akhlaghi Bagherjeri F, Gable RW (2017) J Mol Struct 1135:174–185
11. Sabounchei SJ, Ahmadianpoor M, Yousefi A, Hashemi A, Bayat M, Sedghi A, Akhlaghi Bagherjeri F, Gable RW (2016) RSC Adv 6:28308–28315
12. Clagett M, Gooch A, Graham P, Holy N, Mains B, Strunk J (1976) J Org Chem 41:4033–4035
13. Lu L-Q, Chen J-R, Xiao W-J (2012) Acc Chem Res 45:1278–1293
14. Chen J-R, Dong W-R, Candy M, Pan F-F, Jörres M, Bolm C (2012) J Am Chem Soc 134:6924–6927
15. Hatcher JM, Coltart DM (2010) J Am Chem Soc 132:4546–4547
16. Li T-R, Tan F, Lu L-Q, Wei Y, Wang Y-N, Liu Y-Y, Yang Q-Q, Chen J-R, Shi D-Q, Xiao W-J (2014) Nat Commun 5:5500
17. Wang Q, Qi X, Lu L-Q, Li T-R, Yuan Z-G, Zhang K, Li B-J, Lan Y, Xiao W-J (2016) Angew Chem Int Ed 55:2840–2844
18. Plietker B (2008) Iron catalysis in organic chemistry: reactions and applications. Wiley-VCH, Weinheim
19. Wang Q, Li T-R, Lu L-Q, Li M-M, Zheng K, Xiao W-J (2016) J Am Chem Soc 138:8360–8363
20. Detz RJ (2009) Triazole-based P,N ligands: discovery of an enantioselective copper catalysed propargylic amination reaction. PhD thesis
21. Nishibayashi Y, Uemura S (2008) Metal vinylidenes and allenylidenes in catalysis. Wiley-VCH Verlag GmbH & Co. KGaA, Weinheim, pp 217–250
22. Xu X, Doyle MP (2014) Acc Chem Res 47:1396–1405
23. Deng Y, Massey LA, Zavalij PY, Doyle MP (2017) Angew Chem Int Ed 56:7479–7483
24. Kramer S, Skrydstrup T (2012) Angew Chem Int Ed 51:4681–4684
25. Huang X, Goddard R, Maulide N (2010) Angew Chem Int Ed 49:8979–8983
26. Huang X, Peng B, Luparia M, Gomes LFR, Veiros LF, Maulide N (2012) Angew Chem Int Ed 51:8886–8890
27. Klimczyk S, Huang X, Kählig H, Veiros LF, Maulide N (2015) J Org Chem 80:5719–5729
28. Klimczyk S, Misale A, Huang X, Maulide N (2015) Angew Chem Int Ed 54:10365–10369
29. Sabbatani J, Huang X, Veiros LF, Maulide N (2014) Chem Eur J 20:10636–10639
30. Unthank MG, Hussain N, Aggarwal VK (2006) Angew Chem Int Ed 45:7066–7069
31. Yar M, McGarrigle EM, Aggarwal VK (2008) Angew Chem Int Ed 47:3784–3786
32. Unthank MG, Tavassoli B, Aggarwal VK (2008) Org Lett 10:1501–1504
33. Matlock JV, Svejstrup TD, Songara P, Overington S, McGarrigle EM, Aggarwal VK (2015) Org Lett 17:5044–5047
34. Klose I, Misale A, Maulide N (2016) J Org Chem 81:7201–7210
35. Huang X, Goddard R, Maulide N (2013) Chem Commun 49:4292–4294
36. Liu Y-Y, Yang X-H, Huang X-C, Wei W-T, Song R-J, Li J-H (2013) J Org Chem 78:10421–10426
37. Wang L, He W, Yu Z (2013) Chem Soc Rev 42:599–621
38. Srogl J, Allred GD, Liebeskind LS (1997) J Am Chem Soc 119:12376–12377
39. Hooper JF, Chaplin AB, González-Rodríguez C, Thompson AL, Weller AS, Willis MC (2012) J Am Chem Soc 134:2906–2909
40. Prier CK, Rankic DA, MacMillan DWC (2013) Chem Rev 113:5322–5363
41. Shaw MH, Twilton J, MacMillan DWC (2016) J Org Chem 81:6898–6926
42. Xia X-D, Lu L-Q, Liu W-Q, Chen D-Z, Zheng Y-H, Wu L-Z, Xiao W-J (2016) Chem Eur J 22:8432–8437
43. Trost BM (1966) J Am Chem Soc 88:1587–1588
44. Burtoloso ACB, Dias RMP, Leonarczyk IA (2013) Eur J Org Chem 2013:5005–5016

45. Zhang Z, Wang J (2008) Tetrahedron 64:6577–6605
46. Deng Y, Qiu H, Srinivas HD, Doyle MP (2016) Curr Org Chem 20:61–81
47. Doyle MP, Duffy R, Ratnikov M, Zhou L (2010) Chem Rev 110:704–724
48. Peña-López M, Beller M (2017) Angew Chem Int Ed 56:46–48
49. Moody CJ (2007) Angew Chem Int Ed 46:9148–9150
50. Cohen T, Herman G, Chapman TM, Kuhn D (1974) J Am Chem Soc 96:5627–5628
51. Cimetière B, Julia M (1991) Synlett 1991:271–272
52. Müller P, Fernandez D, Nury P, Rossier J-C (1999) Helv Chim Acta 82:935–945
53. Duan Y, Lin J-H, Xiao J-C, Gu Y-C (2016) Org Lett 18:2471–2474
54. Duan Y, Lin J-H, Xiao J-C, Gu Y-C (2017) Chem Commun 53:3870–3873
55. Baldwin JE, Adlington RM, Godfrey CRA, Gollins DW, Vaughan JG (1993) J Chem Soc Chem Commun:1434–1435
56. Mangion IK, Nwamba IK, Shevlin M, Huffman MA (2009) Org Lett 11:3566–3569
57. Mangion IK, Weisel M (2010) Tetrahedron Lett 51:5490–5492
58. Molinaro C, Bulger PG, Lee EE, Kosjek B, Lau S, Gauvreau D, Howard ME, Wallace DJ, O'Shea PD (2012) J Org Chem 77:2299–2309
59. Mangion IK, Ruck RT, Rivera N, Huffman MA, Shevlin M (2011) Org Lett 13:5480–5483
60. Phelps AM, Chan VS, Napolitano JG, Krabbe SW, Schomaker JM, Shekhar S (2016) J Org Chem 81:4158–4169
61. Vaitla J, Bayer A, Hopmann KH (2017) Angew Chem Int Ed 56:4277–4281
62. Gandelman M, Rybtchinski B, Ashkenazi N, Gauvin RM, Milstein D (2001) J Am Chem Soc 123:5372–5373
63. Gandelman M, Naing KM, Rybtchinski B, Poverenov E, Ben-David Y, Ashkenazi N, Gauvin RM, Milstein D (2005) J Am Chem Soc 127:15265–15272
64. Suarez AIO, del Río MP, Remerie K, Reek JNH, de Bruin B (2012) ACS Catal 2:2046–2059
65. Padwa A, Hornbuckle SF (1991) Chem Rev 91:263–309
66. Diekmann J (1965) J Org Chem 30:2272–2275
67. Ando W, Yagihara T, Tozune S, Nakaido S, Migita T (1969) Tetrahedron Lett 10:1979–1982
68. Ando W, Yagihara T, Tozune S, Imai I, Suzuki J, Toyama T, Nakaido S, Migita T (1972) J Org Chem 37:1721–1727
69. Gillespie RJ, Porter AEA, Willmott WE (1978) J Chem Soc Chem Commun:83–84
70. Zhang Y, Wang J (2010) Coord Chem Rev 254:941–953
71. Jones AC, May JA, Sarpong R, Stoltz BM (2014) Angew Chem Int Ed 53:2556–2591
72. Sheng Z, Zhang Z, Chu C, Zhang Y, Wang J (2016) Tetrahedron 73:4011–4022
73. Kirmse W, Kapps M (1968) Chem Ber 101:994–1003
74. Doyle MP, Griffin JH, Chinn MS, Van Leusen D (1984) J Org Chem 49:1917–1925
75. Fukuda T, Katsuki T (1997) Tetrahedron Lett 38:3435–3438
76. Davies PW, Albrecht SJC, Assanelli G (2009) Org Biomol Chem 7:1276–1279
77. Greenman KL, Carter DS, Van Vranken DL (2001) Tetrahedron 57:5219–5225
78. Zhou C-Y, Yu W-Y, Chan PWH, Che C-M (2004) J Org Chem 69:7072–7082
79. Peng L, Zhang X, Ma M, Wang J (2007) Angew Chem Int Ed 46:1905–1908
80. Xiao Q, Wang J-B (2007) Acta Chim Sin 65:1733–1735
81. Zhu S-F, Zhou Q-L (2014) Nat Sci Rev 1:580–603
82. Carter DS, Van Vranken DL (2000) Org Lett 2:1303–1305
83. Prabharasuth R, Van Vranken DL (2001) J Org Chem 66:5256–5258
84. Xu X, Li C, Tao Z, Pan Y (2017) Green Chem 19:1245–1249
85. Aviv I, Gross Z (2008) Chem Eur J 14:3995–4005
86. Holzwarth MS, Alt I, Plietker B (2012) Angew Chem Int Ed 51:5351–5354
87. Liao M, Peng L, Wang J (2008) Org Lett 10:693–696
88. Li Y, Shi Y, Huang Z, Wu X, Xu P, Wang J, Zhang Y (2011) Org Lett 13:1210–1213
89. Nishibayashi Y, Ohe K, Uemura S (1995) J Chem Soc Chem Commun:1245–1246
90. Kitagaki S, Yanamoto Y, Okubo H, Nakajima M, Hashimoto S (2001) Heterocycles 54:623–628

91. Aggarwal VK, Ferrara M, Hainz R, Spey SE (1999) Tetrahedron Lett 40:8923–8927
92. Zhang X, Qu Z, Ma Z, Shi W, Jin X, Wang J (2002) J Org Chem 67:5621–5625
93. Ma M, Peng L, Li C, Zhang X, Wang J (2005) J Am Chem Soc 127:15016–15017
94. Trost BM, Hammen RF (1973) J Am Chem Soc 95:962–964
95. Zhang Z, Sheng Z, Yu W, Wu G, Zhang R, Chu W-D, Zhang Y, Wang J (2017) Nat Chem 9:970–976
96. Li Y, Huang Z, Wu X, Xu P-F, Jin J, Zhang Y, Wang J (2012) Tetrahedron 68:5234–5240
97. Miura T, Tanaka T, Yada A, Murakami M (2013) Chem Lett 42:1308–1310
98. Yadagiri D, Anbarasan P (2013) Chem Eur J 19:15115–15119
99. Miki K, Nishino F, Ohe K, Uemura S (2002) J Am Chem Soc 124:5260–5261
100. Kato Y, Miki K, Nishino F, Ohe K, Uemura S (2003) Org Lett 5:2619–2621
101. Davies PW, Albrecht SJC (2008) Chem Commun:238–240
102. Davies PW, Albrecht SJC (2009) Angew Chem Int Ed 48:8372–8375
103. Shapiro ND, Toste FD (2007) J Am Chem Soc 129:4160–4161
104. Li G, Zhang L (2007) Angew Chem Int Ed 46:5156–5159
105. Santos MD, Davies PW (2014) Chem Commun 50:6001–6004
106. Li J, Ji K, Zheng R, Nelson J, Zhang L (2014) Chem Commun 50:4130–4133
107. Zhang H, Wang B, Yi H, Zhang Y, Wang J (2015) Org Lett 17:3322–3325
108. Song Z, Wu Y, Xin T, Jin C, Wen X, Sun H, Xu Q-L (2016) Chem Commun 52:6079–6082
109. Ellis-Holder KK, Peppers BP, Kovalevsky AY, Diver ST (2006) Org Lett 8:2511–2514
110. Nair V, Nair SM, Mathai S, Liebscher J, Ziemer B, Narsimulu K (2004) Tetrahedron Lett 45:5759–5762
111. Lu P, Herrmann AT, Zakarian A (2015) J Org Chem 80:7581–7589
112. Lin R, Cao L, West FG (2017) Org Lett 19:552–555
113. Qu J-P, Xu Z-H, Zhou J, Cao C-L, Sun X-L, Dai L-X, Tang Y (2009) Adv Synth Catal 351:308–312
114. Xu X, Li C, Xiong M, Tao Z, Pan Y (2017) Chem Commun 53:6219–6222
115. Aggarwal VK, Winn CL (2004) Acc Chem Res 37:611–620
116. McGarrigle EM, Aggarwal VK (2007) Enantioselective organocatalysis: reactions and experimental procedures. Wiley-VCH Verlag GmbH & Co. KGaA, Weinheim, pp 357–389
117. Aggarwal VK, Abdel-Rahman H, Jones RVH, Lee HY, Reid BD (1994) J Am Chem Soc 116:5973–5974
118. Aggarwal VK, Abdel-Rahman H, Jones RVH, Standen MCH (1995) Tetrahedron Lett 36:1731–1732
119. Aggarwal VK, Thompson A, Jones RVH, Standen M (1995) Tetrahedron Asymmetry 6:2557–2564
120. Aggarwal VK, Abdel-Rahman H, Fan L, Jones RVH, Standen MCH (1996) Chem Eur J 2:1024–1030
121. Aggarwal VK, Alonso E, Hynd G, Lydon KM, Palmer MJ, Porcelloni M, Studley JR (2001) Angew Chem Int Ed 40:1430–1433
122. Aggarwal VK, Alonso E, Bae I, Hynd G, Lydon KM, Palmer MJ, Patel M, Porcelloni M, Richardson J, Stenson RA, Studley JR, Vasse J-L, Winn CL (2003) J Am Chem Soc 125:10926–10940
123. Aggarwal VK, Thompson A, Jones RVH, Standen MCH (1996) J Org Chem 61:8368–8369
124. Aggarwal VK, Alonso E, Fang G, Ferrara M, Hynd G, Porcelloni M (2001) Angew Chem Int Ed 40:1433–1436
125. Fulton JR, Aggarwal VK, de Vicente J (2005) Eur J Org Chem 2005:1479–1492
126. Aggarwal VK, Smith HW, Hynd G, Jones RVH, Fieldhouse R, Spey SE (2000) J Chem Soc Perkin Trans 1:3267–3276

Reactivity and Applications of α-Metalated Ylides

Viktoria H. Gessner

Abstract α-Metalated ylides, the so-called yldiides, represent a unique class of carbon-centered donor ligands. With two lone pairs of electrons at the central ylidic carbon atom, they are closely related to important organometallic ligand systems, above all bisylides and methandiides, and thus have attracted considerable research interest both from experimental and theoretical points of view. Although the number of isolated and structurally characterized yldiides is still limited, reactivity studies have demonstrated their exciting chemistry. Nowadays applications range from their use as powerful, highly nucleophilic reagents in organic synthesis such as in cascade reactions to their use as strong σ- and π-donor ligands in main group element and transition metal chemistry. The unique reactivity and donor capacity of α-metalated ylides is thereby strongly connected with the availability of the two lone pairs at the ylidic carbon atom, which makes yldiides to a special class of ylidic compounds. This review summarizes the chemistry of yldiides, particularly highlighting recent developments in their isolation and applications, also emphasizing structural and electronic properties of these compounds.

Keywords Carbanions • Catalysis • Coordination chemistry • Electronic structure • Ylide chemistry

Contents

V.H. Gessner (✉)
Lehrstuhl für Anorganische Chemie II, Fakultät für Chemie und Biochemie, Universitätsstraße 150, 44801 Bochum, Germany
e-mail: viktoria.gessner@rub.de

1   Introduction

The first preparation of ylides and their application in organic synthesis already dates back more than 100 years [1]. Since then, these reagents – above all phosphorus ylides – have become important reagents that are used in many transformations such as for the synthesis of natural products or compounds of biological and pharmacological interest. Likewise, metalated derivatives of ylides have early attracted considerable research interest particularly due to their increased reactivity compared to their neutral analogues and their potential as valuable synthetic building blocks with multiple functionalities and nucleophilic centers [2]. In general, treatment of ylides with strong metal bases can result in the formation of different metalated species depending on the position at which the metalation occurs in the molecule. This is schematically depicted in Scheme 1. Historically, diylidic compounds such as **A** had been the first class of metalated ylides. These diylides feature two carbanionic centers – mostly both in α-position to the onium moiety. The first preparation has already been described in the pioneering work by Wittig and Rieber in the 1940s [3]. Especially phosphorus-based diylides have been synthesized since then [4–6] and have been employed in selected organic transformations [2, 7–11] and as bidentate ligands in coordination chemistry, above all for the synthesis of multinuclear gold complexes [12–16]. Nevertheless, applications remained scarce compared to simple ylides. The same holds true for ortho-metalated ylides **B** that have frequently – yet often unintendedly – been observed as final product of metalation reactions of triphenylphosphonium ylides [17, 18].

α-Metalated ylides, the so-called yldiides **C**, have only recently started to receive renewed research interest both from experimental and theoretical points of view [19]. Although attempts to synthesize and apply yldiides as reactive Wittig reagents have early been made [20], the first isolation and structural proof was only achieved years later in 1997 [21]. In contrast to other metalated ylides, yldiides possess formally two lone pairs of electrons at the central ylidic carbon atom and thus exhibit a remarkably high charge concentration at a single atomic site. This property leads to unique donor properties and reactivities, which have been demonstrated by means of many exciting examples over the years.
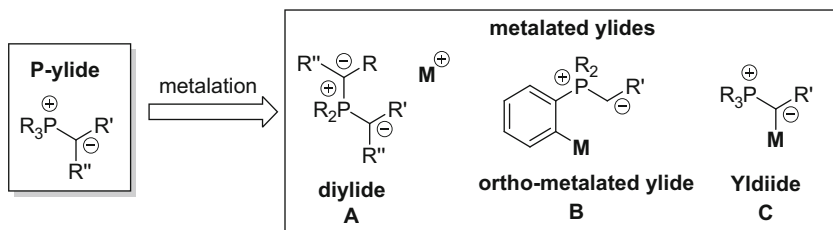
Scheme 1 Structures of different types of metalated ylides

In a structural sense, yldiides are also closely related to bisylides, such as carbodiphosphoranes **D** [22–24] and methandiides **E** (Fig. 1) [25, 26]. Likewise, these compounds exhibit two lone pairs at the central carbon atom but differ in their total charge. As such, bisylides are neutral compounds, in which the two negative formal charges at the carbon atom are equalized by the adjacent positively charged onium moieties. In contrast, methandiides are dianionic compounds that typically form oligomeric structures due to the complexation of the corresponding metal ions. According to the Green formalism of ligands in organometallic chemistry [27], bisylides can be regarded as L_2-type ligands, while methandiides are typically X_2-type ligands. Owing to these properties, both ligand systems have found broad applications in coordination and complex chemistry. For example, methandiides have shown to serve as unusual carbene ligands forming a unique type of carbene complexes with metals covering the whole periodic table by simple salt metathesis reaction [28–31]. The neutral bisylides on the other hand show fascinating electronic properties and have thus been used as versatile ligands such as for the stabilization of unusual bonding situations [24, 32, 33]. The exciting chemistry of bisylidic compounds is summarized in [34, 35].

Overall, yldiides take an intermediate position between these classes of carbon-based donor ligands. In this book chapter, we summarize the chemistry of α-metalated ylides also in comparison with other ylidic compounds and carbon bases. We particularly focus on recent advances in their isolation and the elucidation of their molecular and electronic structure. Furthermore applications in organic synthesis as well as coordination and complex chemistry are presented, which highlight the special properties and reactivities of yldiides as versatile reagents.

2 Preparation, Characterization, and Structures of Metalated Ylides

2.1 Synthesis and Structures of α-Metalated Ylides

Since metalated ylides are the deprotonated version of "normal" ylidic compounds, the most convenient way of their synthesis includes the deprotonation of ylide precursors or the direct double deprotonation of phosphonium salts. Thereby, the CH acidity of the precursor is pivotal for choosing the right base and reaction
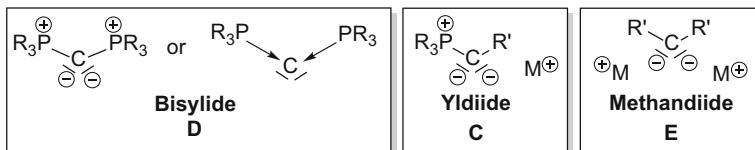
Fig. 1 Comparison between bisylides, yldiides, and methandiides

conditions for successful isolation of the yldiide. Although the deprotonation of many ylides has early been reported, structural proof of the actual formation of an yldiide has only been provided for very few examples. This is mostly because of the lack of sufficient stabilization of the negative charge at the ylidic carbon atom and/or favorable decomposition pathways (e.g., via metal salt elimination), which result in low stabilities and/or follow-up reactions. This, for example, holds true for the first α-metalated ylide reported by Bestmann and coworkers in the 1970s [36]. They reacted ethoxycarbonyl-methylenetriphenylphosphorane (1) with methyl or phenyllithium (Scheme 2) to form the desired yldiide 2. However, 2 was found to be unstable under the reaction conditions and further reacted under loss of lithium ethoxide to the corresponding ylide 3. The same reactivity was observed for the methoxy compound using sodium hexamethyldisilazide (NaHMDS) as base [37].

The simplest phosphorus yldiide, α-lithiomethylenetriphenylphosphorane 4, had been the subject of contradicting studies. Corey and coworkers reported the facile synthesis of 4 by treatment of methylenetriphenylphosphorane (5) with different organolithium bases (Scheme 3) [20]. 4 was successfully applied as "activated" ylide capable of performing Wittig-type reactions with difficult substances such as sterically hindered ketones, which – in contrast – showed no reaction with the corresponding ylide, methylenetriphenylphosphorane (5). Although these results were again later confirmed by the same authors [38], it contrasts reports by Schlosser and coworkers, who showed that treatment of ylide 5 with alkyllithium bases also leads to the formation of considerable amounts of further metalated species, in particular the *ortho*-metalated compound 6 [39]. Despite these contradictions, yldiide 4 was later reported to be more conveniently accessible via metal/halogen exchange using (bromomethy1)phosphonium bromide 8 (Scheme 3) [38, 40], a method which is often used in alkali and alkaline earth metal chemistry but scarcely in the preparation of yldiides.

Despite these early reports on the in situ preparation and application of yldiides, the first isolation was only achieved in the late 1980s by Bestmann and coworkers [41]. The cyano-functionalized yldiide 9 was prepared by a straightforward metalation procedure from the corresponding ylide 9-H using NaHMDS as base (Scheme 4). Thus, 9 was obtained as yellow and air- and moisture-sensitive solid and characterized by IR as well as NMR spectroscopy. Interestingly, the nitrile band in 9 was found to appear at smaller wave numbers ($\nu = 2{,}000 \ \text{cm}^{-1}$) compared to the ylide precursor ($\nu = 2{,}130 \ \text{cm}^{-1}$), thus suggesting a decrease in the C–N bond order. Based on these observations, the authors concluded that resonance structure 9′ with a C=N double bond strongly contributes to the electron distribution in 9.
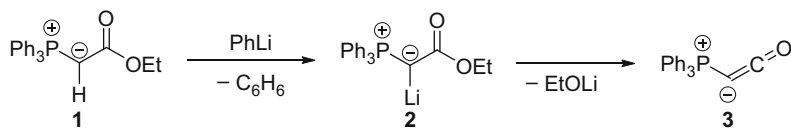
Scheme 2 First attempt to isolate α-metalated ylide **2**
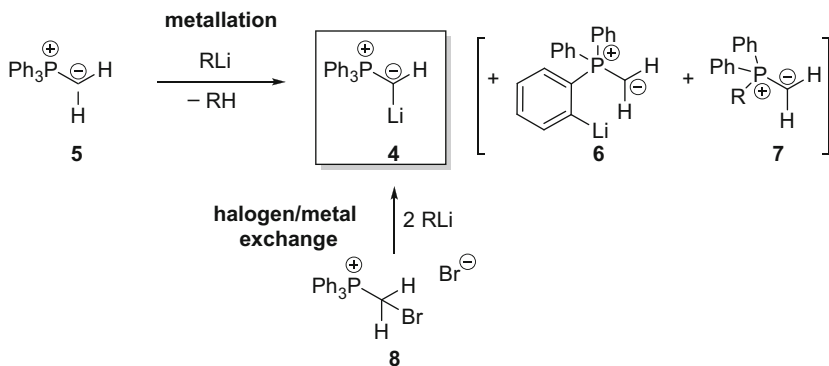
Scheme 3 Preparation of α-lithiomethylenetriphenylphosphorane **4** via metalation and halogen/metal exhange
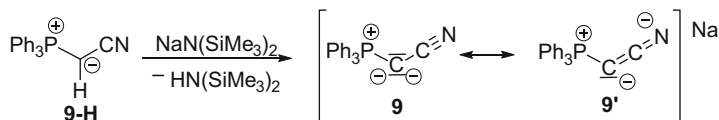
Scheme 4 Preparation and resonance structures of the metalated ylide **9**

However, owing to its reactivity also resonance structure **9** with two pairs of electrons at the ylidic carbon atom was suggested (see below).

Apart from yldiide **9,** four further metalated ylides have been isolated and additionally structurally authenticated to date. The first structural proof was provided by Niecke with lithium phosphoranylidene ylides **10** [21] (Scheme 5). These compounds were prepared by deprotonation of the protonated precursor with butyllithium and isolated as yellow, crystalline solids. It is noteworthy that the ylides **10a** and **10b** can also be regarded as lithiated phosphalkenes with the negative charge residing on the X substituent. However, since the formula depicted in Scheme 5 may also contribute to the electronic structure of the compound, **10** has also to be regarded as metalated ylide. This is also supported by the molecular structure of **10a** and **10b** in which the lithium ion directly binds to the ylidic carbon atom. The coordination sphere of the metal is completed by the coordination of three molecules of THF. An interesting structural feature are the short P–C distances of 1.632(5) and 1.624(5) Å which corroborate with a partial double bond character or increased Coulombic interactions within the $P^{\delta+}$–$C^{\delta-}$ linkage.

Scheme 5 Preparation and
structures of the metalated
ylides **10** and **12**

10a, X = C(SiMe$_3$)$_2$
10b, X = NAr with
Ar = 2,4,6-tBu$_3$C$_6$H$_2$
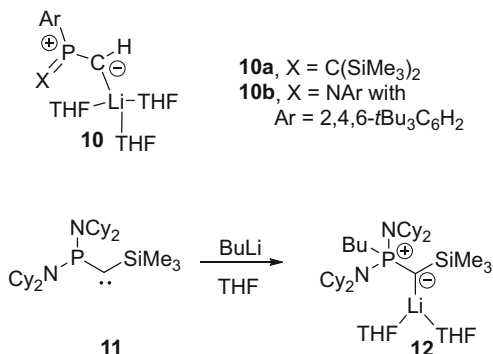
    In contrast to all other metalated ylides, the silyl-substituted system **12** was not
prepared via deprotonation or halogen/metal exchange but by a unique 1,2 addition
reaction of butyllithium to carbene **11** (Scheme 5) [42]. Comparable to the molec-
ular structures of **10**, yldiide **12** features a direct contact between the ylidic carbon
atom and the metal ion, which is further coordinated by solvent molecules (Fig. 2).
The carbon atom features a planar geometry with short P–C (1.636(11) Å) and Si–C
distances (1.755(10) Å) corroborating with increased electrostatic interactions or
strong σ-donation from and π-backbonding to the phosphine ligand (see below for a
detailed discussion on the bonding situation in metalated ylides). Although **10** and
12 had been isolated and structurally authenticated, applications and detailed
studies on their reactivity are missing.
    The first metalated ylide, which is conveniently accessible and isolable also in
gram scale, has only recently been reported by Gessner and coworkers [43]. The
sulfonyl-substituted yldiide **13-M** can be prepared by stepwise deprotonation of the
corresponding phosphonium salt **13-H$_2$** (Scheme 6). Depending on the metal base
used in the second deprotonation step, the lithium, sodium, and potassium com-
pound, respectively, are available and have been characterized in solution as well as
in solid state. The molecular structure of **13-M** was determined with sodium and
potassium as counterions (Fig. 3a, b). In the latter case, complexation by 18-crown-
6 was used to ease crystallization. While the sodium compound features a dimeric
structure with two (NaO)$_4$ cubes connected via one common face, the potassium
analogue forms a monomer, in which the coordination sphere of the metal is
completed by the crown ether. Despite forming different aggregates, both com-
pounds feature a similar coordination behavior of the yldiide toward the metal. As
such, the metal is coordinated by the oxygen atoms of the sulfonyl moiety as well as
by the ylidic carbon atom. Consistently, similar bond lengths and angles have been
found in both structures. Similar to the metalated ylides **10** and **12**, **13-M** also
exhibits considerably shortened P–C distances. This bond shortening nicely reflects
the increased negative partial charge at the central carbon atom. Thus, a continuous
bond shortening is observed in the compound series **13-H$_2$**, **13-H**, and **13-M**. While
the P–C bond in the phosphonium salt amounts to 1.808(3) Å, it shortens to 1.700
(3) Å in ylide **13-H** and even to 1.646(2) in the potassium salt **13-K**. The same trend
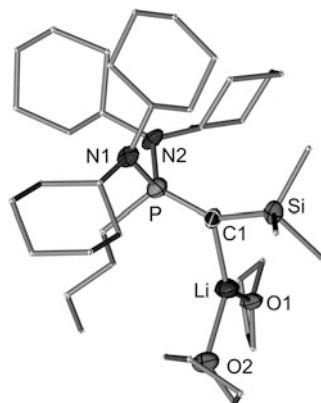
was observed for the S–C bond, thus reflecting the increased electrostatic attraction within the whole P–C–S linkage. It is noteworthy that the short P–C distances reported for the metalated ylides **10**, **12**, and **13-K** are comparable to that found in the molecular structure of hexaphenylcarbodiphosphorane (CDP) (1.635(5) Å) [44]. The same holds true for the sulfoxide system **15-Li** reported by Maerten, Baceiredo, and coworkers [45] (Scheme 6). **15-Li** forms a dimeric structure incorporating a Li_2O_2 core due to coordination of two molecules of THF (Fig. 3c). The yldiide also features contact between the lithium atom and the sulfoxide oxygen atom comparable to **13-M**.

Concerning the identification and characterization of α-metalated ylides, ^{31}P NMR spectroscopy has proven to be particularly helpful. In general, a distinct high-field shift of the ^{31}P NMR signal relative to the ylide precursor or the phosphonium salt is observed upon metalation. This has been demonstrated for the series of compounds **13-H$_2$**, **13-H**, and **13-M** [43] but also for other yldiides. A selection of NMR data for isolated yldiides is given in Table 1. The ^{31}P NMR shift also seems to depend on the nature of the metal and how strongly it is bound to the ylidic carbon atom. As such, a further high-field shift is observed by replacing sodium by potassium in yldiide **13-M** and by addition of the crown ether. Another NMR value indicative for successful yldiide formation is the $^1J_{PC}$ coupling constant. In general, a decrease in the coupling constant was observed upon metalation, for example, by $\Delta J = 40$ Hz in case of the cyano-functionalized yldiide **9** [41] or by even $\Delta J = 121$ Hz in case of sulfoxide **15-Li** [45]. This decrease was attributed to a higher p character in the P–C linkage and an increase of s-electron density at the ylidic carbon atom which also results in the stabilization of the lone pair at the carbon atom [21].

Although a couple of metalated ylides have been isolated and unambiguously been identified, the number of conveniently accessible representatives is still extremely limited. So far, only yldiides with an additional anion-stabilizing group (e.g., CN in **9** or SiMe$_3$ in **12**) have been isolated. For broad applications, a broadening of the scope will be necessary in the future. However, owing to the

Tipp = tri*iso*propylphenyl
R = *iso*-propyl
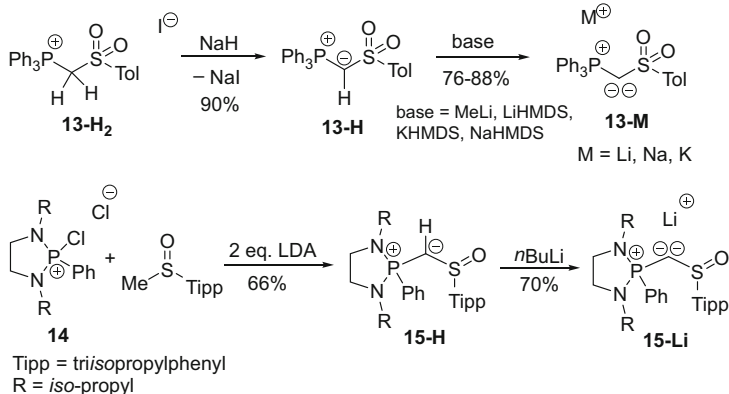
Scheme 6 Preparation of yldiides **13-M** (*top*) and **15-Li** (*bottom*) by deprotonation of the corresponding ylides

high electron density at the yldic carbon atom in yldiides, the isolation of less or non-stabilized systems will be particularly challenging.

2.2 Computational Studies on the Electronic Structure of Yldiides

First computational studies on metalated ylides were already performed by Streitwieser in 1984 on the model system (α-lithiomethylene)phosphorane, $H_3PC(H)Li$ [46]. They particularly focused on the increased reactivity of yldiides compared to their corresponding ylides as had been reported by Corey and coworkers [20]. The performed ab initio SCF-MO calculations indicated that the high reactivity of $H_3PC(H)Li$ is mostly due to its high charge concentration and its existence as contact ion pair, whose chemistry is similar to that of the corresponding free anion and thus shows low steric hindrance. Density functional theory calculations on the metalated ylide **13-M** also showed an increased negative partial charge at the yldic carbon atom in **13-M** ($q_C = -1.33$) compared to **13-H** ($q_C = -1.05$) [43]. This increase of electron density is well in line with the reduced bond distances in the P–C–S linkage found in the molecular structure of **13-M** (see above). Calculations of the molecular orbitals showed that the two highest occupied molecular orbitals (HOMO and HOMO-1, Fig. 4) mostly resemble lone pairs of electrons at the yldic carbon atom, one of σ- (HOMO-1) and one of π-symmetry (HOMO), thus suggesting that the yldiide should potentially act as strong σ- and π-donor ligand. Accordingly, high proton affinities (PA) were calculated for **13-M**. These PAs are higher than those found for CDPs but smaller than those of similar methandiide ligands.

The bonding situation in metalated ylides was only recently addressed. These studies were particularly motivated by continuous controversial discussions on the electronic structure of bisylides such as carbodiphosphoranes [47–49]. While it has early been
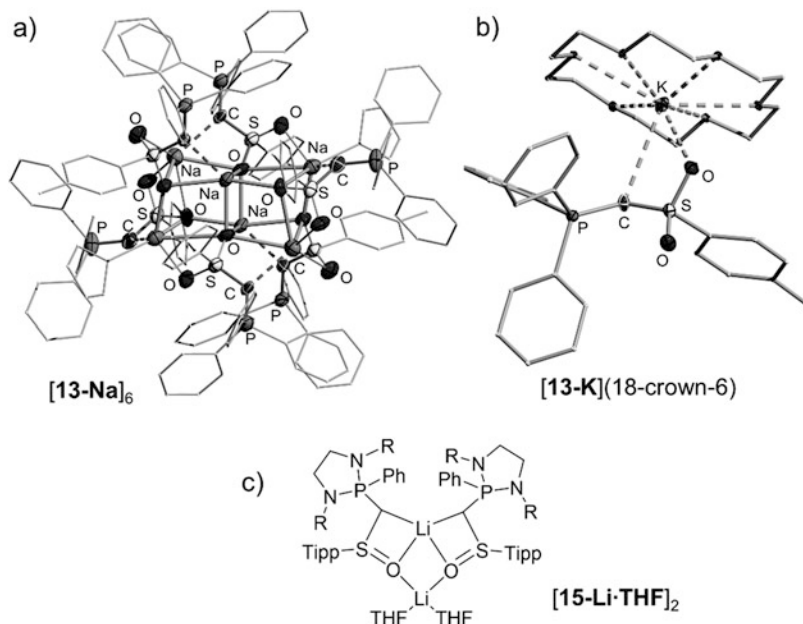
Fig. 3 Solid-state molecular structures of yldiide **13-M** with sodium (**a**) and potassium (**b**) as counterions and (**c**) drawing of the molecular structure of **15-Li**

shown that bisylides – due to the energetically high-lying d-orbitals of phosphorus [50] – cannot be described as heterocumulenes such as **D1** (Fig. 5), the bisylidic structure **D2** with electrostatic interactions in the P^+–C^- linkage has long been considered as the best description of the bonding situations. However, based on theoretical studies, Frenking and coworkers recently suggested that the structure **D3** with donor-acceptor interactions between the phosphine ligand and the central carbon atom better describes the electronics and reactivity of bisylides [51–54]. Here, the bonding is described by a captodative formalism, that is, σ-donation from the ligands (L) to the central carbon atom and π-back-donation of the lone pairs of carbon(0) to L. In contrast to the ylidic bonding situation in **D2**, the carbon atom in **D3** formally exhibits an oxidation state of zero, which led to the denotation of bisylides as carbones. Because of the similarity of this bonding situation to the Dewar-Chatt-Duncanson model [55, 56] used to describe ligand-metal interactions in transition metal chemistry, Fürstner and colleagues concluded in their studies that "carbon is capable of serving as the central atom of a complex – just as a metal can do" [22, 57]. This bonding situation and metal-like behavior of carbon or other main group elements was found to be suitable not only for the description of carbodiphosphoranes but also for other bisylidic compounds such as carbodicarbenes [58, 59] or heavier main group element compounds [60].

For elucidation of the bonding situation in metalated ylides, natural bond orbital (NBO) analyses in combination with energy decomposition analyses (EDA) and calculations of the molecular orbitals were performed [61]. Real systems, such as

Table 1 Comparison of the ^{31}P NMR data of metalated ylides and their protonated precursors

Compound	δ_P (ppm)	$^1J_{PC}$ (Hz)	Compound	δ_P (ppm)	$^1J_{PC}$ (Hz)
13-H$_2$	16.8	45.9	**12-H**	63.5	125.7
13-H	14.2	123.3	**12**	41	Broad signals
13-Na	−11.0	38.0	**9-H**	23.2	135
13-K	−12.3	Broad signals	**9**	2.5	94.6
13-K (with 18-crown-6)	−16.6	Broad signals	**10a-H**	n.d.	126.6
15-H	46.8	151.3	**10a**	148.3	28.2
15-Li	18.0	30.6			
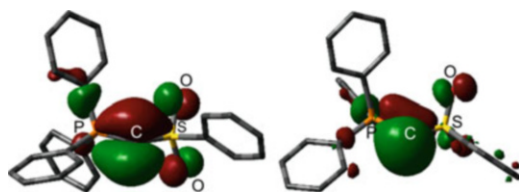
Fig. 4 HOMO (*left*) and HOMO-1 (*right*) of the metalated ylide **13-M**
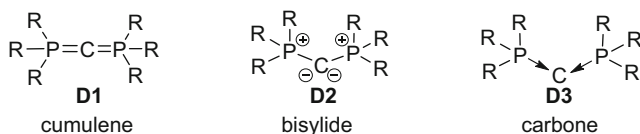
Fig. 5 Possible canonical structures of carbodiphosphoranes

the isolated compounds **9** and **13-M**, as well as further model systems of the general constitution Ph$_3$P–C–L were addressed in order to study the impact of the substituent L on the bonding situation. Additionally, neutral bisylidic analogues of some of the yldiides were examined in order to shed light on the influence of the total charge of the molecule on the electronics of the compound. Due to the unsymmetrical substitution pattern in metalated ylides, also unsymmetrical bonding situations (i.e., combinations of the resonance structures depicted in Fig. 5) were considered. An interesting outcome of these studies concerned the negative charge located at the ylidic carbon atom in metalated ylides compared to that in related bisylidic compounds. Despite the negative total charge, yldiides were found to show similar negative charges than their neutral analogues. For example, the isoelectronic compound pair **9** and **16** (Fig. 6) exhibit comparable charges at the central carbon atom ($q_C = -0.99$ vs. -0.96) and at phosphorus, despite the fact that nitrile **9** is an anionic compound while **16** is a neutral species. Overall, the charge at the carbon atom is more affected by the nature of the substituent than by the total charge of the molecule. Anion-stabilizing groups such as sulfonyl or phosphoryl groups lead to

Fig. 6 Comparison of the
NBO charges in the
metalated ylide **9** and **16**
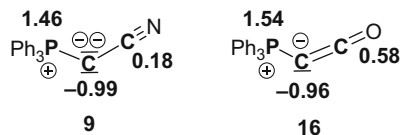
high charge concentrations (e.g., $q_C = -1.29$ in the phenyl-substituted analogue of **13**), while substituents capable for charge delocalization minimize the charge density (e.g., $q_C = -0.99$ in **9**).

With respect to a carbone-like character of metalated ylides, the energy decomposition analyses (as well as the NBO analyses) provided no clear-cut picture [61]. Instead, for most of the yldiides calculated, several fragmentation patterns were found to be equal in energies and thus equally valid. In general, ylidic bonds ($P^+–C^-$ and $L–C^-$) and dative interactions ($P \rightarrow C$ and $C \leftarrow L^-$) as well as combinations of both showed similar energies. For example, for the phenyl-substituted analogue of **13**, the two structures shown in Fig. 10 were calculated to be the best fragmentation pattern of this system. Interestingly, introduction of a positive charge into the molecular backbone resulted in an increased importance of the donor-acceptor bond for the description of the interaction of the ligand L with the central carbon atom. Thus, the neutral compound **17** also exhibited a low-energy structure with an ylidic bond to the phosphine ligand and a dative bond to the sulfonyl substituent (see structure **17′′′** in Fig. 7), which was not found to be suitable for the description of its anionic congener **13_Ph**. Overall, both bonding schemes (ylidic and dative) are suitable for the description of metalated ylides. Thus, they can also be viewed as anionic carbone derivatives. Independent of the exact bonding situation, all fragmentation patterns reflect the presence of two pairs of electrons located at the central carbon atom, which are in line with the molecular orbitals (cf. Fig. 4) and the reactivity of these compounds (see below).

3 Applications of Metalated Ylides in Organic Synthesis

The reactivity of metalated ylides is dominated by the two lone pairs of electrons at the ylidic carbon atom. These electron pairs give rise to high electron density and thus to high basicity and a strong nucleophilic character. Thus, yldiides can be used to functionalize ylides by simple treatment with various electrophilic species. Even though – due to the lack of readily isolable systems – most of the reactions reported made use of in situ generated yldiides, applications are not limited to simple trapping reactions. With the increasing number of isolated metalated ylides in recent years, new applications have been discovered, and many more can be expected in the next years. In this chapter, we discuss the use of metalated ylides in synthetic chemistry. We first focus on applications in organic synthesis for the preparation of functionalized compounds. While the applications discussed here already demonstrate the unique reactivity of
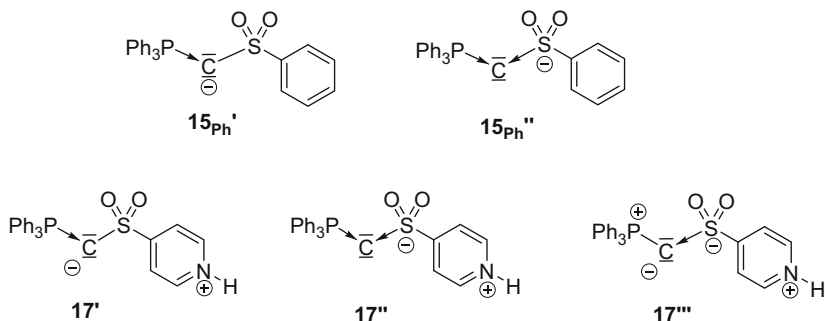
Fig. 7 Most favored structures for 13_{Ph} and its neutral congener **17** according to the EDA

yldiides connected with the two lone pairs at carbon, the subsequent chapters concentrate on their ligand properties and their use in main group and transition metal chemistry.

3.1 Reactivity Toward Carbonyl Compounds and Epoxides

The synthetic value of "simple" ylidic compounds is strongly connected with their use in Wittig-type reactions. While the Wittig reactivity of simple ylides has been studied intensively over many years [62–64], the reactivity of metalated ylides toward carbonyl compounds is by far less explored. Nonetheless, the first experiments on Wittig-type reactions with metalated ylides were already reported in the 1980s. Corey and coworkers demonstrated an increased reactivity of α-lithiomethylenetriphenylphosphorane (**4**) compared to its protonated ylide analogue (methylenetriphenylphosphorane) in Wittig reactions with sterically demanding ketones [20, 38]. As such, **4** reacted with fenchone (**18**) to the corresponding exo-methylene derivative **19**, while methylenetriphenylphosphorane showed no conversion (Scheme 7a). The synthetic utility was also demonstrated by the reactions of **4** with 2 equiv. benzaldehyde or hexanal, which were both converted to the trans-allylic alcohols **20** and **21**, respectively (Scheme 7b). In this reaction, the metalated ylide showed two distinct reactivities: at first, it acted as a typical organolithium species undergoing a 1,2-addition to the carbonyl group, while it subsequently performed a classical Wittig olefination reaction. This already demonstrated the applicability of metalated ylides in cascade reactions, which was later also applied for other types of reactions (see Sect. 3.2).

In contrast to the Wittig reactivity observed by Corey, a different behavior toward aldehydes was reported by Gessner and coworkers using the isolated sodium yldiides **9** and **13-Na** [43]. Instead of forming trans-allylic alcohols as found for yldiide
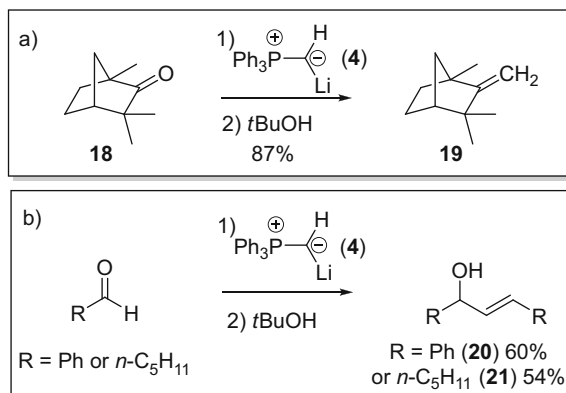
Scheme 7 Reactions of lithiomethylenetriphenylphosphorane **4** with carbonyl compounds: (**a**) with a sterically demanding ketone and (**b**) with aldehydes

4 (Scheme 7b), **9** and **13-Na** reacted with benzaldehyde and pentafluorobenzaldehyde to the novel carbonyl compounds **22–24** as main products (Scheme 8). Mechanistically, this reaction presumably also proceeds at first via a 1,2-addition of the metalated ylide to the carbonyl group. However, the formed intermediate sodium alcoholate is a highly stabilized ylide which thus does not (or only slowly) undergo Wittig olefination. Instead, the high electron density leads to the formal elimination of a β-substituent. Thus, in case of benzaldehyde sodium, hydride is formally eliminated, while in case of the fluorinated compound, pentafluorophenyl sodium is lost. This reaction impressively demonstrates the tunability of the reactivity of metalated ylides. Hence, the α-substituents are important not only for the stabilization of these compounds but also for tailoring their reactivity.

The synthetic utility of metalated ylides was also demonstrated by means of their reactivity toward epoxides. Several examples were reported in which yldiides cleanly reacted with epoxides in a ring-opening reaction and formation of alcohols after hydrolysis, among α-lithiomethylenetriphenylphosphorane (**4**) [20] and the Bestmann's yldiide **9**. Due to the cyano-functionalization, **9** also gave way to interesting further reaction products after hydrolysis of the alcoholate **25** initially formed after epoxide opening (Scheme 9) [65]. As such, acidic workup first leads to protonation and formation of the intermediates **26-Int**, which subsequently hydro-lyze via phosphine oxide elimination to γ-hydroxynitriles **26** in overall yields of 63–72%. In contrast, hydrolysis of **25** under basic conditions results in the additional hydrolysis of the nitrile group. The thus formed carboxylates **27-Int** then furnishes lactones **27** after protonation and cyclization in overall yields between 60 and 77%. Hence, the metalated ylide **9** proved to be a particularly versatile reagent, due to the additional reactivity of the cyano group.
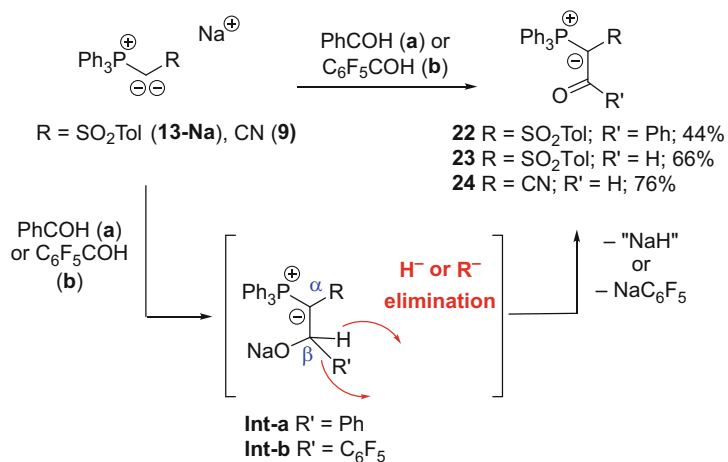
Scheme 8 Reaction of the isolated yldiides **9** and **13-Na** with aldehydes: acylation reaction via an intermediate alcoholate
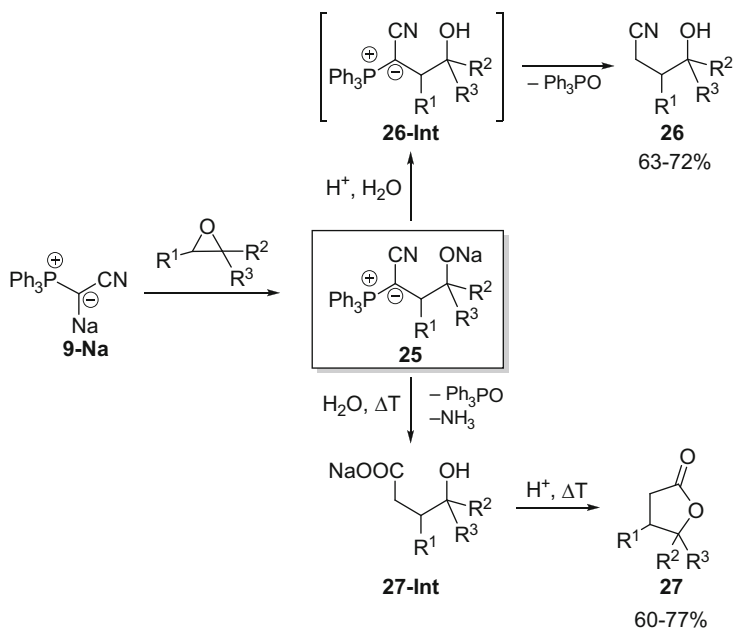
Scheme 9 Ring opening of epoxides with yldiide **9** and subsequent hydrolysis reactions

3.2   Cascade Reactions

Because of the two lone pairs at the ylidic carbon atom, metalated ylides can both react as highly nucleophilic carbon bases but also as ylidic compounds. This makes yldiides particularly interesting reagents for cascade reactions, using both types of reactivities. This has first been demonstrated by the reaction of the metalated ylide **4** with two equivalents of aldehyde, resulting in a 1,2-addition reaction followed by a Wittig olefination to yield trans-allylic alcohols (Scheme 7) [20]. However, also two different reaction partners can be employed to introduce different groups and functionalities and to address different reaction pathways. Bestmann and coworkers used this approach for a series of cascade reactions starting from the cyano system **9** [41]. Until today, **9** remains the metalated ylide, which has most intensively been studied in cascade reactions. This can probably be referred to its convenient preparation and stability, thus suggesting that the isolation of further yldiides may be attractive for the development of new domino reactions.

A selection of cascade reactions performed with yldiide **9** is shown in Scheme 10. Starting with simple substitution reactions using acetale functionalized halogen compounds, Bestmann and coworkers accomplished elegant cyclization reactions to monocyclic and bicyclic compounds. After substitution, subsequent cleavage of the acetale to the aldehyde and intramolecular Wittig reaction yielded the α,-β-unsaturated nitriles **28** and **29**. Also, dienes were found to be accessible from **9** employing different aldehydes [41]. Here, the first step involves the 1,2-addition of the metalated ylide to *n*-pentanal followed by treatment with trimethylchlorosilane to yield the α,β-unsaturated cyano ylide **30-Int** via loss of trimethylsilanol (Me$_3$SiOH) from the intermediate silyl ether. **30-Int** subsequently reacts with a further equivalent of aldehyde in a Wittig reaction to form the corresponding dienes **30a** and **30b** in moderate to good yields (48–72%). Cyanoacetylenes **31a** and **31b** were also found to be accessible from **9** by its reaction with carboxylic esters. The initially obtained acyl cyano ylides **31-Int** undergo thermolysis to the corresponding alkyne carbonitriles by elimination of triphenylphosphine oxide (Scheme 10).

4   Ylide Functionalization in Main Group Element Chemistry

The two lone pairs at the ylidic carbon atom and the resulting high donor capacity of metalated ylides suggest that these compounds may serve as potent donor ligands to support electron-deficient and/or low valent main group element compounds. Due to the so far extremely limited number of readily isolable yldiides, this chemistry is still in its infancy. However, the examples reported and summarized in the following chapter already demonstrate the utility of metalated ylides to stabilize and electronically manipulate main group element species.
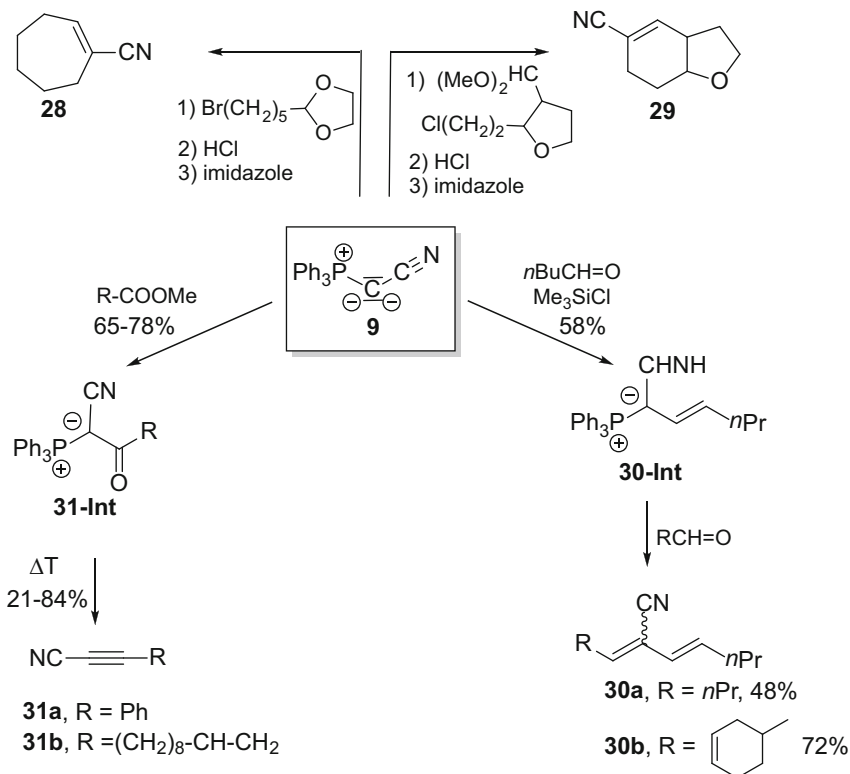
Scheme 10 Cascade reactions with yldiide **9**

4.1 Ylide-Stabilized Carbenes and Silylenes

Singlet carbenes have experienced a remarkable renaissance over the past three decades. With the development of stable, isolable, and even bottable systems, these compounds have turned from laboratory curiosities into versatile reagents with a myriad of applications [66–70]. For example, singlet carbenes have been recognized as powerful ligands in transition metal catalysis [71–74] and main group element chemistry [75], as organocatalysts [76, 77] or as reactive species in bond activation reactions [78–81]. Decisive factor in this chemistry has been the stabilization of these low-valent carbon compounds to facilitate their handling and isolation. In most of the cases, stabilization is achieved by α-nitrogen substituents [e.g., in diaminocarbenes, above all *N*-heterocyclic carbenes (NHC), or cyclic alkyl (amino)carbenes (cAAC), Fig. 8]. These substituents stabilize the singlet ground state through π-interaction, i.e., the lone pair of the heteroelement interacts with the vacant p_π orbital of the carbene. Similar stabilizing abilities can be envisioned for ylide substituents, which thus may be used for the stabilization of singlet carbenes and the manipulation of their electron-donating properties. Since the α-carbon atom

Fig. 8 Different types of stabilized carbenes
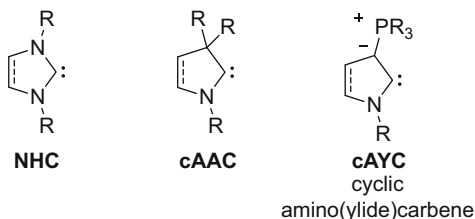
in ylide-substituted carbenes is less electronegative than the nitrogen in NHCs but capable of π-donation, ylide-functionalized carbenes are expected to be strongly σ-donating ligands with pronounced electron-releasing capacities and thus attractive ancillary ligands for applications in homogenous catalysis. Due to these promising features, ylide-substituted carbenes (as well as silylenes) have been subject of experimental as well as theoretical investigations over the past 10 years.

4.1.1   Synthesis and Properties

Transition metal complexes of cyclic amino(ylide)carbene (cAYC) (Fig. 9) had early been reported [82–86] but had only little impact compared with NHC complexes. These cAYC complexes were synthesized through intramolecular cyclization from the corresponding transition metal isocyanide complexes bearing a phosphorus ylide at the ortho position and not from the corresponding isolated carbenes. In contrast, free cAYCs have only recently been synthesized. In 2008, Kawashima and Fürstner independently reported of the preparation and properties of the phosphorus- and sulfur ylide-functionalized carbenes **32–35** depicted in Fig. 12 [87–89]. Although the ylide moiety in these systems was not introduced by using isolated metalated ylides, the synthesized AYCs impressively demonstrated the unique donor properties of such carbene ligands as result of ylide functionalization.

The preparation of cAYCs **32–35** was accomplished by deprotonation of the protonated precursors comparable to diaminocarbenes. In a typical protocol, metal bases such as mesityllithium (MesLi) or potassium hexamethyldisilazide (KHMDS) were added to solutions of the onium salts at low reaction temperatures. Scheme 11 exemplarily depicts the synthesis of **32** reported by Kawashima [87]. Despite the facile synthesis of the carbenes **32–35,** their isolation at room temperature failed due to the higher reactivity of these species compared to NHCs. For example, **32** was shown to undergo transfer of one of the phosphonium-bound phenyl groups to the carbenic carbon atom to give phosphine **36** [87]. However, chemical evidence for the carbene character of **33–35** was unambiguously provided by the reaction with elemental sulfur to yield the corresponding thioamides.

The donor property of AYCs was assessed by the preparation of the *cis*-[RhCl(CO)₂L] complexes of **32–35**. The carbonyl stretching frequencies in these complexes are recognized as an index of the electron-donating properties of L-type ligands such as carbenes [90, 91]. In all cases, lower frequencies compared to analogous diaminocarbenes were
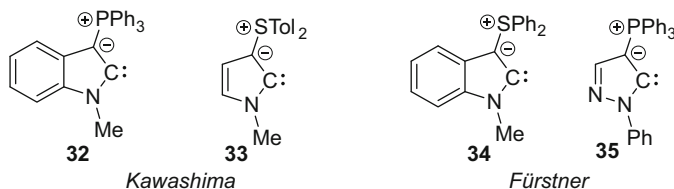
Fig. 9 Cyclic amino(ylide)carbenes synthesized by Kawashima and Fürstner
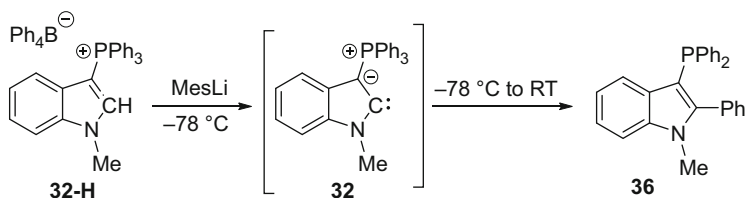
Scheme 11 Synthesis and decomposition of amino(ylide)carbene **32**

observed. For example, the rhodium complex **37** of AYC **35** showed a frequency no less than 44 cm^{-1} lower than that of the corresponding triazolyl-2-ylidene complex **38** (Fig. 10) [89]. This indicates that introduction of an ylide substituent has a tremendous effect on the electronics of a given carbene system. In general, the electron-releasing property of AYCs surpasses that of traditional NHCs. Despite of these features, applications of AYCs **32**–**35** in catalysis remain scarce until today. The only example was provided with AYC **32**, which was applied in a Buchwald-Hartwig-type C–N coupling reaction [82].

Ylide-substituted carbenes were presumably also the active ligands in palladium-catalyzed coupling reactions with the 1,3-diphosphorus ylide cyclopentadienylium salts [(C$_5$H$_3$)(PPh$_3$)$_2$]I and its tolyl derivative {(C$_5$H$_3$)[P(4-CH$_3$-Ph)$_3$]$_2$}I [92]. Although the corresponding bis(ylide)-stabilized carbenes **39** were neither isolated nor their formation unambiguously confirmed by their reactivity (e.g., trapping with elemental sulfur or in metal complexes), their proposed formation was well in line with the high activity of these ligands in Buchwald-Hartwig and Suzuki coupling reactions of aryl chlorides at room temperature (Fig. 11). This was further confirmed by density functional theory (DFT) studies showing that these purely ylide-functionalized carbenes possess exceptionally high donor abilities.

Silylene systems analogous to **39** were reported by Driess and coworkers. Their synthesis was accomplished by deprotonation of the bisphosphonium salts **40** with four molar equivalents of potassium hexamethyldisilazide (KHMDS) in the presence of SiBr$_4$ followed by reduction of the corresponding dibromo precursors (Fig. 12, top) [93]. Due to the generally higher stability of silylenes compared to their carbon congeners [94], **41b** could be isolated and characterized in solution. Despite the absence of any amino substituent, **41a** and **41b** turned out to be remarkably stable, showing no significant decomposition reactions in aromatic solvents after 3 months
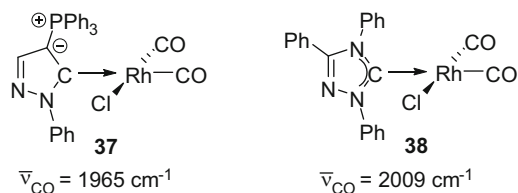
Fig. 10 Rhodium complexes **37** and **38** with AYC **35** and the corresponding triazolyl-2-ylidene as ligands
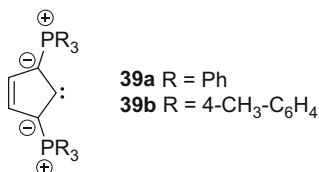
Fig. 11 Bis(ylide)-stabilized carbenes **39**

at room temperature. The ^{29}Si NMR signal of the silylenes appeared considerably downfield shifted ($\delta = 213.3$ and 212.4 ppm) compared to that of reported NHSis ($\delta = 78$–119 ppm) [94]. Likewise, the ylidic carbon atom also appeared downfield at $\delta = 90$ ppm, which is atypical for the carbanionic center of a phosphorus ylide. This change in chemical shift was explained by the generation of a ring current as illustrated by the silacyclopentadienide-like resonance structures **41A** and **41B** shown in Fig. 12 (bottom). The aromatic character was further confirmed by DFT studies. As such, nucleus-independent chemical shift (NICS) [95, 96] calculations showed a NICS(1) [97] value of -4.0, and the molecular orbitals showed π-bonding orbitals delocalized over the whole ring system. Interestingly, the lowest unoccupied molecular orbital with significant π character on silicon was found to be LUMO+8 (LUMO: lowest unoccupied molecular orbital), thus indicating that the silylene center in **41** is less electrophilic and more electron-rich compared to that of N-heterocyclic silylenes (NHSi).

More recently, Kato and coworkers came to the same conclusions by means of amino(ylide)silylene **42** prepared by reduction of the dichloro precursor with potassium at 80°C (Scheme 12) [98]. Determination of the Tolman electronic parameter (TEP) [99, 100] to estimate ligand donor properties showed that the electron-donor ability of **42** ($\nu_{CO} = 2051$ cm^{-1}) is as strong as that of classical NHC ligands and considerably stronger than that of NHSis. This was also reflected in the high reactivity of **42**. For example, reaction with 2,3-dimethyl-1,3-butadiene gave the corresponding [4+1]-cycloadduct **43**, while treatment with white phosphorus resulted in the insertion of the silylene into the σ-P–P bond to give the SiP$_4$ cage compound **44**.

Overall, the synthesized ylide-functionalized carbenes and silylenes demonstrate the ability of ylide substituents to stabilize low-valent species and to tailor their electronic properties. So far, only a limited number of compounds has been synthesized and isolated. This limitation, however, might be overcome with the development of readily

40a R = Ph
40b R = 3-CH$_3$-C$_6$H$_4$
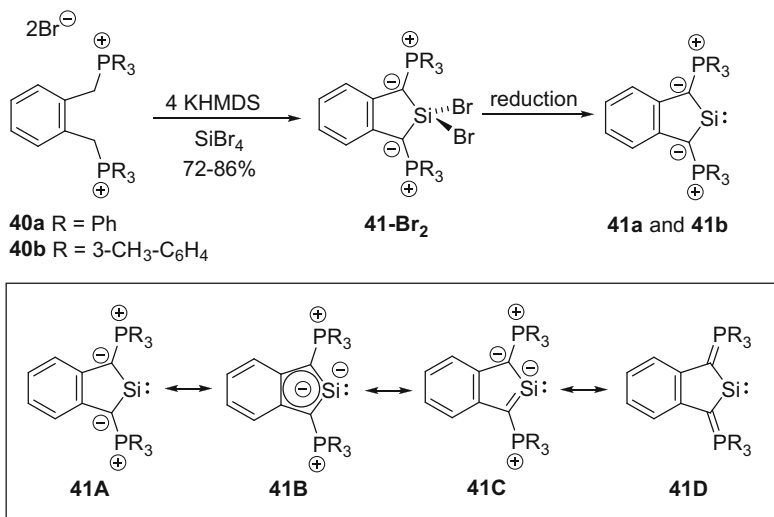
Fig. 12 (*Top*) Synthesis of the bisylide-stabilized silylenes **41** and (*bottom*) resonance structures of **41**
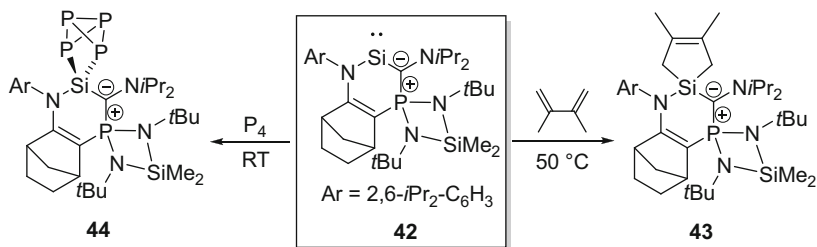
Scheme 12 Structure and reactivity of amino(ylide)silylene **42**

accessible metalated ylides for facile ylide functionalization. This will also be beneficial for further applications of these carbenes, such as in homogenous catalysis.

4.1.2 DFT Calculations

The influence of ylide substitution on the properties and reactivities of carbenes and silylenes has also been subject to intensive computational studies. Pukhan and coworkers investigated the impact of ylide groups on the stability and reactivity compared to known NHCs, cAACs, as well as bisylides and other carbon(0) derivatives (Fig. 13) [101]. Calculations of the molecular orbitals showed that the smaller –I effect and the larger π-donating ability of an ylide group relative to a nitrogen substituent result in an increase of the energies of the σ- and π-donating orbitals. Thus, the amino(ylide)carbene **47** and bis(ylide) carbene **48** are more basic than NHC **45** and cAAC **46**. Interestingly, the σ- and π-donor
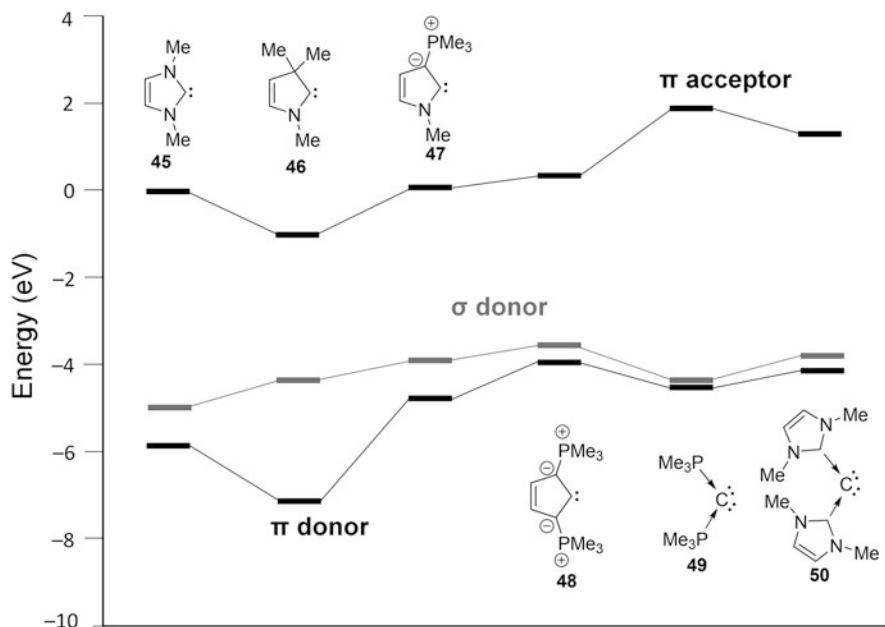
Fig. 13 Energies (eV) of the molecular orbitals of carbenes and carbon(0) compounds responsible for the σ- and π-donating as well as π-accepting properties of the central carbon atom

abilities were found to be equal or even higher than those of the carbon(0) compounds **49** and **50**. Thus, introduction of ylide moieties adjacent to the carbenic carbon renders the basicities of these carbenes comparable to that of known carbon(0) compounds. However, in contrast to carbones, ylide-substituted carbenes still possess moderate to strong π-acceptor properties. The σ- and π-donating abilities in the range of carbon(0) compounds are particularly remarkable, since the high basicity associated with carbon(0) compounds can be referred to the presence of two high-energy lone pair orbitals, while in case of carbenes, it is related to the presence of only one lone pair orbital at the carbenic center together with a 3c–2e π-donor orbital. The same tendencies observed for the σ- and π-donating abilities of compounds **45–50** were also found for the first and second proton affinities as well as for the bond dissociation energies of one molecule AuCl from the mono or diaurated complexes [LAuCl and L(AuCl)$_2$] of these ligands. These properties have been used to distinguish between carbenes and carbones [102–104]. The calculations, however, indicate that with introduction of ylide substituents, this distinction becomes blurred, thus manifesting the unique properties of amino(ylide)carbenes (AYCs) and bis(ylide)carbene (Y$_2$Cs). This special electronic character of AYCs and Y$_2$Cs – as well as of cyclic ylide-stabilized silylenes [105] – was also confirmed in further theoretical studies [106–109]. Kassaee and coworkers additionally examined the influence of different ylide moieties as well as different backbones (noncyclic vs. cyclic, saturated vs. unsaturated) on the stability of AYCs. Ammonium ylides were found to exert the highest stabilizing effect on the carbenic center resulting, for example, in larger

singlet-triplet energy gaps and broader HOMO-LUMO gaps than in phosphorus or sulfur ylides [109]. Comparable to aminocarbenes, aromatic cyclic systems are more stable than their saturated cyclic analogues, which are in turn more stable than their acyclic counterparts.

Recent studies by Phukan and coworkers also focused on the applicability of ylide-substituted carbenes in bond activation chemistry. While NHCs are generally ineffective in direct bond activation reactions, cAACs have shown to activate a series of element hydrogen bonds [110], among the H–H bond in dihydrogen as well as the N–H bond of ammonia [78]. This can be referred to the smaller HOMO-LUMO gap in cAACs and the increased nucleophilicity and electrophilicity. This ambiphilicity allows for an efficient interaction of the HOMO and LUMO with the σ- and σ*-orbitals of the respective bond in the transition state analogous to interactions found in bond activation reactions with transition metals (Fig. 14, left). Due to the generally larger HOMO-LUMO gaps in ylide-functionalized carbenes, these systems were found to be inactive in dihydrogen activation [108]. Interestingly, this lack of activity can already be seen in the transition states characterized for these carbenes (Fig. 16, right), which were found to be quite different compared to those of cAACs. While the positively polarized hydrogen atom of dihydrogen interacts effectively with the lone pair orbital of the ylide-stabilized carbenes, the hydridic hydrogen is far away from the formally vacant p_π orbital at the carbon atom. This results in a much weaker carbene-H_2 interaction and thus in a weaker activation. Hence, the poor π-accepting property of ylide-functionalized carbenes seems to be responsible for their inability (or at least low effectiveness) in bond activation reactions (cf. Fig. 13). Nevertheless, experimental proof of this observation is so far missing.

Overall, all calculations demonstrate that ylide functionalization results in an efficient stabilization of the single state of a carbene and in large singlet-triplet separations. Thus, the isolation of AYC and Y_2C also at room temperature should be possible. Such an isolation would be particularly important to further experimentally evaluate the σ- and π-donating properties of these systems and to develop applications in coordination chemistry and catalysis.
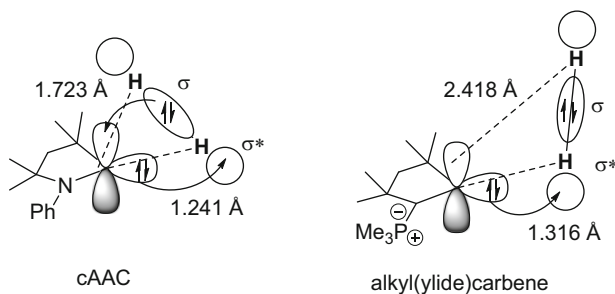
Fig. 14 Orbital interactions important for the activation of dihydrogen by cAACs (*left*) and alkyl (ylide)carbenes (*right*); bond lengths correspond to the distances between the carbenic carbon atom and dihydrogen in the transition state

4.2 Ylide-Stabilized Cationic Main Group Element Compounds

As impressively demonstrated by the preparation of ylide-stabilized carbenes and silylenes, the functionalization of main group element compounds by ylide moieties can efficiently be used to tune the properties of a given system. Due to the strong donor properties of the ylide moiety, electron-deficient species are particularly interesting target molecules. Besides the low-valent group, 14 species also cationic compounds have been stabilized by means of ylide functionalization.

4.2.1 Boron Compounds

Due to the three valence electrons of boron, boron compounds are inherently electron-deficient. Hence, their general properties, bonding modes, and reactivities are dictated by their tendency to overcome this deficiency, such as by adduct formation or oligomerization. Often amido or aryl groups are applied in boron chemistry which allow for efficient π-donation to the boron center and electronic stabilization of the compounds. With their σ- and π-donor properties, metalated ylides are ideal ligands to stabilize boranes or even boron cations. The first application of ylide ligands in boron chemistry was reported by Bestmann and coworkers [111]. They reacted the cyano-functionalized ylide **9-H** with $BH_3 \cdot SMe_2$ to selectively deliver the neutral compound **51** (Scheme 13). In contrast to systems with non-stabilized ylides, which underwent thermal rearrangement to phosphine-coordinated boranes [112], **51** revealed to be thermally stable and could be further converted to lithium borate **52** by addition of *n*-butyllithium. Although **52** has not been prepared directly from the metalated ylide **9**, it can be regarded as an yldiide adduct of BH_3. The molecular structure of **52** was also determined by single-crystal X-ray diffraction analysis. In the solid state, the THF-solvated metal solely coordinates to the nitrile moiety and not to the hydrides at boron or the ylidic carbon center.

The formation of **52** is in contrast to recent results by Gessner and coworkers with the sulfonyl-stabilized metalated ylide **13-M** [43]. Reaction of **13-M** with $BH_3 \cdot THF$ selectively led to the formation of the bisylide-functionalized borane **53**, instead of a borate analogous to **52** (Scheme 14). This can be explained by the high donor ability of **15** which renders the initially formed sodium borate **53-Int** highly electron-rich. Thus, it further reacts with a further equivalent of borane THF adduct under hydride transfer and formation of sodium boron hydride. The thus formed mono-ylide-substituted borane reacts with a second equivalent of yldiide to a further borate intermediate which again eliminates a hydride to form **53**. Hence, the different reactivities of **52** and **53-Int** reflect the differences in the donor properties of the corresponding metalated ylides **9** and **13-M**. Because **9** can delocalize the negative charge into the cyano moiety, it is less basic than **15** and hence borate **51** more stable than **53-Int**. Notably, borane **53** is – in contrast to many
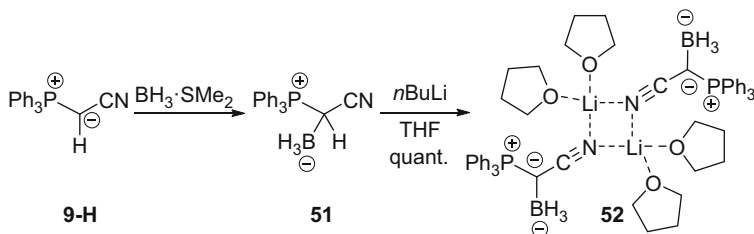
Scheme 13 Preparation of the ylide-functionalized borate **52**
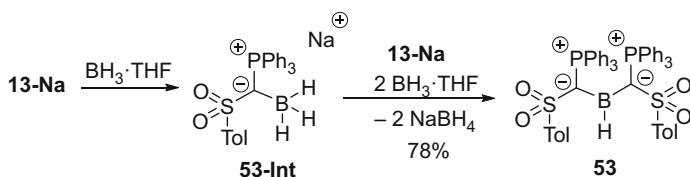
Scheme 14 Formation of borane **53** from the metalated ylide **13-M**
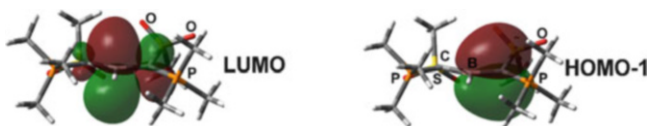
Fig. 15 Molecular orbitals of a methyl-substituted model system of the bis(ylide)-substituted borane **53**

other boranes – monomeric. Dimerization is inhibited due to steric but also electronic effects due to the π-donation from the ylide ligand. This can be seen from the molecular orbitals (Fig. 15), which clearly show π-interaction between boron and the ylide ligand.

The high donor capacity of **13-M** was also used to stabilize boron cations. Cationic boron species are naturally even more reactive than their neutral analogues due to their higher electron deficiency [113]. Nevertheless, hydride abstraction from **53** was found to be facile employing different trityl salts with non-coordinating anions (Scheme 15) [114]. Also, tris(pentafluorophenyl)borane could be used for hydride abstraction thus already indicating that ylide substitution makes the resulting cationic boron species less Lewis acidic than $B(C_6F_5)_3$ itself. Consistently, the cations were also found to be thermally robust, showing no decomposition in the solid state up to 200°C.

X-ray crystallographic studies (Fig. 16) of the hexafluorophosphate salt **54e** showed that the boron center in **54** is coordinated not only by the two ylide substituents but also by one sulfonyl moiety [114]. The B–C distances were found to be shorter than typical single bonds, thus reflecting the π-donation from the ylide substituents. This is also in line with the planarity of the whole Y–C–Y moiety (Y = PCS). Computational studies further confirmed the π-interaction within the
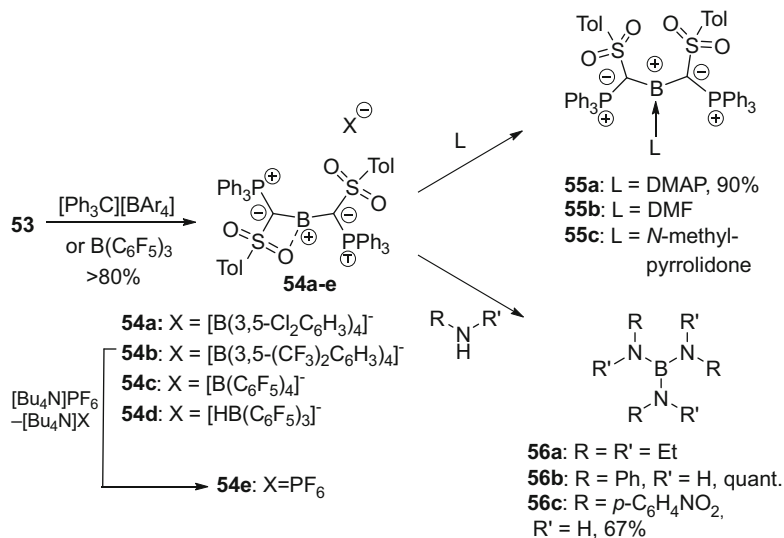
Scheme 15 Synthesis of the bis(ylide)-stabilized boron cations **54** and their reactivity toward amines and Lewis bases L
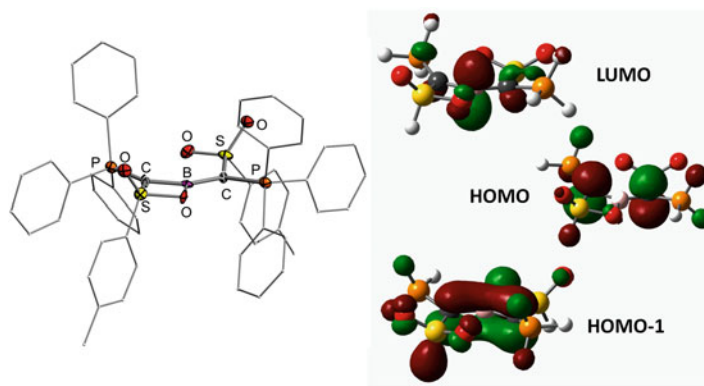
Fig. 16 (*Left*) Crystal structure of the cation of **54e** and (*right*) display of the calculated molecular orbitals of a methyl-substituted model system of **54**

central C–B–C linkage. As such, the HOMO represents the two lone pairs at the carbon atoms, while the HOMO-1 is the bonding π-interaction over the whole C–B–C linkage and the LUMO its antibonding counterpart (Fig. 16, right). Despite this π-delocalization, electrostatic interactions were also found to contribute to the bonding situation in **54**. Hence, large negative charges were observed at the ylidic carbon atoms ($q_C = -1.26$ and -1.30) and a large positive charge at the boron center ($q_B = 0.90$), thus reflecting the special donor properties of the stabilized yldiide **15**. This polar bonding situation also determines the reactivity of the boron cation.

Treatment with strong Lewis bases such as *N,N*-dimethylaminopyridine (DMAP) results in the formation of the expected Lewis base adducts **55** (Scheme 15) with de-coordination of the sulfonyl group. In contrast, primary and secondary amines lead to the activation of the N–H bond across the B–C bond, thus furnishing the corresponding tris(amino)boranes **56** via cleavage of the B–C bond and elimination of ylide **13-H** and phosphonium salt **13-H$_2$**.

4.2.2 Phosphorus Compounds

Ylide functionalization of phosphorus compounds was early reported. In general, three synthetic strategies have been used in this chemistry (Scheme 16): (1) reaction of ylides with phosphorus halides in the presence of base (Route A) [115, 116], (2) chlorosilane elimination (trans-silylation) by reaction of silyl-substituted ylides with phosphorus chlorides (Route B) [117–119], and (3) reaction of metalated ylides with chlorophosphines (Route C) [42, 43].

   The influence of ylide substitution on the electronics of the phosphorus center was particularly addressed by Schmidpeter and coworkers. They observed that introduction of an ylide substituent into halogen phosphorus compounds results in a strong polarization of the P–Hal bond [120, 121]. Depending on the electronics of further substituents at the phosphorus center in **57**, this polarization can even result in the spontaneous dissociation of the halide from the phosphorus to give the corresponding cations **57′** (Scheme 17). This spontaneous dissociation was observed in bisylide functionalized systems such as **57g** and **57h** as well as in compounds **57f** with R′ being an amino substituent [122]. For all other ylide-functionalized halophosphines, elongated P–Cl bonds were observed, and the halide could easily be abstracted by addition of group III halides such as AlCl$_3$ or GaCl$_3$ to form the corresponding cations [123]. For example, compound **57d** with R = Ph and R′ = Me exhibited the longest P–Cl bond (2.262(1) Å) observed for an acyclic chlorophosphine at that time [124]. The facile phosphenium cation formation in these systems can be explained by the π-donation of the ylide substituent and the stabilization of the resulting cation. This is expressed by the
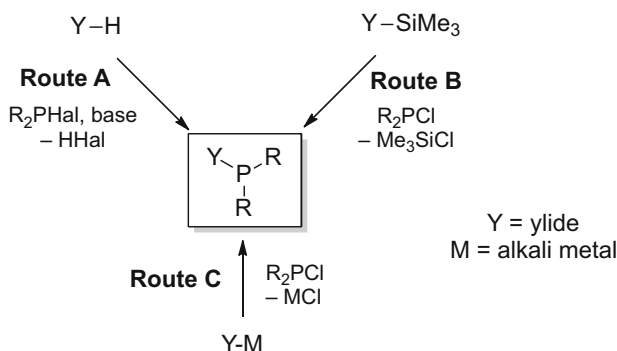
Scheme 16 Preparation methods for ylide-functionalized phosphorus compounds

a: R = H, R' = Cl
b: R = Me, R' = Cl
c: R = Ph, R' = Cl
d: R = Ph, R' = Me

e: R = SiMe$_3$, R' = Cl
f: R = NEt$_2$, R' = Cl
g: R = Ph, R' = C(Ph)PPh$_3$
h: R = Me, R' = C(Me)PPh$_3$
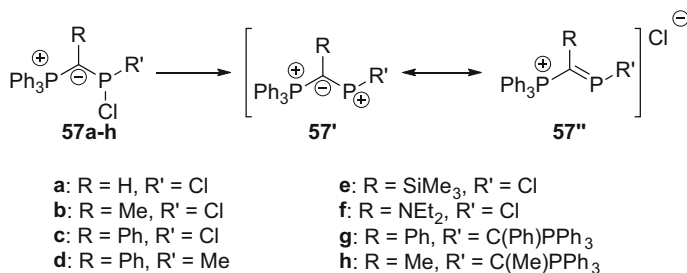
Scheme 17 Phosphenium ion generation by P–Cl bond dissociation in ylide-substituted phosphorus compounds

phosphonium ion resonance structure **57″** depicted in Scheme 17. Consistently large P–C–P–R dihedral angles of approx. 180° were found in the crystal structures of these compounds.

Systematic studies by Schmidpeter on the electronic effects of different ylide groups showed that ylide substitution results in a P–Hal bond polarization already in dihalogenphosphines YPHal$_2$ (**57** wit R′=Hal). Crystallographic studies of these compounds revealed the full range of compounds from symmetric systems with equal P–Hal bonds to compounds with one P–Hal bond being extremely elongated [121]. In these structures, the dichlorophosphine moiety always prefers the conformation, in which one of the P–Cl bond stands roughly perpendicular to the plane P–C–(R)–P plane (Fig. 17, left). This gives rice to an almost parallel orientation of this bond to the p_z orbital at the ylidic carbon atom and thus to effective charge transfer from the carbon atom to the antibonding orbital of the P–Cl bond. This charge transfer finally results in the bond lengthening and weakening. Consistently, the halogen atom perpendicular to the ylide plane is more easily abstracted than the other one in dihalogenphosphines. This can, for example, be seen in the cation of **57e** with R = SiMe$_3$ and R′ = Cl formed after chloride abstraction with GaCl$_3$ (Fig. 17, right) [124]. The P–Cl bond polarization and ionization of **57** to **57′** were also traced by NMR spectroscopy in solution. In general, the ^{31}P NMR signals of acyclic monochlorophosphines can be found at $\delta_P < 200$ ppm, while those of phosphenium ions appear at $\delta_P > 260$ ppm [124]. This spectroscopic difference between **57** and **57′** was used to determine solvent effects on the dissociation equilibrium. Thereby, the most pronounced solvent dependency was observed for the enamine functionalized chlorophosphine **58** (Fig. 18). Here, the equilibrium shifted almost completely from the covalent to the ionic side within a rather narrow range of solvent composition (20–70 vol% dichloromethane in benzene). Overall, the studies on the polarization of P–Hal bonds in ylide-substituted halophosphines clearly demonstrate the tunability of the electronics of the ylide substituent by variation of the R group (such as in **57**) and its impact on the fragments it is bound to.
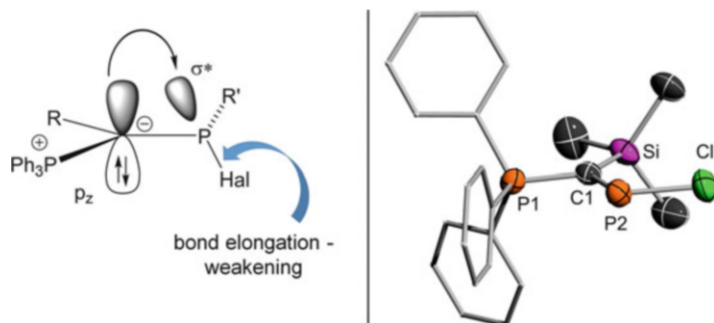
Fig. 17 (*Left*) Orbital interactions in the preferred conformation of ylide-substituted halophosphines; (*right*) cation in the molecular structure of **57e** (GaCl$_4$ counterion omitted for clarity)
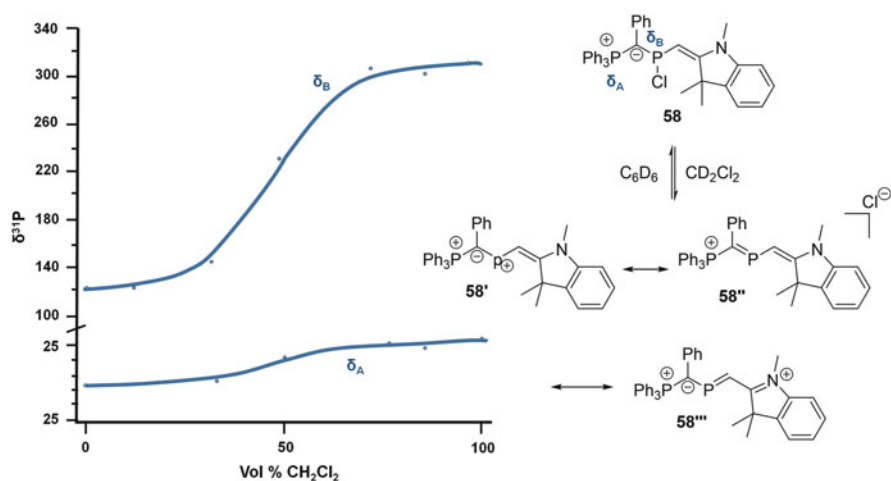
Fig. 18 (*Left*) Chemical shifts of the phosphorus atoms of enamine **58** (δ_A: phosphonium group, δ_B: phosphenium center) depending on the solvent mixture; (*right*) resonance structures of **58**

5 Yldiides as Ligands in Transition Metal Chemistry

5.1 General Bonding Properties

Due to their capability to act as σ- as well as π-donors, α-metalated ylides also represent interesting ligands for transition metal compounds to form either carbene-like structures or dimetalated species. Transition metal complexes with various types of ylides have been known for many years. However, the number of complexes with yldiides as ligands is still limited particularly compared with carbenes. This is on the one hand due to the lack of readily available yldiides and on the other hand due to side reactions often occurring in the metalation step, such as ortho-

metalations, C–P bond activations, or carbene transfer reactions [18]. This has, for example, been demonstrated by Schuhmann and coworkers by means of luthenium complex **59**. Instead of generating the corresponding yldiide complex **60** when treated with methylenetriphenylphosphorane (**3**), the cyclometalated complex **61** was formed after elimination of methane [125]. In contrast, a dinuclear complex with yldiide ligands is formed using the methoxyphenyl substituted ylide **62**. This ylide gives way to complex **64** with the yldiide ligand adopting a bridging position. No complex with a terminal coordination mode of the yldiide such as in the hypothetical carbene-like complex **63** was observed (Scheme 18) [126].

As indicated by means of the two different luthenium complexes **63** and **64,** yldiides can bind to a metal in a bridging mode to coordinate two metals in a μ^2-type fashion or in a terminal coordination mode, thus forming either dinuclear complexes such as **F** or carbene-like complexes (phosphonium alkylidenes) such as **G** depicted in Fig. 20. The latter can exhibit different bonding situations between the metal and the carbon atom. Depending on the electronics of the yldiide ligand and the metal fragment, the ylide ligand can act as two- or four-electron donor ligand. Thus, either carbene complexes with a metal carbon double bond or complexes with ylidic metal carbon interactions can be formed. This is reflected by the different resonance structures **G** and **G′** (Fig. 19). While in the ylidic structure the p_π lone pair remains at the ylidic carbon atom, it is directly involved in the metal-carbon interaction in the carbene-like systems. Thus, the latter are preferentially formed with electron-poor, acidic metal centers. Independent of the final coordination mode, yldiides should – owing to their negative charge – formally act as X,L-type ligands according to Green's covalent bond classification (CBC) method [27]. This substantially distinguishes yldiides from neutral carbenes and carbodiphosphoranes as well as from dianionic methandiides. However, as
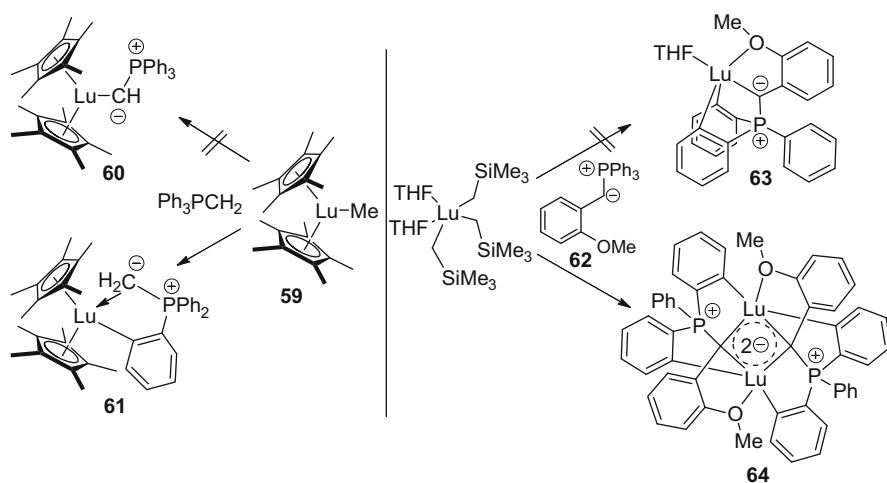
Scheme 18 Formation of cyclometalated or dinuclear luthenium complexes with different ylide ligands
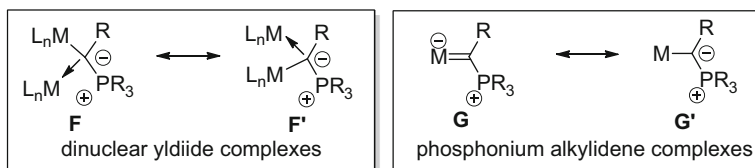
Fig. 19 Different coordination modes of yldiides with transition metals: (*left*) bimetallic complexes and (*right*) carbene-like systems

shown by many complexes synthesized, the actual ligand behavior depends on various factors including reaction partner and synthesis method (vide infra).

The following two chapters address the two different coordination modes **F** and **G** of yldiides in transition metal chemistry. These chapters are not meant to be exhaustive but to provide an overview over bonding modes and applications. Further examples can be found in other review articles [18, 62].

5.2 Ylide Ligands in Gold Complexes

Dimetallic complexes of ylide ligands − including yldiides − have particularly been prepared with gold as metal [127–132]. In these complexes, the geminal coordination of both metals by the ylidic carbon atom supports strong aurophilic interactions, which had been subject of experimental and theoretical investigations [133]. In contrast to carbodiphosphoranes, which act as neutral L_2 ligands and typically replace the L ligand in the reaction with the LAuCl precursor (e.g., **65**, Fig. 20) [134], yldiides should function as anionic L,X ligand. However, coordination of ylide ligands was shown to be somewhat more complex. As such, studies by Schmidbaur [135] as well as Alcarazo and Fürstner [136] also showed that even neutral carbodiphosphoranes may react as X,L- or even X_2-type ligand. For example, reaction of carbodiphosphorane $(MePh_2P)_2C$ with $[(PPh_3)AuBr]$ lead to the cationic complex **67** by replacement of the bromo instead of the phosphine ligand, while reaction of a pyridine-substituted carbodiphosphorane with $[(Me_2S)AuCl]$ allowed the isolation of the mono-cationic complex **66**. Gold complexes of yldiides have, for example, been prepared with the cyano-functionalized system **9**, albeit not directly formed from the metalated ylide **9-H** but via the so-called acac method using $[(PPh_3)Au(acac)]$ (acac=acetylacetonate) as gold(I) source [137, 138]. Here, acac acts as internal base to deprotonate the used ylide precursor to the corresponding yldiide. In case of **9-H**, this synthetic strategy leads to the formation of complex **68** with the yldiide ligand acting as X_2 ligand. In contrast to bisylides, yldiide ligands have so far only acted as anionic X_2 ligands resulting in cationic digold complexes such as **68** or **69** and **70** (Fig. 20) [129, 139]. Nonetheless, none of the complexes has been synthesized from an isolated metalated ylide.

A particularly interesting example of a series of gold complexes of an ylidic ligand system was reported by Vicente et al. [139]. Starting from the simple
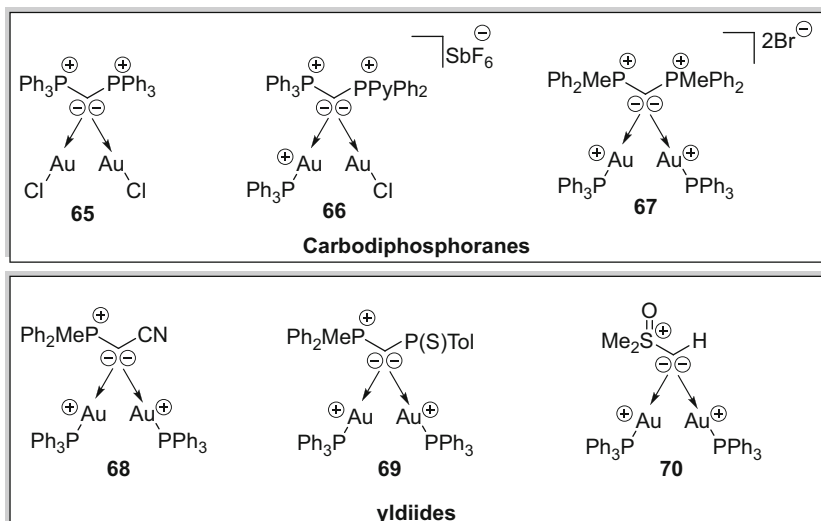
Fig. 20 Diaurated complexes of (*top*) carbodiphosphoranes and (*bottom*) yldiides

sulfoxonium salt [Me$_3$SO]ClO$_4$ and varying amounts of [(PPh$_3$)Au(acac)], they obtained the monoaurated complex [Me$_2$S(O)CH$_2$AuPPh$_3$]ClO$_4$ (**71**), the di- (**70**), tri- (**72**), and even the tetragold complex **73**. The latter features a hyperconjugate carbon atom which in the molecular structure adopts the apex of a square pyramid with the four gold atoms forming the base (Scheme 19a). In the trigold complex **72**, the ylide likewise coordinates on top of a gold triangle. Such a structural motif had also been reported by Schmidbaur and coworkers starting from the silylated ylide **74** (Scheme 19b) [135]. The generation of the formally di-anionic ylide ligand in **75** made use of the low stability of the C–Si bond in silyl-substituted ylides – as used for the syntheses of phosphorus compounds (Scheme 16) – as well as a second equivalent of **74** serving as base.

5.3 Carbene-Like Complexes Based on Yldiides

Carbene-like complexes based on yldiide ligands can be expected to exhibit unique electronic properties due to the flexible M–C bonding situation (c.f. **G** and **G′** in Fig. 20) arising from the fact that yldiides may act as two- or four-electron donor ligands. In cases that yldiides function as σ- and π-donor ligands, carbene complexes can be formed – analogous to methandiides – via donation of four electrons from the carbon to the metal center. However, the donation of the π- lone pair into empty metal d-orbitals is usually facing a competitive situation with π-bonding into the σ*-molecular orbitals of the triphenylphosphonium substituent (negative hyperconjugation). This typically leads to a stronger polarization of the metal carbon bond compared with that in classical carbene

a)

b)
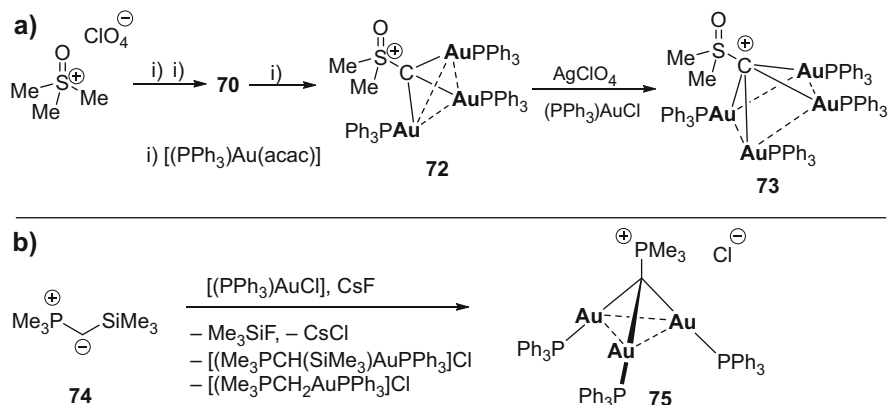
Scheme 19 Multi-nuclear gold complexes with ylide ligands: (**a**) Synthesis of a tetragold and (**b**) of a trigold complex

complexes. Hence, the M–C bond is in general less stable and the phosphonium alkylidenes thus more reactive. The continuous range of different bonding situations in these complexes is also reflected by the ^{13}C NMR signals of the ylidic carbon atom in the metal complexes. While the dimetalated complexes in general showed high-field shifted signals, the carbon atom in phosphonium alkylidenes usually appears upfield shifted depending on the degree of π-donation (see below).

Detailed studies on triphenylphosphonium methylidene complexes have been reported by Sundermeyer and coworkers with group V–VII metals [140–143]. These complexes were synthesized by transylidation using one sacrificial equivalent of ylide for deprotonation to the yldiide ligand. As such, the molybdenum and tungsten imido complexes **77a** and **77b** were obtained from the dichloro precursors, [Mo(NtBu)$_2$Cl$_2$] and [W(NtBu)$_2$Cl$_2$(py)$_2$], with four equivalents of methylenetriphenylphosphorane (Fig. 21, left) [140]. These complexes were particularly interesting since the [M=CH–PR$_3$$^+$] moiety is isoelectronic to [M=CH–SiR$_3$] used in Schrock-type complexes that are active in olefin metathesis catalysis [144]. The formation of the yldiide ligands proceeds via the intermediate ylide complexes **76-Int**. These complexes are usually formed in transylidation reactions but are not always isolable due to the often fast deprotonation step. In the solid state, **77b** showed short W=C bonds, falling in the upper range for double bonds. The different degrees of π-donation to the metal center and double bond character in **76** and **77** can be assumed from their ^{13}C NMR signals. As such, the mono-alkylidene complexes **76** exhibited significantly more downfield shifted signals (e.g., $\delta_C = 127.8$ ppm for **76a**) than the di-alkylidene analogues **77** (e.g., $\delta_C = 73.6$ ppm for **77a**). This can probably be referred to the smaller degree of M=C double bond character in **77** due to the competing π-donation from the imido and alkylidene ligands in **76** and particularly in **77**. The resulting reactivity of the metal carbon linkage in phosphonium alkylidenes was, for example, demonstrated by the facile insertion of carbon monoxide or isonitrile into the M–C bond in **76** thus leading to a complete break of the metal-ylide interaction [142].
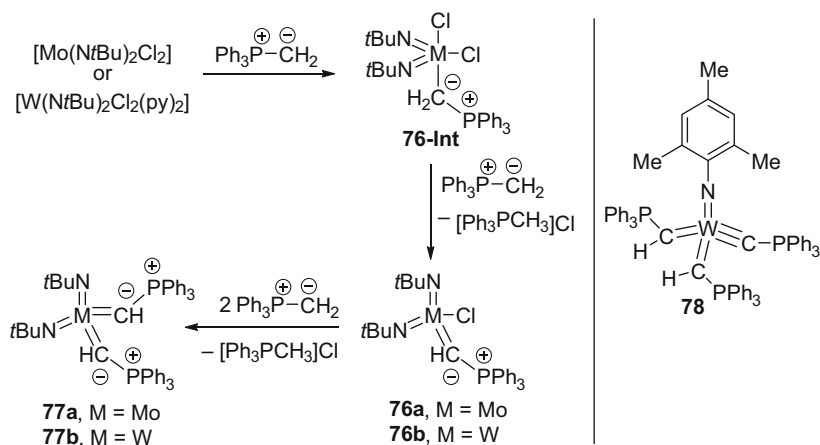
Fig. 21 Synthesis of molybdenum and tungsten phosphonium alkylidene complexes

A particularly interesting tungsten complex with respect to metal-ylide interactions has also been reported by Sundermeyer and coworkers [145]. Complex **78** with phosphonium alkylidene and alkylidyne ligands was formed by an analogous transylidation strategy with seven equivalents of ylide (Fig. 21, right). This complex formally features two M=C double bonds as well as a metal carbon triple bond. Comparable to the yldiide ligand, the phosphonium methylidyne functionality can be described by different resonance structures, $[M^-\equiv C–PPh_3^+]$ or $[M=C^-–PPh_3^+]$. However, due to the strong π-bond competition of the four π-donor ligands in **78,** only partial π-donation from the ylide ligands can occur. This, for example, leads to a considerably bent M–C–P linkage with an angle of 154.0(4)°.

While most of the yldiides complexes were so far synthesized via deprotonation of ylide complexes (see above), Kreissl and coworkers reported on a unique alternative method via addition of a phosphine to a carbyne complex. This has first been demonstrated by means of complex **79** and trimethylphosphine which resulted in the selective formation of the cationic chromium yldiides **80** (Fig. 22, left) [146]. The ^{13}C NMR signal of the metal-bound carbon atom experiences a high-field shift upon PMe$_3$ addition from 349 ppm in **79** to 307 ppm in **80**. A similar procedure has also been employed for other yldiides complexes [147–149].

The bonding situation in an yldiide rhodium complex was addressed by Chauvin by means of computational methods [150]. Deprotonation of a cationic rhodium precursor with a chelating phosphine ligand afforded the yldiide complex **81** (Fig. 22, right). The ^{13}C NMR signal of the yldiidic carbon atom appeared rather high-field shifted at 41.5 ppm, thus already indicating weak alkylidene character. This was confirmed by DFT studies. As such, the HOMO of a model system of **81** was shown to represent the antibonding π interaction of the M–C bond, while electron-localization function (ELF) analysis yielded the bonding mode with only a M–C single bond as the most important resonance form. Comparative studies with neutral bisylide ligands showed that the
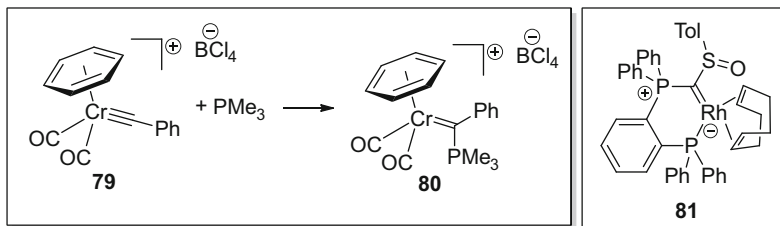
Fig. 22 (*Right*) Chauvin's rhodium yldiide complex **81** and (*left*) chromium yldiide **80** synthesized from corresponding carbyne complex **79**
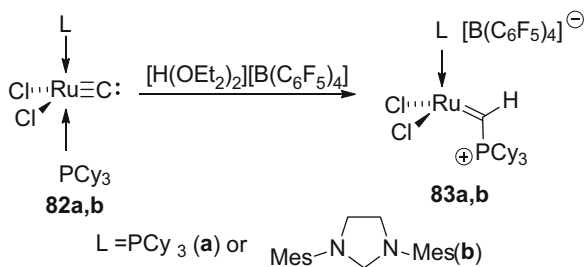
Fig. 23 Piers' phosphonium alkylidene complexes used in olefin metathesis

overall charge of the yldiide ligand exerts only a very weak influence on the bonding properties of the ligand.

The only but extremely impressive example of a catalytic application of an yldiide complex was given by Piers and coworkers by means of ruthenium complexes **83a** and **83b** (Fig. 23) [151]. These complexes were synthesized by a unique strategy based upon the synthetic route to chromium yldiides via phosphine addition to the corresponding carbyne complexes (see above) [146]: initial protonation of the carbide complexes **82** with [H(OEt$_2$)$_2$][B(C$_6$F$_5$)$_4$] resulted in the subsequent transfer of the tricyclohexylphosphine ligand from the metal to carbide atom to yield the yldiide complexes in good yields. Complexes **83a** and **83b** represent close structural models for the proposed four-coordinate 14-electron active species in the Grubbs' catalyst family and were thus applied in olefin metathesis. These studies revealed that particularly **83b** is an extremely fast-initiating catalyst, even surpassing the activity of the highly reactive Schrock catalyst [144]. The reason for this high activity is the fact that no ligand dissociation is required in order for the complex to enter the catalytic cycle. Furthermore, the complexes **83a** and **83b** also allowed the observation of ruthenacyclobutanes [152–154], which are supposed to be the relevant intermediates for the metathesis reaction.

Overall, the selected yldiide complexes demonstrate the unique metal-carbon interaction in these systems. Here, the yldiide ligand not only does give way to dinuclear as well as carbene-like (alkylidene) complexes with a range of different bonding situations but also allows for the stabilization of metal species with unique

reactivities. Owing to the fact that all complexes synthesized so far have not been prepared directly from a metalated ylide, the potential of this ligand class is probably still underdeveloped, and further advancements can be expected with the introduction of more readily available and isolable yldiides.

6 Conclusions and Outlook

In conclusion, yldiides are a unique type of σ- and π-donor ligands that have found applications from organic synthesis to main group metal and transition metal chemistry. The myriad of applications is especially impressive keeping in mind that only an extremely limited number of metalated ylides has so far been isolated. Instead, often detours have been undertaken to realize ylide functionalization or yldiide coordination. It can thus be expected that the preparation of isolable stabilized metalated ylides will open new avenues in the chemistry of yldiides. This is indicated by the cyano- and sulfonyl-stabilized systems **9** and **13-M**, which have already demonstrated their versatility in synthesis and coordination chemistry. However, the generation of further representatives will be important to tailor the structures, electronics, and donor properties of these ligands and hence their capability for advanced applications such as in the stabilization of reactive species or support catalytically active complexes.

References

1. Michaelis A, Gimborn HV (1894) Chem Ber 27:272–277
2. Cristau H-J (1994) Chem Rev 94:1299–1313
3. Wittig G, Rieber M (1949) Justus Liebigs Ann Chem 562:177–187
4. Schröder FG, Sundermeyer J (2015) Organometallics 34:1017–1020
5. Cramer RE, Bruck MA, Gilje JW (1986) Organometallics 5:1496–1499
6. Less RJ, Naseri V, Wright DS (2009) Organometallics 28:3594–3596
7. Cristau HJ, Ribeil Y (1988) J Organomet Chem 352:C51–C53
8. Cristau HJ, Ribeil Y, Chiche L, Plénat F (1988) J Organomet Chem 352:C47–C50
9. McKenna EG, Walker BJ (1988) Tetrahedron Lett 29:485–488
10. McKenna EG, Walker BJ (1989) J Chem Soc Chem Commun 568–569. doi: https://doi.org/10.1039/C39890000568
11. Taillefer M, Cristau HJ, Fruchier A, Vicente V (2001) J Organomet Chem 624:307–315
12. Usón R, Laguna A, Laguna M, Jiménez J, Jones PG (1991) Angew Chem 103:190–191
13. Schmidbaur H, Hartmann C, Reber G, Müller G (1987) Angew Chem 99:1189–1191
14. Basil JD, Murray HH, Fackler JP, Tocher J, Mazany AM, Trzcinska-Bancroft B, Knachel H, Dudis D, Delord TJ, Marler D (1985) J Am Chem Soc 107:6908–6915
15. Mohr F, Sanz S, Tiekink ERT, Laguna M (2006) Organometallics 25:3084–3087
16. Méndez LA, Jiménez J, Cerrada E, Mohr F, Laguna M (2005) J Am Chem Soc 127:852–853
17. Navarro R, Urriolabeitia EP (1999) Dalton Trans 4111–4122
18. Urriolabeitia EP (2008) Dalton Trans 5673–5686
19. Scharf LT, Gessner VG (2017) Inorg Chem 56:8599–8607
20. Corey EJ, Kang J (1982) J Am Chem Soc 104:4724–4725
21. Baumgarnter T, Schinkels B, Gudat D, Nieger M, Niecke E (1997) J Am Chem Soc 119:12410–12411

22. Dyker CA, Bertrand G (2009) Nat Chem 1:265–266
23. Schmidbaur H, Schier A (2012) Angew Chem Int Ed 52:176–186
24. Zhao L, Hermann M, Holzmann N, Frenking G (2017) Coord Chem Rev 344:163–204
25. Harder S (2011) Coord Chem Rev 255:1252–1267
26. Marek I (2000) Chem Rev 100:2887–2900
27. Green MLH (1995) J Organomet Chem 500:127–148
28. Jones ND, Cavell RG (2005) J Organomet Chem 690:5485–5496
29. Cantat T, Mézailles N, Auffrant A, Le Floch P (2008) Dalton Trans 1957–1972
30. Liddle ST, Mills DP, Wooles AJ (2011) Chem Soc Rev 40:2164–2176
31. Gessner VH, Becker J, Feichtner K-S (2015) Eur J Inorg Chem 1841–1859
32. Petz W (2015) Coord Chem Rev 291:1–27
33. Alcarazo M (2011) Dalton Trans 40:1839–1845
34. Alcarazo M (2017) Synthesis, structure, and reactivity of carbodiphosphoranes, carbo-dicarbenes, and related species. Struct Bond. https://doi.org/10.1007/430_2017_19 (this volume)
35. Liu S, Chen W-C, Ong T-G (2017) Synthesis and structure of carbodicarbenes and their application in catalysis. Struct Bond. https://doi.org/10.1007/430_2017_20 (this volume)
36. Bestmann HJ, Besold R, Sandmeier D (1975) Tetrahedron Lett 16:2293–2294
37. Bestmann HJ, Sandmeier D (1975) Angew Chem 87:630
38. Corey EJ, Kang J, Kyler K (1985) Tetrahedron Lett 26:555–558
39. Schaub B, Jenny T, Schlosser M (1984) Tetrahedron Lett 25:4097–4100
40. Schaub B, Schlosser M (1985) Tetrahedron Lett 26:1623–1626
41. Bestmann HJ, Schmidt M (1987) Angew Chem Int Ed Eng 26:79–81
42. Goumri-Magnet S, Gornitzka H, Baceiredo A, Bertrand G (1999) Angew Chem Int Ed 38:678–680
43. Scherpf T, Wirth R, Molitor S, Feichtner K-S, Gessner VH (2015) Angew Chem Int Ed 54:8542–8546
44. Hardy GE, Zink JI, Kaska WC, Baldwin JC (1978) J Am Chem Soc 100:8001–8002
45. Garduno-Alvia A, Lenk R, Escudié Y, González ML, Bousquet L, Saffon-Merceron N, Toledano CA, Bagan X, Branchadell V, Maerten E, Baceiredo A (2017) Eur J Inorg Chem 3494–3497
46. McDowell RS, Streitwieser A Jr (1984) J Am Chem Soc 106:4047–4048
47. Himmel D, Krossing I, Schnepf A (2014) Angew Chem Int Ed 53:370–374
48. Frenking G (2014) Angew Chem Int Ed 53:6040–6046
49. Himmel D, Krossing I, Schnepf A (2014) Angew Chem Int Ed 53:6047–6048
50. Lischka H (1977) J Am Chem Soc 99:353–360
51. Tonner R, Öxler F, Neumüller B, Petz W, Frenking G (2006) Angew Chem Int Ed 45:8038–8042
52. Tonner R, Frenking G (2008) Chem Eur J 14:3260–3272
53. Tonner R, Frenking G (2008) Chem Eur J 14:3273–3289
54. Tonner R, Frenking G (2009) Pure Appl Chem 81:597–614
55. Dewar M (1951) Bull Soc Chim Fr 18:C79
56. Chatt J, Duncanson LA (1953) J Chem Soc 2939–2947
57. Alcarazo M, Lehman CW, Anoop A, Thiel W, Fürstner A (2009) Nat Chem 1:295–301
58. Tonner R, Frenking G (2007) Angew Chem Int Ed 46:8695–8698
59. Klein S, Tonner R, Frenking G (2010) Chem Eur J 16:10160–10170
60. Takagi N, Tonner R, Frenking G (2012) Chem Eur J 18:1772–1780
61. Scharf LT, Andrada DM, Frenking G, Gessner VH (2017) Chem Eur J 23:4432–4434
62. Kolodiazhnyi OI (1999) Phosphorus ylides; chemistry and application in organic synthesis. Wiley-VCH, Weinheim
63. Maryanoff BE, Reitz AB (1989) Chem Rev 89:863–927
64. Byrne PA, Gilheany DG (2013) Chem Soc Rev 42:6670–6696
65. Bestmann HJ, Schmidt M (1987) Tetrahedron Lett 28:2111–2114
66. Igau A, Grützmacher H, Baceiredo A, Bertrand G (1988) J Am Chem Soc 110:6463–6466
67. Arduengo AJ, Harlow LM, Kine M (1991) J Am Chem Soc 113:361–363

68. Vignolle J, Cattoën X, Bourissou D (2009) Chem Rev 109:3333–3384
69. Soleilhavoup M, Bertrand G (2014) Acc Chem Res 48:256–266
70. Melaimi M, Soleilhavoup M, Bertrand G (2010) Angew Chem Int Ed 49:8810–8849
71. Rovis T, Nolan SP (2013) Synlett 24:1188–1189
72. Arduengo AJ, Bertrand G (2009) Chem Rev 109:3209–3210
73. Schuster O, Yang L, Raubenheimer HG, Albrecht M (2009) Chem Rev 109:3445–3478
74. Dötz KH, Stendel J (2009) Chem Rev 109:3227–3274
75. Wang Y, Robinson GH (2011) Inorg Chem 50:12326–12337
76. Bugaut X, Glorius F (2012) Chem Soc Rev 41:3511–3522
77. Ender D, Niemeier O, Henseler A (2007) Chem Rev 107:5606–5655
78. Frey GD, Lavalla V, Donnadieu B, Schoeller WW, Bertrand G (2007) Science 316:439–441
79. Back O, Kuchenbeiser G, Donnadieu B, Bertrand G (2009) Angew Chem Int Ed 48:
    5530–5533
80. Schmidt D, Bertel JHJ, Pietsch S, Radius U (2012) Angew Chem Int Ed 51:8881–8885
81. Lavigne F, Maerten E, Alcaraz G, Branchadell V, Saffon-Merceron N, Baceiredo A (2012)
    Angew Chem Int Ed 51:2489–2492
82. Facchin G, Campostrini R, Michelin RA (1985) J Organomet Chem 294:C21–C25
83. Michelin RA, Facchin G, Braga D, Sabatino P (1986) Organometallics 5:2265–2274
84. Michelin RA, Mozzon M, Facchin G, Braga D, Sabatino P (1988) J Chem Soc Dalton Trans
    1803–1811
85. Facchin G, Mozzon M, Michelin RA, Ribeiro MTA, Pombeiro AJL (1992) J Chem Soc
    Dalton Trans 2827–2835
86. Pombeiro AJL (2005) J Organomet Chem 690:6021–6040
87. Nakafuji S, Kobayashi J, Kawashima T (2008) Angew Chem Int Ed 47:1141–1144
88. Kobayashi J, Nakafuji S, Yatabe A, Kawashima T (2008) Chem Commun 6233–6235
89. Fürstner A, Alcarazo M, Radkowski K, Lehmann CW (2008) Angew Chem Int Ed 47:
    8302–8306
90. Nelson DJ, Nolan SP (2013) Chem Soc Rev 42:6723–6753
91. Wolf S, Plenio J (2009) J Organomet Chem 694:1487–1492
92. Xu C, Wang Z-Q, Li Z, Wang W-Z, Hao X-Q, Fu W-J, Gong J-F, Ji B-M, Song M-P (2012)
    Organometallics 31:798–801
93. Asay M, Inoue S, Driess M (2011) Angew Chem Int Ed 50:9589–9592
94. Asay M, Jones C, Driess M (2011) Chem Rev 111:354–396
95. Schleyer PR, Maerker C, Dransfeld A, Jiao H, Hommes NJRE (1996) J Am Chem Soc 118:
    6317–6318
96. Chen Z, Wannere CS, Corminboeuf C, Puchta R, Schleyer PR (2005) Chem Rev 105:
    3842–3888
97. Schleyer PR, Jiao H, Hommes NJRE, Malkin VG, Malkina O (1997) J Am Chem Soc 119:
    12669–12670
98. Alvarado-Beltran I, Baceiredo A, Saffon-Merceron N, Branchadell V, Kato T (2016)
    Angew Chem Int Ed 55:16141–16144
99. Tolman CA (1977) Chem Rev 77:313–348
100. Crabtree RH (2005) The organometallic chemistry of the transition metals. Wiley, Hoboken
101. Guha AK, Gogoi U, Phukan AK (2013) Int J Quantum Chem 113:2471–2477
102. Esterhuysen C, Frenking G (2011) Chem Eur J 17:9944–9956
103. Fürstner A, Alcarazo M, Goddard R, Lehmann CW (2008) Angew Chem Int Ed 47:
     3210–3215
104. Alcarazo M, Suárez RM, Goddard R, Fürstner A (2010) Chem Eur J 16:9746–9749
105. Karni M, Apeloig Y (2012) Organometallics 31:2403–2415
106. Borthakur B, Silvi B, Dewhurst RD, Phukan AK (2016) J Comput Chem 37:1484–1490
107. Borthakur B, Phukan AK (2015) Chem Eur J 21:11603–11609
108. Bharadwaz P, Chetia P, Phukan AK (2017) Chem Eur J 23:9926–9936

109. Haerizade BN, Kassaee MZ, Zandi H, Koohi M, Ahmadi AA (2014) J Phys Org Chem 27: 902–908
110. Melaimi M, Jazzar R, Soleilhavoup M, Bertrand G (2017) Angew Chem Int Ed 56: 10046–10068
111. Bestmann HJ, Röder T, Bremer M, Löw D (1991) Chem Ber 124:199–202
112. Köster E, Rickborn B (1967) J Am Chem Soc 89:2782–2784
113. Piers WE, Bourke SC, Conroy KD (2005) Angew Chem Int Ed 44:5016–5036
114. Scherpf T, Feichtner K-S, Gessner VH (2017) Angew Chem Int Ed 56:3275–3279
115. Heckmann G, Plass W, Fluck E (1991) Z Anorg Allg Chem 596:139–148
116. Schmidbaur H, Tronich W (1968) Chem Ber 101:3545–3555
117. Schmidbaur H (1975) Acc Chem Res 8:62–70
118. Schmidbaur H, Malisch W (1970) Angew Chem Int Ed Eng 9:70–71
119. Schmidbaur H, Malisch W (1971) Chem Ber 104:150–159
120. Schmidpeter A, Jochem G (1992) Tetrahedron Lett 33:471–474
121. Schmidpeter A, Nöth H, Jochem G, Schrödel H-P, Karaghiosoff K (1995) Chem Ber 128: 379–393
122. Schmidpeter A, Jochem G, Robl C, Nöth H (1997) J Organomet Chem 529:87–102
123. Schrödel H-P, Schmidpeter A, Nöth H (1996) Heteroat Chem 7:355–358
124. Jochem G, Breitsameter F, Schier A, Schmidpeter A (1996) Heteroat Chem 7:239–247
125. Schuhmann H, Reiher F-W (1984) J Organomet Chem 269:21–27
126. Rufanov KA, Müller BH, Spannenberg A, Rosenthal U (2005) New J Chem 30:29–31
127. Schmidbaur H, Gasser O (1976) Angew Chem Int Ed Eng 15:502–503
128. Smyslova EI, Perevalova EG, Dyadchenko VP, Grandberg KI, Slovokhotov YL, Struchkov YT (1981) J Organomet Chem 215:269–279
129. Gimeno MC, Laguna A, Laguna M, Sanmartin F, Jones PG (1993) Organometallics 12: 3984–3991
130. Vicente J, Chicote M-T, Saura-Llamas I, Jones PG, Meyer-Bäse K, Erdbrügger CF (1988) Organometallics 7:997–1006
131. Vicente J, Chicote M-T, Lagunas M-C, Jones PG, Ahrens B (1997) Inorg Chem 36: 4938–4944
132. Vicente J, Chicote M-T, Cayuelas JA, Fernandez-Baeza J, Jones PG, Sheldrick GM, Espinet P (1985) J Chem Soc Dalton Trans 1163–1168
133. Schmidbaur H, Schier A (2012) Chem Soc Rev 41:370–412
134. Vicente J, Singhal AR, Jones PG (2002) Organometallics 21:5887–5900
135. Schmidbaur H, Scherbaum F, Huber B, Müller G (1988) Angew Chem Int Ed Eng 27: 419–421
136. Alcarazo M, Radkowski K, Mehler G, Goddard R, Fürstner A (2013) Chem Commun 49: 3140–3142
137. Vicente J, Chicote MT (1999) Coord Chem Rev 193–195:1143–1161
138. Vicente J, Chicote MT, Lagumas M-C (1999) Helv Chim Acta 82:1202–1210
139. Vicente J, Chicote M-T, Guerrero R, Jones PG (1996) J Am Chem Soc 118:699–700
140. Sundermeyer J, Weber K, Nürnberg O (1992) J Chem Soc Chem Commun 1631–1633
141. Sundermeyer J, Putterlik J, Pritzkow H (1993) Chem Ber 126:289–296
142. Sundermeyer J, Weber K, Pritzkow H (1993) Angew Chem 105:751–753
143. Li X, Wang A, Wang L, Sun H, Harms K, Sundermeyer J (2007) Organometallics 27: 1411–1413
144. Schrock RR, Hoveyda AH (2003) Angew Chem Int Ed 42:4592–4633
145. Li X, Schopf M, Stephan J, Harms K, Sundermeyer J (2002) Organometallics 21:2356–2358
146. Kreissl FR, Stueckler P (1976) J Organomet Chem 110:C9–C11
147. Valyaev DA, Lugan N, Lavigne G, Ustynyuk NA (2008) Organometallics 27:5180–5183
148. Kreissl FR, Stueckler P, Meineke EW (1977) Chem Ber 110:3040–3045
149. Filippou AC, Wössner D, Kociok-Köhn G, Hinz I (1997) J Organomet Chem 541:333–343

150. Zurawinski R, Lepetit C, Canac Y, Mikolajczyk M, Chauvin R (2009) Inorg Chem 48: 2147–2155
151. Romero PE, Piers WE, McDonald R (2004) Angew Chem Int Ed 43:6161–6165
152. Romero PE, Piers WE (2005) J Am Chem Soc 127:5032–5033
153. Wenzel AG, Grubbs RH (2006) J Am Chem Soc 128:16048–16049
154. Van der Eide EF, Romero PE, Piers WE (2008) J Am Chem Soc 130:4485–4491

Index